MSE 991 Special Topic:

Computational Materials Science

Part II

Yue Qi
Philip Eisenlohr

Chemical Engineering and Materials Science
Michigan State University

contact

- eisenlohr@egr.msu.edu
- +1 517 432-4506
- room 3520

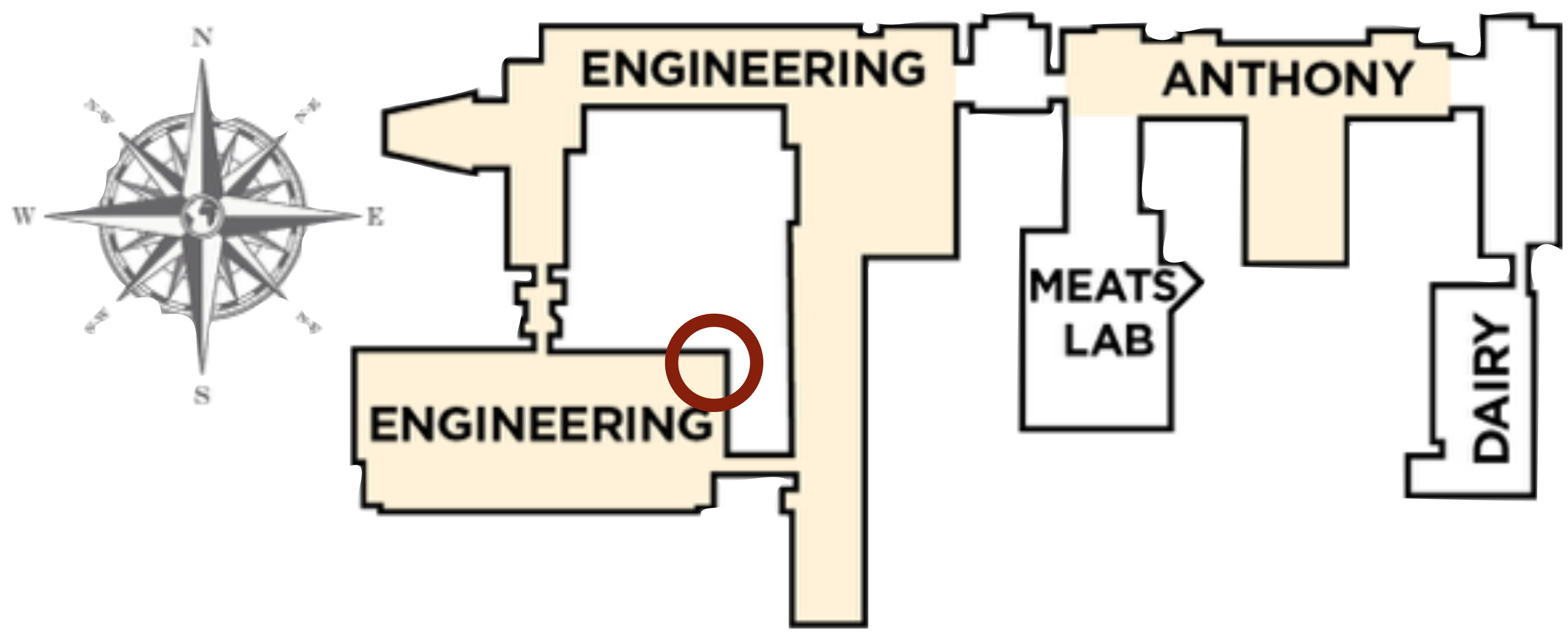

materials in structural applications

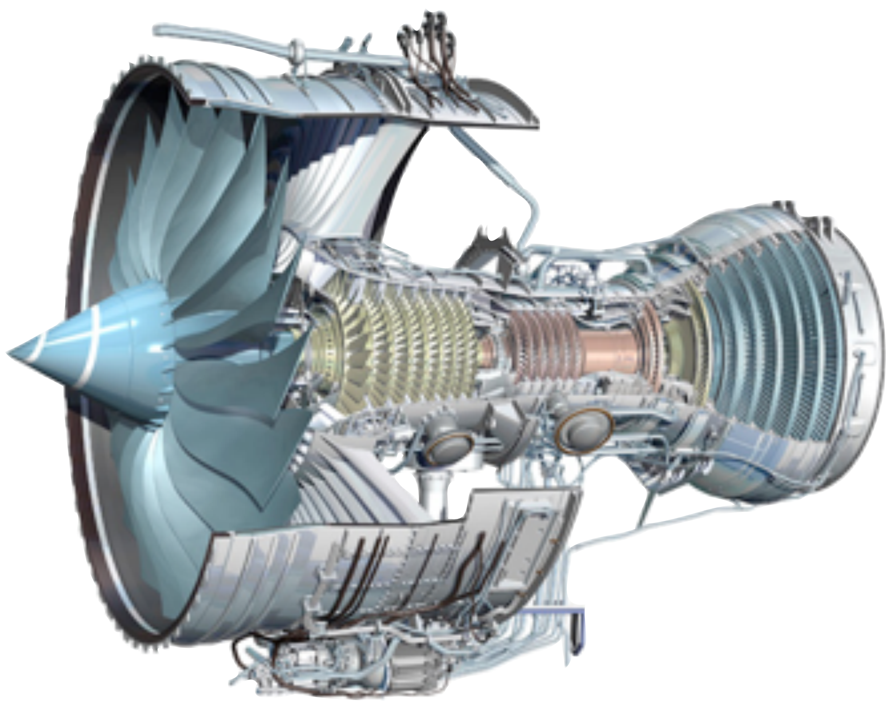

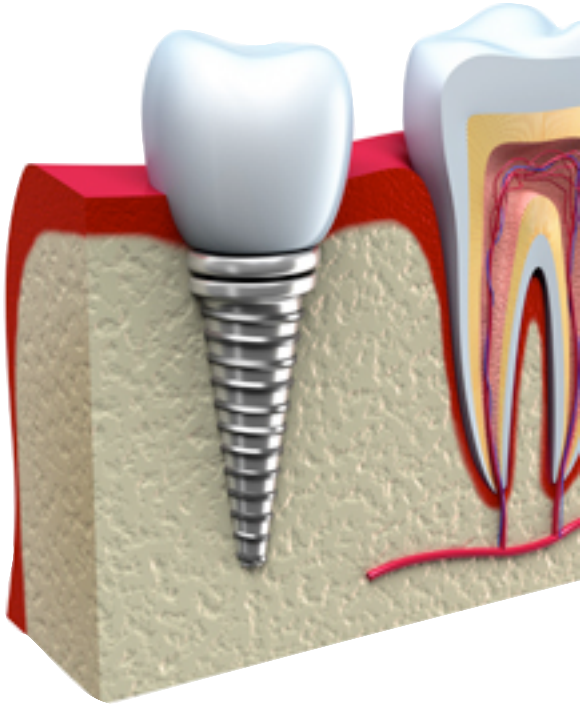

deformation in manufacturing

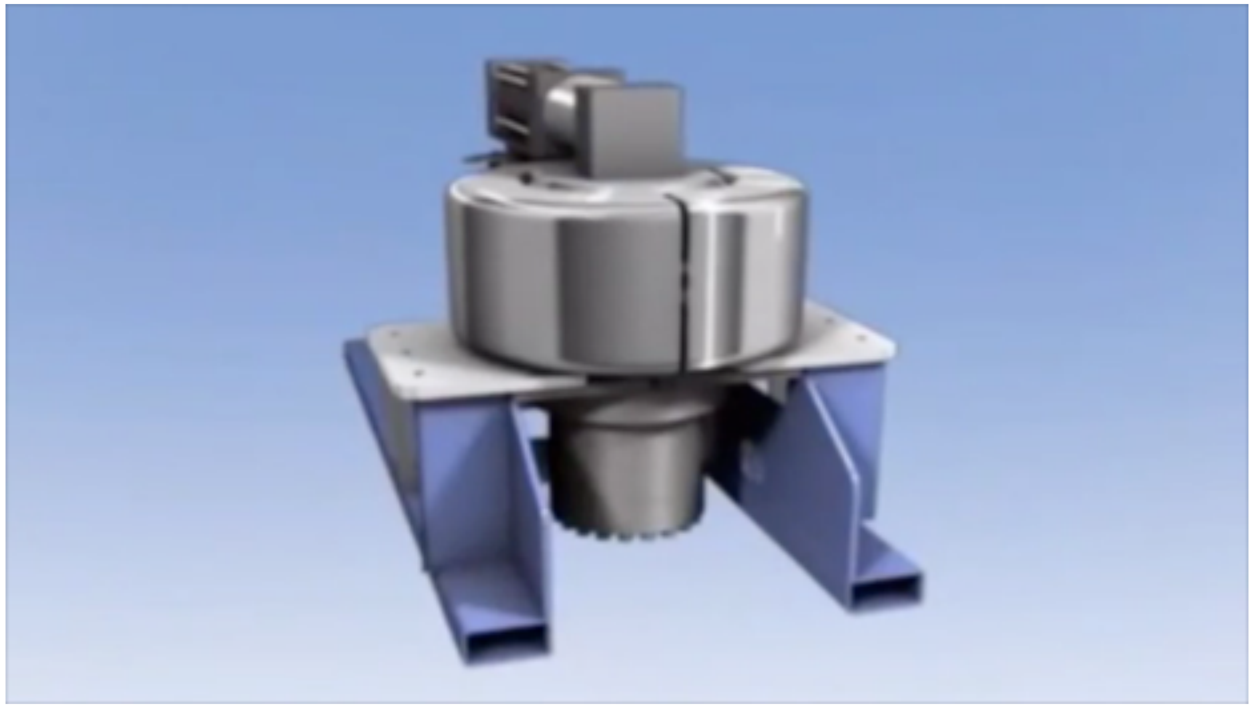

deformation in manufacturing

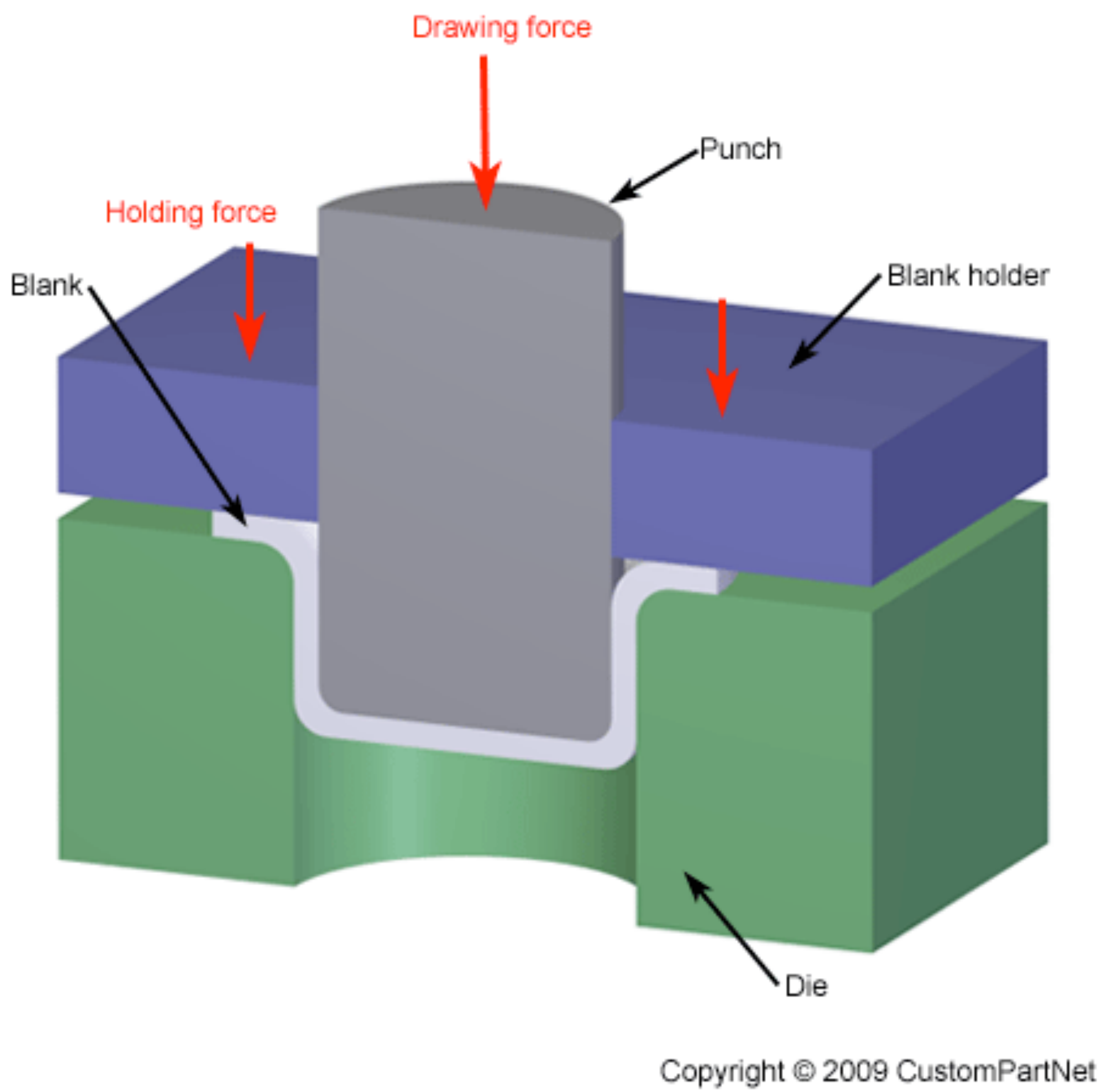

deep drawing

MICHIGAN STATE UNIVERSITY

deformation in manufacturing

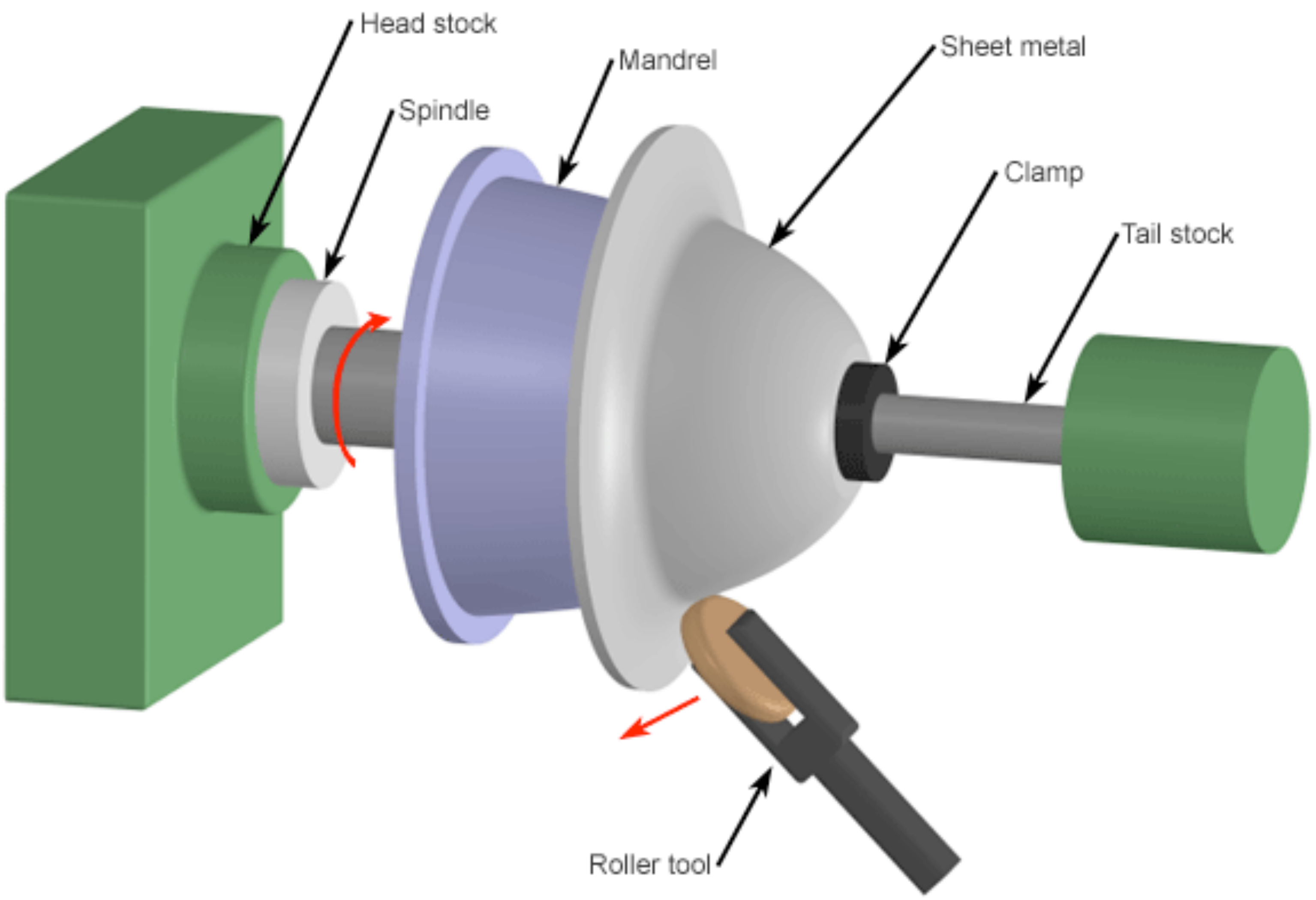

spinning

MICHIGAN STATE UNIVERSITY

deformation in manufacturing

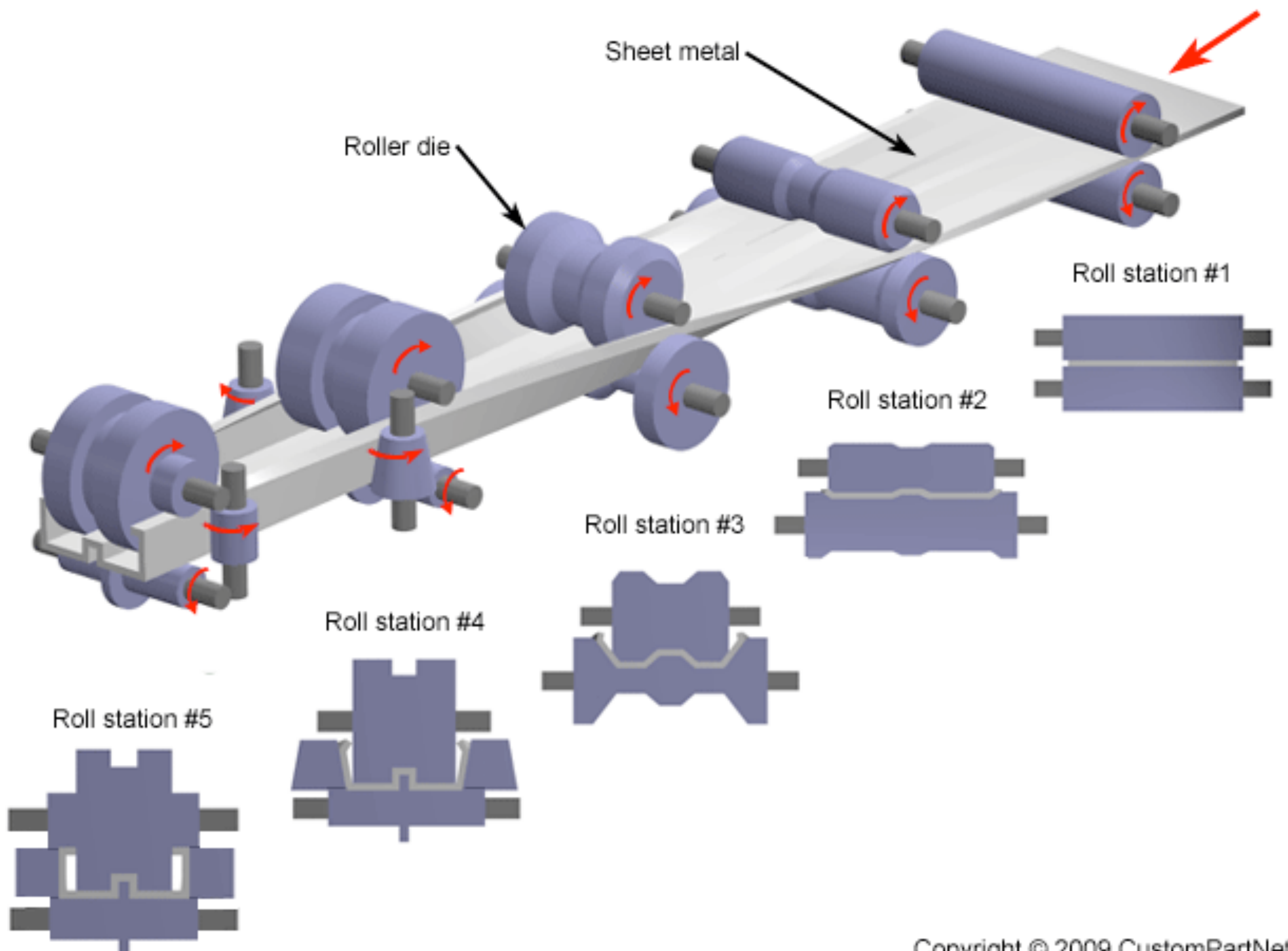

roll forming

deformation in service

deformation in service

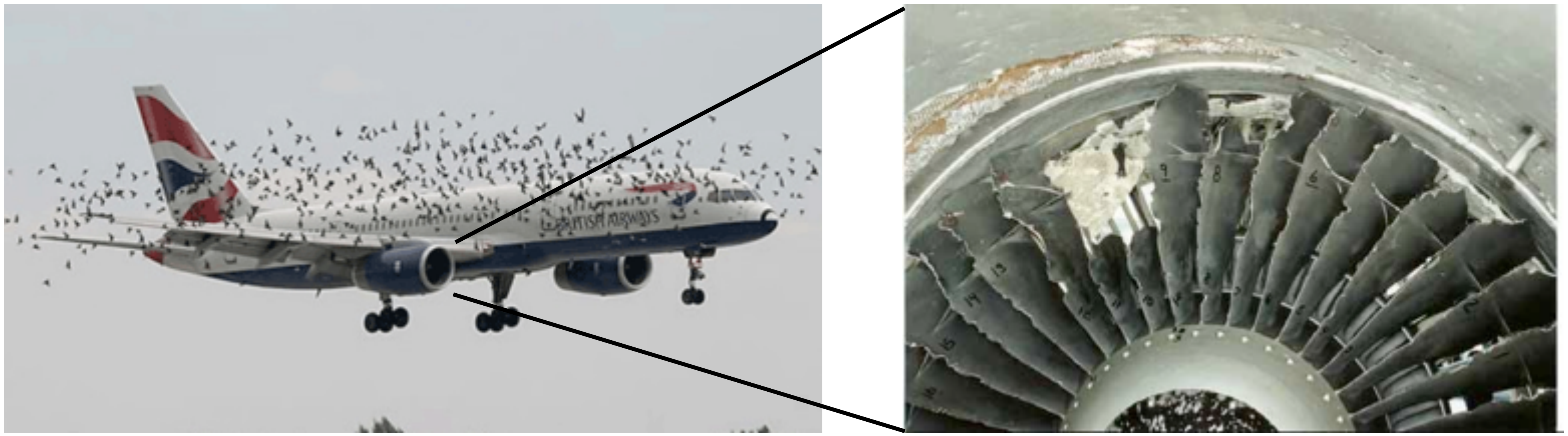

beneficial mechanical properties

- strength / creep resistance
- ductility
- toughness
- fatigue resistance

MICHIGAN STATE UNIVERSITY

materials have multiscale hierarchy

the challenges: polycrystallinity

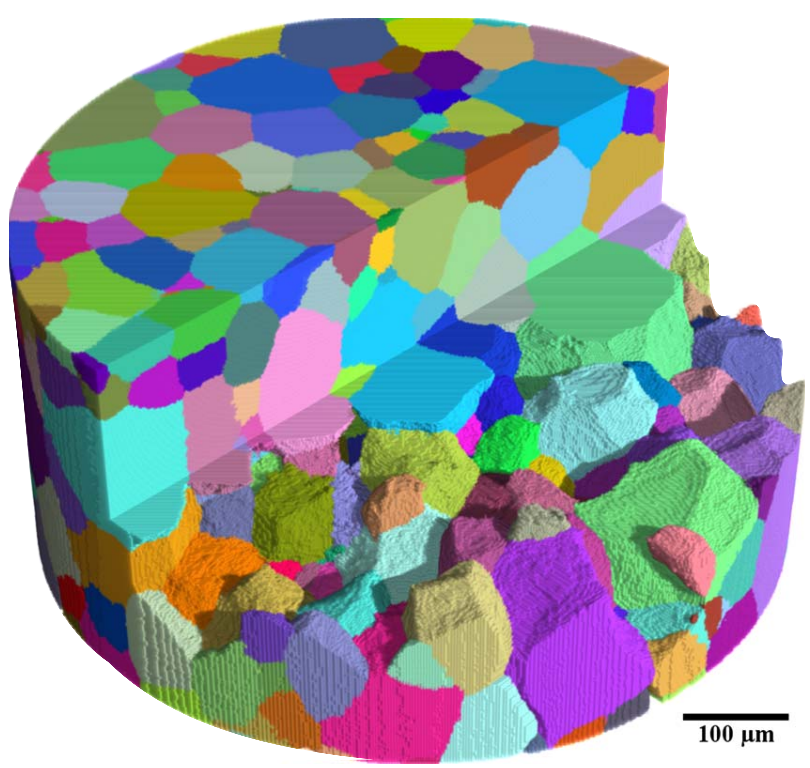

10.1063/1.3100200

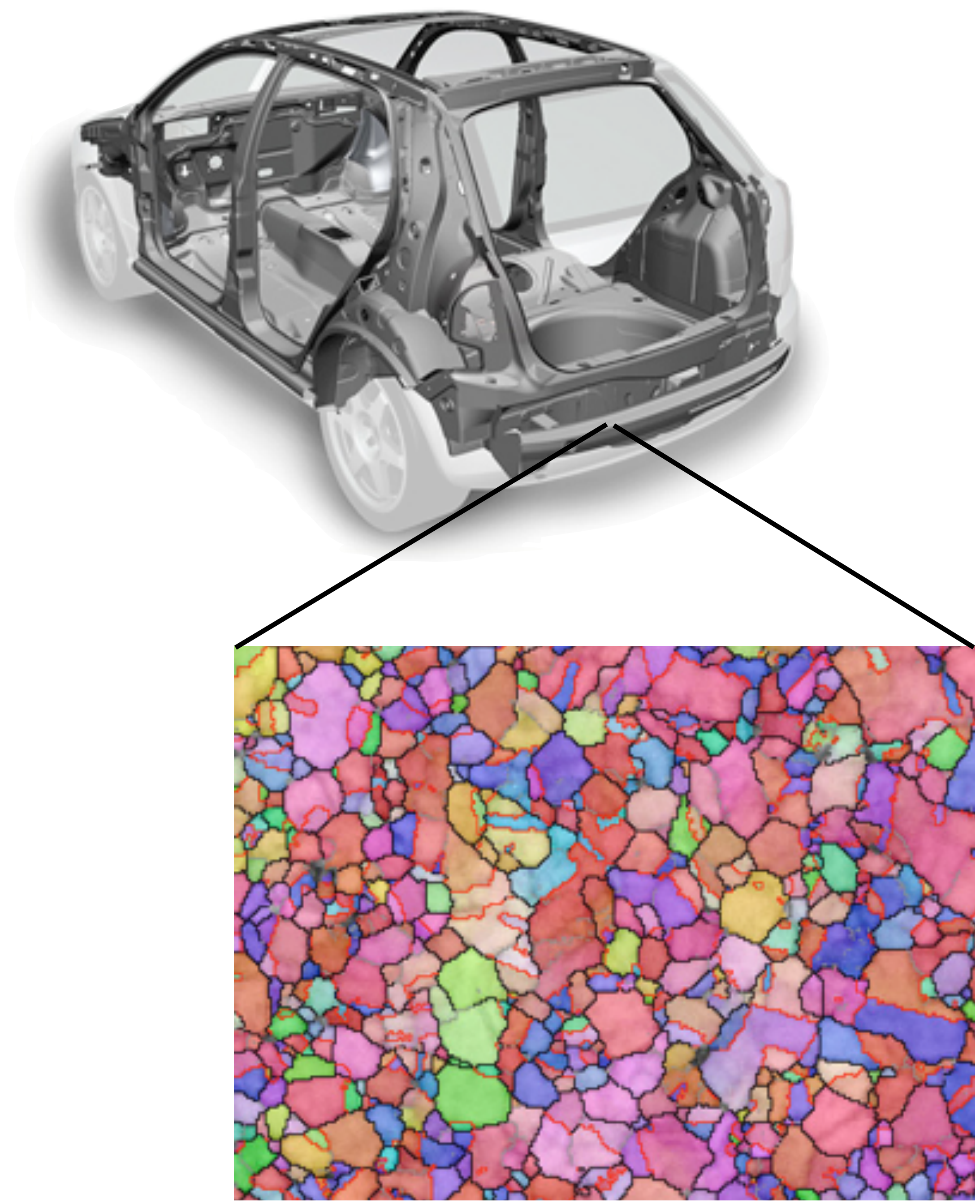

the challenges: microstructure

- ferritic–martensitic steel
- Al-4%Cu
- Mg-5%Zn
- Ni-base alloy

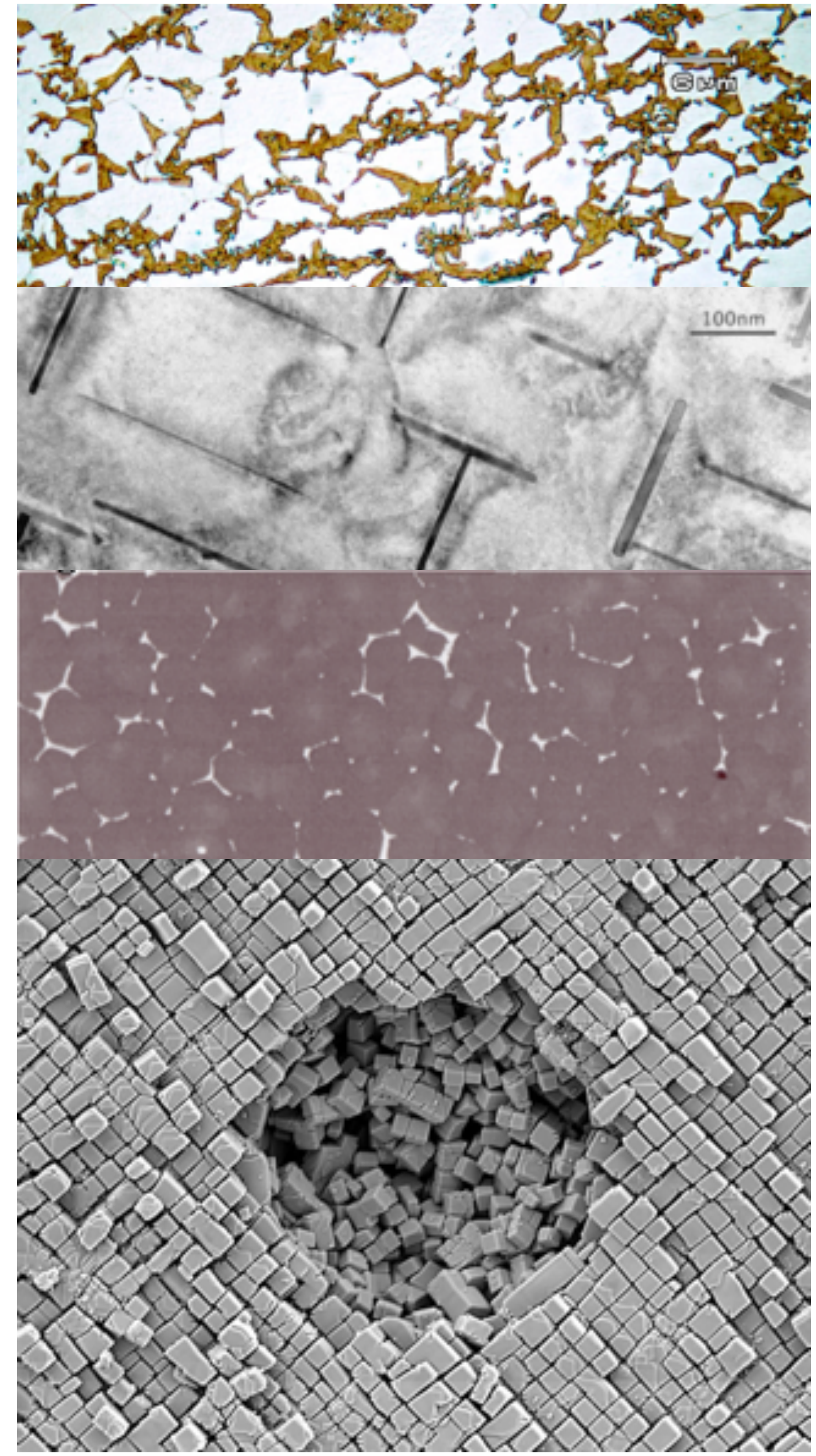

the challenges: deformation mechanisms

- dislocation slip
- dislocation structure evolution
- mechanical twinning / displacive transformation

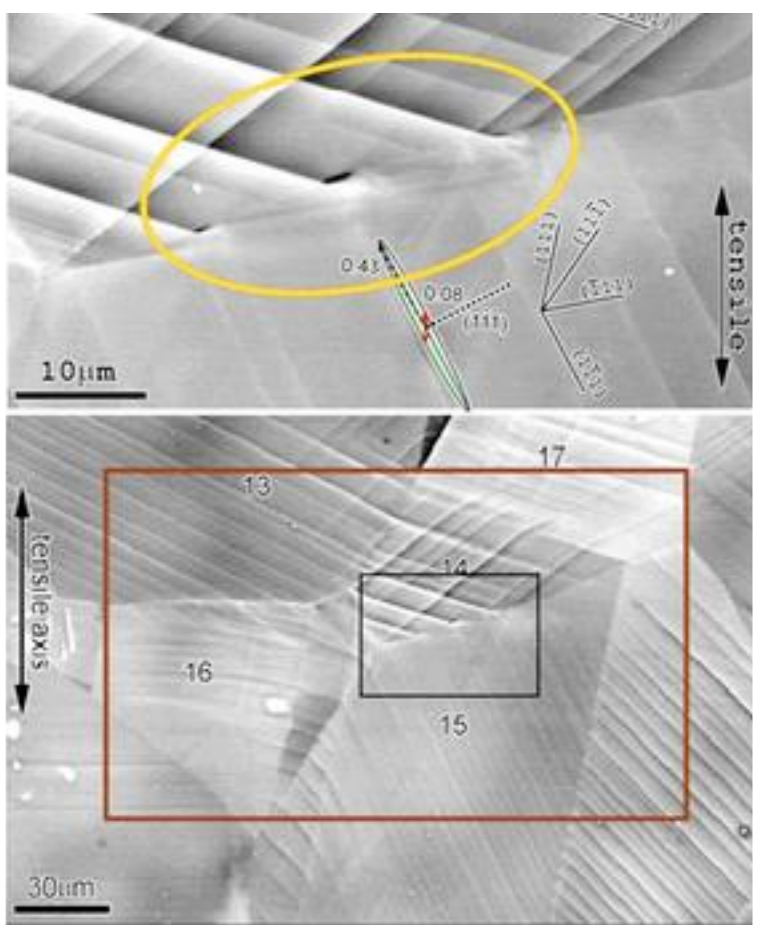

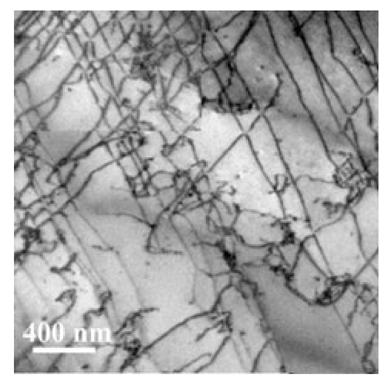

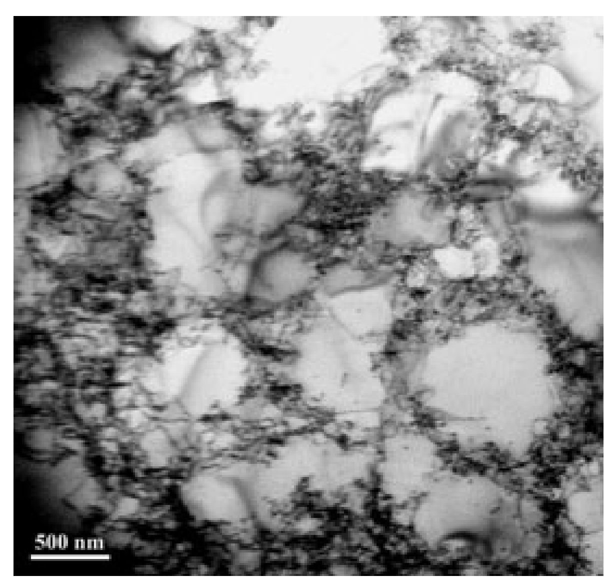

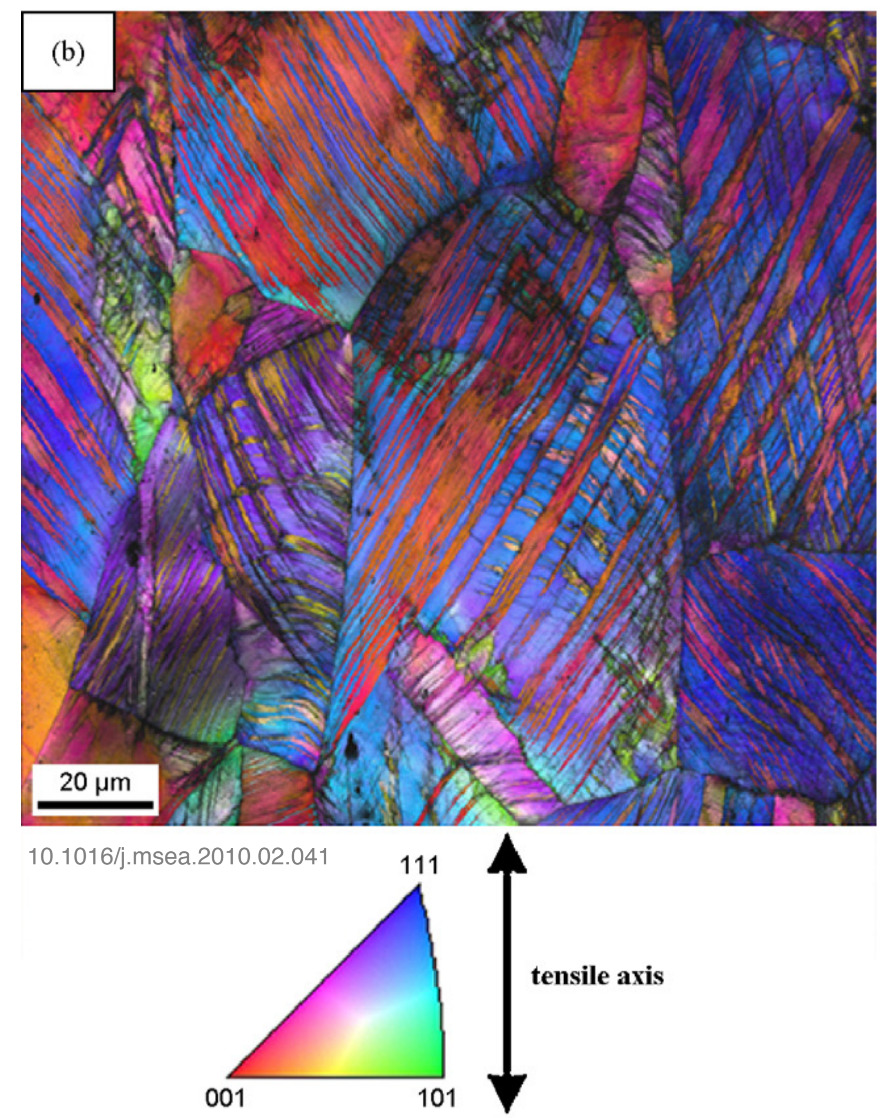

10.1016/j.msea.2010.02.041

MICHIGAN STATE UNIVERSITY

hierarchical modeling

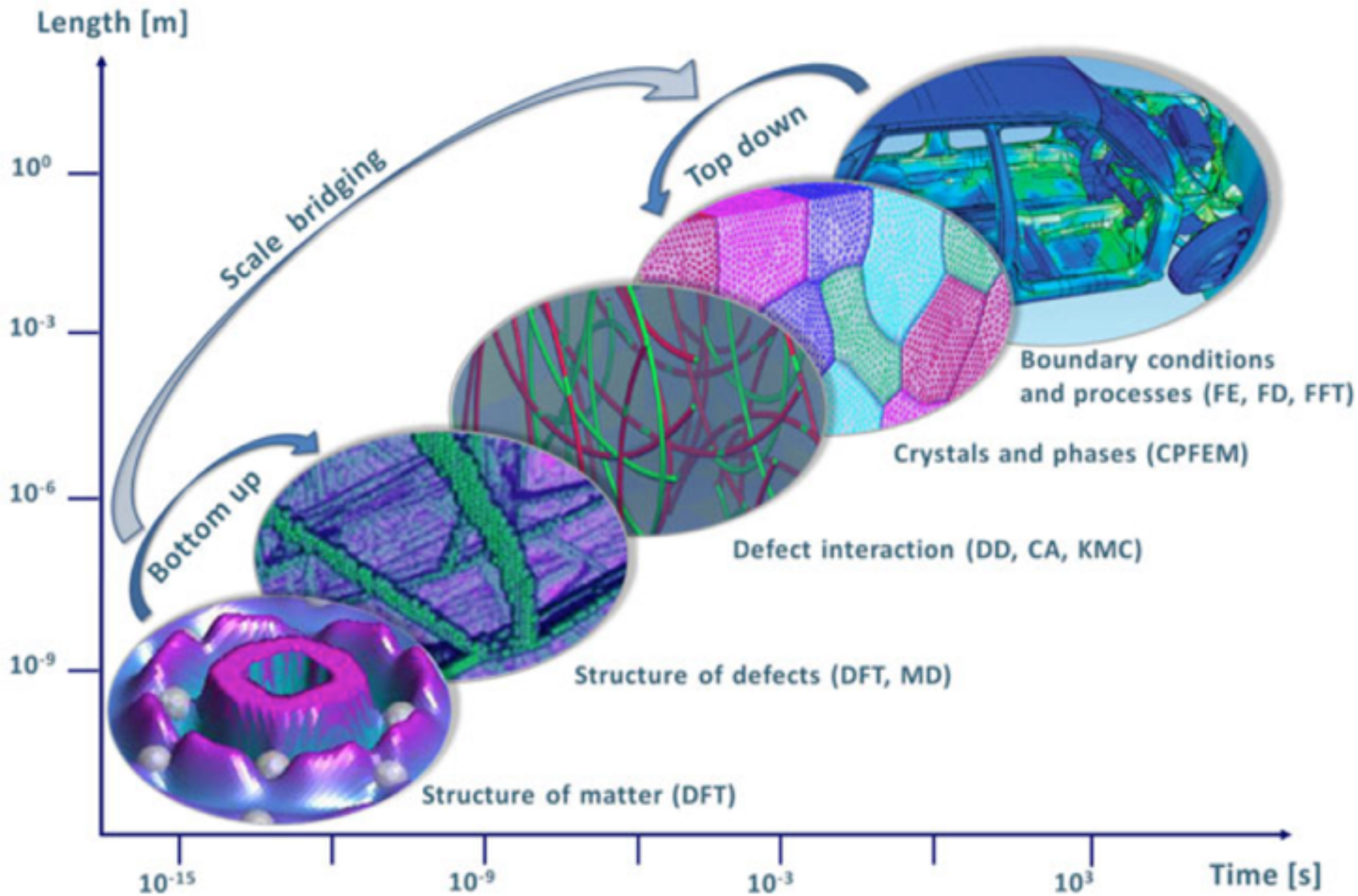

hierarchical modeling

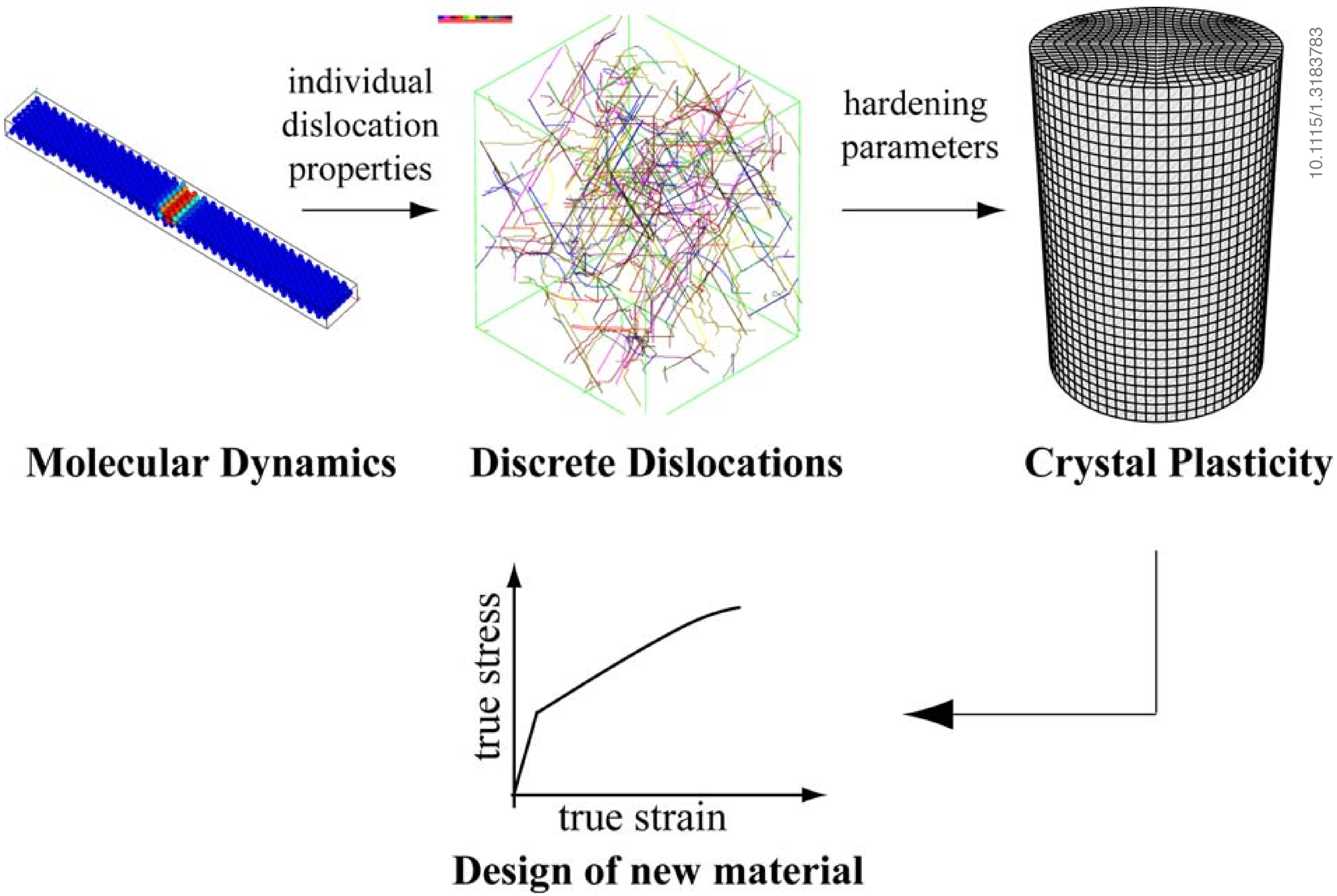

the plan…

	reading assignments	Tuesday	Thursday	Friday Lab	homework
Mar 24	Bulatov, Cai: ***Computer simulation of dislocations*** Groh, Zbib: ***Advances in DDD and multi-scale modeling***	Basic idea of discrete dislocation dynamics (DDD), spatial discretizations	DDD mobility tensor, topological updates, inputs from atomistic scales, stress-field calculations	Long-range elastic field of edge dislocation from 2D MD	
Mar 31	Roters, Eisenlohr, Bieler, Raabe: ***Crystal Plasticity Finite Element Methods in Mater. Sci. and Eng.***	Continuum mechanical background of finite strain crystal plasticity	Flexible and modular setup of crystal plasticity simulation	DDD of Frank–Read source, forest interaction	Identify strongest FCC dislocation interaction
Apr 7		Constitutive descriptions of crystal plasticity	Phenomenological approaches, Dislocation mechanics	Install and familiarize with DAMASK	consult / improve DAMASK documentation
Apr 14		Elasto-plastic decomposition, configurations, numerical solution strategies	Polycrystal plasticity, grain interactions	single crystals and bi-crystals under tension	lattice orientation evolution in bicrystal deformation

the plan…

	reading assignments	Tuesday	Thursday	Friday Lab	homework
Apr 21		Homogenization schemes	Single-point, mean-field, interaction, full-field	Grain aggregate deformation with orientation shuffling	Dependence of strength on composition in two-phase polycrystal
Apr 28		Finite element method	Spectral method	Sheet metal forming	
Bonus		Spectral methods for strong property contrast	Spectral methods for strong property contrast	Performance comparison: spectral and finite element method	
Finals		to be decided…			

what is a dislocation?

(linear) boundary of a plane through which atoms have been dislocated

- dislocated in-plane (conservative)

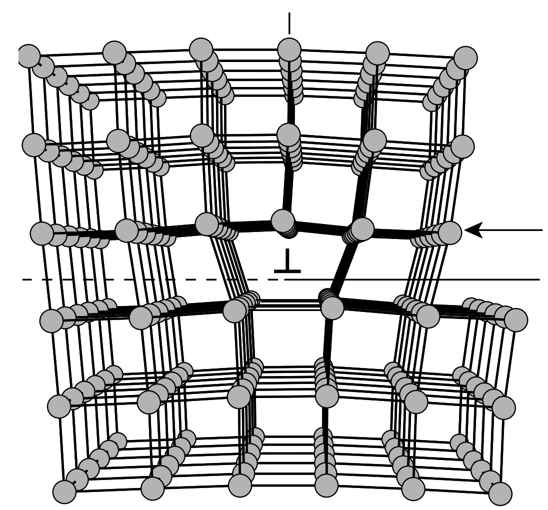

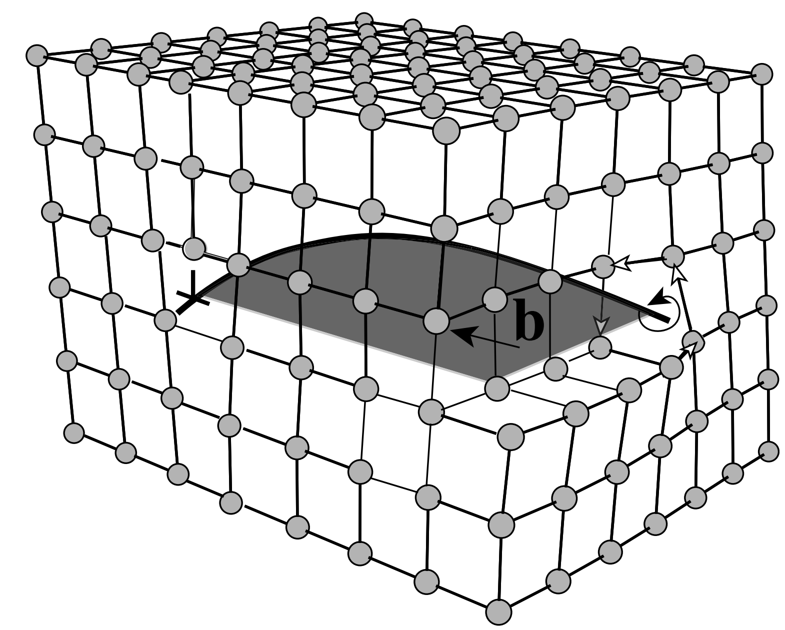

- dislocated out-of-plane (non-conservative)

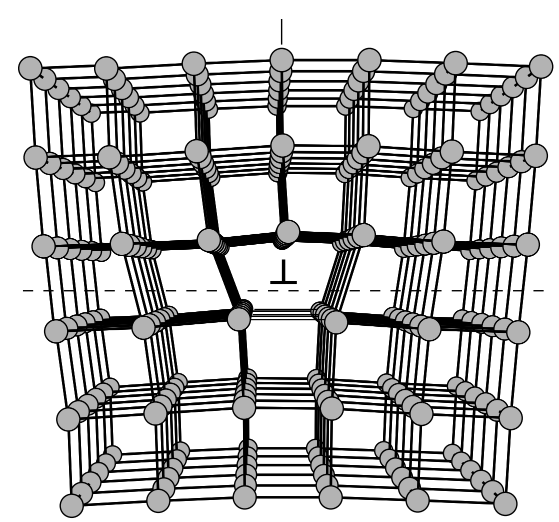

geometrical characterization of dislocations

- Burgers circuit

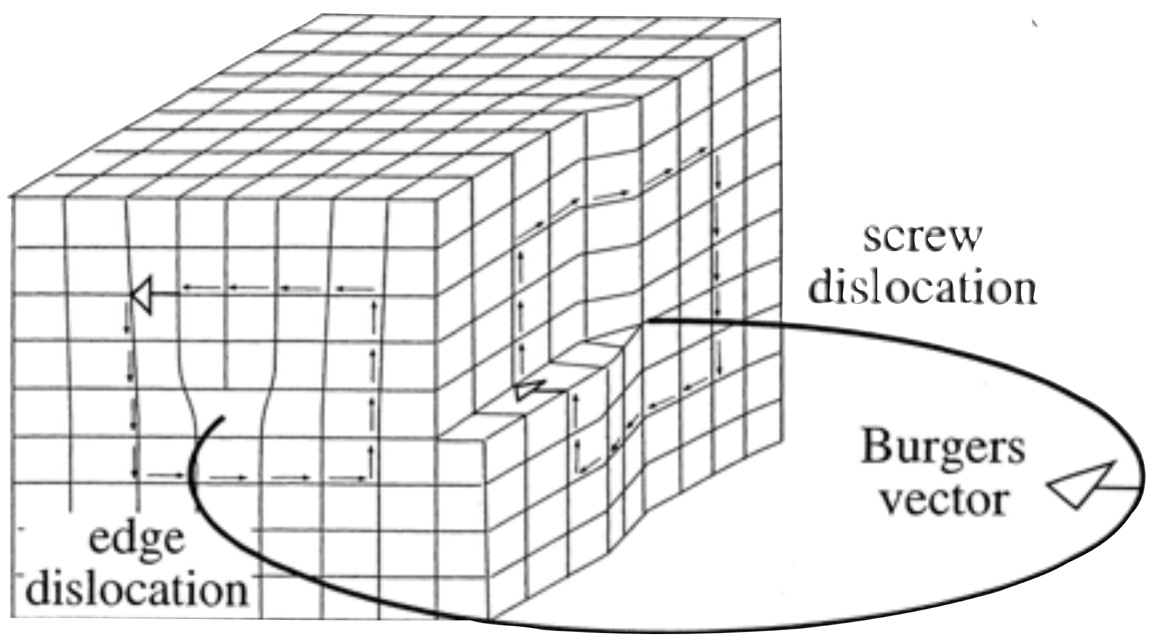

- Burgers vector

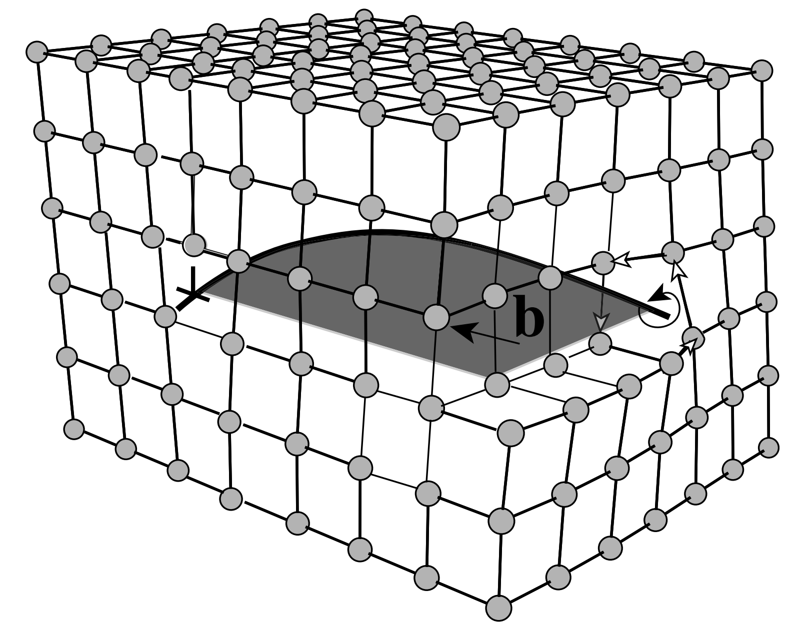

geometrical characterization of dislocations

- Burgers circuit

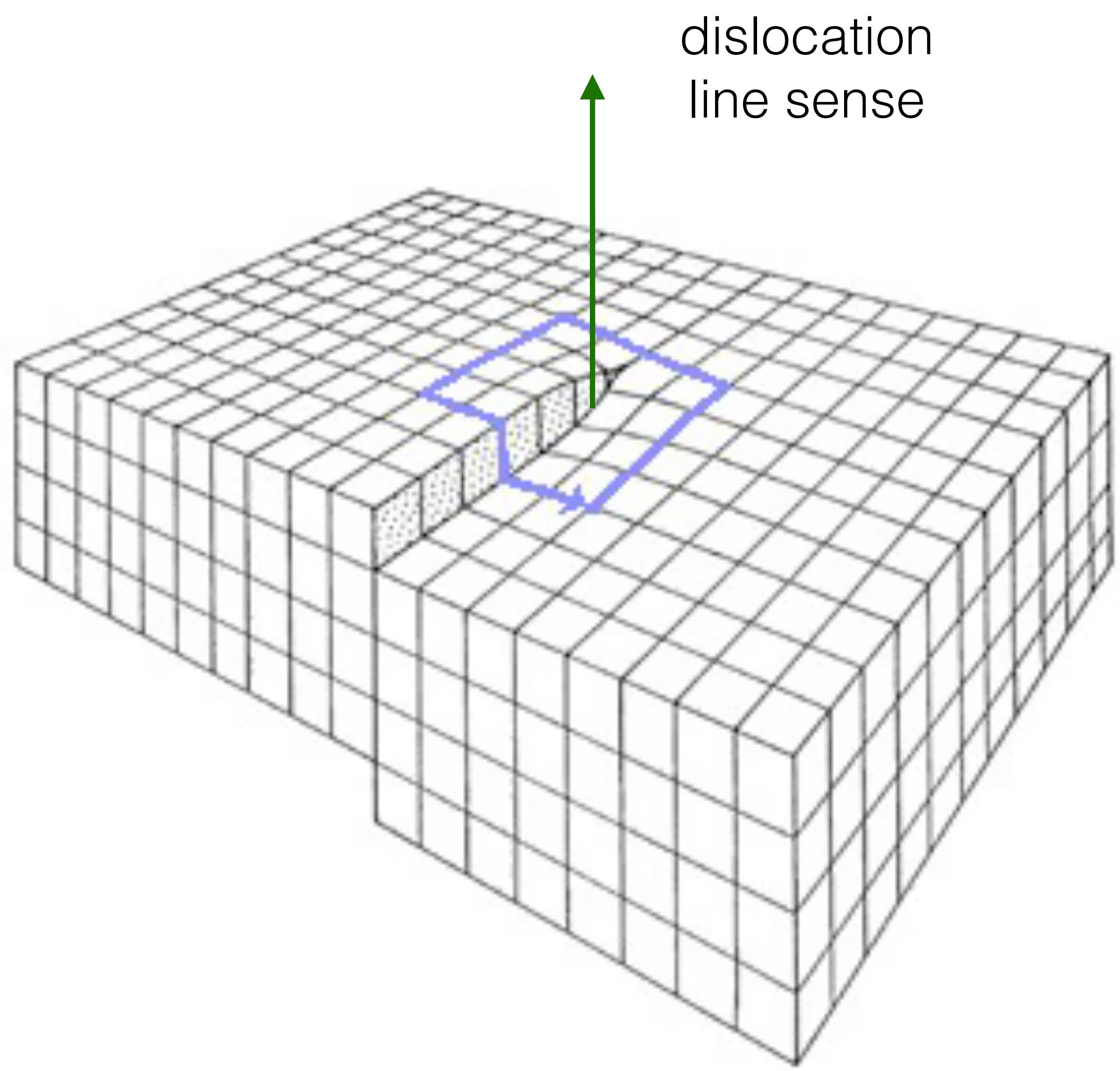

geometrical characterization of dislocations

- Burgers vector conservation

Burgers circuit q and p enclose the same dislocation:

$$\mathbf{b}_1 = \mathbf{b}_2 + \mathbf{b}_3$$

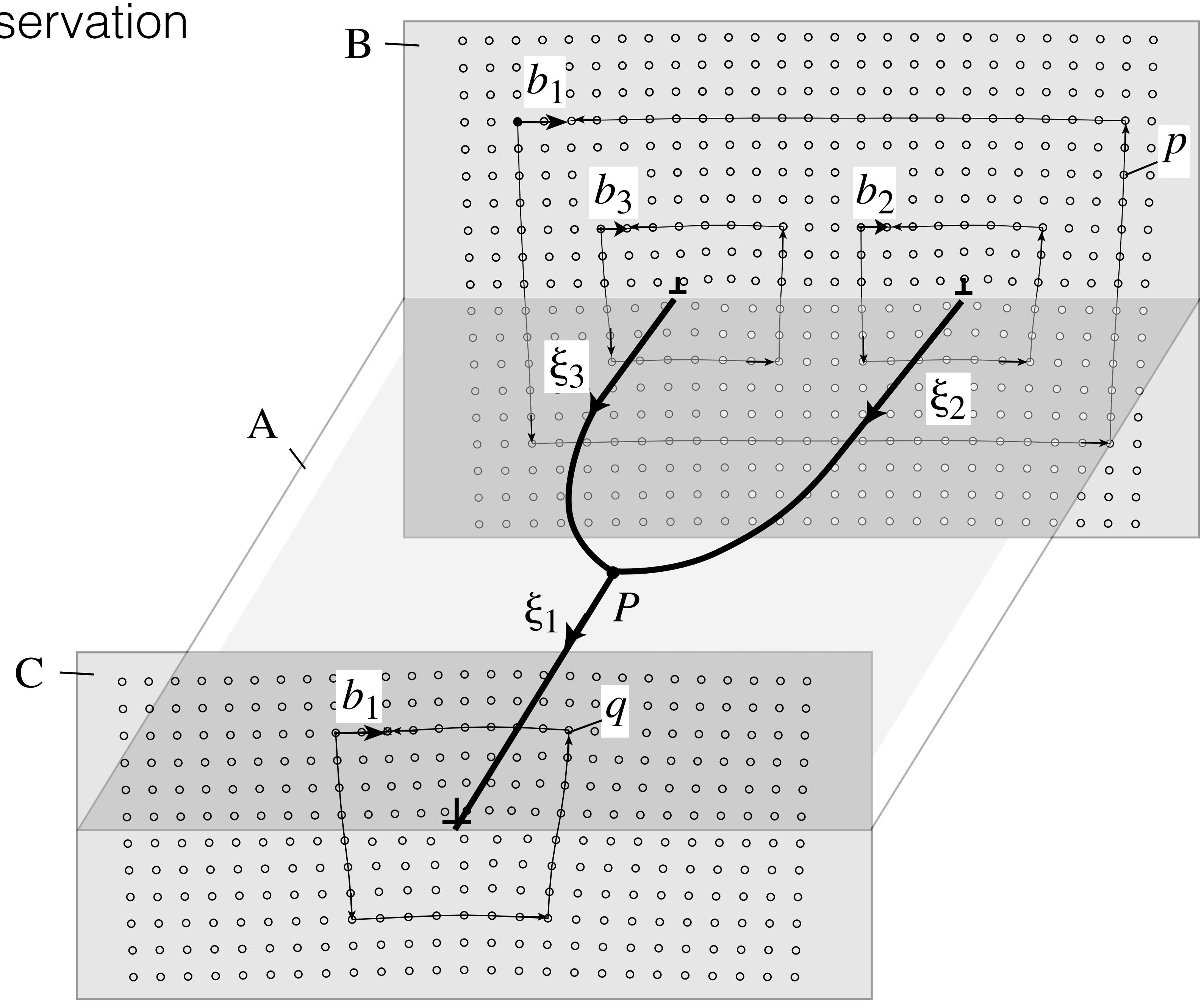

geometrical characterization of dislocations

- Burgers vector conservation

adopt outward-pointing line sense at dislocation node:

$$\sum_i^N \mathbf{b}_i = \mathbf{0}$$

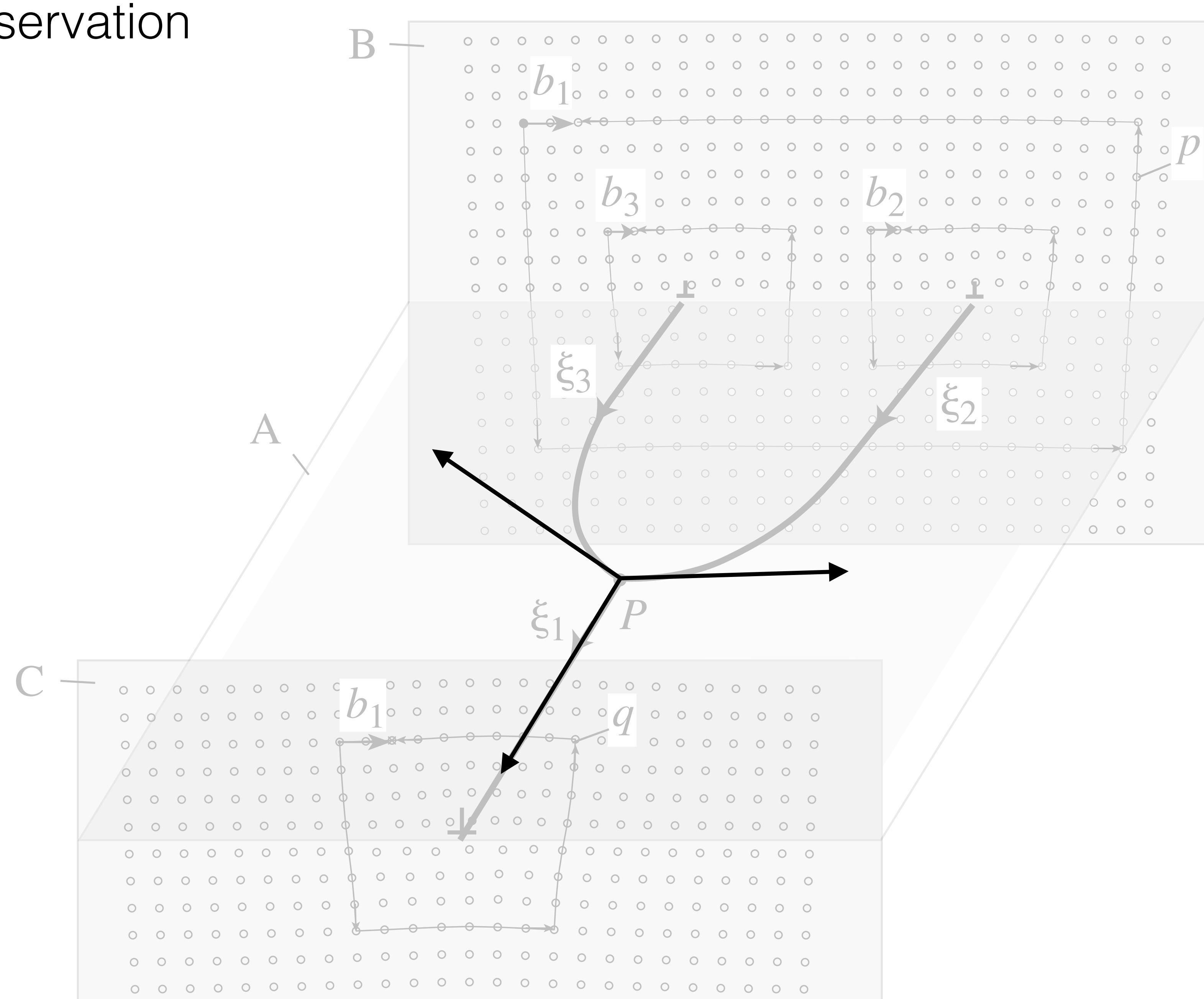

dislocation character

- edge type
- mixed type
- screw type

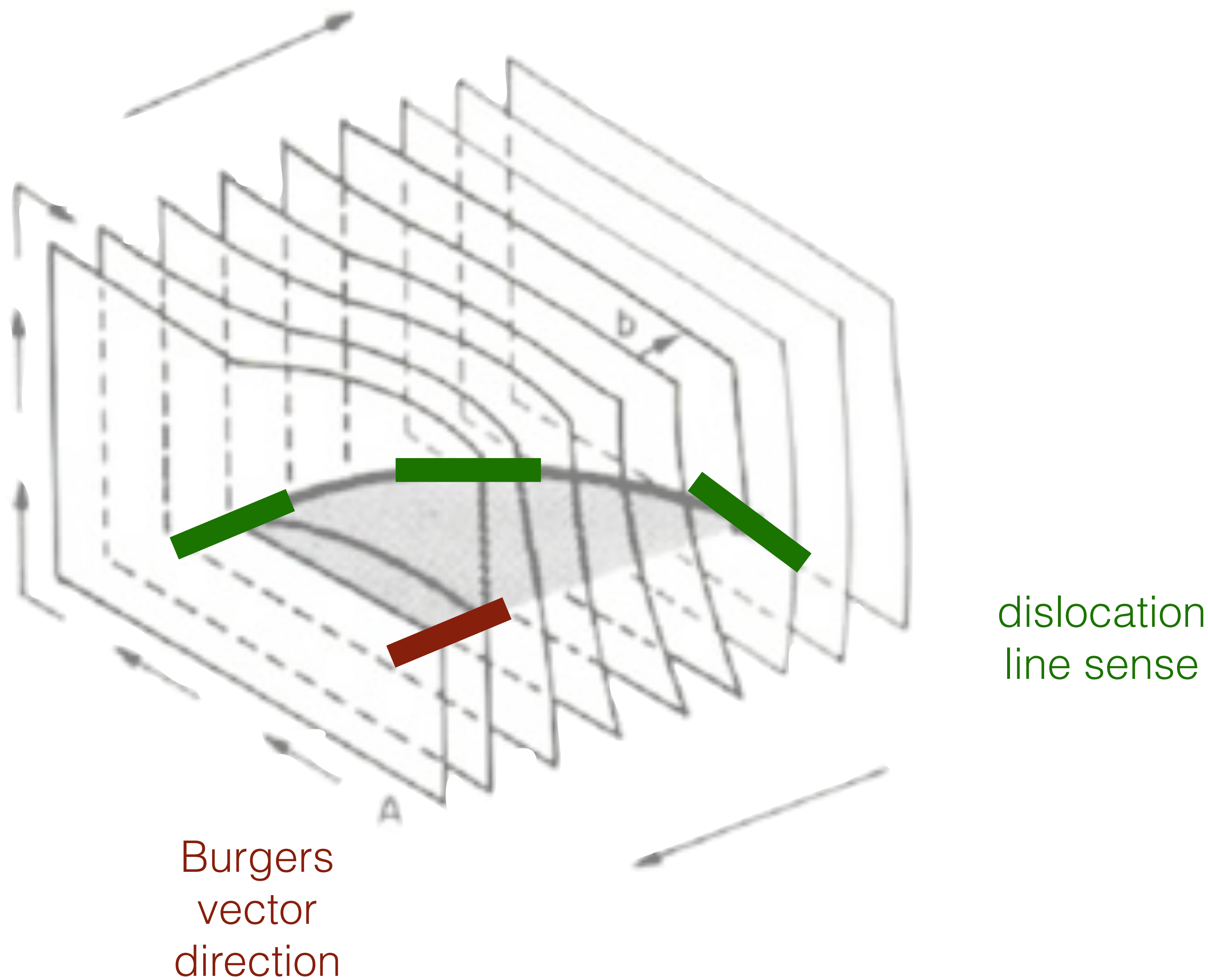

basic idea of DDD

compute and follow the dynamics of dislocation line network

- insight into origin of dislocation patterning
- evolution mechanisms of dislocation structure
- relationship between dislocation structure and strength

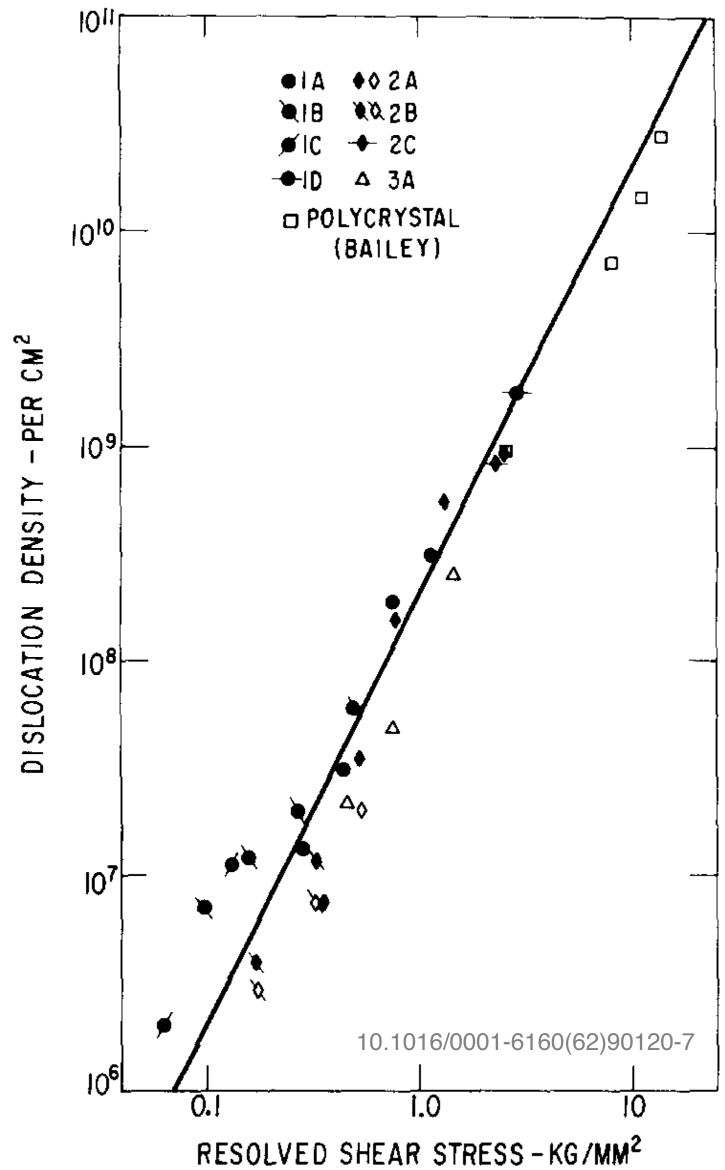

10.1016/0001-6160(62)90120-7

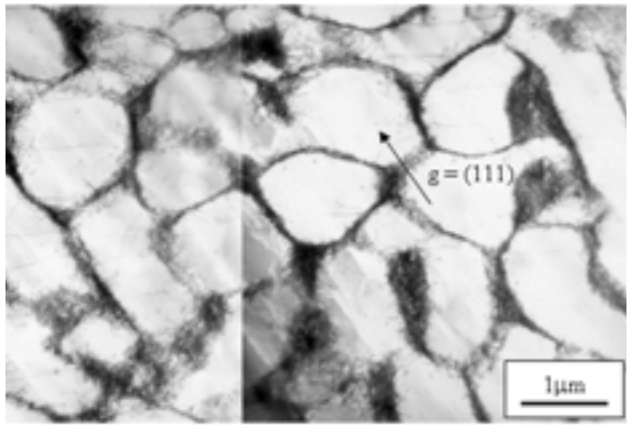

http://engr.unr.edu/~yjiang/jixi_zhang.html

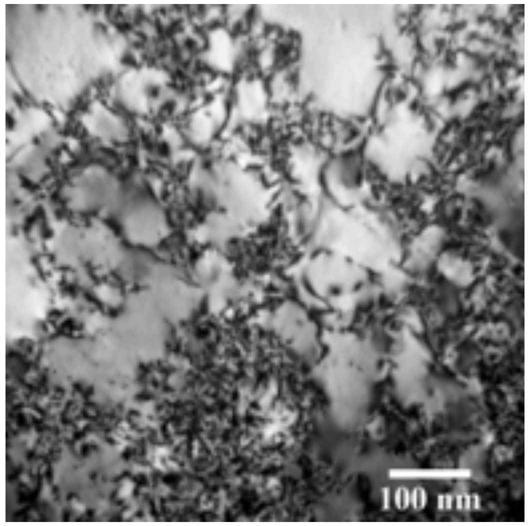

10.1007/s11661-009-9863-8

basic idea of DDD

compute and follow the dynamics
of dislocation line network

- spatial discretization
- driving forces
- mobility
- topological changes

spatial discretization

- eigenstrain field

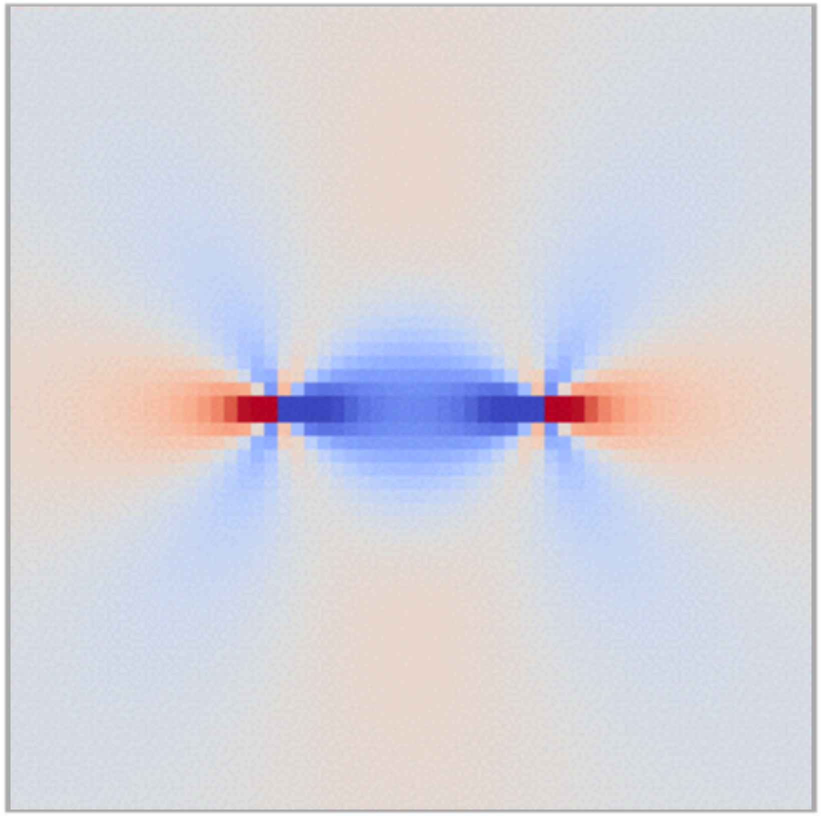

- front tracking

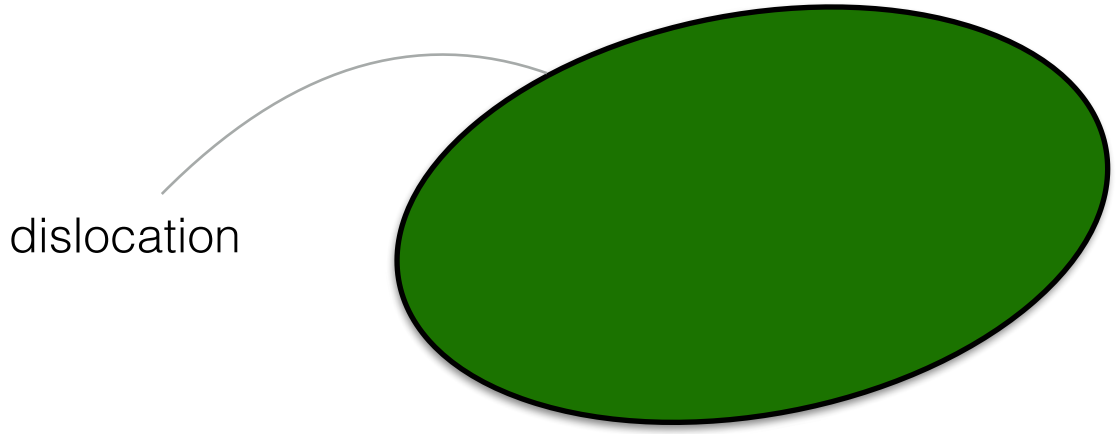

two-dimensional spatial discretization

- assumption of straight dislocation lines —> points on plane
- positive / negative Burgers vector or line sense
- multiple slip

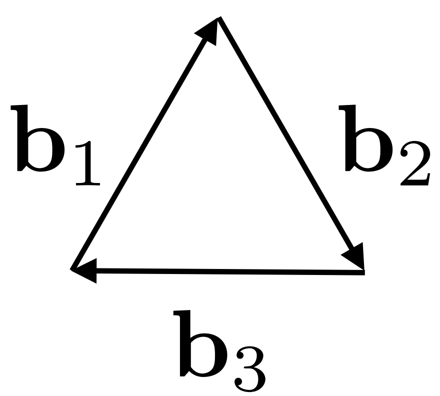

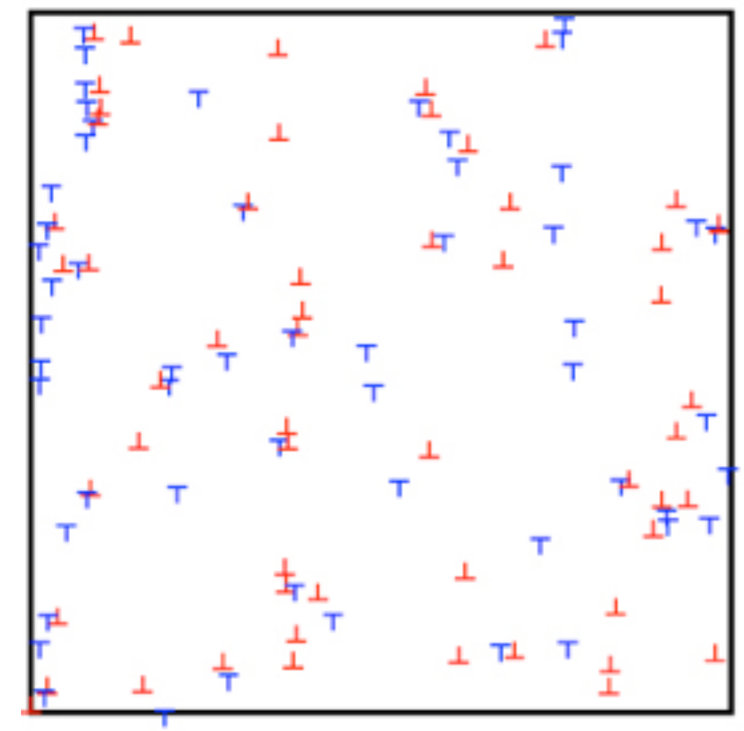

two-dimensional spatial discretization

advantages

- smaller amount of data
- easier to implement
- much faster
- easy visualization

drawbacks

- only one dislocation character
- limited slip system interaction / reaction products
  - cutting
  - jog formation
- no curvature effects
- dislocation sources?

three-dimensional spatial discretization

- nodes connected by segments
  - linear spline [Bulatov, Zbib, Kubin]
  - cubic spline [Ghoniem]
  - arc [Schwarz]

MICHIGAN STATE UNIVERSITY

three-dimensional spatial discretization

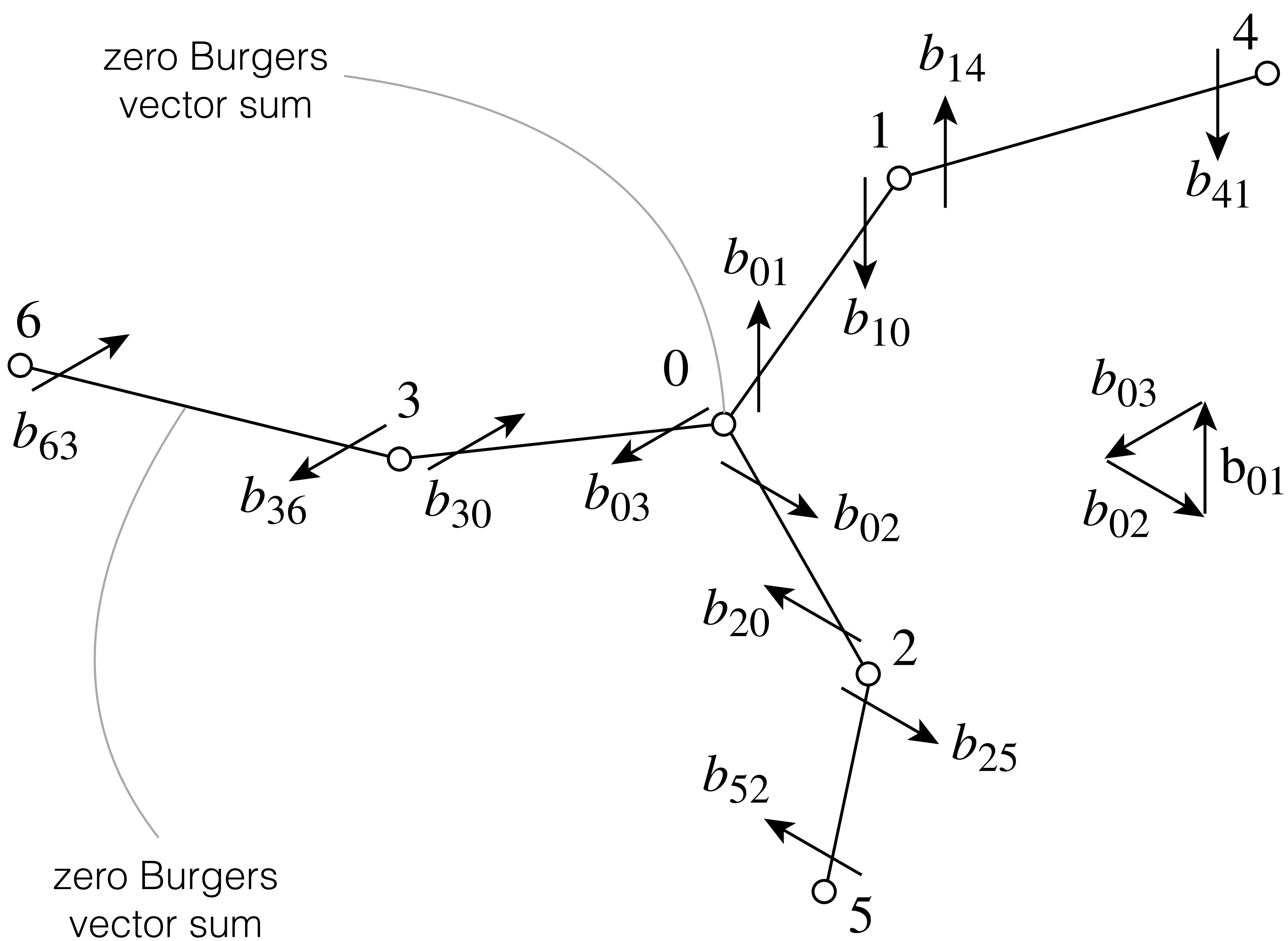

three-dimensional spatial discretization

- degrees of freedom
  - positions of nodes
  - Burgers vectors (connectivity) at node

$$\{\mathbf{r}_i, \mathbf{b}_{ij}\}$$

node

segment

three-dimensional spatial discretization

advantages

- dislocation sources
- curved dislocations
- dislocation cutting / reaction products

drawbacks

- rapid growth of segment count
- computationally demanding
- topological updates

MICHIGAN STATE UNIVERSITY

three-dimensional spatial discretization

exemplary simulation of dislocation penetration through low angle grain boundary
(i.e. dislocation mesh)

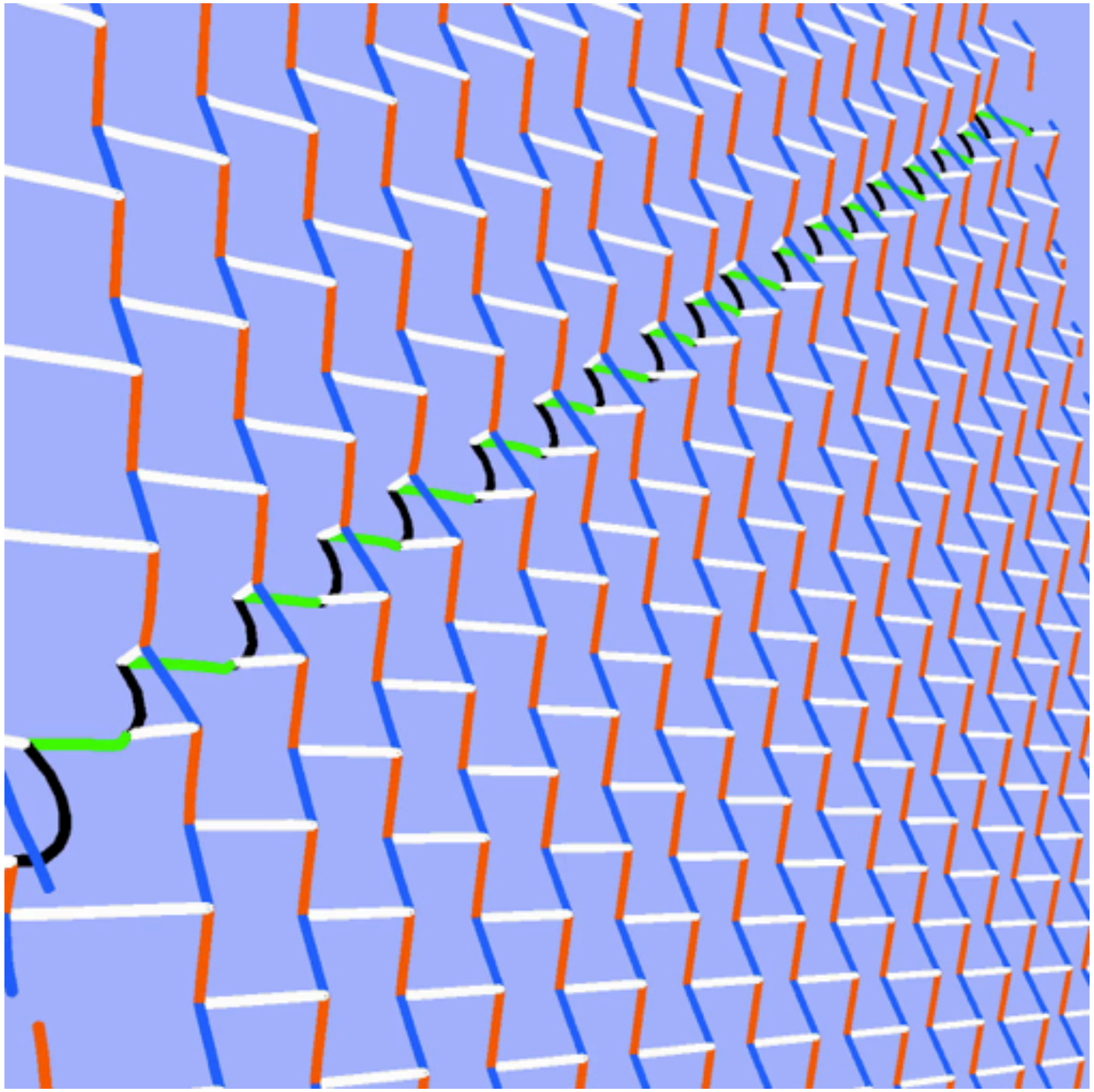

driving force

force acting on a dislocation (segment) by either

- Energy variation with position $$\mathbf{f}_i = -\frac{\partial E_{\mathrm{tot}}(\{\mathbf{r}_i, \mathbf{b}_{ij}\})}{\partial \mathbf{r}_i}$$
- Peach–Koehler force

driving force

energy of dislocation network

$$E_{\rm tot}(C) = E_{\rm el}(C, r_{\rm c}) + E_{\rm core}(C, r_{\rm c})$$

- elastic interaction
- *non-local*

- dislocation core energy
- *local*

driving force

energy of dislocation network

$$E_{\text{tot}}(C) = E_{\text{el}}(C, r_{\text{c}}) + E_{\text{core}}(C, r_{\text{c}})$$

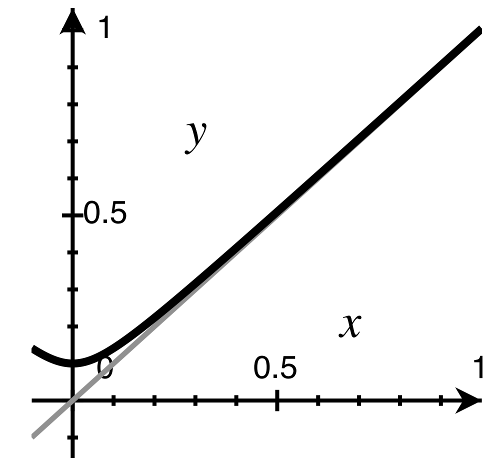

$$E_{\text{el}}(C, r_c) = \frac{\mu}{16\pi} \oint_C \oint_C b_i b'_j \partial_k \partial_k R_a \, \mathrm{dx}_i \mathrm{dx}'_j$$
$$- \frac{\mu}{8\pi} \oint_C \oint_C \epsilon_{ijq} \epsilon_{mnq} b_i b'_j \partial_k \partial_k R_a \, \mathrm{dx}_m \mathrm{dx}'_n$$
$$+ \frac{\mu}{8\pi\,(1-\nu)} \oint_C \oint_C \epsilon_{ikl} \epsilon_{jmn} b_k b'_m \partial_i \partial_j R_a \, \mathrm{dx}_l \mathrm{dx}'_n .$$

see Hirth & Lothe (1982)
"Theory of dislocations"
for details

driving force

energy of dislocation network

$$E_{\mathrm{tot}}(C) = E_{\mathrm{el}}(C, r_{\mathrm{c}}) + E_{\mathrm{core}}(C, r_{\mathrm{c}})$$

- analytic expression for integrals
- (double) sum over straight segments

$$\mathbf{f}_i^{\mathrm{el}} = -\frac{\partial E_{\mathrm{el}}}{\partial \mathbf{r}_i}$$

driving force

energy of dislocation network

$$E_{\mathrm{tot}}(C) = E_{\mathrm{el}}(C, r_{\mathrm{c}}) + E_{\mathrm{core}}(C, r_{\mathrm{c}})$$

$$E_{\mathrm{core}}(C, r_c) = \oint_C E_{\mathrm{c}}(\mathbf{x}; r_c)\, \mathrm{d}L(\mathbf{x})$$

- depends on local line direction
- from atomistic energy minus elastic
- tension to reduce line length
- torque towards low-energy directions

driving force

energy of dislocation network

$$E_{\mathrm{tot}}(C) = E_{\mathrm{el}}(C, r_{\mathrm{c}}) + E_{\mathrm{core}}(C, r_{\mathrm{c}})$$

$$E_{\mathrm{core}}(C, r_c) = \sum_{(i-j)} E_c(\theta_{i-j}, \phi_{i-j}; r_c)\, \|\mathbf{r}_i - \mathbf{r}_j\|$$

- tabulated (interpolated) by direction
- sum over straight segments

$$\mathbf{f}_i^{\mathrm{core}} = -\frac{\partial E_{\mathrm{core}}}{\partial \mathbf{r}_i}$$

driving force

force acting on a dislocation (segment)

- Energy variation with position
- Peach–Koehler force $$\mathbf{f}^{\mathrm{PK}}(\mathbf{x}) = (\boldsymbol{\sigma}(\mathbf{x}) \cdot \mathbf{b}) \times \boldsymbol{\xi}(\mathbf{x})$$

driving force

change in elastic energy from Peach–Koehler force

$$\delta E_{\mathrm{el}} = - \oint_C \mathbf{f}^{\mathrm{PK}}(\mathbf{x}) \cdot \delta \mathbf{r}(\mathbf{x})\, \mathrm{d}L(\mathbf{x})$$

$$\delta E_{\mathrm{el}} = - \oint_C \mathbf{f}^{\mathrm{PK}}(\mathbf{x}) \cdot N_i(\mathbf{x}) \delta \mathbf{r}_i\, \mathrm{d}L(\mathbf{x})$$

energy variation

displacement variation

$$\mathbf{f}_i^{\mathrm{el}} = - \frac{\delta E_{\mathrm{el}}}{\delta \mathbf{r}_i} = \oint_C \mathbf{f}^{\mathrm{PK}}(\mathbf{x})\, N_i(\mathbf{x})\, \mathrm{d}L(\mathbf{x})$$

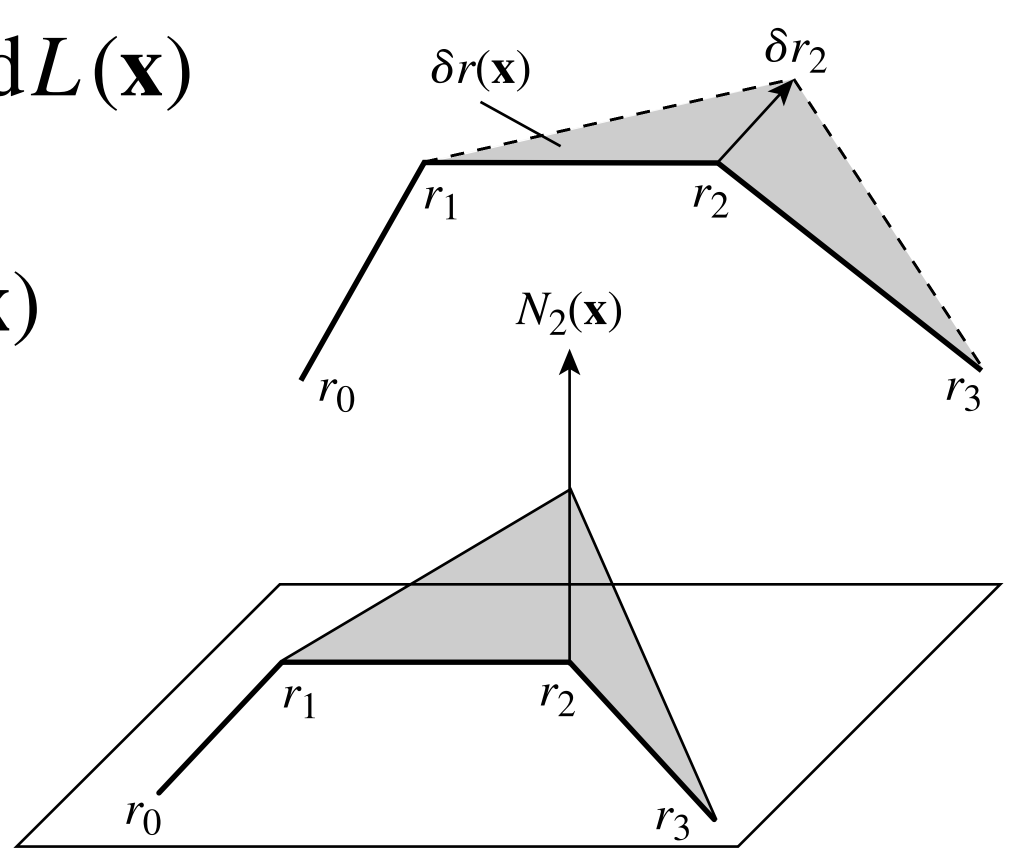

- introduce shape function

$$N_i(\mathbf{x}) = \frac{\|\mathbf{x} - \mathbf{r}_j\|}{\|\mathbf{r}_i - \mathbf{r}_j\|}$$

driving force

stress from the dislocation network

$$\sigma_{\alpha\beta}(\mathbf{x}) = \frac{\mu}{8\pi}\oint_C \partial_i\partial_p\partial_p R_a \left(b_m\epsilon_{im\alpha}\mathrm{dx}'_\beta + b_m\epsilon_{im\beta}\mathrm{dx}'_\alpha\right) + \frac{\mu}{4\pi(1-\nu)}\oint_C b_m\epsilon_{imk}\left(\partial_i\partial_\alpha\partial_\beta R_a - \delta_{\alpha\beta}\partial_i\partial_p\partial_p R_a\right)\mathrm{dx}'_k$$

see Hirth & Lothe (1982) "Theory of dislocations" for details

$$\sigma_{\alpha\beta}(\mathbf{x}) = \sum_{(k-l)} \sigma_{\alpha\beta}(\mathbf{x}; k-l)$$

$$\mathbf{f}_i^{\mathrm{el}} = \sum_j \sum_{(k-l)} \mathbf{f}_i^{\mathrm{el}}(i-j; k-l)$$

nodal mobility

contrary to atom motion in molecular dynamics (MD), mobility of (discretization) nodes in dislocation line dynamics is

- typically over-damped
- strongly anisotropic
  - depends on direction of motion ϕ
  - depends on line direction θ

nodal mobility

mobility function for over-damped motion

$$\mathbf{v}_i = \mathbf{M}(\{\mathbf{f}_j\})$$

nodal velocity

nodal forces

nodal mobility

assumption of dislocation drag force

$$\mathbf{f}^{\mathrm{drag}}(\mathbf{x}) = -\mathcal{B}(\boldsymbol{\xi}(\mathbf{x}))\mathbf{v}(\mathbf{x})$$

per line length

drag tensor

local force equilibrium (no acceleration)

$$\sum_j \mathbf{v}_j N_j(\mathbf{x})$$

$$\mathbf{f}^{\mathrm{drag}}(\mathbf{x}) + \mathbf{f}^{\mathrm{drive}}(\mathbf{x}) = \mathbf{0}$$

$$\mathbf{f}^{\mathrm{drive}}(\mathbf{x}) = \mathcal{B}(\boldsymbol{\xi}(\mathbf{x}))\mathbf{v}(\mathbf{x})$$

nodal mobility

weak(er) form of force balance

$$\oint_C N_i(\mathbf{x})[\mathbf{f}^{\mathrm{drag}}(\mathbf{x}) + \mathbf{f}^{\mathrm{drive}}(\mathbf{x})]\, dL(\mathbf{x}) = \mathbf{0}$$

exemplary mobility tensor: face-centered cubic

(possible) anisotropy of glide mobility for edge and screw

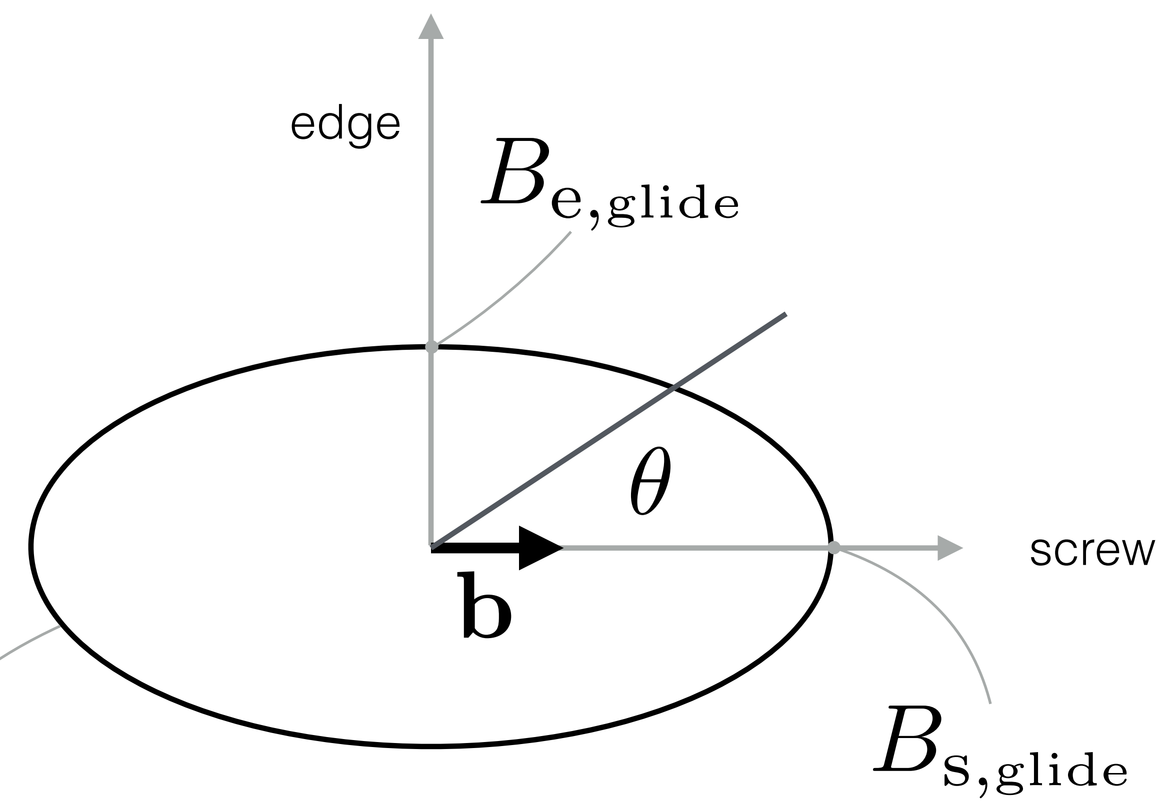

$$B_{\mathrm{s,glide}} \cos^2\theta + B_{\mathrm{e,glide}} \sin^2\theta$$

exemplary drag tensor: face-centered cubic

(strong) anisotropy between glide and climb motion

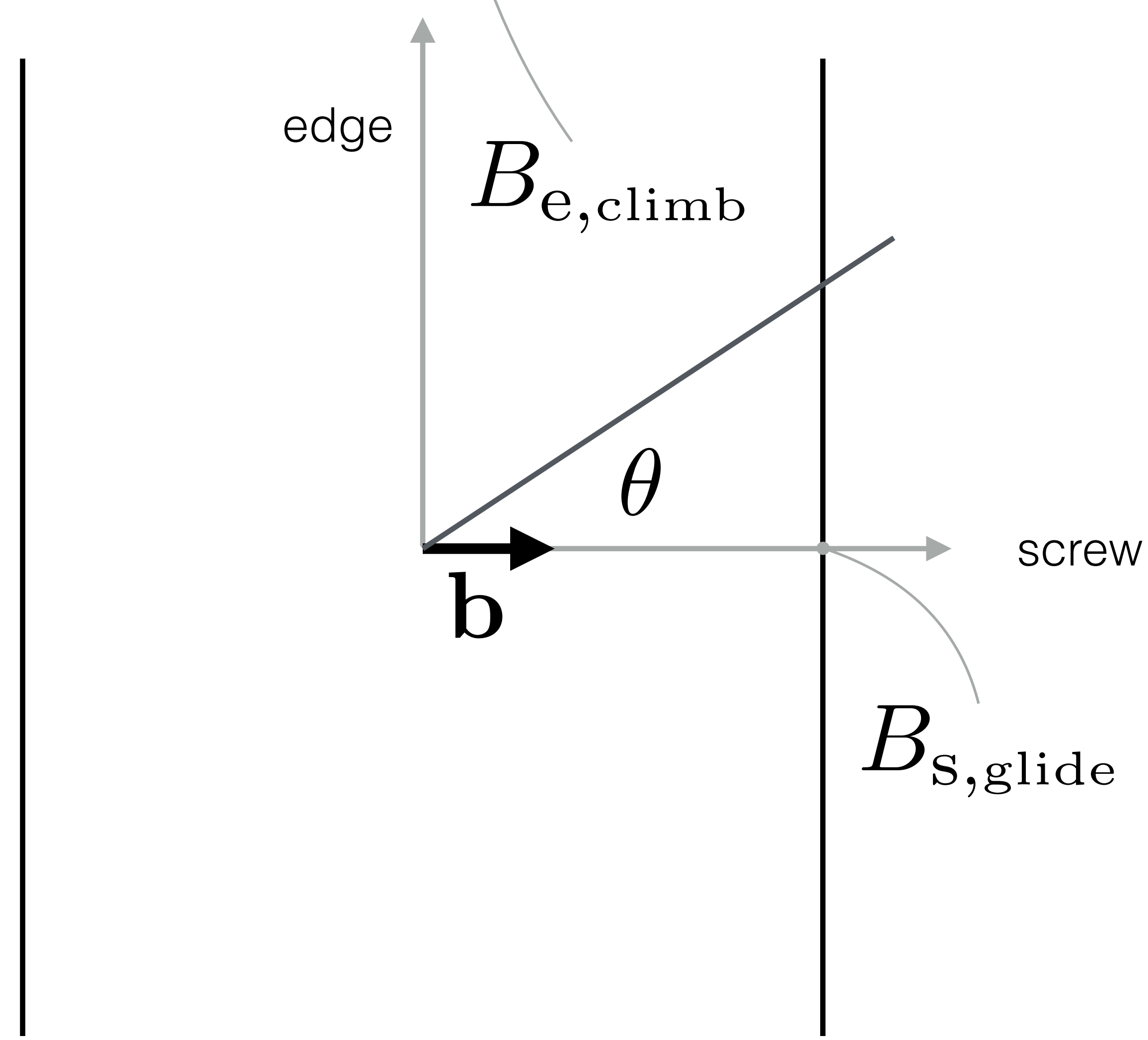

exemplary drag tensor: face-centered cubic

partial dislocation split restricts screw to glide plane

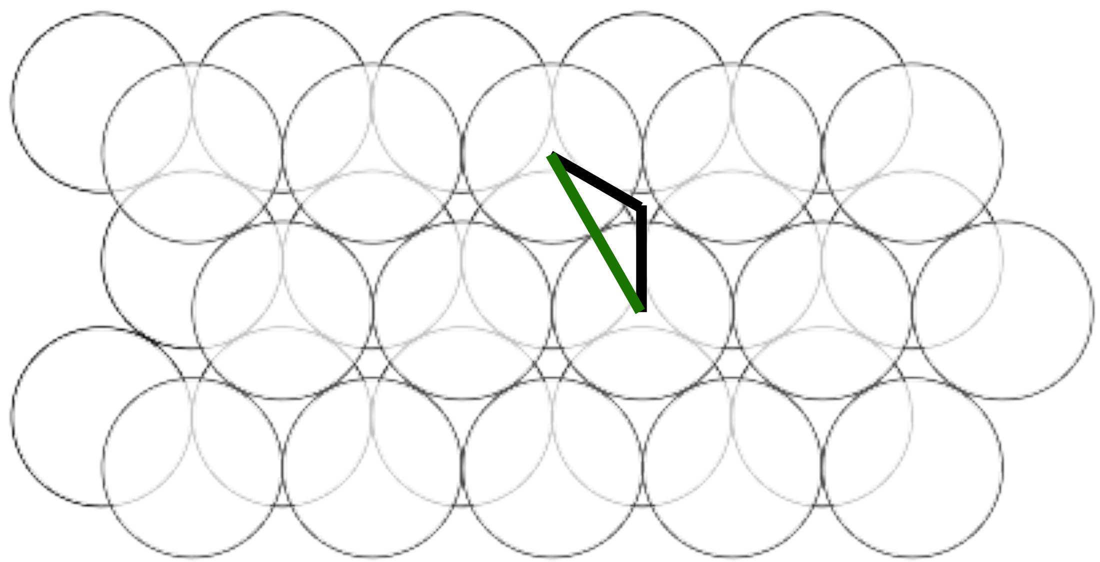

$\{1\,1\,1\}$

exemplary drag tensor: face-centered cubic

efficient correction of velocities

- no out-of-plane component

$$\mathbf{v}_i \cdot \mathbf{n}_{ij} = 0$$

- remove normal components

$$\mathbf{v}_i^{\mathrm{glide}} = \left(\mathbf{I} - \sum_j \mathbf{n}_{ij} \otimes \mathbf{n}_{ij} \right) \mathbf{v}_i$$

exemplary drag tensor: face-centered cubic

restrict velocity to be normal to segment

$$\mathcal{B}(\boldsymbol{\xi}) \propto \mathbf{I} - \boldsymbol{\xi} \otimes \boldsymbol{\xi}$$

exemplary drag tensor: face-centered cubic

$$\mathcal{B}(\boldsymbol{\xi}) = (B_{\mathrm{s,glide}} \cos^2\theta + B_{\mathrm{e,glide}} \sin^2\theta)(\mathbf{I} - \boldsymbol{\xi} \otimes \boldsymbol{\xi})$$

$$\mathcal{B}(\boldsymbol{\xi}) = B(\mathbf{I} - \boldsymbol{\xi} \otimes \boldsymbol{\xi})$$

MICHIGAN STATE UNIVERSITY

exemplary drag tensor: body-centered cubic

- pure screw $$\mathcal{B}(\boldsymbol{\xi}) = B_{\mathrm{s}}(\mathbf{I} - \boldsymbol{\xi} \otimes \boldsymbol{\xi})$$
- mixed $$\mathcal{B}(\boldsymbol{\xi}) = B_{\mathrm{glide}}\, \mathbf{m} \otimes \mathbf{m} + B_{\mathrm{climb}}\, \mathbf{n} \otimes \mathbf{n}$$

$$B_{\mathrm{glide}}^{-2} = B_{\mathrm{e,glide}}^{-2}\, |\mathbf{b} \times \boldsymbol{\xi}|^2 + B_{\mathrm{s}}^{-2}(\mathbf{b} \cdot \boldsymbol{\xi})^2$$

$$B_{\mathrm{climb}}^{2} = B_{\mathrm{e,climb}}^{2}\, |\mathbf{b} \times \boldsymbol{\xi}|^2 + B_{\mathrm{s}}^{2}(\mathbf{b} \cdot \boldsymbol{\xi})^2$$

topological changes

possible reasons

- rediscretization (numerical)

- junction formation (physical)

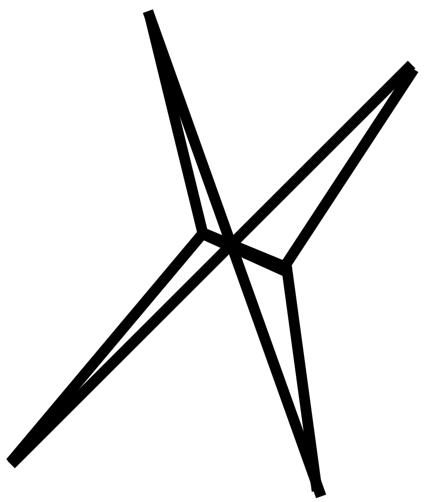

topological changes: example

junction formation in a low-angle grain boundary

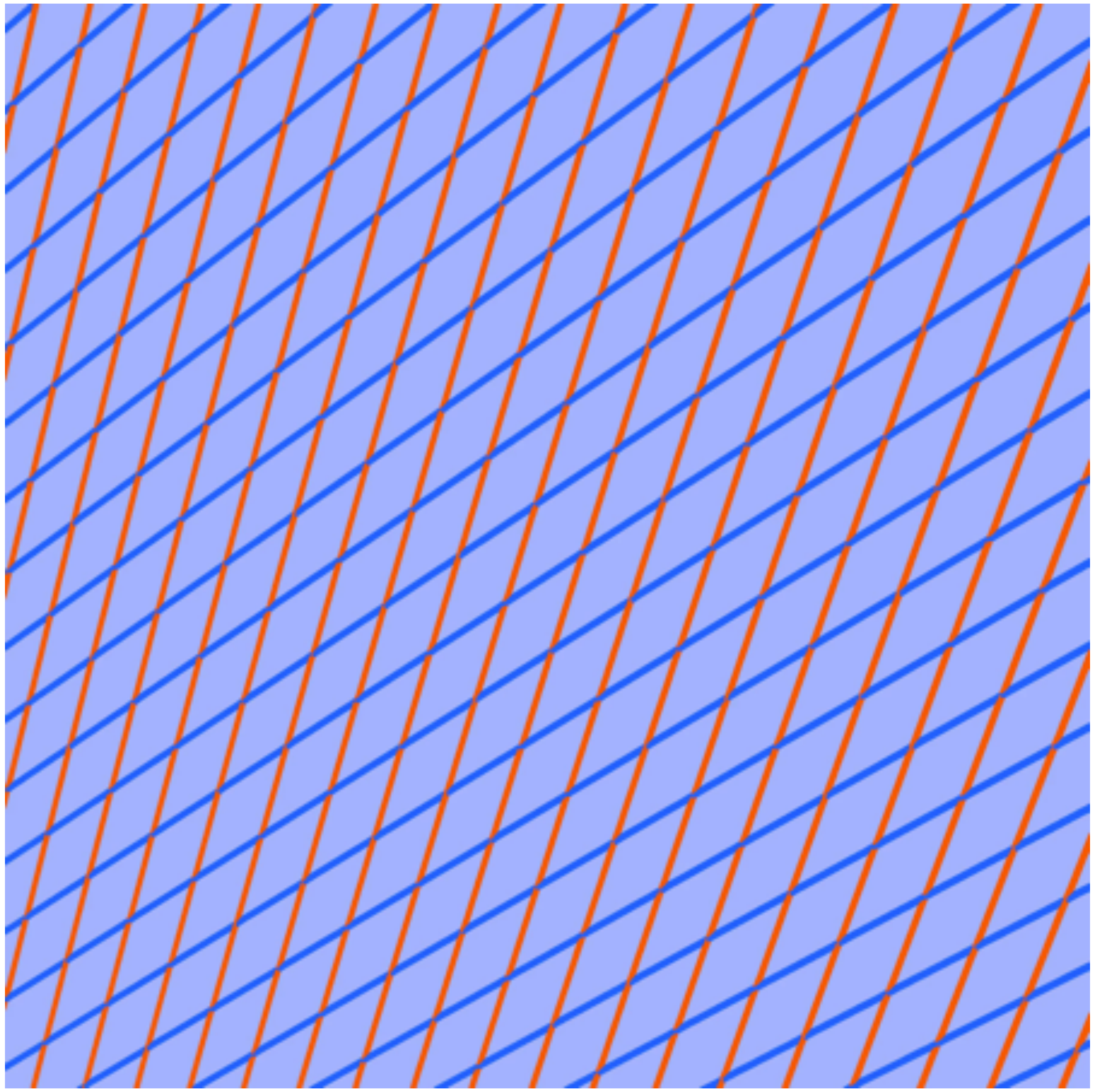

topological changes: rediscretization

elementary topological operators

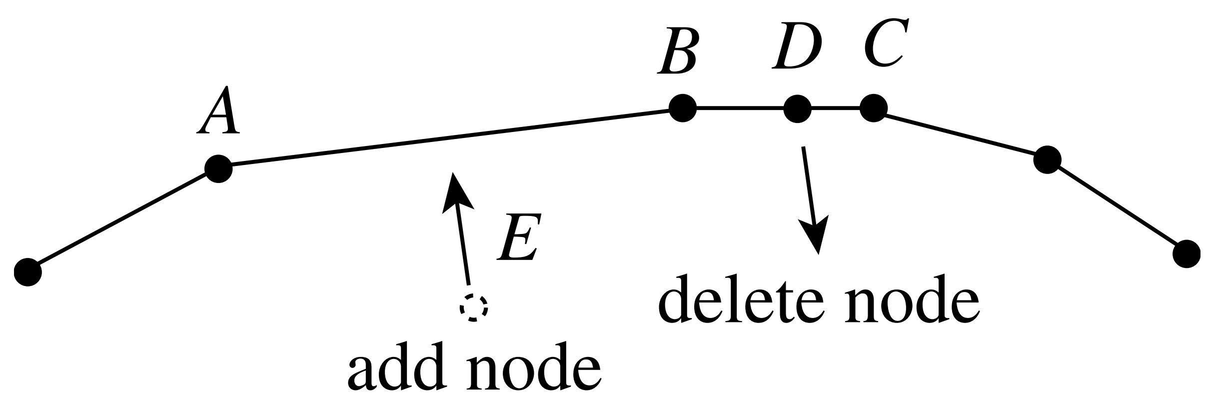

- add

$$\mathbf{b}_{\mathrm{AE}} := \mathbf{b}_{\mathrm{AB}} \text{ and } \mathbf{b}_{\mathrm{EA}} := \mathbf{b}_{\mathrm{BA}}$$

$$\mathbf{b}_{\mathrm{BE}} := \mathbf{b}_{\mathrm{BA}} \text{ and } \mathbf{b}_{\mathrm{EB}} := \mathbf{b}_{\mathrm{AB}}$$

- delete

$$\mathbf{b}_{\mathrm{BC}} := \mathbf{b}_{\mathrm{BD}} \text{ and } \mathbf{b}_{\mathrm{CB}} := \mathbf{b}_{\mathrm{CD}}$$

topological changes: rediscretization

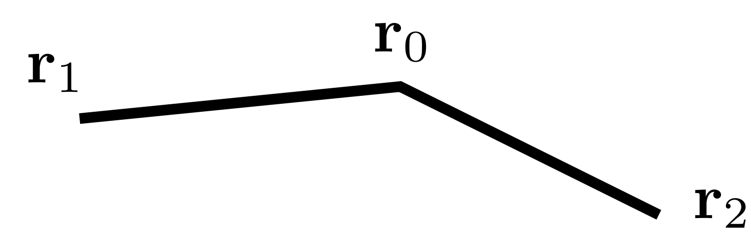

algorithm

1. If node N_0 has more than two arms, go to 7. Otherwise, find nodes N_1 and N_2 connected to node N_0. Obtain positions $\mathbf{r}_0$, $\mathbf{r}_1$, $\mathbf{r}_2$ and velocities $\mathbf{v}_0$, $\mathbf{v}_1$, $\mathbf{v}_2$ of nodes N_0, N_1, N_2.

topological changes: junctions

elementary topological operators

- split

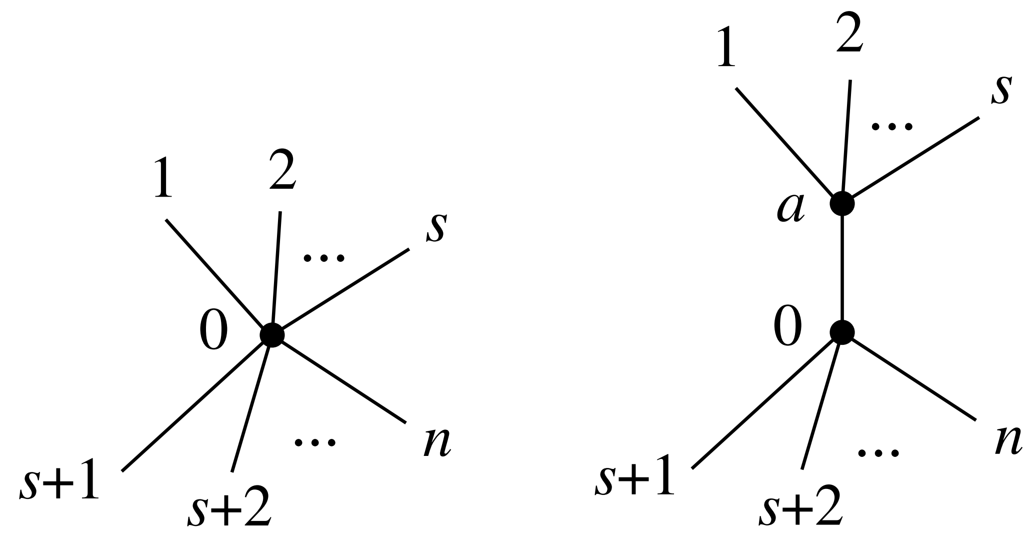

(a) (b)

$$\mathbf{b}_{ai} := \mathbf{b}_{0i} \text{ and } \mathbf{b}_{ia} := \mathbf{b}_{i0} \quad i = 1, \ldots, s$$

$$-\mathbf{b}_{a0} = \mathbf{b}_{0a} = \Delta\mathbf{b} = \sum_{i=1}^{s} \mathbf{b}_{ai} \quad \text{if} \quad \Delta\mathbf{b} \neq \mathbf{0}$$

topological changes: junctions

elementary topological operators

- merge

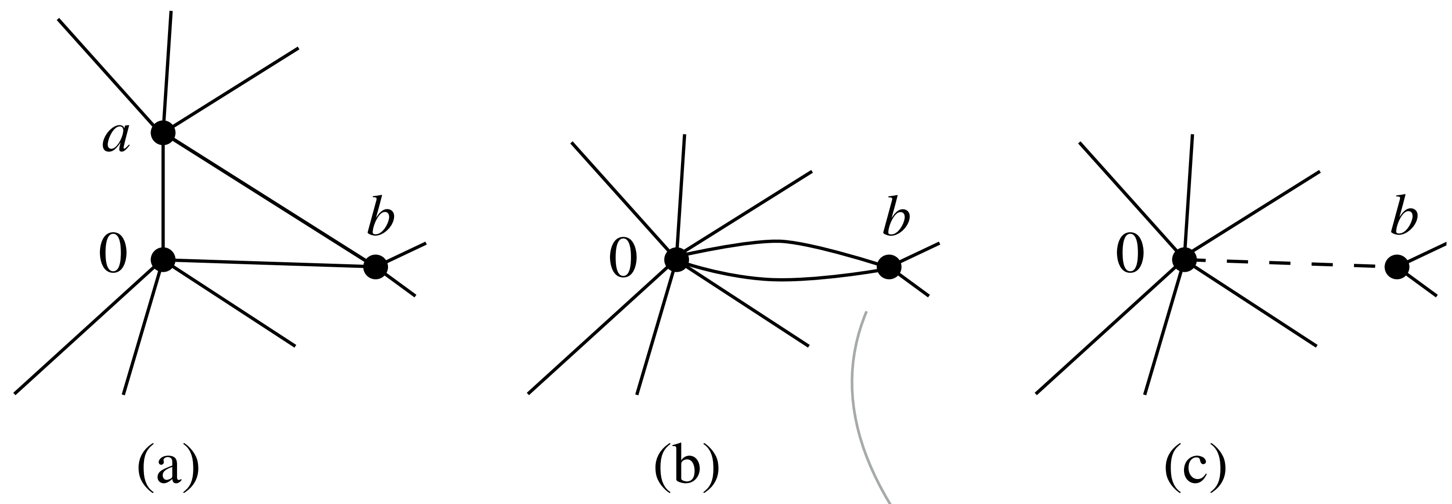

check for double connectivity

$$\mathbf{b}_{0i} := \mathbf{b}_{ai} \text{ and } \mathbf{b}_{i0} := \mathbf{b}_{ia} \quad i = 1, \ldots, s$$

topological changes: junctions

when to merge

- segment collision

  $d < r_\mathrm{a}$

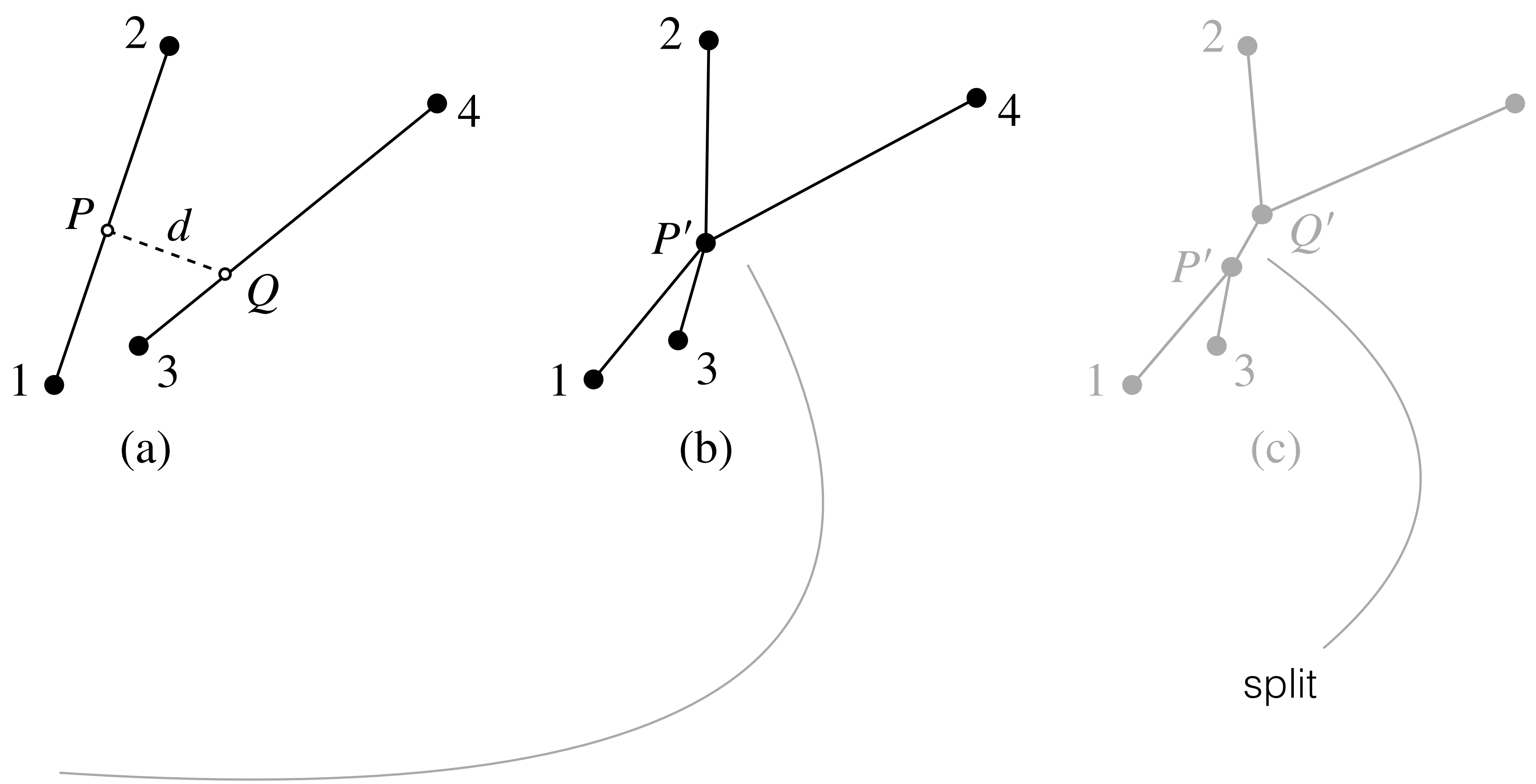

- minimum nodal separation

  $d < r_\mathrm{a}$

topological changes: junctions

when to split

- multi-arm node with more than 3 segments

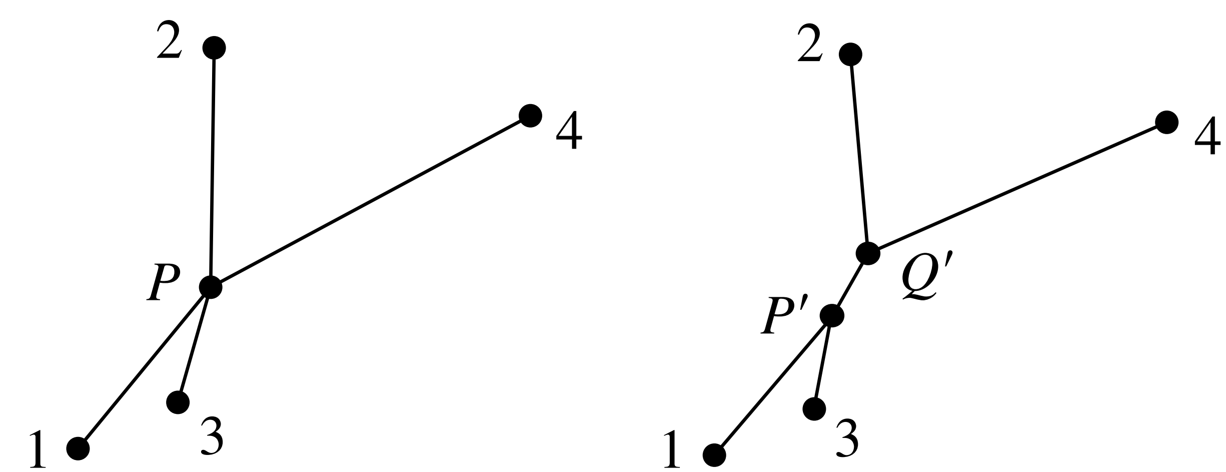

(b) (c)

- select maximum dissipation rate among possible splits

$$\dot{Q}_P = \mathbf{f}_P \cdot \mathbf{v}_P < \mathbf{f}_{P'} \cdot \mathbf{v}_{P'} + \mathbf{f}_{Q'} \cdot \mathbf{v}_{Q'} = \dot{Q}_{P'Q'}$$

summary of 3D line DD

- spatial discretization of dislocation network via nodes connected by (straight) segments
- arbitrary topological changes through “split” and “merge” operations
- nodal driving force results from (isotropic) elastic interaction between all segments (and core energy variation)
- mobility (drag) tensor connects nodal forces to velocities and can be derived from atomistic calculations of dislocation motion
- omitted: time integration algorithms

suggested background reading

- Jirásek & Bazant: “Inelastic Analysis of Structures”
  John Wiley & Sons, 2002
- Chadwick: “Continuum Mechanics”
  Dover Publications, 1999
- course follows
  Roters, Eisenlohr, Bieler, & Raabe: “Crystal Plasticity Finite Element Methods in Materials Science and Engineering”, chapter 3
  Wiley-VCH, 2010

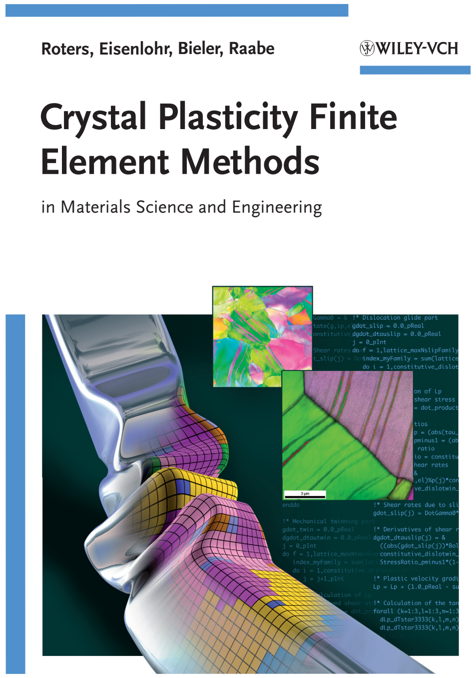

content

- kinematics:

  study of (typically position-dependent) displacements and, if considering time-dependence, motions of a material body without explicitly asking about the forces that are causing them

- mechanical equilibrium:

  conditions for forces acting on the body of material and causing above kinematic reactions

MICHIGAN STATE UNIVERSITY

material points and configurations

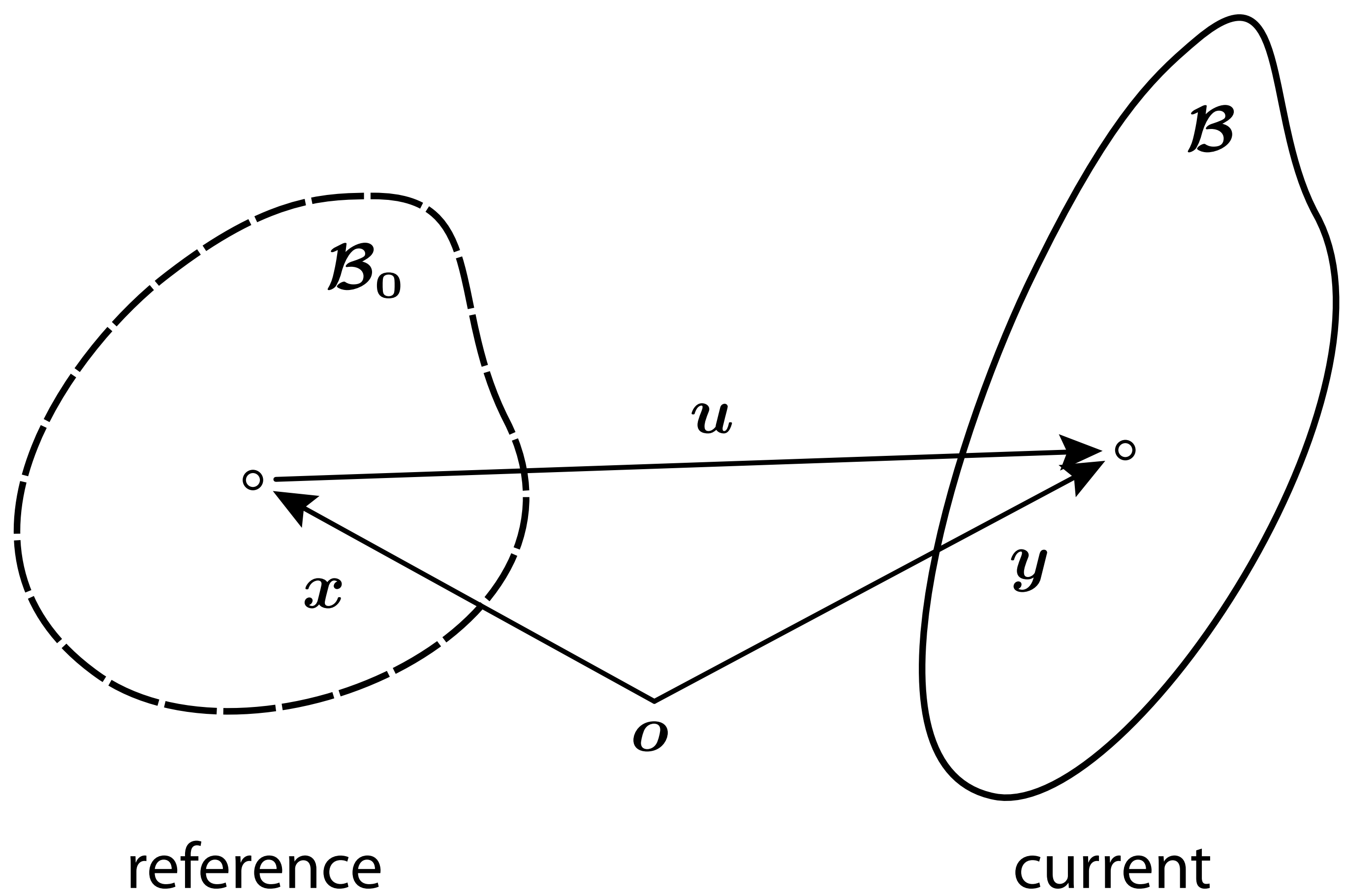

$$\mathbf{y}(\mathbf{x}) : \mathbf{x} \in \mathcal{B}_0 \longmapsto \mathbf{y} \in \mathcal{B}$$

deformation gradient

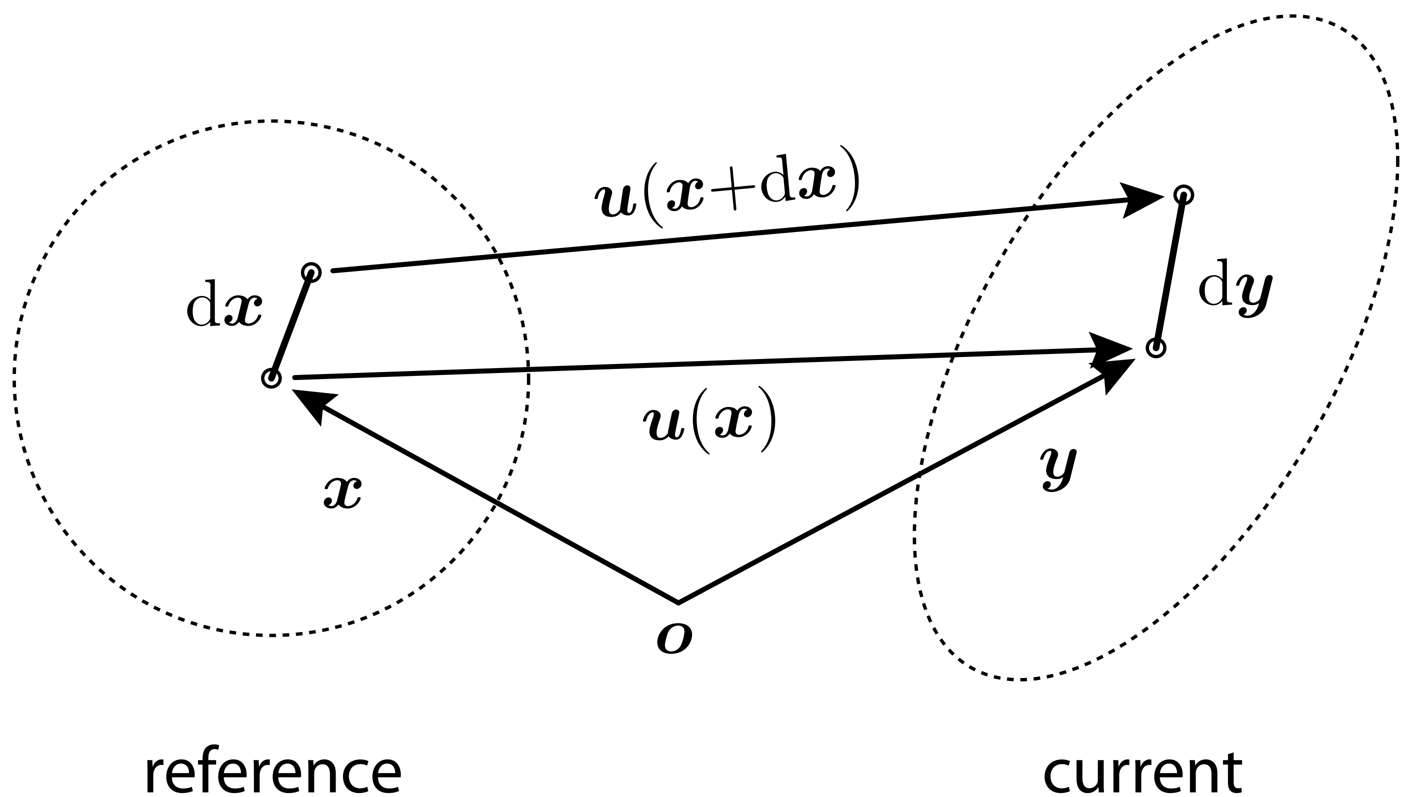

$$\mathbf{y} + \mathrm{d}\mathbf{y} = \mathbf{y}(\mathbf{x}) + \frac{\partial \mathbf{y}}{\partial \mathbf{x}}\,\mathrm{d}\mathbf{x} + \mathcal{O}(\mathrm{d}\mathbf{x}^2)$$

$$\mathrm{d}\mathbf{y} = \frac{\partial \mathbf{y}}{\partial \mathbf{x}}\,\mathrm{d}\mathbf{x} = \mathbf{F}\,\mathrm{d}\mathbf{x}$$

MICHIGAN STATE UNIVERSITY

deformation gradient

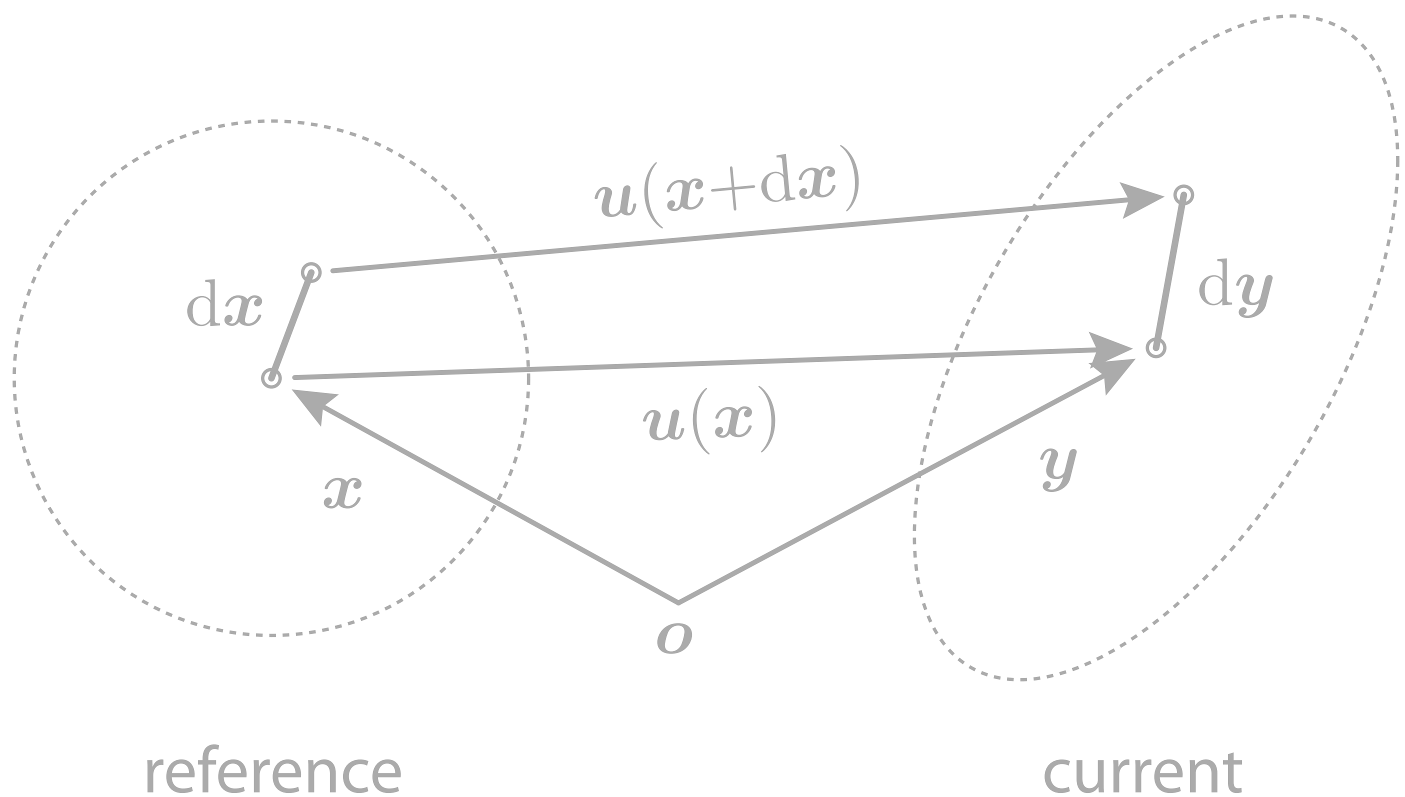

$$\mathbf{F} = \frac{\partial \mathbf{y}}{\partial \mathbf{x}} = \mathrm{Grad}\,\mathbf{y} \quad \text{or}$$

$F_{ij} = \partial y_i / \partial x_j$ in Cartesian components.

deformation gradient

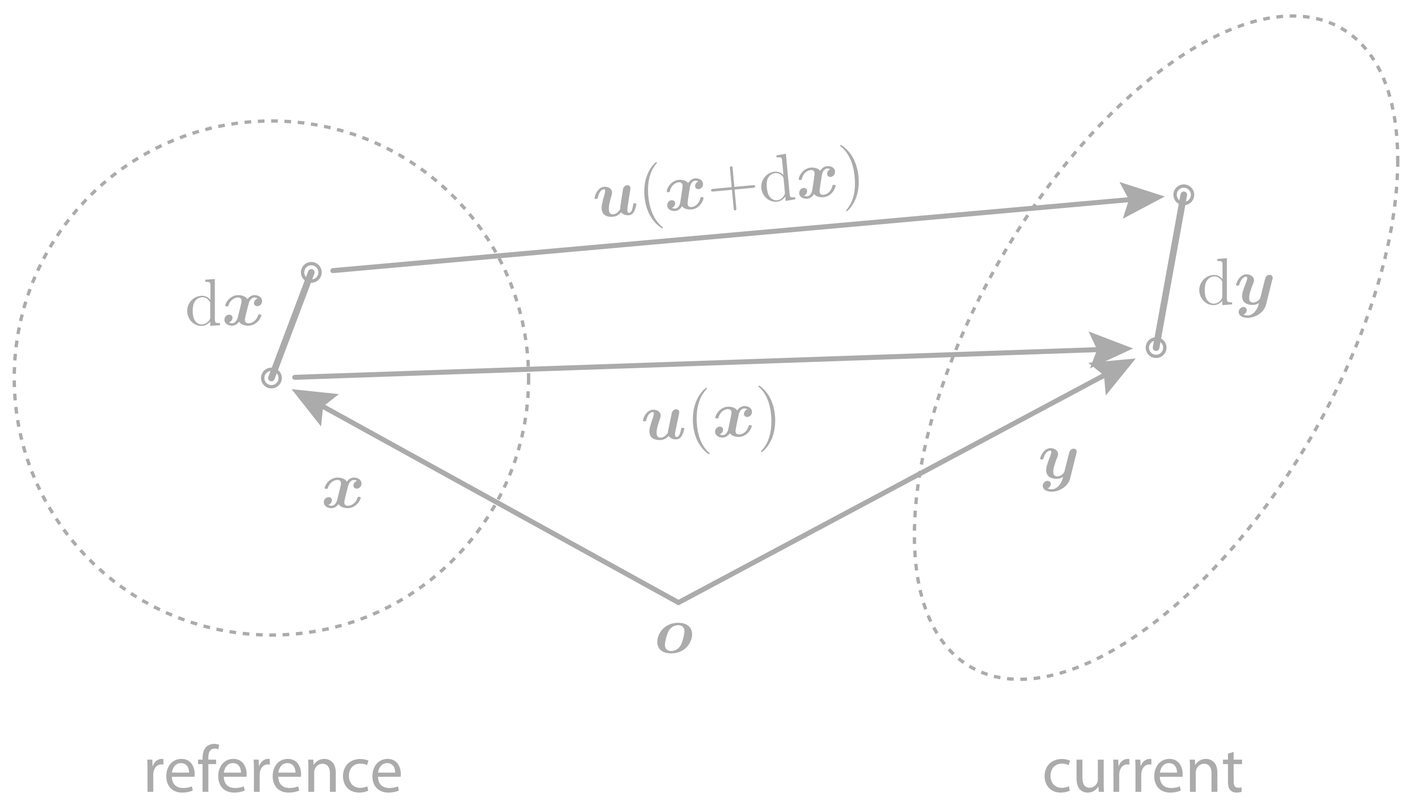

$$\mathbf{F}^{-1} = \frac{\partial \mathbf{x}}{\partial \mathbf{y}} = \operatorname{grad} \mathbf{x} \quad \text{or}$$

$${F_{ij}}^{-1} = \partial x_i / \partial y_j \quad \text{in Cartesian components.}$$

deformation gradient

mapping of general second-rank tensors between reference and current configuration

- push forward: $$\mathbf{A} = \mathbf{F}\,\mathbf{A}_0\,\mathbf{F}^{-1}$$

  acting in reference configuration

- pull back $$\mathbf{A}_0 = \mathbf{F}^{-1}\,\mathbf{A}\,\mathbf{F}$$

  acting in current configuration

change in volume

- Jacobian $$J = \det \mathbf{F} = \frac{\mathrm{d}V}{\mathrm{d}V_0} = \frac{\rho_0}{\rho}$$

change in area

- directed surface $\mathrm{d}\mathbf{n} = J\mathbf{F}^{-\mathrm{T}}\mathrm{d}\mathbf{n}_0$

MICHIGAN STATE UNIVERSITY

change in length

$$\mathrm{d}\mathbf{x} = \mathrm{d}l_0\,\mathbf{a}$$
$$\mathrm{d}\mathbf{y} = \mathrm{d}l\,\mathbf{b}$$

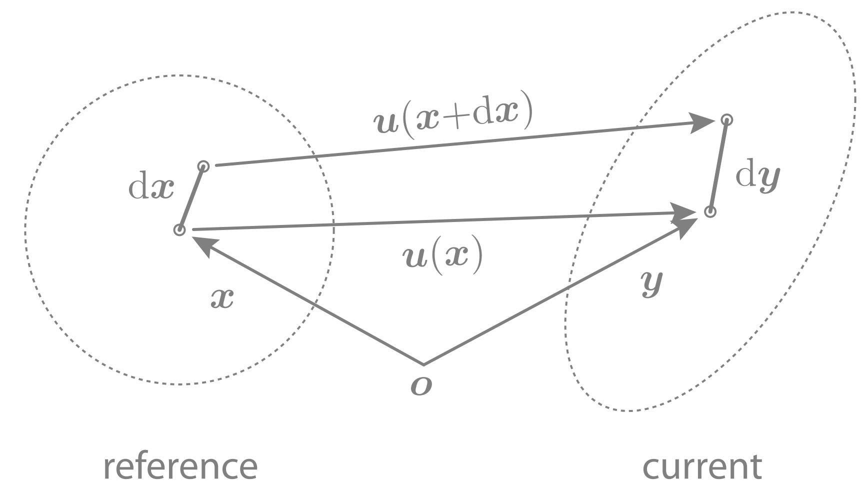

- stretch

$$\mathrm{d}\mathbf{y}\cdot\mathrm{d}\mathbf{y} = \mathbf{F}\,\mathrm{d}\mathbf{x}\cdot\mathbf{F}\,\mathrm{d}\mathbf{x}$$
$$\left(\frac{\mathrm{d}l}{\mathrm{d}l_0}\right)^2 = \mathbf{F}\,\mathbf{a}\cdot\mathbf{F}\,\mathbf{a} = \mathbf{a}\cdot\mathbf{F}^{\mathrm{T}}\mathbf{F}\,\mathbf{a} = \mathbf{a}\cdot\mathbf{C}\,\mathbf{a} = \lambda^2$$

$$\mathrm{d}\mathbf{x}\cdot\mathrm{d}\mathbf{x} = \mathbf{F}^{-1}\mathrm{d}\mathbf{y}\cdot\mathbf{F}^{-1}\mathrm{d}\mathbf{y}$$
$$\left(\frac{\mathrm{d}l_0}{\mathrm{d}l}\right)^2 = \mathbf{F}^{-1}\mathbf{b}\cdot\mathbf{F}^{-1}\mathbf{b} = \mathbf{b}\cdot\mathbf{F}^{-\mathrm{T}}\mathbf{F}^{-1}\mathbf{b} = \mathbf{b}\cdot(\mathbf{F}\mathbf{F}^{\mathrm{T}})^{-1}\mathbf{b} = \mathbf{b}\cdot\mathbf{B}^{-1}\mathbf{b} = \lambda^{-2}$$

right Cauchy–Green tensor

left Cauchy–Green tensor

change in angle

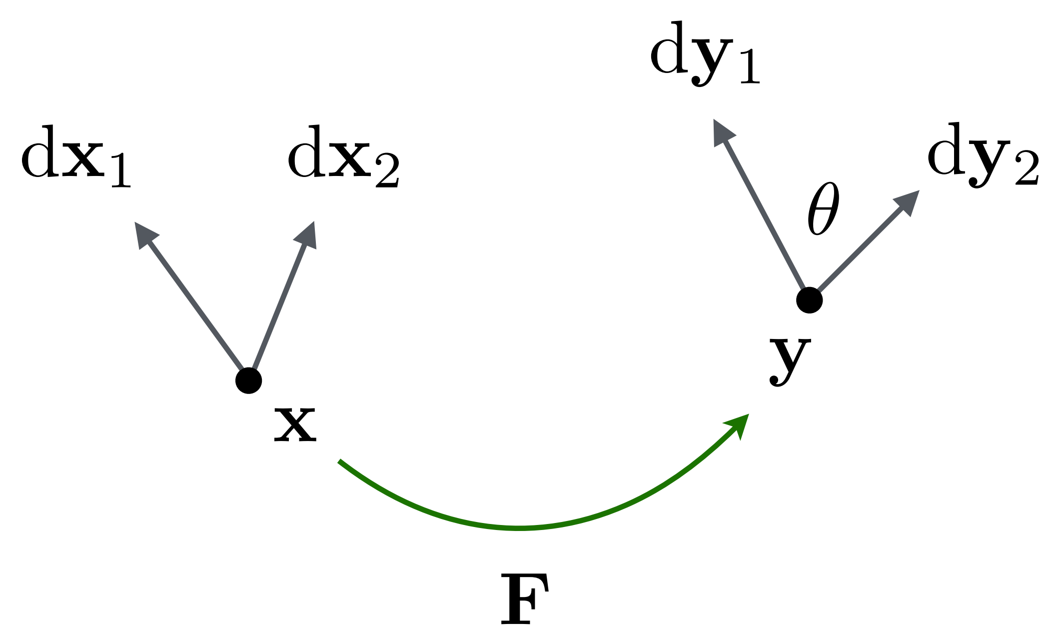

$$\lambda_1 \lambda_2 \cos\theta = \mathbf{a}_1 \cdot \mathbf{C}\, \mathbf{a}_2$$

symmetry of Cauchy–Green tensors

- right Cauchy–Green tensor

$$
\begin{aligned}
\mathbf{C} :&= \mathbf{F}^{\mathrm{T}}\mathbf{F} \\
&= \mathbf{F}^{\mathrm{T}}\left(\mathbf{F}^{\mathrm{T}}\right)^{\mathrm{T}} = \left(\mathbf{F}^{\mathrm{T}}\mathbf{F}\right)^{\mathrm{T}} \\
&= \mathbf{C}^{\mathrm{T}}
\end{aligned}
$$

- left Cauchy–Green tensor

$$
\begin{aligned}
\mathbf{B} :&= \mathbf{F}\mathbf{F}^{\mathrm{T}} \\
&= \left(\mathbf{F}^{\mathrm{T}}\right)^{\mathrm{T}}\mathbf{F}^{\mathrm{T}} = \left(\mathbf{F}\mathbf{F}^{\mathrm{T}}\right)^{\mathrm{T}} \\
&= \mathbf{B}^{\mathrm{T}}
\end{aligned}
$$

spectral decomposition of Cauchy–Green tensors

- $\mathbf{C}$ is symmetric and positive-definite $\qquad \mathbf{C} = \sum_{i=1}^{3} \mu_i \, \mathbf{n}_i \otimes \mathbf{n}_i$
- real and positive eigenvalues $\qquad \mu_1, \mu_2, \mu_3$
- orthogonal eigenvectors $\qquad \mathbf{n}_1, \mathbf{n}_2, \mathbf{n}_3$

spectral decomposition of Cauchy–Green tensors

stretches along eigenvectors

$$
\begin{aligned}
{\lambda_j}^2 &= \mathbf{n}_j \cdot \mathbf{C}\,\mathbf{n}_j \\
&= \mathbf{n}_j \cdot \left(\sum_{i=1}^{3} \mu_i\, \mathbf{n}_i \otimes \mathbf{n}_i \right) \mathbf{n}_j \\
&= \mathbf{n}_j \cdot \left(\sum_{i=1}^{3} \mu_i\, \mathbf{n}_i\, (\mathbf{n}_i \cdot \mathbf{n}_j) \right) \\
&= \mathbf{n}_j \cdot \left(\sum_{i=1}^{3} \mu_i\, \mathbf{n}_i\, \delta_{ij} \right) \\
&= \mu_j\, \mathbf{n}_j \cdot \mathbf{n}_j \\
&= \mu_j
\end{aligned}
$$

relation between Cauchy–Green and stretch tensor

- right Cauchy–Green tensor

$$\mathbf{C} = \sum_{i=1}^{3} {\lambda_i}^2 \, \mathbf{n}_i \otimes \mathbf{n}_i$$

$$\mathbf{U}\mathbf{U} = \mathbf{U}^2 = \mathbf{C}$$

- right stretch tensor

$$\mathbf{U} = \sum_{i=1}^{3} \lambda_i \, \mathbf{n}_i \otimes \mathbf{n}_i$$

polar decomposition of deformation gradient

- invertible tensor $\mathbf{F}$

$$\mathbf{F} = \mathbf{R}\mathbf{U} = \mathbf{V}\mathbf{R}$$

- $\mathbf{R}$ is proper orthogonal (rotation)

- $\mathbf{U}$, $\mathbf{V}$ are positive-definite and symmetric

polar decomposition of deformation gradient

relation to Cauchy–Green tensors

$$\mathbf{F} = \mathbf{R}\mathbf{U} = \mathbf{V}\mathbf{R}$$

$$\begin{aligned} \mathbf{C} &= \mathbf{F}^{\mathrm{T}}\mathbf{F} \\ &= (\mathbf{R}\mathbf{U})^{\mathrm{T}}(\mathbf{R}\mathbf{U}) \\ &= \mathbf{U}^{\mathrm{T}}\mathbf{R}^{\mathrm{T}}\mathbf{R}\mathbf{U} \\ &= \mathbf{U}^{\mathrm{T}}\mathbf{U} \\ &= \mathbf{U}^2 \end{aligned} \qquad \begin{aligned} \mathbf{B} &= \mathbf{F}\mathbf{F}^{\mathrm{T}} \\ &= (\mathbf{V}\mathbf{R})(\mathbf{V}\mathbf{R})^{\mathrm{T}} \\ &= \mathbf{V}\mathbf{R}\mathbf{R}^{\mathrm{T}}\mathbf{V}^{\mathrm{T}} \\ &= \mathbf{V}\mathbf{V}^{\mathrm{T}} \\ &= \mathbf{V}^2 \end{aligned}$$

MICHIGAN STATE UNIVERSITY

strain measures

connection to strains and rotations
from infinitesimal framework

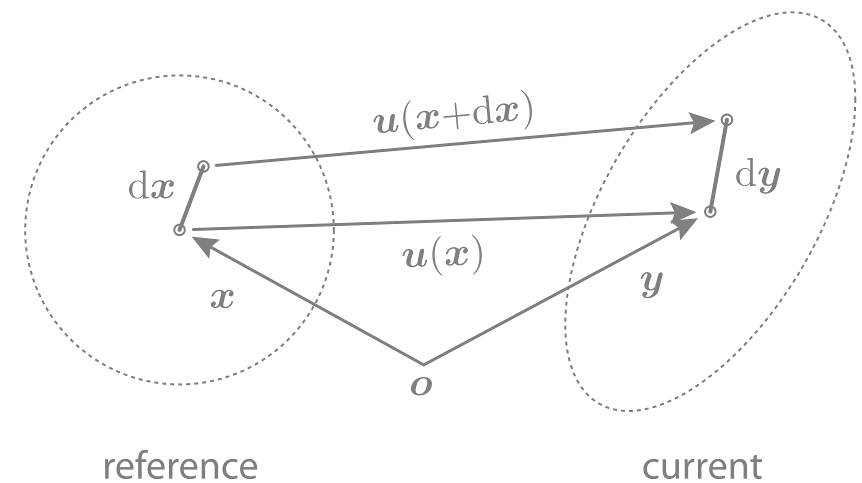

$$\begin{aligned}
\mathbf{F} = \frac{\partial \mathbf{y}}{\partial \mathbf{x}} &= \frac{\partial(\mathbf{x}+\mathbf{u})}{\partial \mathbf{x}} \\
&= \mathbf{I} + \frac{\partial \mathbf{u}}{\partial \mathbf{x}} \\
&= \mathbf{I} + \frac{1}{2}\left[\frac{\partial \mathbf{u}}{\partial \mathbf{x}} + \left(\frac{\partial \mathbf{u}}{\partial \mathbf{x}}\right)^{\mathrm{T}}\right] + \frac{1}{2}\left[\frac{\partial \mathbf{u}}{\partial \mathbf{x}} - \left(\frac{\partial \mathbf{u}}{\partial \mathbf{x}}\right)^{\mathrm{T}}\right] \\
&= \mathbf{I} + \left(\frac{\partial \mathbf{u}}{\partial \mathbf{x}}\right)_{\mathrm{sym}} + \left(\frac{\partial \mathbf{u}}{\partial \mathbf{x}}\right)_{\mathrm{skew}} \\
&= \mathbf{I} + \varepsilon + \omega
\end{aligned}$$

strain measures

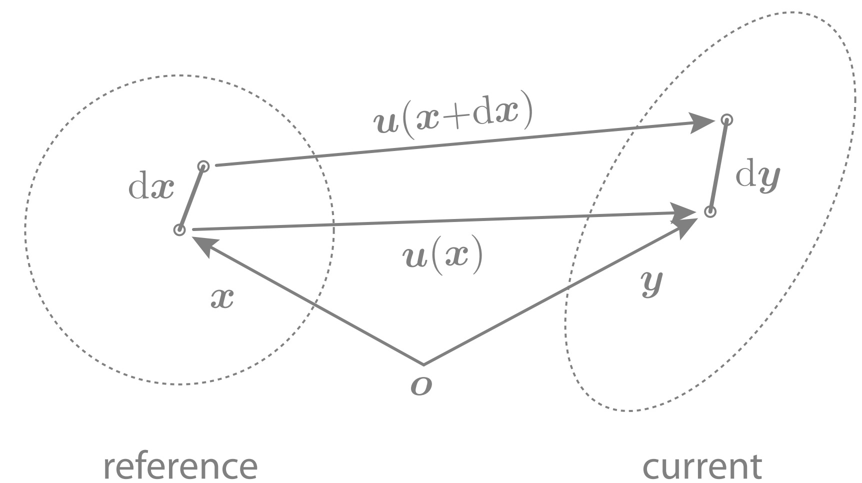

$$
\begin{aligned}
\mathbf{C} = \mathbf{F}^{\mathrm{T}}\mathbf{F} &= \left(\mathbf{I} + \frac{\partial \mathbf{u}}{\partial \mathbf{x}}\right)^{\mathrm{T}} \left(\mathbf{I} + \frac{\partial \mathbf{u}}{\partial \mathbf{x}}\right) \\
&= \mathbf{I} + \left(\frac{\partial \mathbf{u}}{\partial \mathbf{x}}\right)^{\mathrm{T}} + \frac{\partial \mathbf{u}}{\partial \mathbf{x}} + \left(\frac{\partial \mathbf{u}}{\partial \mathbf{x}}\right)^{\mathrm{T}} \left(\frac{\partial \mathbf{u}}{\partial \mathbf{x}}\right) \\
&\approx \mathbf{I} + 2\varepsilon
\end{aligned}
$$

$$
\mathbf{U} = \mathbf{C}^{1/2} \approx \mathbf{I} + \varepsilon
$$

strain measures

strains based on right stretch tensor $\mathbf{U}$

- Biot $$\mathbf{E}^{(1)} = \mathbf{U} - \mathbf{I}$$
- Green's Lagrangian $$\mathbf{E} = \mathbf{E}^{(2)} = \frac{1}{2}\left(\mathbf{U}^2 - \mathbf{I}\right) = \frac{1}{2}\left(\mathbf{C} - \mathbf{I}\right) = \frac{1}{2}\left(\mathbf{F}^{\mathrm{T}}\mathbf{F} - \mathbf{I}\right)$$
- Doyle–Ericksen $$\mathbf{E}^{(m)} = \frac{1}{m}\left(\mathbf{U}^m - \mathbf{I}\right)$$

velocity gradient

time-dependent displacement, *motion* $\mathbf{y}(t)$

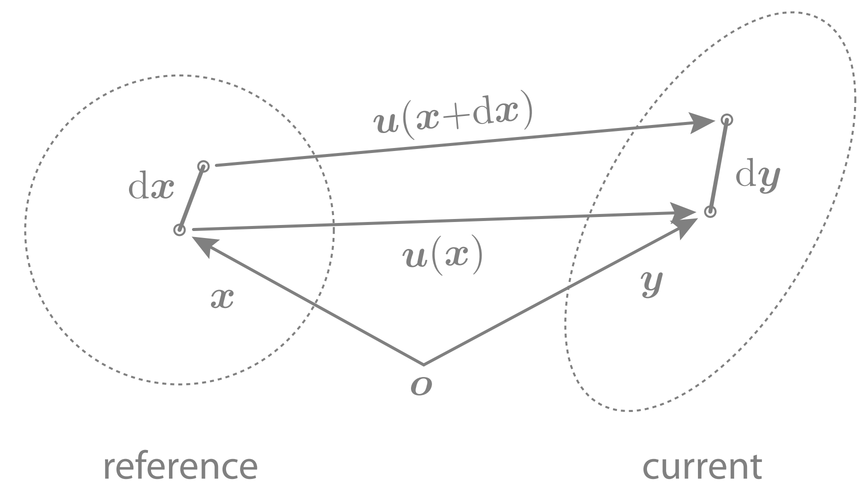

- velocity field $$\mathbf{v} = \frac{\mathrm{d}}{\mathrm{d}t}\mathbf{u} = \dot{\mathbf{u}} = \dot{\mathbf{y}}$$

- spatial velocity gradient $$\mathbf{L} = \frac{\partial \mathbf{v}}{\partial \mathbf{y}} = \operatorname{grad} \mathbf{v}$$

  (relative velocity between two points in current configuration)

velocity gradient

relation to rate of change of deformation gradient

change in velocity $\equiv$ rate of change of relative position

$$\mathbf{L}\,\mathrm{d}\mathbf{y} = \frac{\partial \mathbf{v}}{\partial \mathbf{y}}\,\mathrm{d}\mathbf{y} \equiv \frac{\mathrm{d}}{\mathrm{d}t}\,\mathrm{d}\mathbf{y} = \frac{\mathrm{d}}{\mathrm{d}t}\,\mathbf{F}\,\mathrm{d}\mathbf{x} = \dot{\mathbf{F}}\,\mathrm{d}\mathbf{x} = \dot{\mathbf{F}}\mathbf{F}^{-1}\,\mathrm{d}\mathbf{y}$$

$$\mathbf{L} = \dot{\mathbf{F}}\mathbf{F}^{-1}$$

$$\dot{\mathbf{F}} = \mathbf{L}\mathbf{F}$$

velocity gradient

material time derivatives

$$
\begin{aligned}
(\mathrm{d}\mathbf{y})^{\cdot} &= (\mathbf{F}\,\mathrm{d}\mathbf{x})^{\cdot} \\
&= \dot{\mathbf{F}}\,\mathrm{d}\mathbf{x} + \mathbf{F}\,(\mathrm{d}\mathbf{x})^{\cdot} \\
&= \dot{\mathbf{F}}\,\mathrm{d}\mathbf{x} \\
&= \mathbf{L}\mathbf{F}\,\mathrm{d}\mathbf{x} \\
&= \mathbf{L}\,\mathrm{d}\mathbf{y}
\end{aligned}
$$

$$
\begin{aligned}
(\mathrm{d}\mathbf{y})^{\cdot} &= \mathbf{L}\,\mathrm{d}\mathbf{y} \\
(\mathrm{d}l\,\mathbf{b})^{\cdot} &= \mathbf{L}\,\mathrm{d}l\,\mathbf{b} \\
(\mathrm{d}l)^{\cdot}\,\mathbf{b} + \mathrm{d}l\,\dot{\mathbf{b}} &= \mathbf{L}\,\mathrm{d}l\,\mathbf{b} \\
\mathbf{b}\cdot\mathbf{b}(\mathrm{d}l)^{\cdot} + \mathbf{b}\cdot\dot{\mathbf{b}}\,\mathrm{d}l &= \mathbf{b}\cdot\mathbf{L}\,\mathrm{d}l\,\mathbf{b} \\
(\mathrm{d}l)^{\cdot} &= \mathbf{b}\cdot\mathbf{L}\,\mathrm{d}l\,\mathbf{b}
\end{aligned}
$$

velocity gradient

additive decomposition

stretch rate tensor

$$\mathbf{L} = \mathbf{L}_{\text{sym}} + \mathbf{L}_{\text{skew}} = \frac{1}{2}\left(\mathbf{L} + \mathbf{L}^{\text{T}}\right) + \frac{1}{2}\left(\mathbf{L} - \mathbf{L}^{\text{T}}\right) = \mathbf{D} + \mathbf{W}$$

spin rate tensor

elasto-plastic decomposition

- crystalline solid
- elastic and/or plastic shape change
- pure plastic is lattice-invariant and stress-free

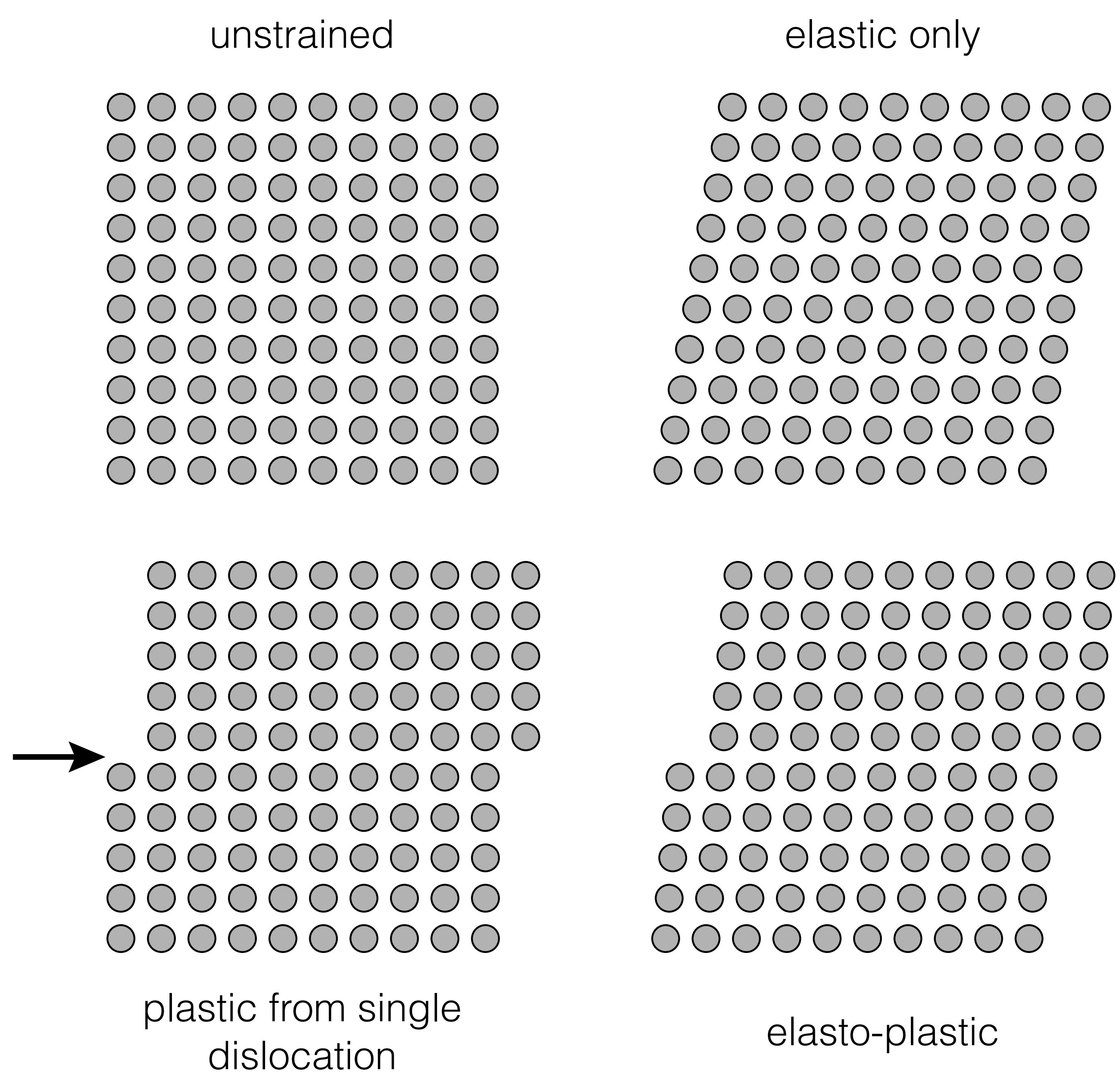

elasto-plastic decomposition

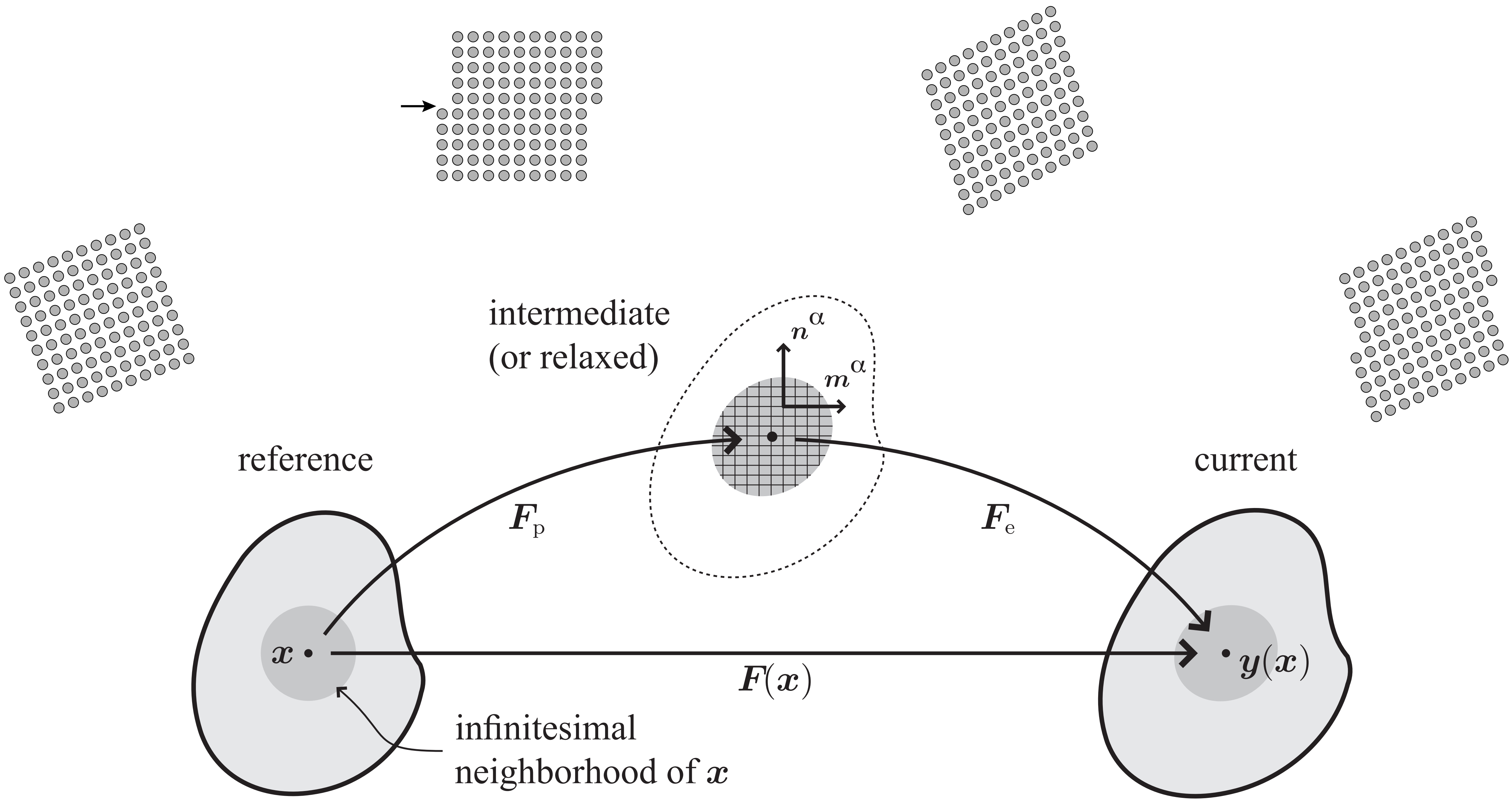

elasto-plastic decomposition

$$\mathbf{F} = \mathbf{F}_{\mathrm{e}}\mathbf{F}_{\mathrm{p}}$$

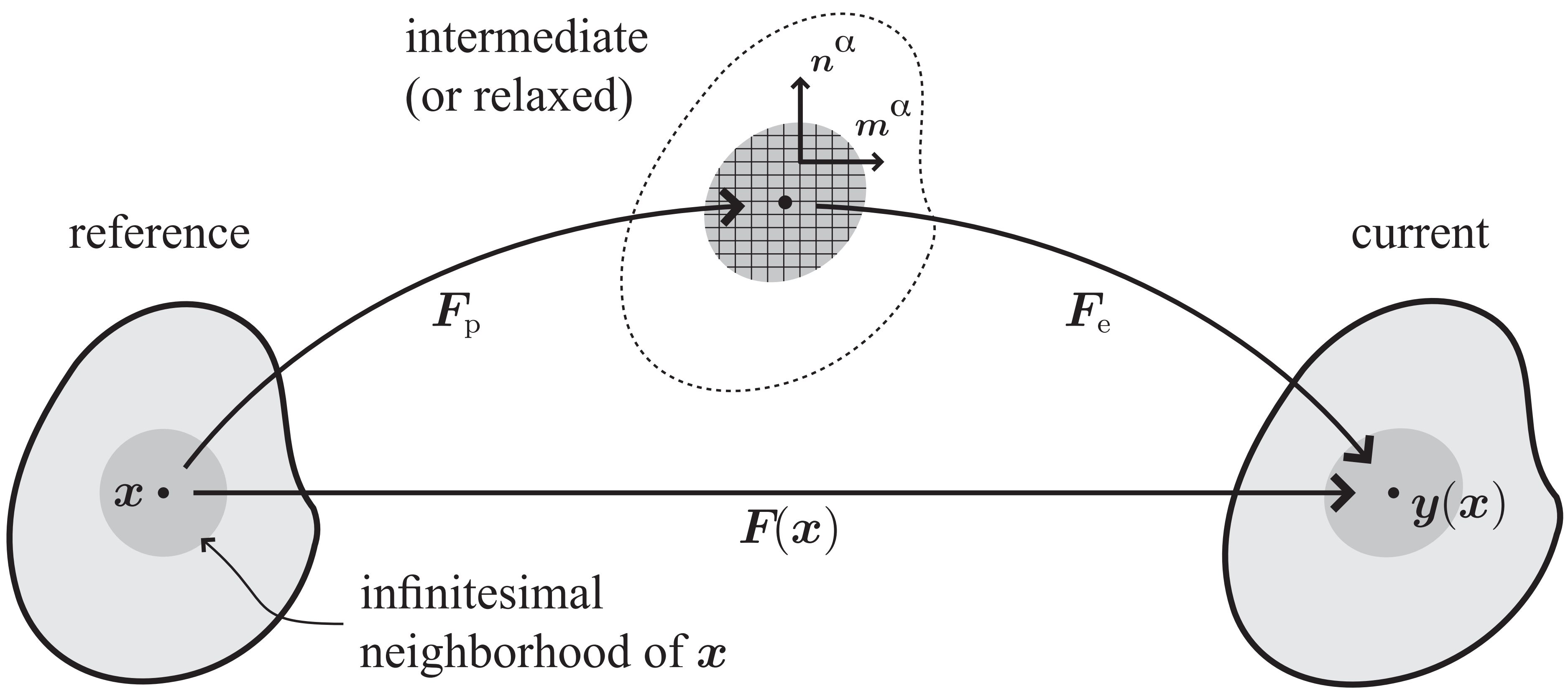

elasto-plastic decomposition

velocity gradient decomposition

$$
\begin{aligned}
\mathbf{L} &= \dot{\mathbf{F}}\mathbf{F}^{-1} \\
&= (\mathbf{F}_{\mathrm{e}}\mathbf{F}_{\mathrm{p}})^{\cdot}\,\mathbf{F}_{\mathrm{p}}{}^{-1}\mathbf{F}_{\mathrm{e}}{}^{-1} \\
&= \dot{\mathbf{F}}_{\mathrm{e}}\mathbf{F}_{\mathrm{p}}\mathbf{F}_{\mathrm{p}}{}^{-1}\mathbf{F}_{\mathrm{e}}{}^{-1} + \mathbf{F}_{\mathrm{e}}\dot{\mathbf{F}}_{\mathrm{p}}\mathbf{F}_{\mathrm{p}}{}^{-1}\mathbf{F}_{\mathrm{e}}{}^{-1} \\
&= \dot{\mathbf{F}}_{\mathrm{e}}\mathbf{F}_{\mathrm{e}}{}^{-1} + \mathbf{F}_{\mathrm{e}}\,\dot{\mathbf{F}}_{\mathrm{p}}\mathbf{F}_{\mathrm{p}}{}^{-1}\,\mathbf{F}_{\mathrm{e}}{}^{-1} \\
&= \mathbf{L}_{\mathrm{e}} + \mathbf{F}_{\mathrm{e}}\,\mathbf{L}_{\mathrm{p}}\,\mathbf{F}_{\mathrm{e}}{}^{-1}
\end{aligned}
$$

acts in current configuration

acts in intermediate configuration

total force acting on body

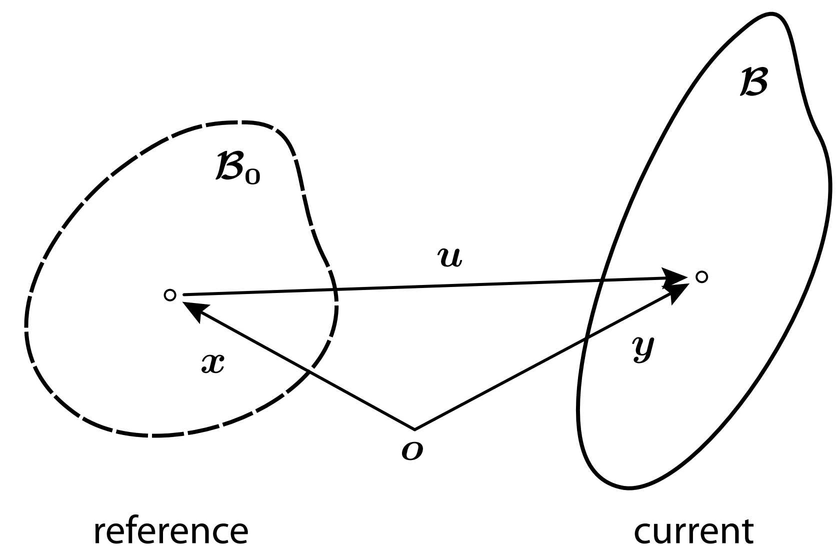

- body force field $\mathbf{g}$
- surface tractions

$$\mathbf{k} = \int_{\mathcal{S}_0} \mathbf{t}_0 \, \mathrm{d}S_0 = \int_{\mathcal{S}} \mathbf{t} \, \mathrm{d}S$$

$$= \int_{\mathcal{S}_0} \mathbf{P} \, \mathrm{d}\mathbf{n}_0 = \int_{\mathcal{S}} \boldsymbol{\sigma} \, \mathrm{d}\mathbf{n}$$

first Piola–Kirchhoff (nominal) stress

Cauchy stress

total force acting on body

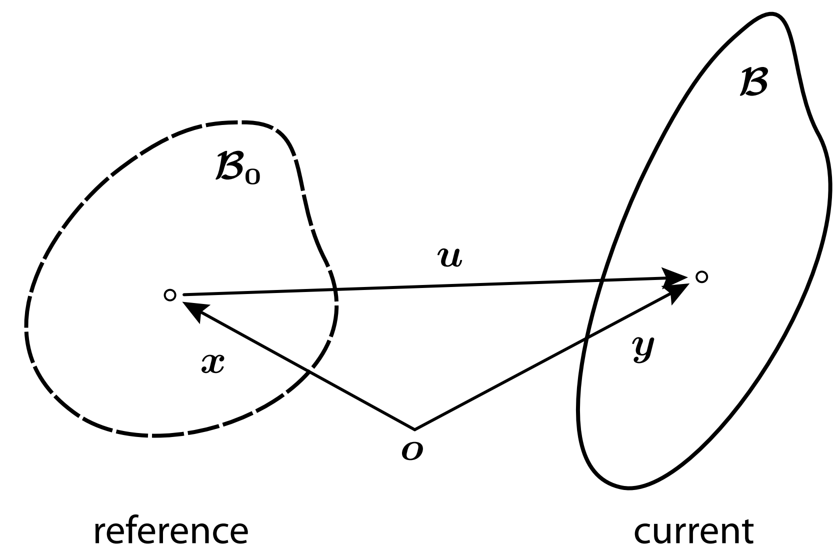

- body force field
- surface tractions

$$\mathbf{k} = \int_{\mathcal{S}_0} \mathbf{P}\,\mathrm{d}\mathbf{n}_0 = \int_{\mathcal{S}} \boldsymbol{\sigma}\,\mathrm{d}\mathbf{n}$$

$$\mathrm{d}\mathbf{n} = J\mathbf{F}^{-\mathrm{T}}\mathrm{d}\mathbf{n}_0$$

$$\mathbf{P} = J\boldsymbol{\sigma}\mathbf{F}^{-\mathrm{T}}$$

total force acting on body

integration of body forces
and surface tractions

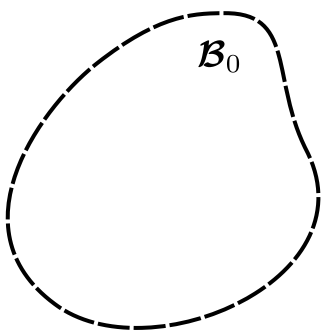

reference

$$\mathbf{f} = \int_{\mathcal{B}_0} \rho_0 \, \dot{\mathbf{v}} \, \mathrm{d}V_0 = \int_{\mathcal{B}_0} \rho_0 \, \mathbf{g} \, \mathrm{d}V_0 + \int_{\mathcal{S}_0} \mathbf{t}_0 \, \mathrm{d}S_0$$

MICHIGAN STATE UNIVERSITY

balance of linear momentum

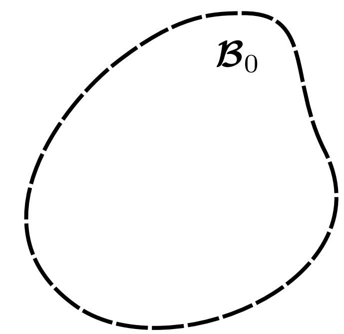

reference

$$\mathbf{0} = \int_{\mathcal{B}_0} \left(\rho_0 \, \mathbf{g} + \frac{\partial \mathbf{P}}{\partial \mathbf{x}} - \rho_0 \, \dot{\mathbf{v}} \right) \mathrm{d}V_0$$

$$= \int_{\mathcal{B}_0} \left(\mathrm{Div} \, \mathbf{P} + \rho_0 \left(\mathbf{g} - \dot{\mathbf{v}} \right) \right) \mathrm{d}V_0$$

$$\mathrm{Div} \, \mathbf{P} = \rho_0 \left(\dot{\mathbf{v}} - \mathbf{g} \right)$$

$$= \mathbf{0}$$

negligible body forces and acceleration

balance of angular momentum

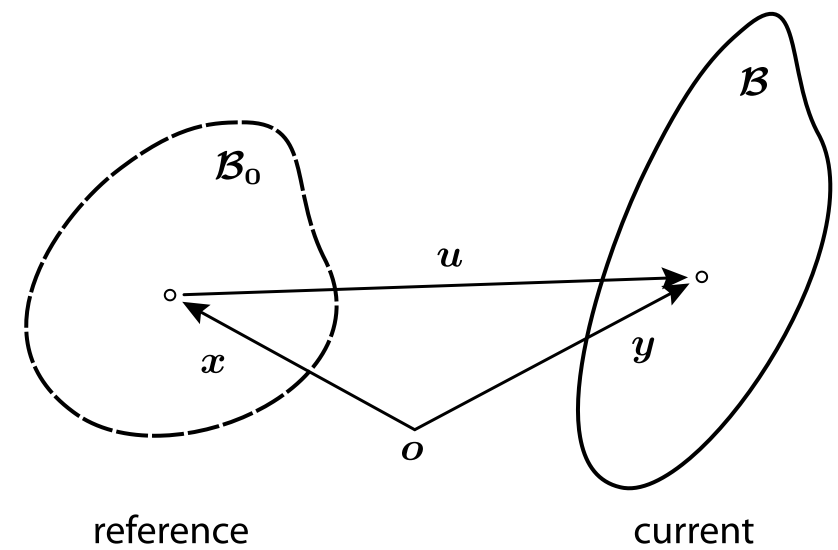

$$\mathbf{P}\mathbf{F}^{\mathrm{T}} = \mathbf{F}\mathbf{P}^{\mathrm{T}} \qquad \Longleftrightarrow \qquad \boldsymbol{\sigma} = \boldsymbol{\sigma}^{\mathrm{T}}$$

overview

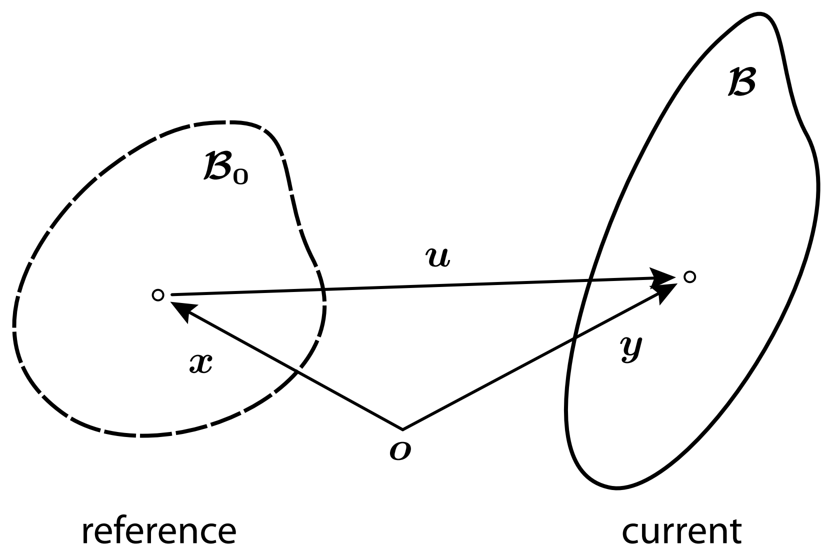

- modeling objective
- material point
- hierarchical simulation framework

modeling objective

crystalline solid

why consider crystallinity at all?

- anisotropy
- physically-based model

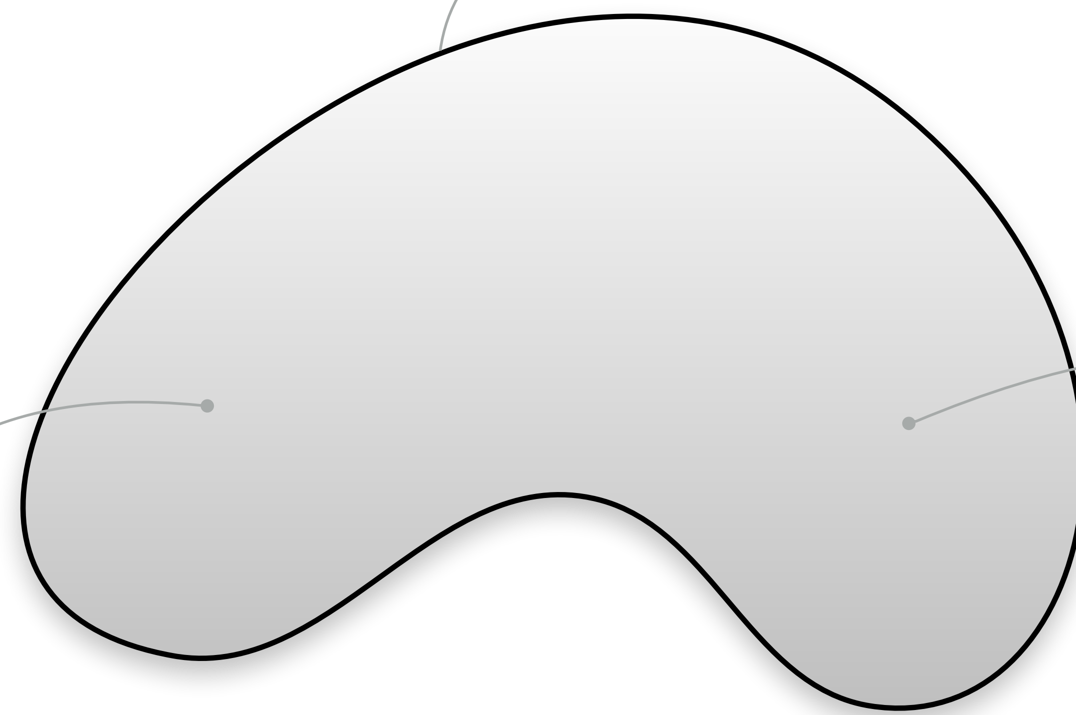

solve partial differential equation system under time-varying boundary conditions

$$\mathrm{Div}\,\mathbf{P} = \mathbf{0}$$

$$\mathrm{Curl}\,\mathbf{F} = \mathbf{0}$$

mechanical response ?

- traction, displacement
- temperature
- other fields…

solution methods

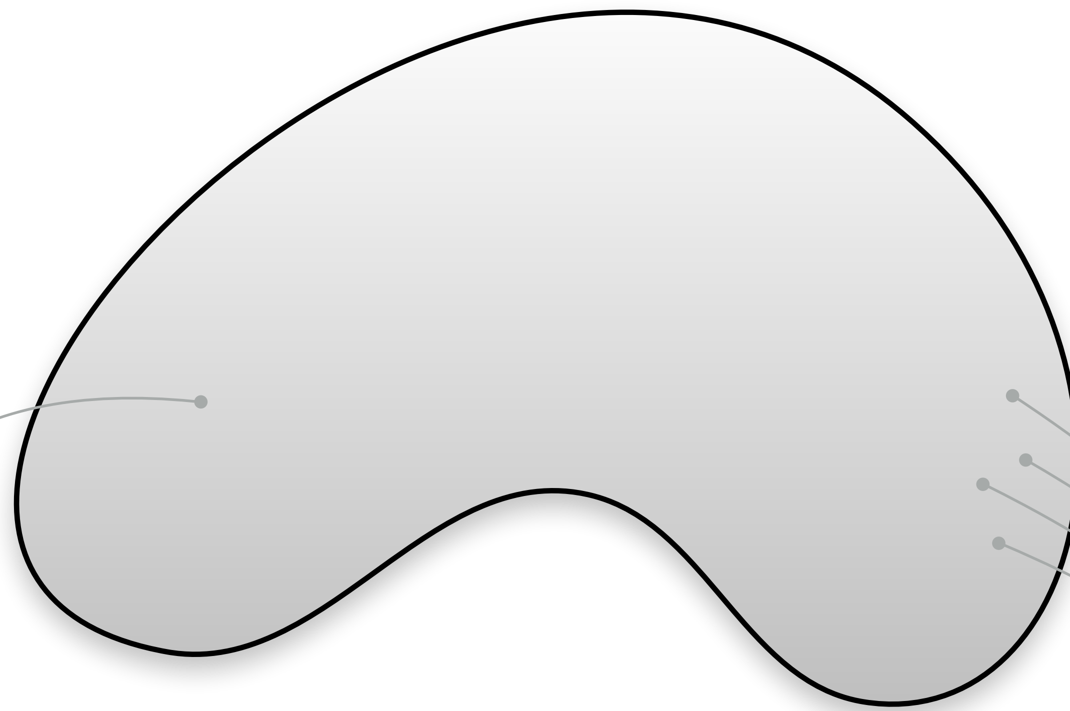

- finite differences
- spectral collocation / Green's function
- finite elements

solve partial differential equation system under time-varying boundary conditions

$$\mathrm{Div}\,\mathbf{P} = \mathbf{0}$$

$$\mathrm{Curl}\,\mathbf{F} = \mathbf{0}$$

+ spatial discretization

point-wise evaluation of $\overline{\mathbf{P}}(\overline{\mathbf{F}})$

material point

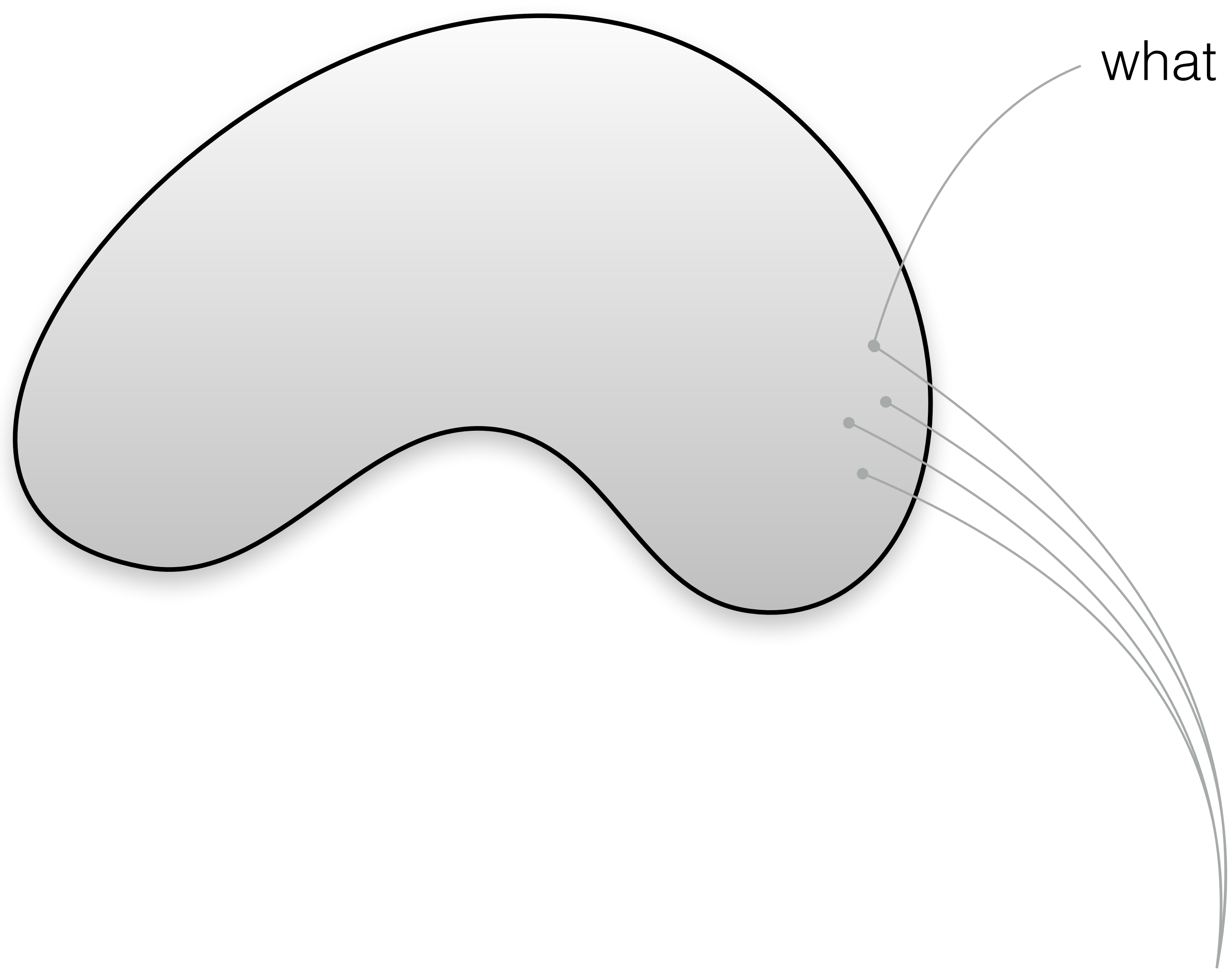

what is there?

$\overline{\mathbf{P}}(\overline{\mathbf{F}})$?

material point

local material constitution depends on
ratio of mesh size / microstructure size

- direct crystal plasticity (mesh finer than crystallites)
- statistical crystal plasticity (mesh larger than crystallites)

material point constitution

direct crystal plasticity

10.1016/j.ijfatigue.2012.04.022

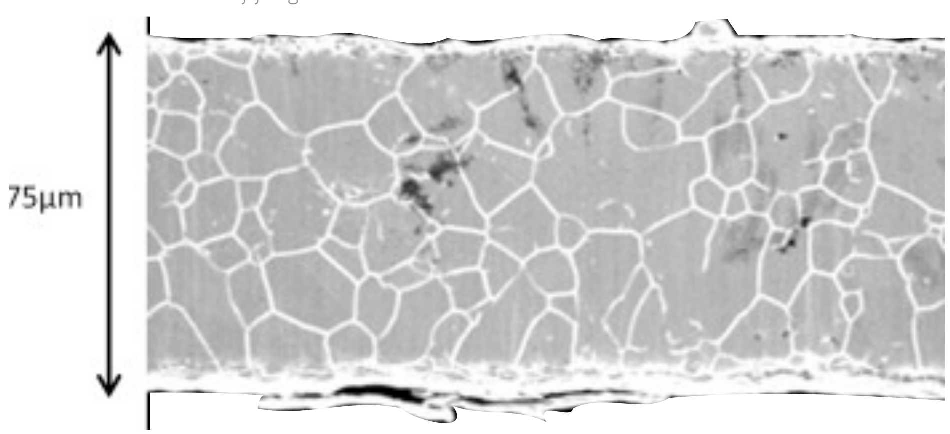

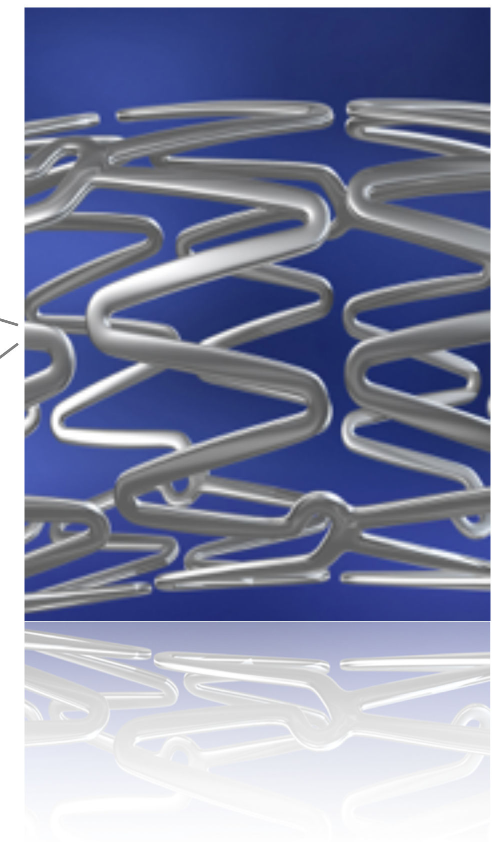

http://axisorigin.com/hkane/wp-content/uploads/Stent_01.jpg

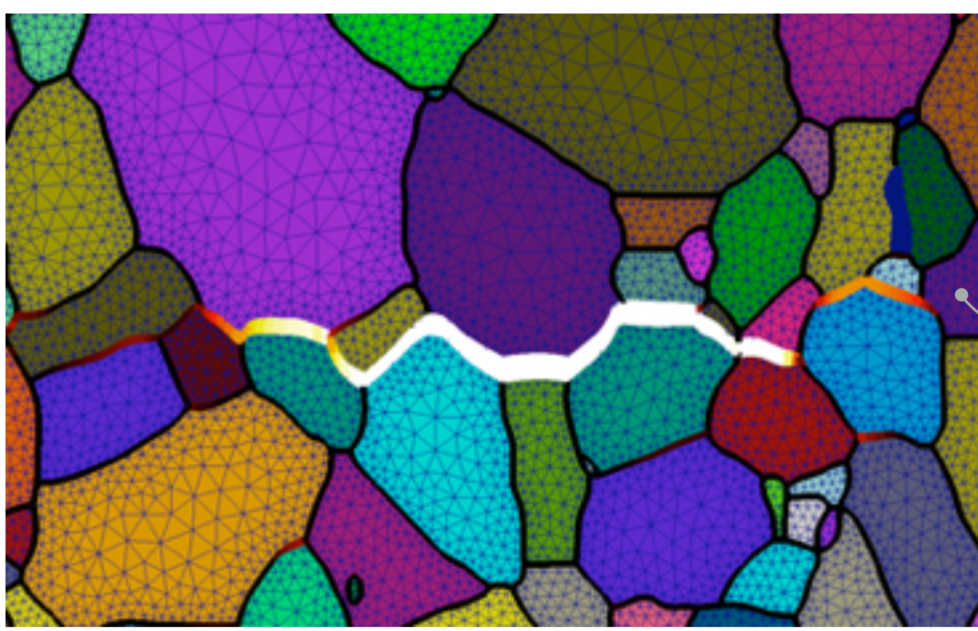

$$\mathbf{F} = \overline{\mathbf{F}}$$

$$\overline{\mathbf{P}} = \mathbf{P}(\mathbf{F})$$

material point constitution

statistical crystal plasticity

- composite response $\overline{\mathbf{P}}(\overline{\mathbf{F}})$?
- approximations required
- subdivision into tractable problems

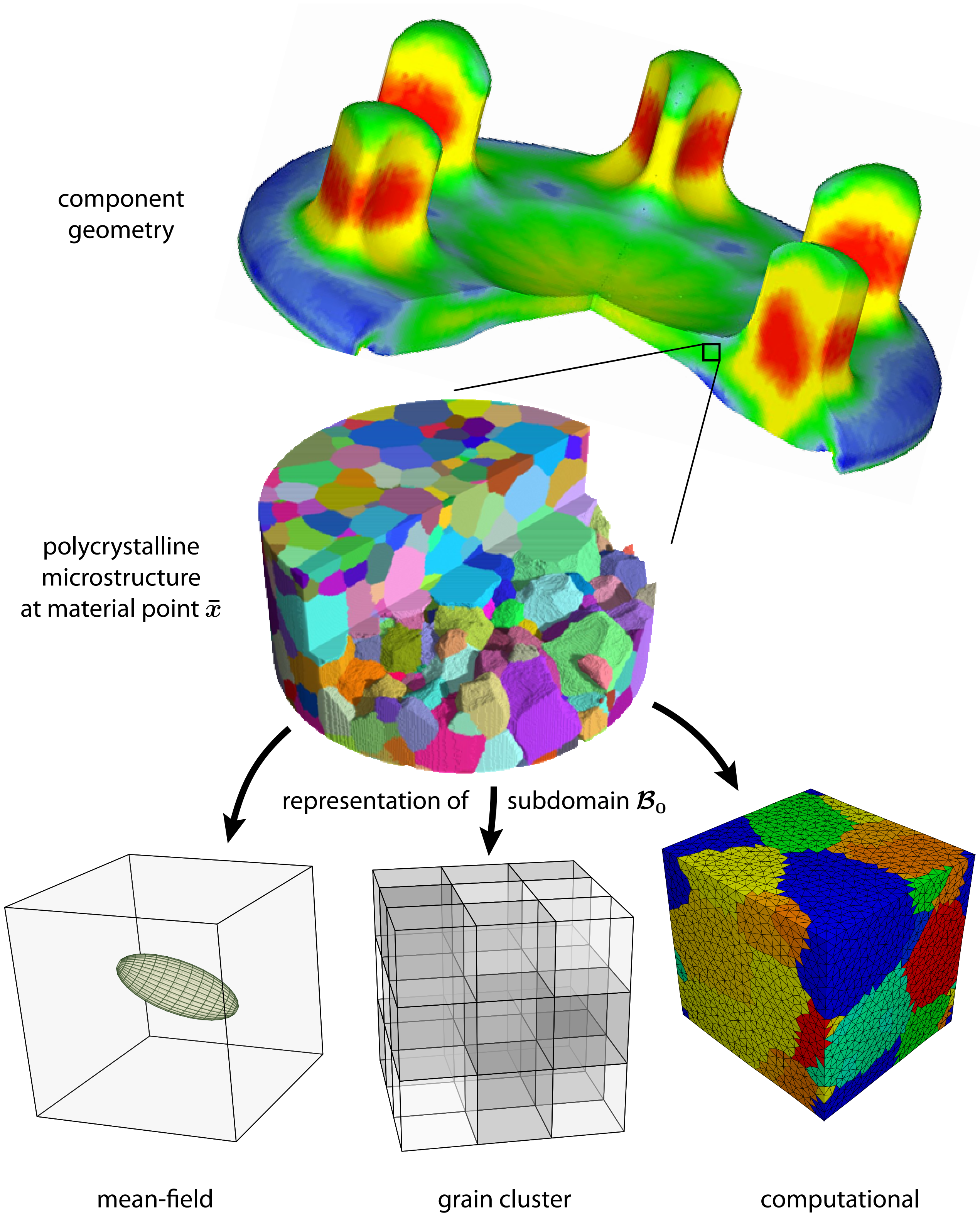

material point constitution

subdivision into tractable problems

$$
\begin{tikzcd}
 & \mathbf{F}_1 \arrow[r] & \mathbf{P}_1 \arrow[ddr] & \\
 & \mathbf{F}_2 \arrow[r] & \mathbf{P}_2 \arrow[dr] & \\
\overline{\mathbf{F}} \arrow[uur] \arrow[ur] \arrow[r] \arrow[dr] & \vdots \arrow[r] & \vdots \arrow[r] & \overline{\mathbf{P}} \\
 & \mathbf{F}_N \arrow[r] & \mathbf{P}_N \arrow[ur] &
\end{tikzcd}
$$

deformation partitioning

single crystallite constitutive relation $\mathbf{P}(\mathbf{F})$

stress homogenization

single crystal constitution

elasto-plasticity

- $\mathbf{P}(\mathbf{F})$ is known for purely elastic deformation
- in general, $\mathbf{P}(\mathbf{F})$ is not directly accessible since rate of plasticity is driven by stress

(recall part on driving force in DDD lecture)

single crystal constitution

Maxwell model of elasto-plasticity

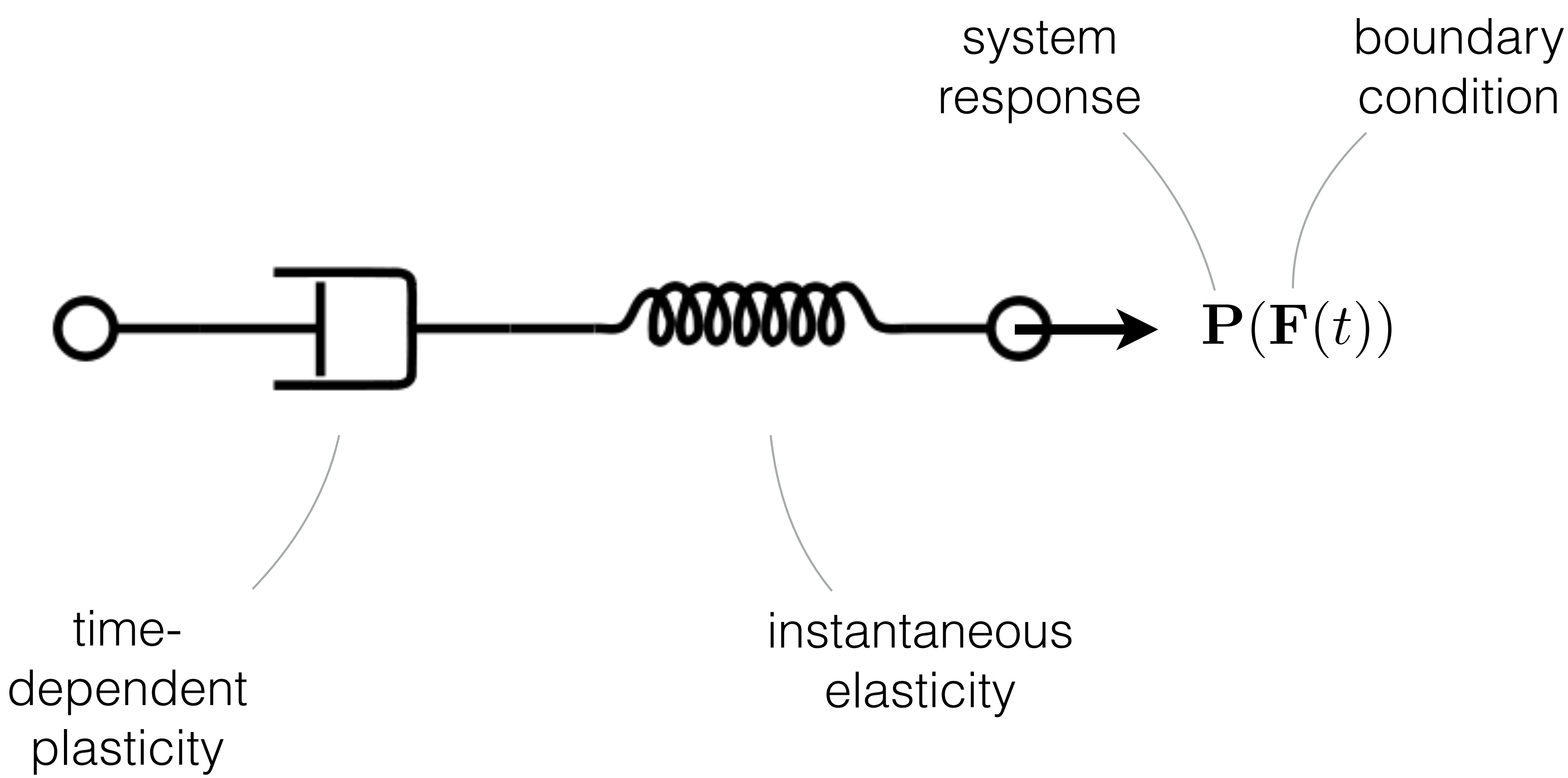

elasto-plastic decomposition

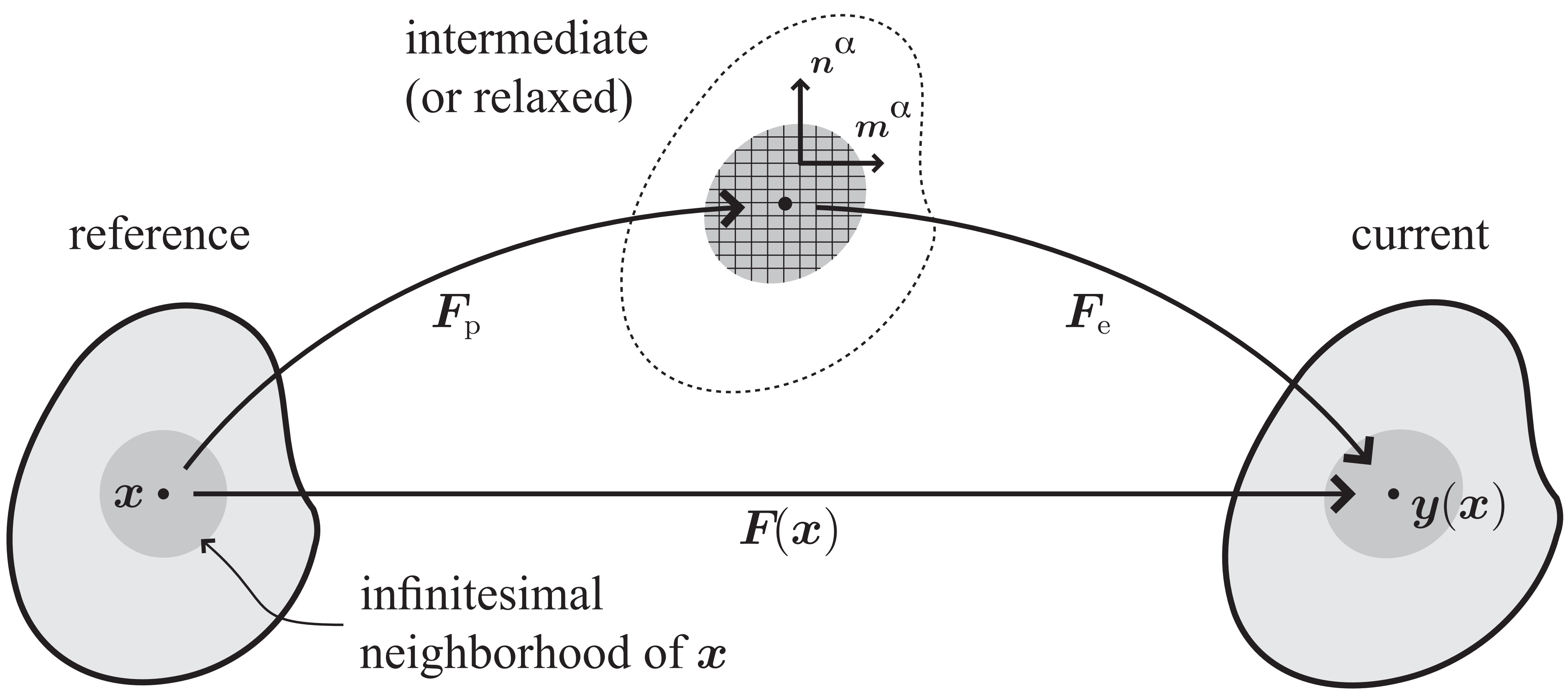

elasto-plastic consistency

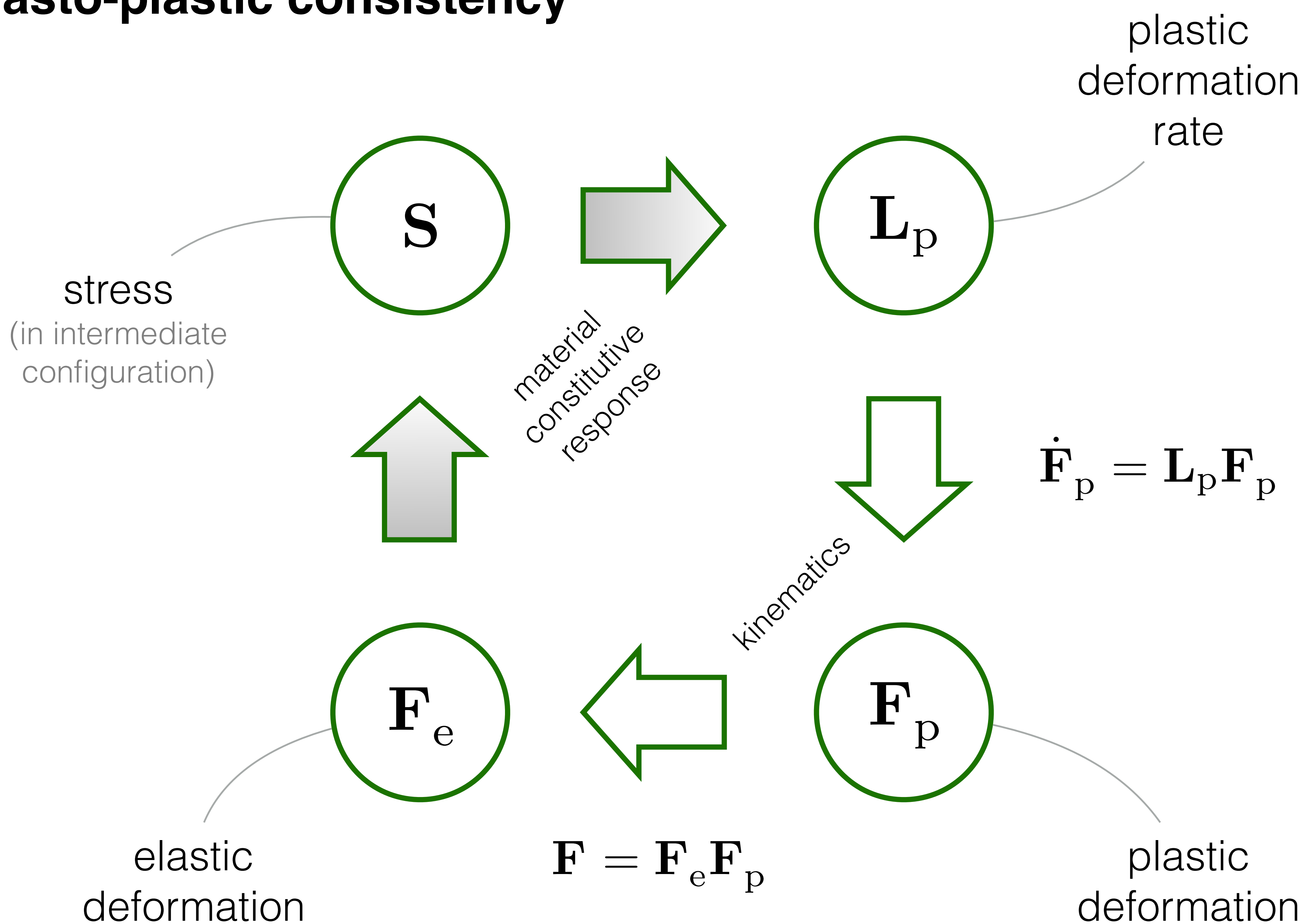

single crystal constitutive law

- internal state variables $\mathbf{s}$
- elastic stress $\mathbf{S} = \mathbf{S}(\mathbf{F}_\mathrm{e}, \mathbf{s})$

$$= \mathbb{C} : \mathbf{E} = \mathbb{C} : ({\mathbf{F}_\mathrm{e}}^\mathrm{T}\mathbf{F}_\mathrm{e} - \mathbf{I})/2$$

- plastic velocity gradient $\mathbf{L}_\mathrm{p} = \mathbf{L}_\mathrm{p}(\mathbf{S}, \mathbf{s})$
- rate of internal state evolution $\dot{\mathbf{s}} = \dot{\mathbf{s}}(\mathbf{S}, \mathbf{s})$

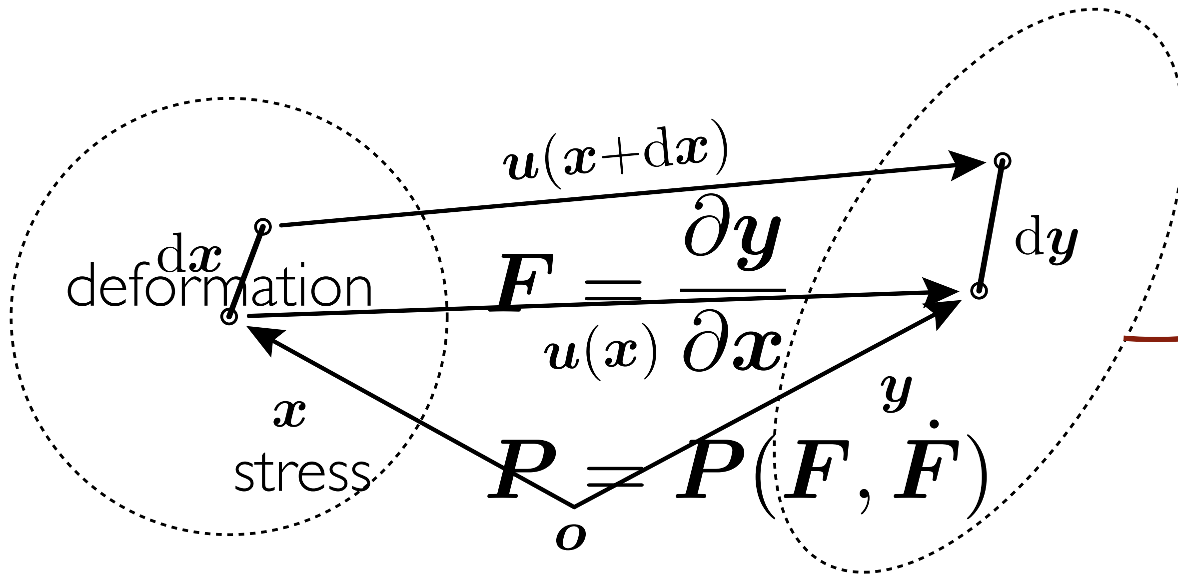

reference current

continuum

DAMASK *(Düsseldorf Advanced Materials Simulation Kit)*

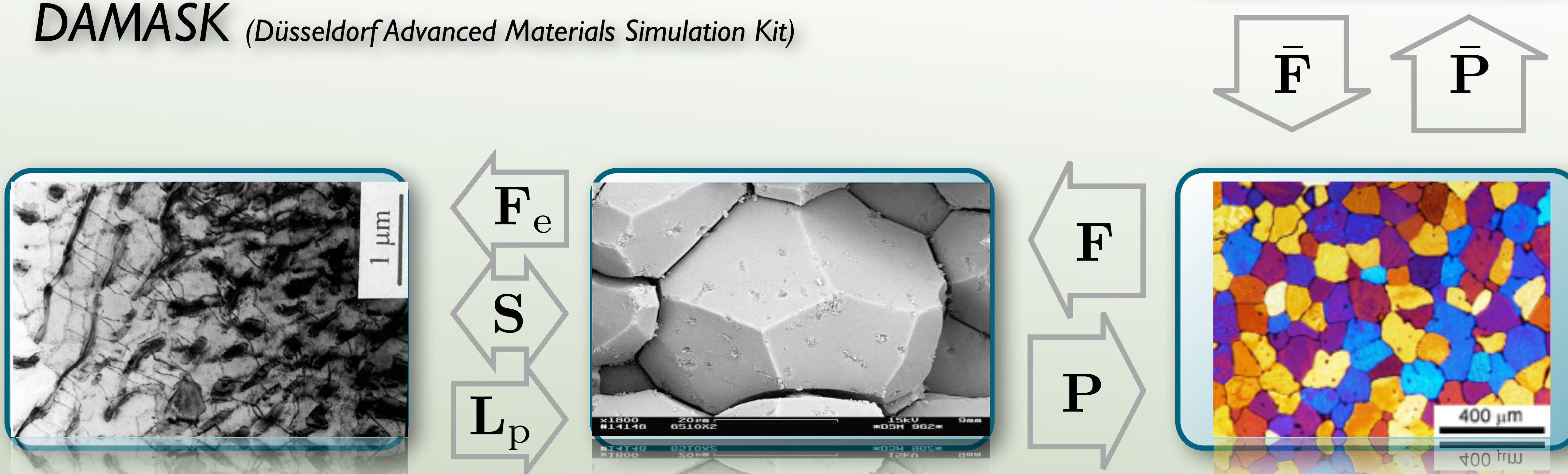

physics of deformation crystallite aggregate

upcoming lectures

- constitutive descriptions of single crystal plasticity
- time integration and numerical solution schemes
- polycrystal plasticity, microstructure homogenization
- solution methods for full-field mechanical boundary value problem

flexible material point setup

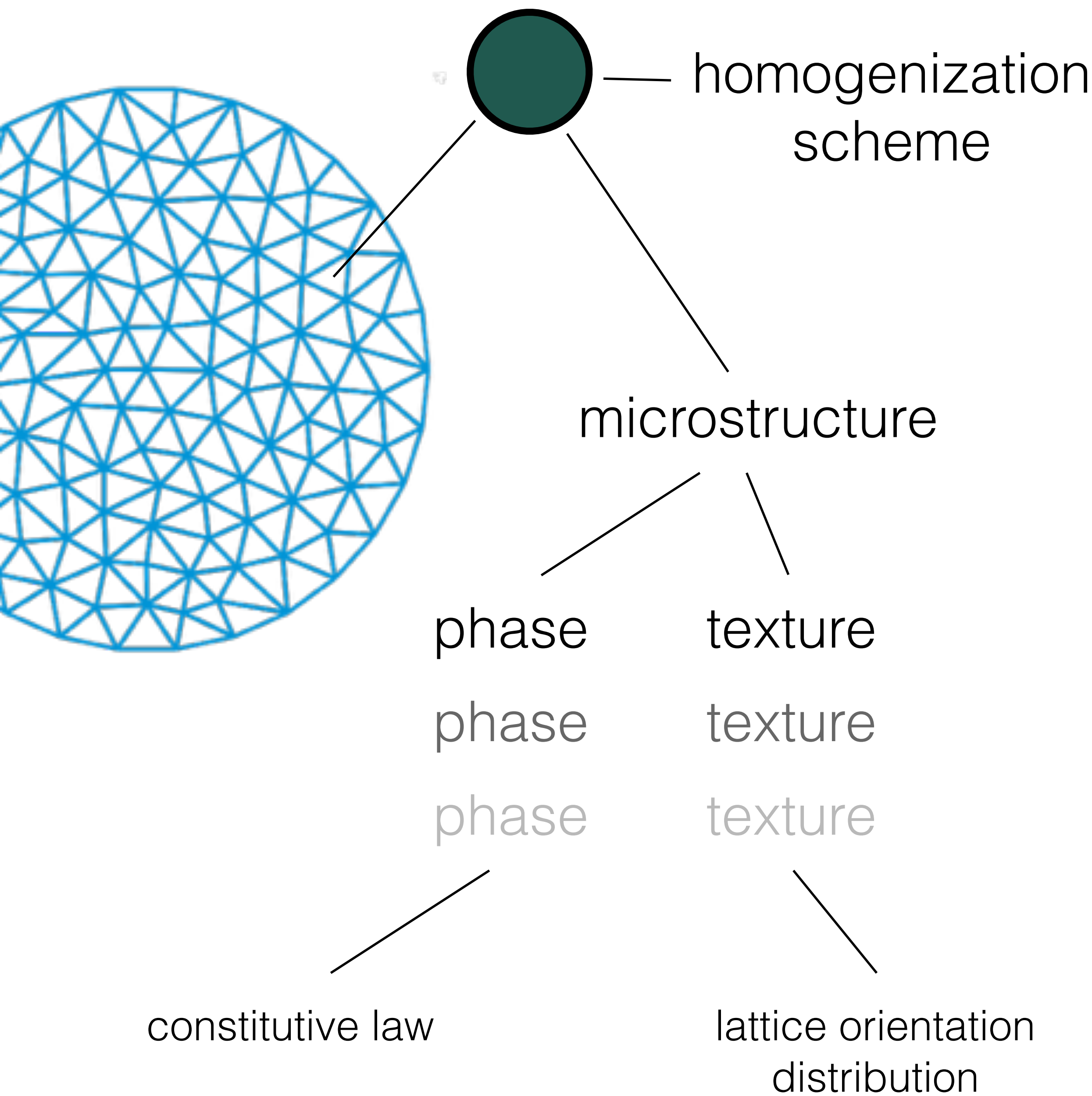


```
[illegible]

[illegible]

  [illegible]
  [illegible]          phase 1      texture 1     fraction 1.0

[illegible]            flowstress
  (output)             strainrate
  [illegible]          [illegible]
  [illegible]          [illegible]  texture 1     fraction  0.82
  [illegible]          [illegible]  texture 1     fraction  0.18
  taylorfactor         3
  tau0         31e6
   ...
```

overview

- lattice slip kinematics and resolved stress
- experimental background
- phenomenological descriptions
- dislocation density-based descriptions

resolved stress

- work done by dislocation motion

slipped area

$$W = \mathrm{d}A\, \tau\, b$$

force per area in direction of slip

$$\tau = (\boldsymbol{\sigma}\, \mathbf{n}) \cdot \mathbf{m}$$
$$= \boldsymbol{\sigma} \cdot (\mathbf{m} \otimes \mathbf{n})$$

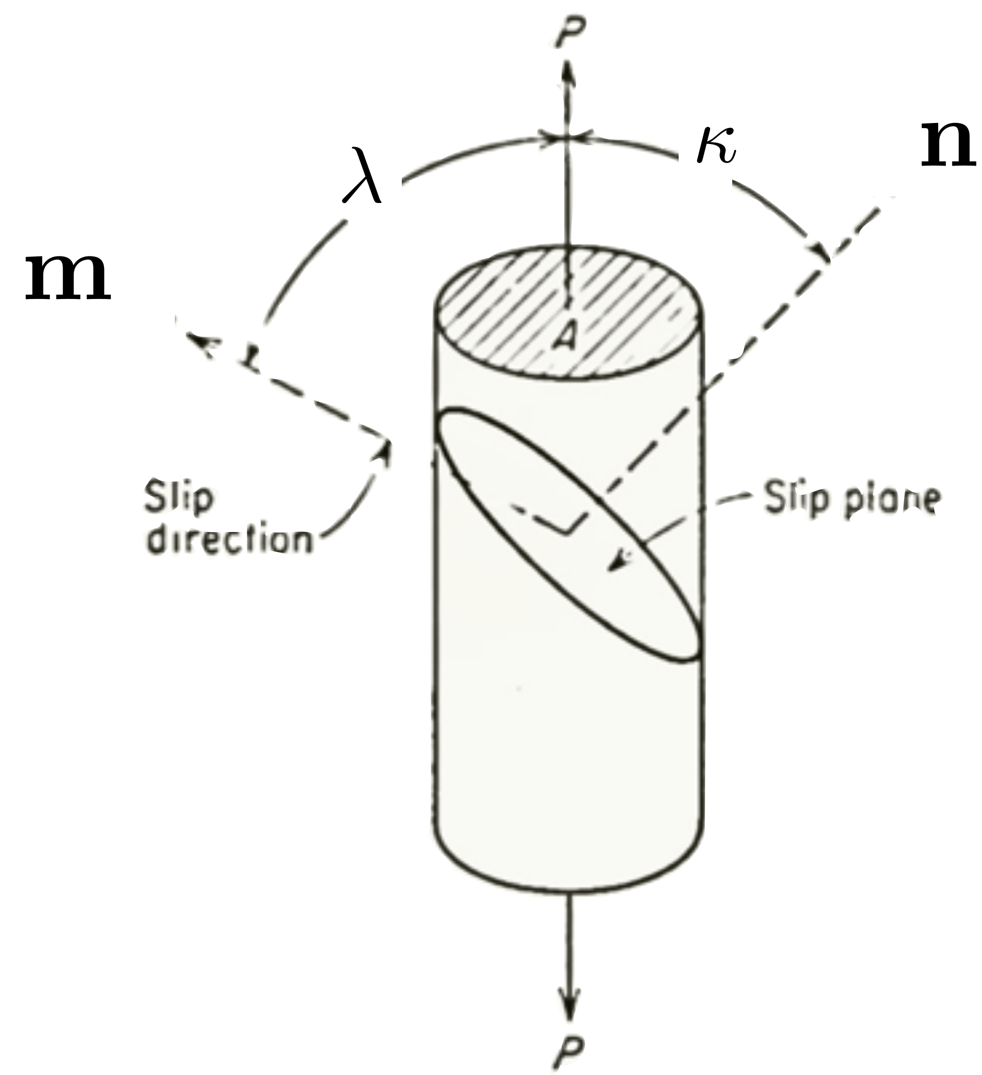

lattice slip kinematics

- rotation of slip direction and slip plane normal

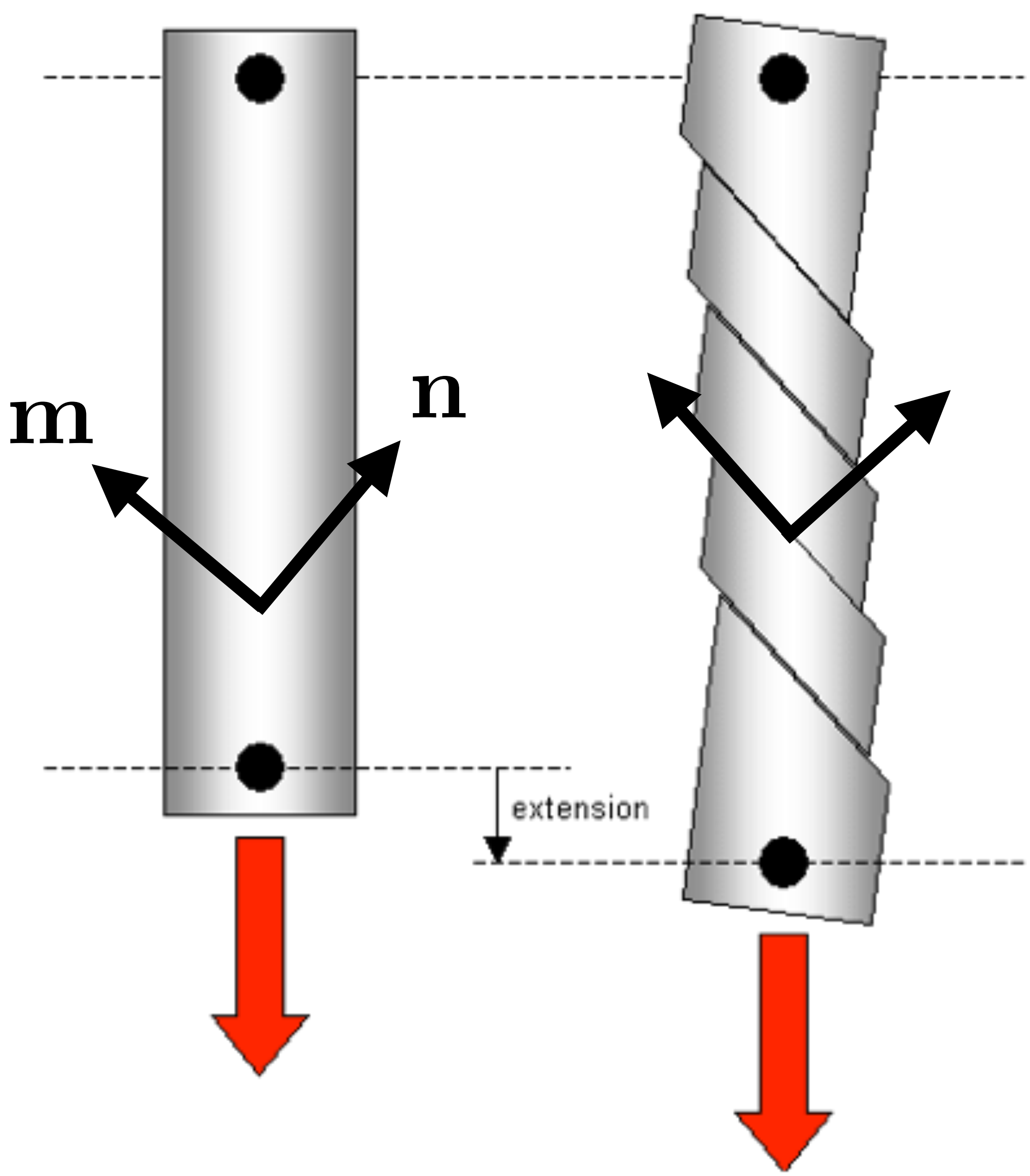

Unslipped single crystal fixed at top end.

Single crystal after plastic deformation by tensile stress in the direction of the arrow. Slip occurs on distinct parallel planes.

lattice slip kinematics

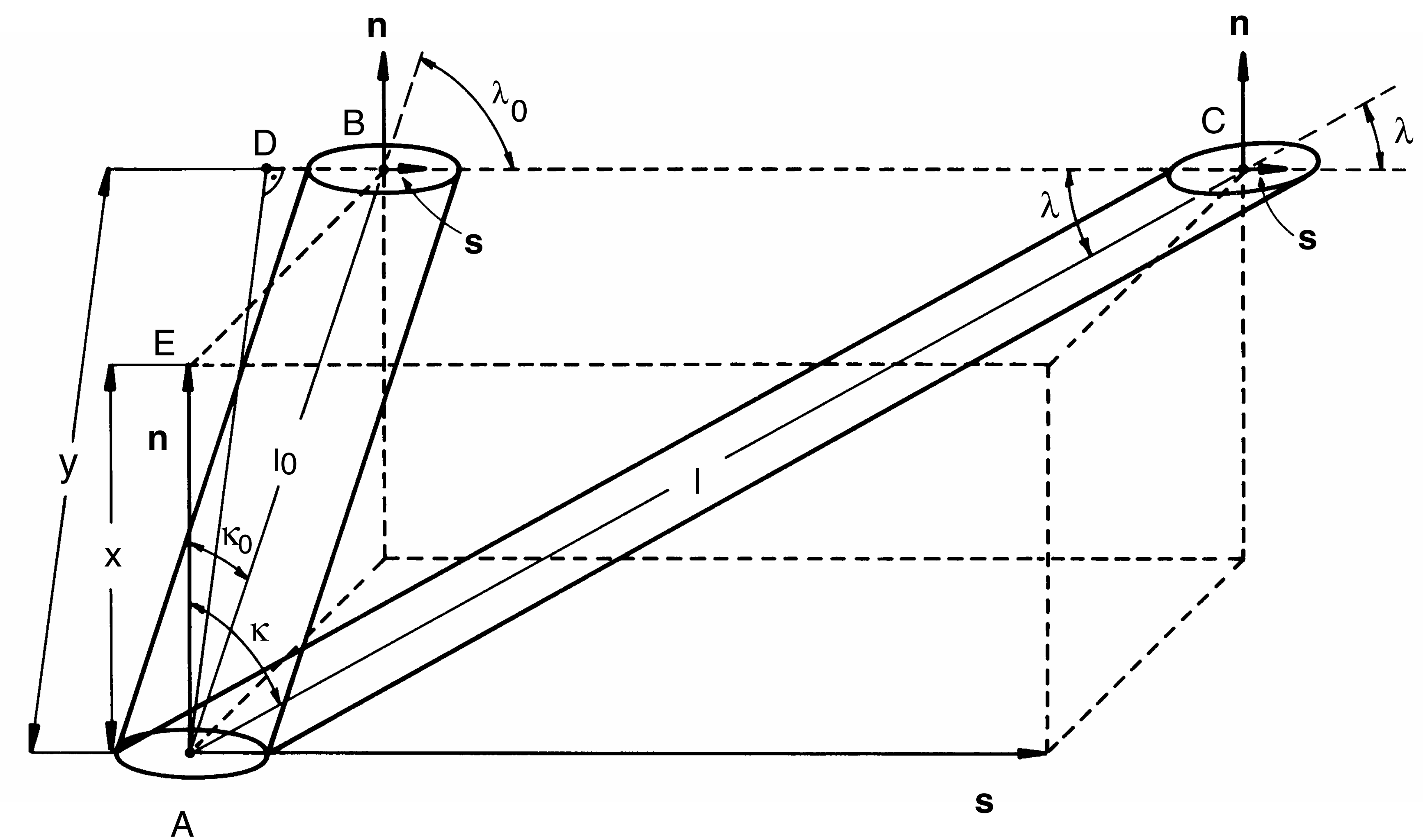

$$l \cos \kappa = l_0 \cos \kappa_0$$

$$l \sin \lambda = l_0 \sin \lambda_0$$

lattice slip kinematics (tension)

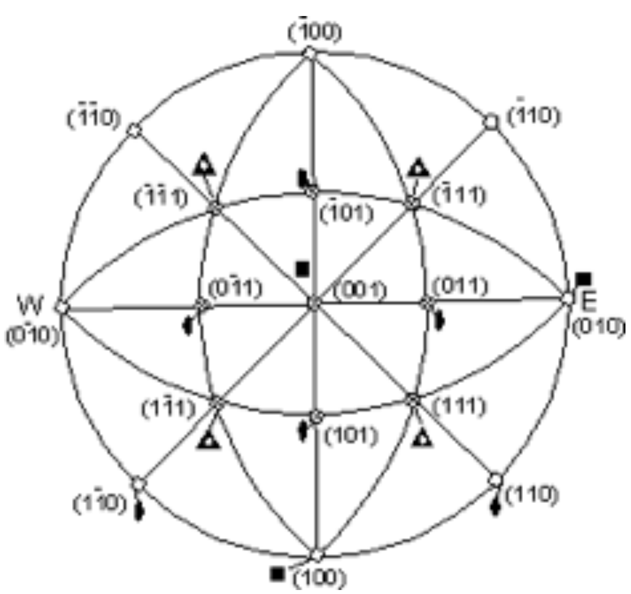

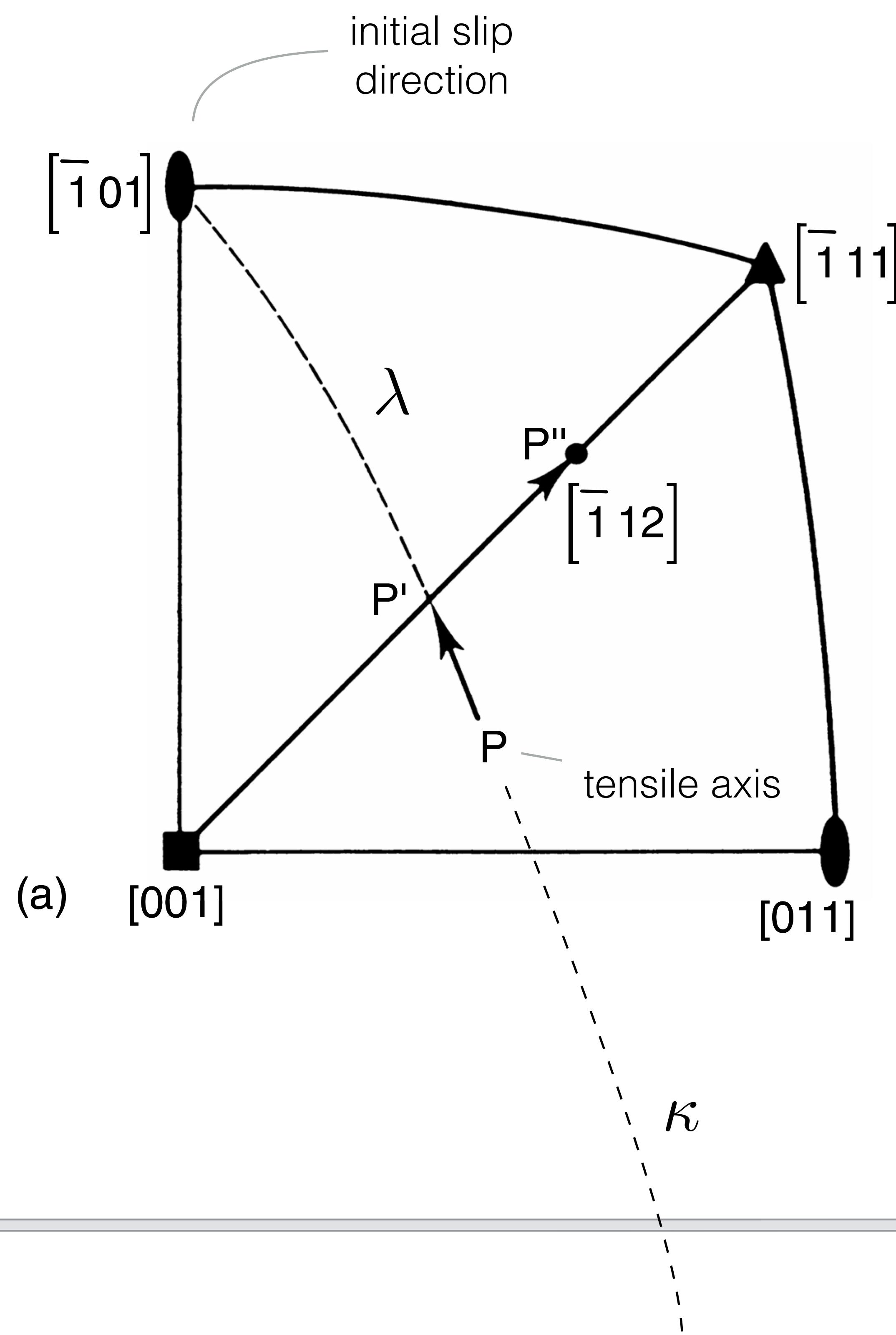

$$l \cos \kappa = l_0 \cos \kappa_0$$

$$l \sin \lambda = l_0 \sin \lambda_0$$

lattice slip kinematics

$$\frac{\partial \mathbf{u}}{\partial \mathbf{y}}\,\mathbf{h} = \mathbf{b}$$

$$\frac{\partial \mathbf{u}}{\partial \mathbf{y}}\,h\,\mathbf{n} = b\,\mathbf{m}$$

$$\frac{\partial \mathbf{u}}{\partial \mathbf{y}} = \frac{b}{h}\,\mathbf{m}\otimes\mathbf{n}$$

$$\frac{\partial \mathbf{u}}{\partial \mathbf{y}} = \frac{b\,A}{V}\,\mathbf{m}\otimes\mathbf{n} = \gamma\,\mathbf{m}\otimes\mathbf{n}$$

$$\frac{\partial \mathbf{v}}{\partial \mathbf{y}} = \frac{b\,\dot{A}}{V}\,\mathbf{m}\otimes\mathbf{n} = \dot{\gamma}\,\underbrace{\mathbf{m}\otimes\mathbf{n}}_{\text{slip system geometry}}$$

lattice slip kinematics

$$\mathbf{L}_{\mathrm{p}} = \sum_{\alpha} \dot{\gamma}^{\alpha}\, \mathbf{m}^{\alpha} \otimes \mathbf{n}^{\alpha}$$

experimental background

single crystal deformation

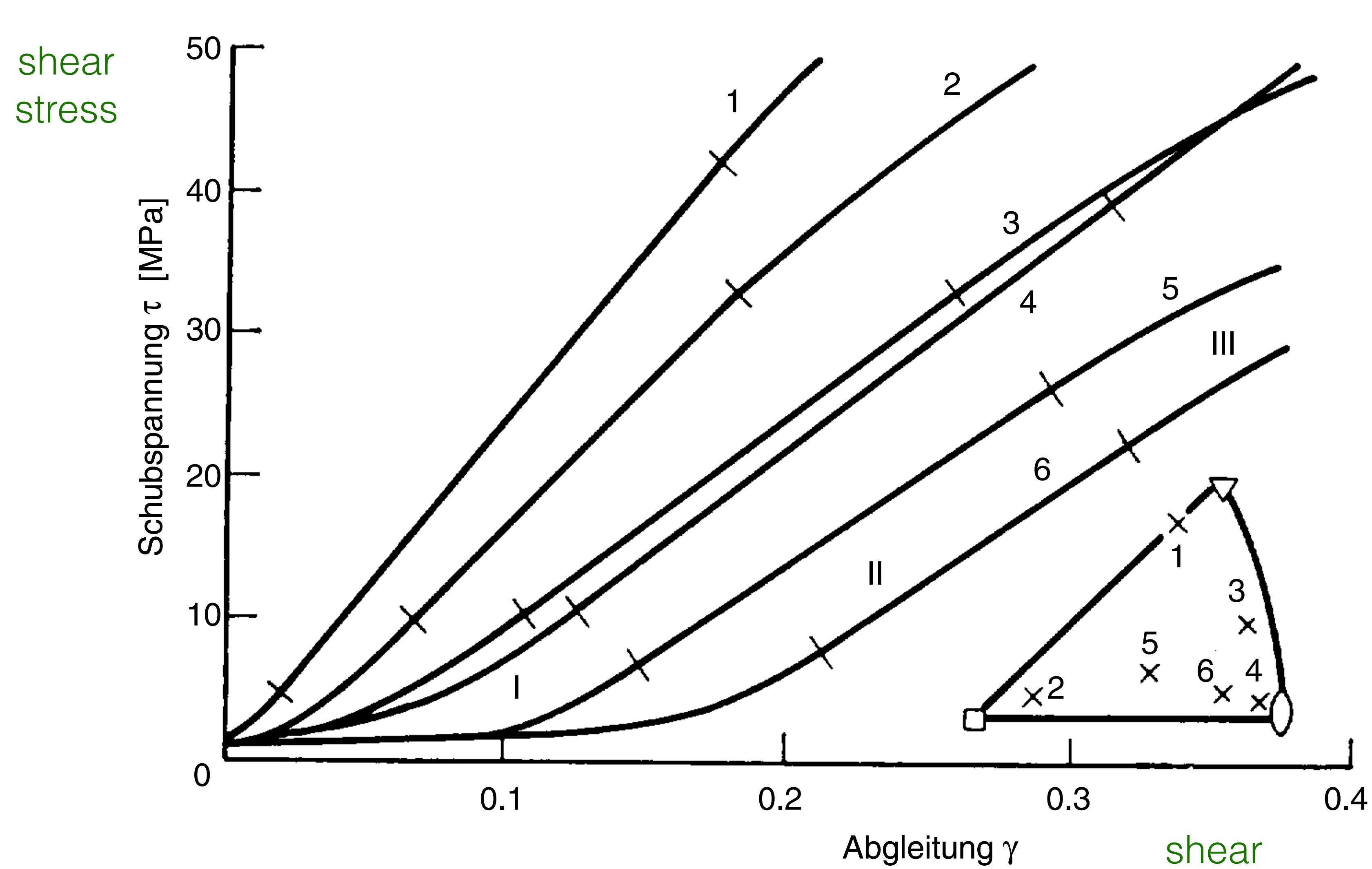

experimental background

single crystal deformation

- I: slip over large areas, little dislocation deposition on 2nd systems
- II: formation of locked configurations, fresh dislocations required
- III: increasing influence of dynamic annihilation

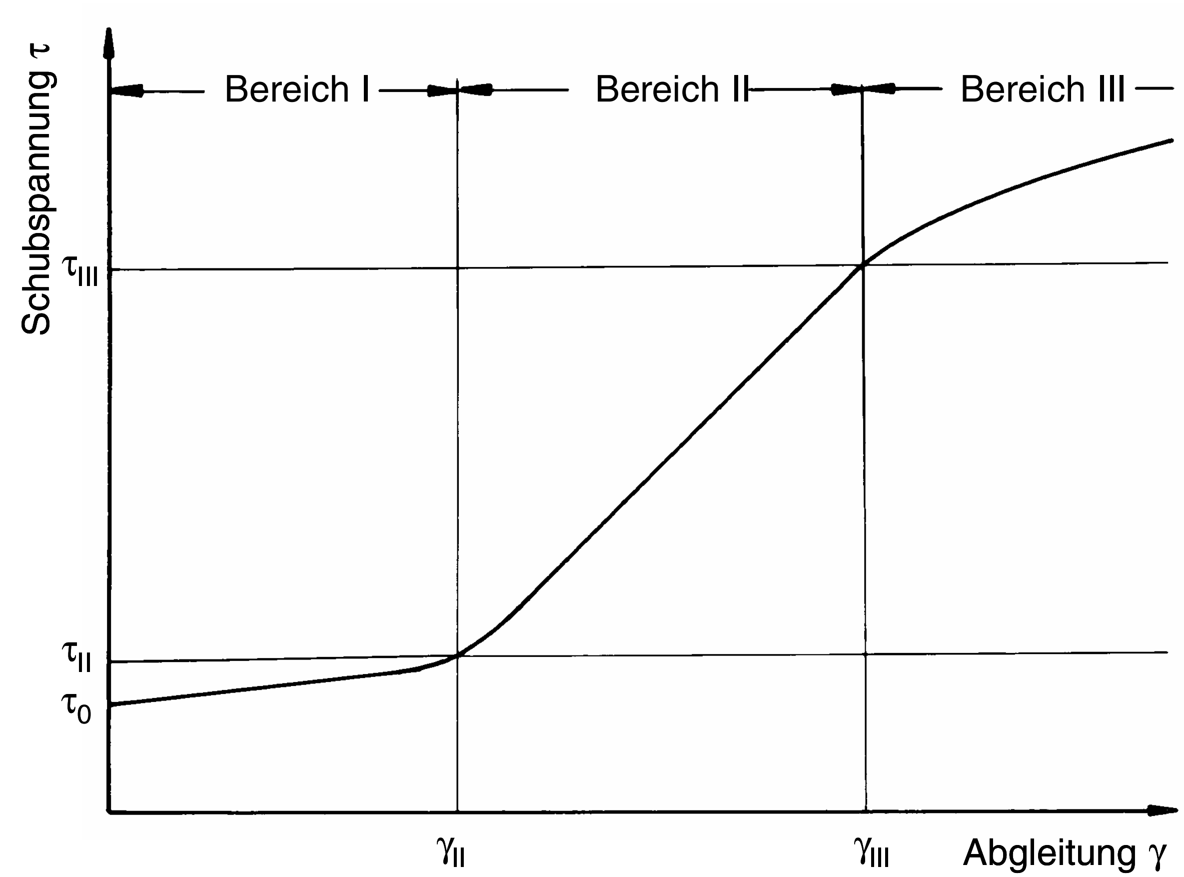

phenomenological description

- internal state parameterization
- internal state evolution
- slip kinetics

phenomenological description

internal state parameterization

- resistance to deformation on each slip system g^α

positive *and* negative sense

phenomenological description

internal state evolution

- slip causes change in deformation resistance

$$\mathrm{d}g^{\alpha} = h^{\alpha\beta} \left|\mathrm{d}\gamma^{\beta}\right|$$

$$\begin{aligned} \dot{g}^{\alpha} &= h^{\alpha\beta} \left|\dot{\gamma}^{\beta}\right| \\ &= q^{\alpha\beta}\, h_0 \left[\operatorname{sgn}\left(1 - \frac{g}{g_\infty}\right) \left|1 - \frac{g}{g_\infty}\right|^{a}\right] \left|\dot{\gamma}^{\beta}\right| \end{aligned}$$

slip system interaction

saturation level

phenomenological description

slip kinetics

- non-linear relation between deformation rate and applied stress

stress sensitivity or rate insensitivity

$$\dot{\gamma}^\alpha = \dot{\gamma}_0 \left| \frac{\tau^\alpha}{g^\alpha} \right|^n \operatorname{sgn}(\tau^\alpha)$$

phenomenological description

advantages

- relatively simple
- 10 parameters

drawbacks

- no intrinsic temperature dependence
- no clear mechanism(s) for internal state evolution

dislocation density-based description

- internal state parameterization
- internal state evolution
- slip kinetics

dislocation density-based description

internal state parameterization

- dislocation density on each slip system ϱ^α

dislocation density-based description

internal state evolution

- dislocation production $\dot{\varrho}^{\alpha}_{+}$
- dislocation annihilation $\dot{\varrho}^{\alpha}_{-}$

dislocation density-based description

internal state evolution: production

- dislocations get stuck while slipping
- geometric parameter: slipped area per deposited dislocation length

$$\Lambda$$

- rate of dislocation density increase

$$b\,\Lambda\,\frac{V}{V} = \frac{\mathrm{d}\gamma^\alpha}{\mathrm{d}\varrho^\alpha}$$

dislocation density-based description

internal state evolution: production

- geometric parameter is structure dependent

$$\Lambda \propto \varrho^{-0.5}$$

$$\mathrm{d}\varrho^\alpha = \frac{\sqrt{\varrho^\alpha}}{b\,c_\Lambda}\,|\mathrm{d}\gamma^\alpha|$$

$$\dot{\varrho}^\alpha = \frac{\sqrt{\varrho^\alpha}}{b\,c_\Lambda}\,|\dot{\gamma}^\alpha|$$

dislocation density-based description

internal state evolution: annihilation

- encounter of compatible slipped area
- sampled volume fraction

$$\begin{aligned}\mathrm{d}\varrho_-^\alpha &= 2\varrho^\alpha\,\mathrm{dln}V \\ &= 2\cdot 2\varrho^\alpha\,\frac{d^\star}{b}\,|\mathrm{d}\gamma^\alpha|\end{aligned}$$

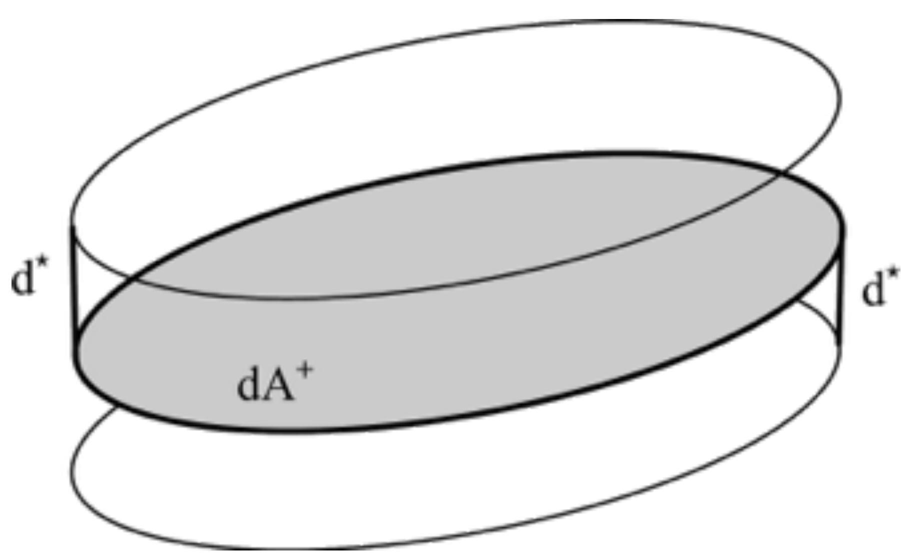

$$\begin{aligned}\mathrm{dln}V &= \frac{\mathrm{d}A^+}{V}\,2d^\star \\ &= \frac{\mathrm{d}\gamma}{b}\,2d^\star\end{aligned}$$

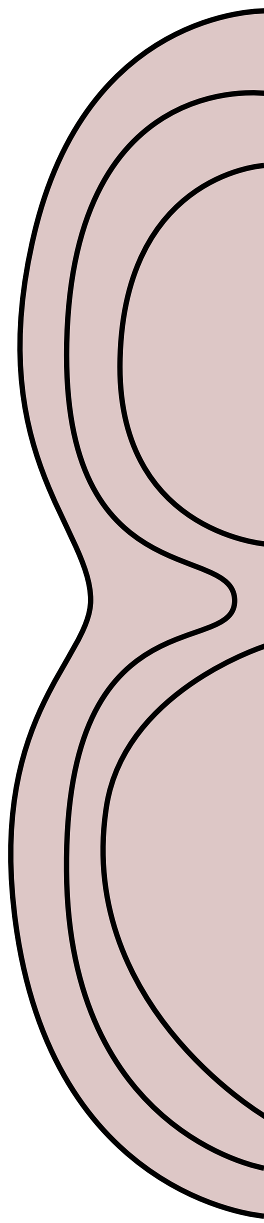

dislocation density-based description

internal state evolution: additional states

- stable dipoles as precursor for annihilation following glide-independent process
- locked dislocation situations
- …

dislocation density-based description

slip kinetics

- Orowan equation $$\dot{\gamma}^\alpha = \varrho^\alpha \, b \, v^\alpha$$

velocity of
dislocation motion

dislocation density-based description

possible obstacles to dislocation motion

- dislocation structure
- Peierls barrier
- solute atoms (or clusters)

dislocation density-based description

dislocation density as obstacle to dislocation motion

- no thermal activation possible
- mechanical threshold

$$\tau_{\text{eff}} = \begin{cases} \left(|\tau| - \tau_{\text{cr}}\right) \operatorname{sgn}(\tau) & \text{if } |\tau| > \tau_{\text{cr}} \\ 0 & \text{if } |\tau| \leq \tau_{\text{cr}} \end{cases}$$

- slip system interaction

$$\tau_{\text{cr}}^{\alpha} = \mu\, b \sqrt{a_{\alpha\beta}\, \varrho^{\beta}}$$

dislocation density-based description

slip system interactions (fcc)

- self
- coplanar
- collinear
- Hirth lock
- Lomer lock
- glissile junction

$\zeta \backslash \xi$	1	2	3	4	5	6	7	8	9	10	11	12
1	s	cp	cp	h	l	g	cl	g	g	h	g	l
2	cp	s	cp	l	h	g	g	h	l	g	cl	g
3	cp	cp	s	g	g	cl	g	l	h	l	g	h
4	h	l	g	s	cp	cp	h	g	l	cl	g	g
5	l	h	g	cp	s	cp	g	cl	g	g	h	l
6	g	g	cl	cp	cp	s	l	g	h	g	l	h
7	cl	g	g	h	g	l	s	cp	cp	h	l	g
8	g	h	l	g	cl	g	cp	s	cp	l	h	g
9	g	l	h	l	g	h	cp	cp	s	g	g	cl
10	h	g	l	cl	g	g	h	l	g	s	cp	cp
11	g	cl	g	g	h	l	l	h	g	cp	s	cp
12	l	g	h	g	l	h	g	g	cl	cp	cp	s

dislocation density-based description

slip system interactions (fcc)

- determination of interaction strength from computational experiments using discrete dislocation dynamics

interaction type	interaction coefficient
self	0
coplanar	0
collinear	0.625
Hirth	0.07
glissile	0.137
Lomer	0.122

Kubin et al. 2008
PhD thesis Kords 2013

dislocation density-based description

thermally activated obstacles

- solid solution atoms
- Peierls barrier

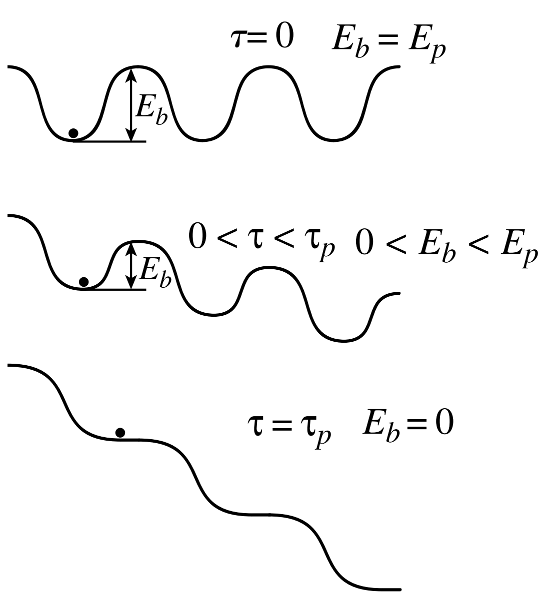

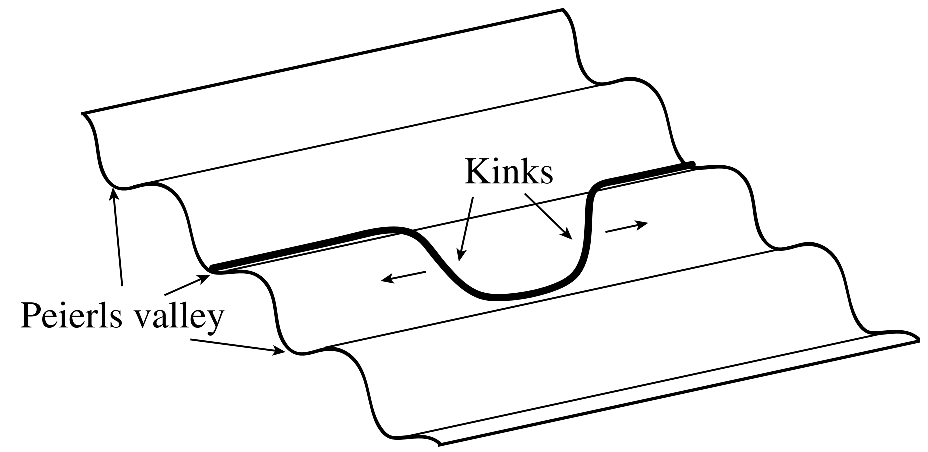

dislocation density-based description

thermally activated obstacles

- solid solution atoms
- Peierls barrier
- probability to overcome obstacle

activation energy $Q = \hat{\tau}\, A\, b = \hat{\tau}\, l\, s\, b$

$$P = \exp\left(-\frac{Q}{k_\mathrm{B} T}\left(1 - \left(\frac{|\tau_\mathrm{eff}|}{\hat{\tau}}\right)^p\right)^q\right)$$

dislocation density-based description

thermally activated obstacles

- solid solution atoms $l_\mathrm{S} = \dfrac{b}{\sqrt{c_\mathrm{at}}}$ $s_\mathrm{S} = d_\mathrm{obst}$
- Peierls barrier $l_\mathrm{p} = w_\mathrm{kink}$ $s_\mathrm{p} = b$

activation energy $Q = \hat{\tau}\, A\, b = \hat{\tau}\, l\, s\, b$

- probability to overcome obstacle

$$P = \exp\left(-\frac{Q}{k_\mathrm{B} T}\left(1 - \left(\frac{|\tau_\mathrm{eff}|}{\hat{\tau}}\right)^p\right)^q\right)$$

dislocation density-based description

effective velocity of obstacle overcoming

attempt frequency

- waiting time at obstacle $$t = (\nu_\mathrm{a}\, P)^{-1}$$

- average travel distance between obstacles $$\lambda_\mathrm{S} = \frac{b}{\sqrt{c_\mathrm{at}}} \qquad \lambda_\mathrm{P} = b$$

- travel velocity between obstacles $$v_\mathrm{T} = M\,|\tau_\mathrm{eff}|$$

dislocation density-based description

effective velocity of obstacle overcoming

$$v = \frac{\lambda}{t + \frac{\lambda}{v_\mathrm{T}}} = \left(\frac{t}{\lambda} + \frac{1}{v_\mathrm{T}} \right)^{-1}$$

$$\frac{t}{\lambda} = \frac{t_\mathrm{P}}{\lambda_\mathrm{P}} + \frac{t_\mathrm{S}}{\lambda_\mathrm{S}} + \ldots$$

tension of a single crystal compared to a bicrystal

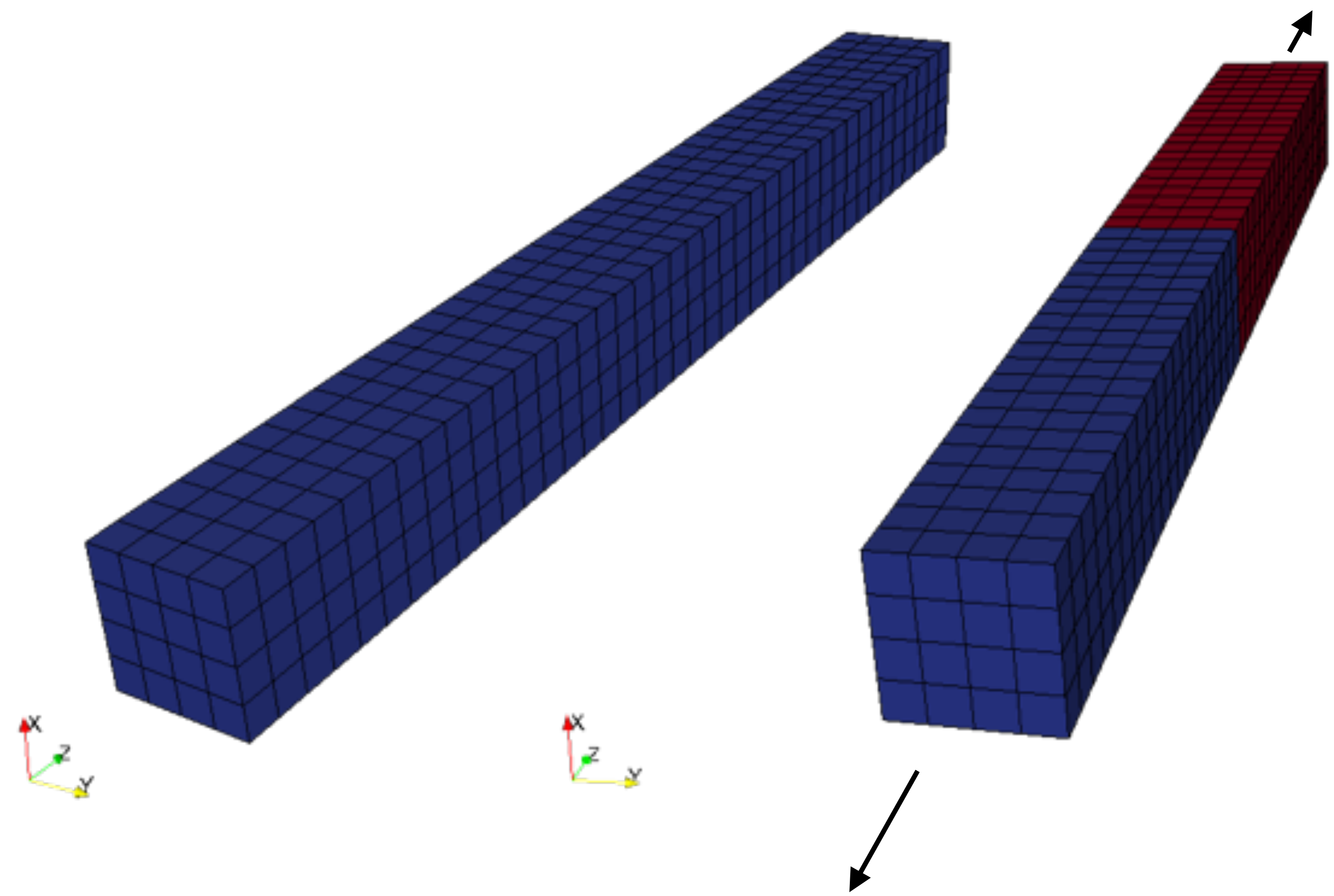

homogenization schemes

problem

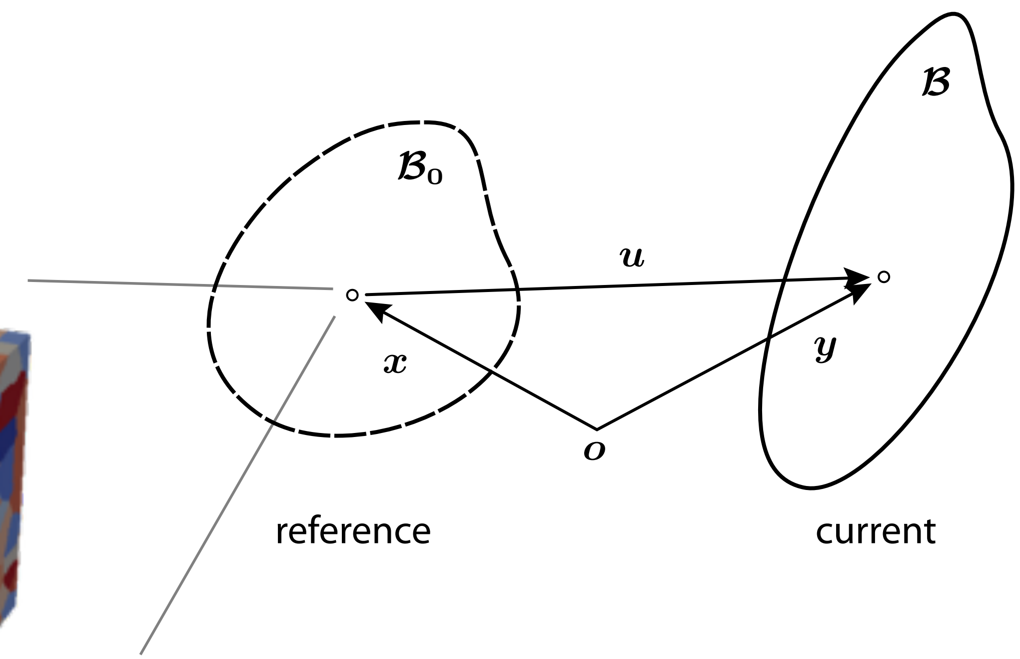

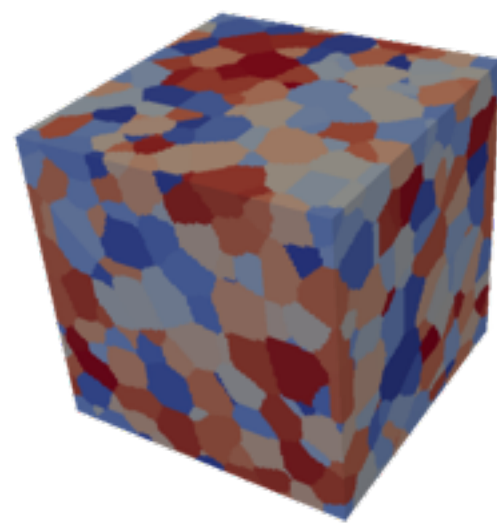

known

$\overline{\mathbf{F}}$ → $\overline{\mathbf{P}}$

$\overline{\mathbf{P}}$ → $\overline{\mathbf{F}}$

unknown

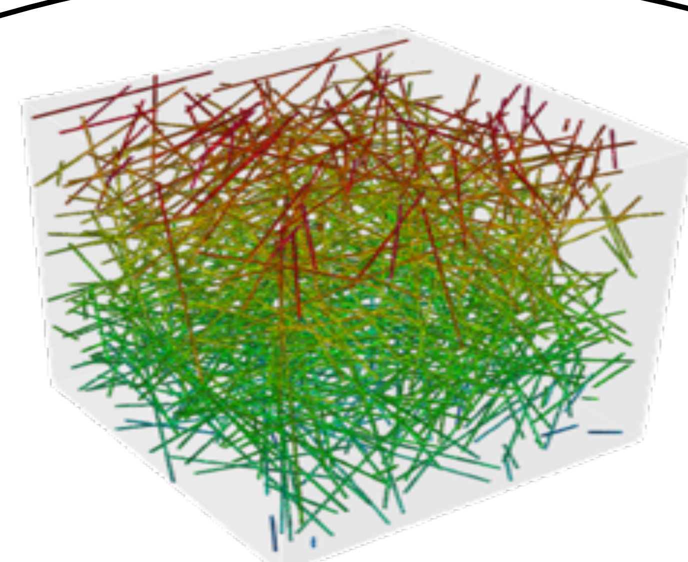

solutions

- mean-field methods
- grain cluster approaches
- computational homogenization

mean-field methods

- no rigorous solution of microscopic boundary value problem

- spatially averaged quantities

homogeneous in inclusion (i)

$$\overline{\mathbf{F}} = \frac{1}{V_0} \sum V_0^{(i)} \mathbf{F}^{(i)} = \langle \mathbf{F}^{(i)} \rangle$$

$$\overline{\mathbf{P}} = \frac{1}{V_0} \sum V_0^{(i)} \mathbf{P}^{(i)} = \langle \mathbf{P}^{(i)} \rangle$$

mean-field methods

iso-strain

$$\mathbf{F}^{(i)} = \overline{\mathbf{F}}$$

$$\overline{\mathbf{P}} = \langle \mathbf{P}^{(i)} \rangle$$

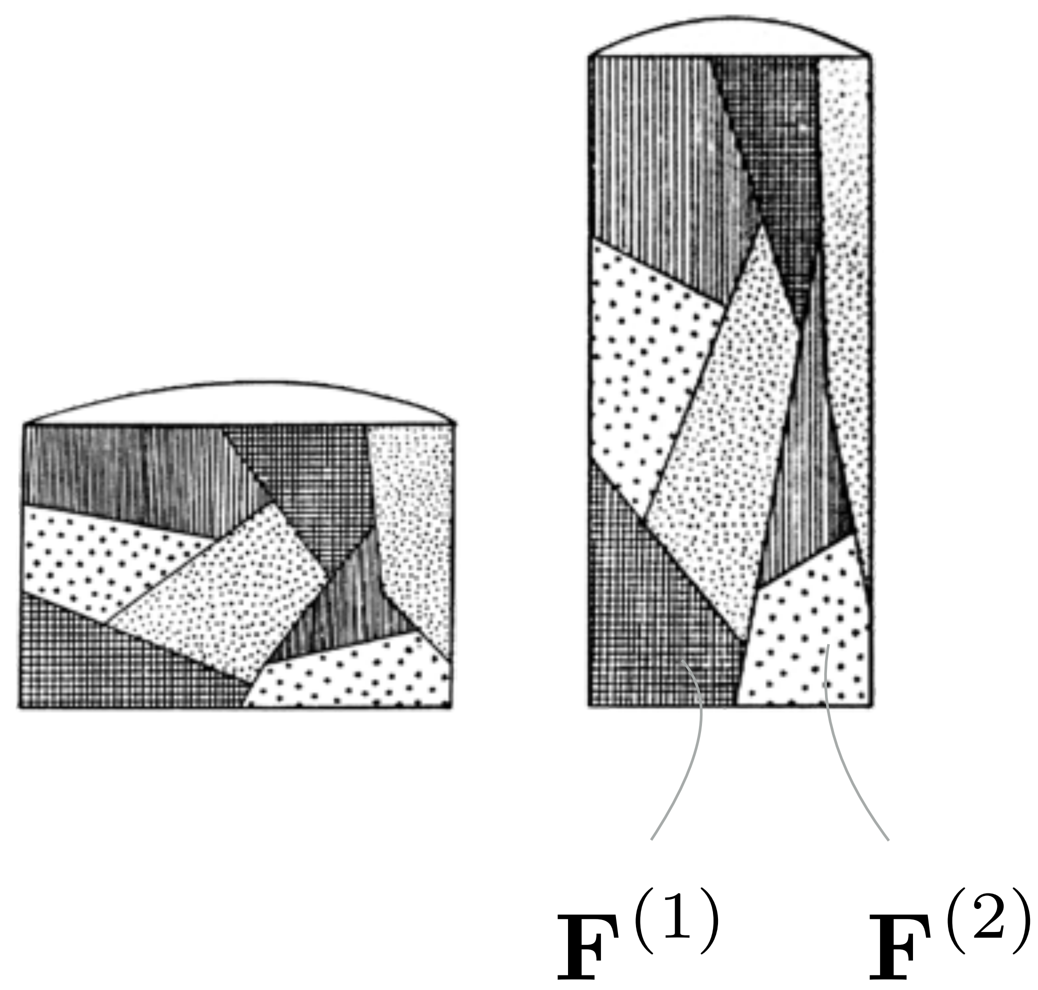

Taylor, G. I. (1938). Plastic strain in metals. J. Inst. Metals, 62, 307–324.

mean-field methods

iso-stress

$$\mathbf{P}^{(i)} = \overline{\mathbf{P}}$$

$$\overline{\mathbf{F}} = \langle \mathbf{F}^{(i)} \rangle$$

mean-field methods

ratio of shear stress to
maximum resolved shear stress

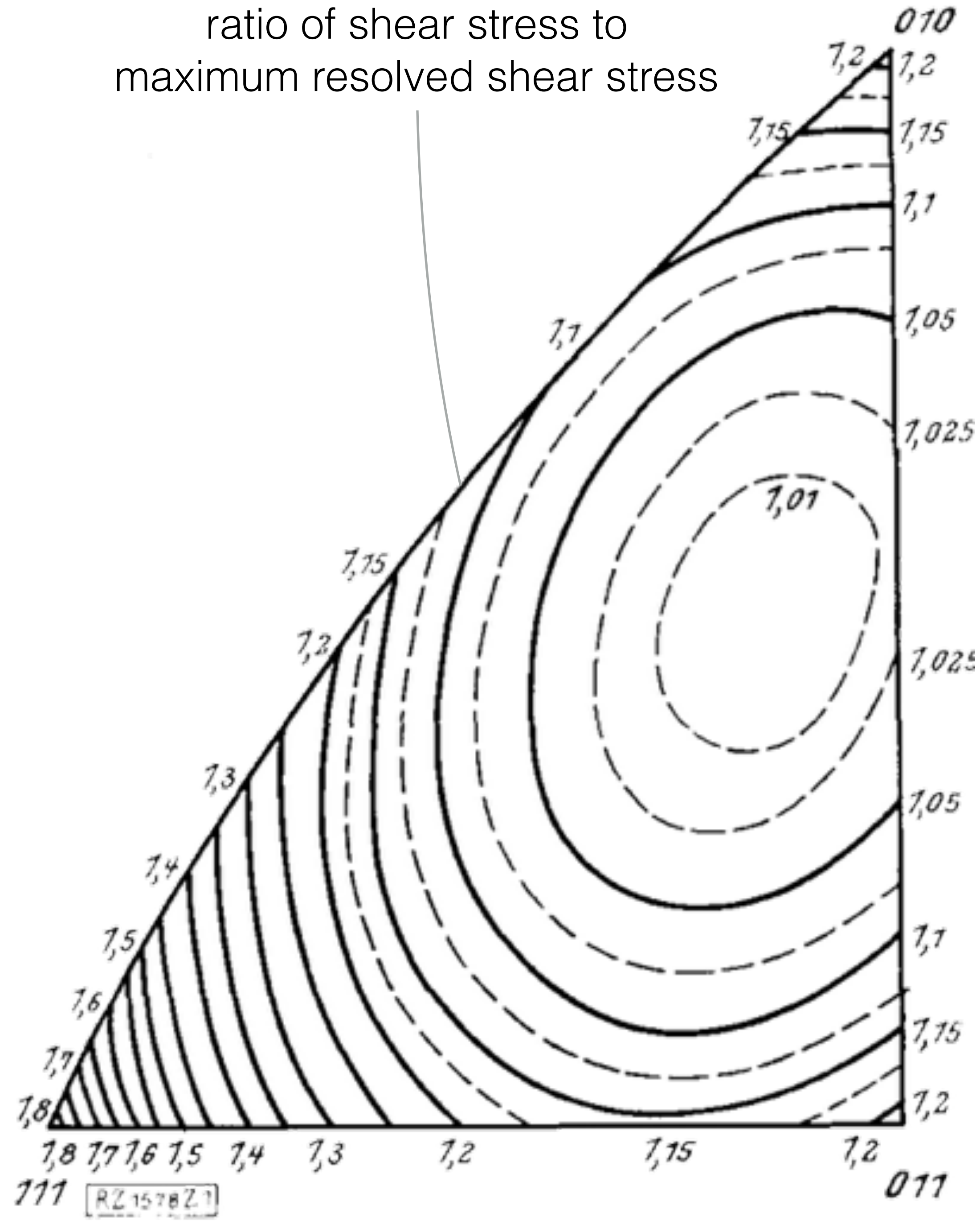

equal resolved stress

assumed stress state
(unit tensor)

$$\mathbf{P}^{(i)} = \lambda^{(i)}\mathbf{P}^{*}$$

selected such that critical resolved
shear stress is reached on most
highly stressed slip system

$$\overline{\mathbf{F}} = \langle \mathbf{F}^{(i)} \rangle$$

Sachs, G. (1928). Zur Ableitung einer Fließbedingung.
Z. Ver. Deutsch. Ing., 72, 734–736.

mean-field methods

iso-work rate

- variable deformation rate $$\dot{\mathbf{F}}^{(i)} = \lambda^{(i)} \dot{\bar{\mathbf{F}}}$$
- volume average $$\dot{\bar{\mathbf{F}}} = \sum \nu^{(i)} \dot{\mathbf{F}}^{(i)}$$
- constraint $$\sum \nu^{(i)} \lambda^{(i)} = 1$$

Tjahjanto, D. D., Roters, F., & Eisenlohr, P. (2007). Iso-work-rate weighted-Taylor homogenization scheme for multiphase steels assisted by transformation-induced plasticity effect. steel research, 78(10-11), 777–783.

mean-field methods

iso-work rate

- equivalent rate of work $$\mathbf{P}^{(i)} \cdot \dot{\mathbf{F}}^{(i)} = \mathbf{P}^{(N)} \cdot \dot{\mathbf{F}}^{(N)}$$

- non-linear equation system for free parameters $$\left[\lambda^{(i)}\mathbf{P}^{(i)}(\lambda^{(i)}) - \lambda^{(N)}\mathbf{P}^{(N)}(\lambda^{(N)})\right] \cdot \dot{\bar{\mathbf{F}}} = 0$$

Tjahjanto, D. D., Roters, F., & Eisenlohr, P. (2007). Iso-work-rate weighted-Taylor homogenization scheme for multiphase steels assisted by transformation-induced plasticity effect. steel research, 78(10-11), 777–783.

mean-field methods

(elastic) composites

$$\boldsymbol{\sigma}_0 = \mathbb{C}_0 \boldsymbol{\epsilon}_0$$

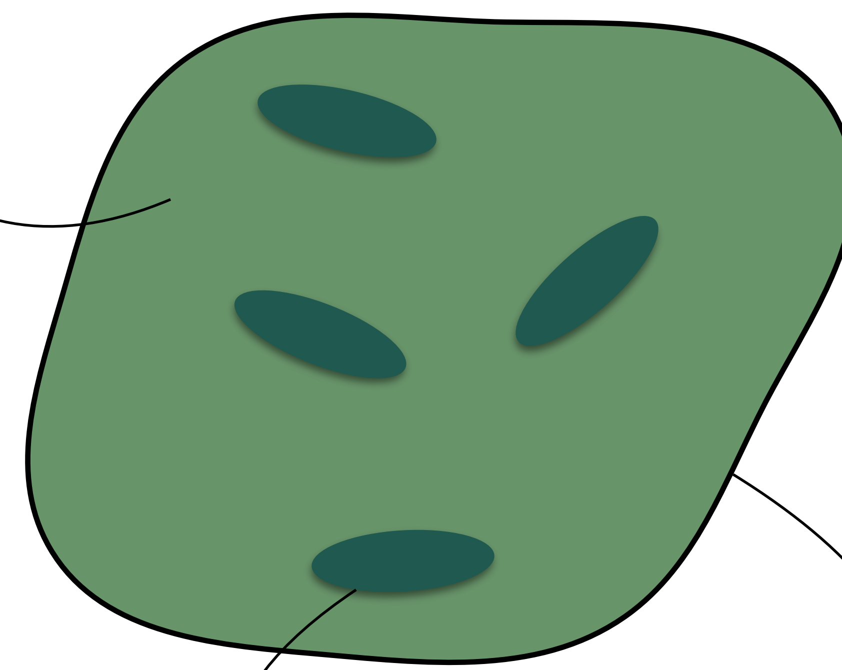

- strain localization tensors

$$\boldsymbol{\epsilon}_1 = \mathbb{A}\boldsymbol{\epsilon}$$

$$\boldsymbol{\epsilon}_1 = \mathbb{B}\boldsymbol{\epsilon}_0$$

$$\mathbb{A} = \mathbb{B} : \left[\nu_0 \mathbb{I} + \nu_1 \mathbb{B}\right]^{-1}$$

$$\boldsymbol{\sigma}_1 = \mathbb{C}_1 \boldsymbol{\epsilon}_1$$

$$\boldsymbol{\sigma} = \nu_0 \boldsymbol{\sigma}_0 + \nu_1 \boldsymbol{\sigma}_1$$

$$\boldsymbol{\epsilon} = \nu_0 \boldsymbol{\epsilon}_0 + \nu_1 \boldsymbol{\epsilon}_1$$

mean-field methods

(elastic) composites

$$\boldsymbol{\sigma}_0 = \mathbb{C}_0 \boldsymbol{\epsilon}_0$$

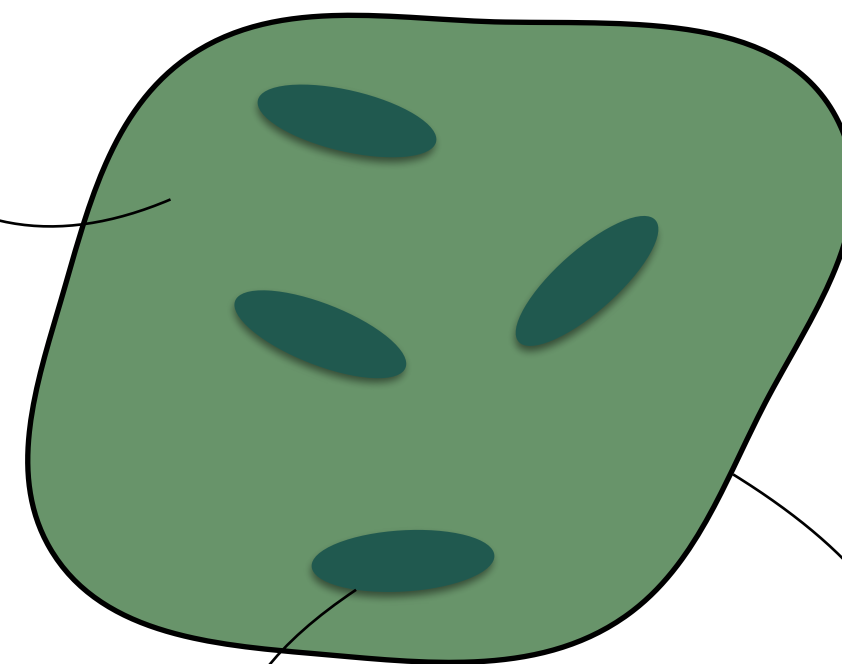

- macro stiffness

$$\boldsymbol{\sigma} = \mathbb{C}\, \boldsymbol{\epsilon}$$

$$\boldsymbol{\sigma}_1 = \mathbb{C}_1 \boldsymbol{\epsilon}_1$$

$$\mathbb{C} = [\nu_0 \mathbb{C}_0 + \nu_1 \mathbb{C}_1 : \mathbb{B}] : [\nu_0 \mathbb{I} + \nu_1 \mathbb{B}]^{-1}$$

$$\boldsymbol{\sigma} = \nu_0 \boldsymbol{\sigma}_0 + \nu_1 \boldsymbol{\sigma}_1$$

$$\boldsymbol{\epsilon} = \nu_0 \boldsymbol{\epsilon}_0 + \nu_1 \boldsymbol{\epsilon}_1$$

mean-field methods

(elastic) composites

- macro stiffness
$$\mathbb{C} = [\nu_0 \mathbb{C}_0 + \nu_1 \mathbb{C}_1 : \mathbb{B}] : [\nu_0 \mathbb{I} + \nu_1 \mathbb{B}]^{-1}$$
- iso-strain
$$\mathbb{B} = \mathbb{I}$$
- iso-stress
$$\mathbb{B} = \mathbb{C}_1{}^{-1} : \mathbb{C}_0$$

mean-field methods

Eshelby formalism

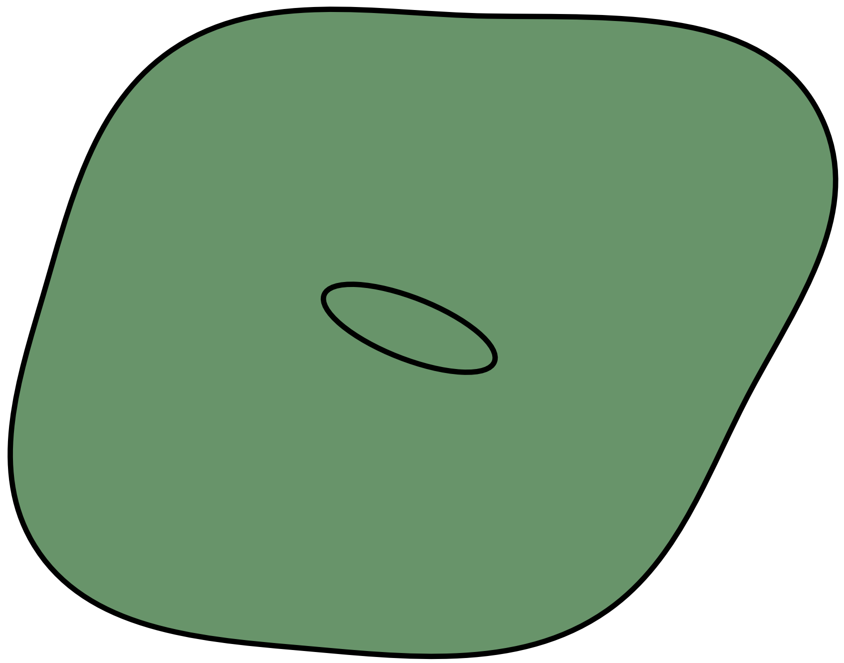

mean-field methods

Eshelby formalism

- cut out

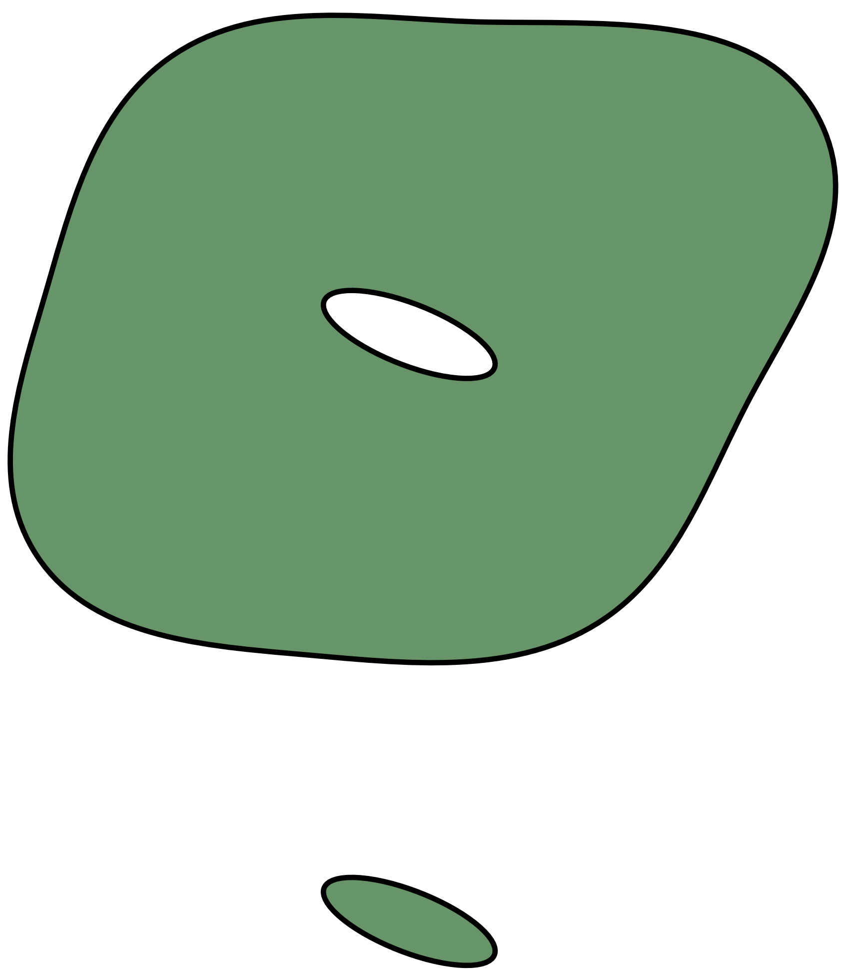

mean-field methods

Eshelby formalism

- cut out
- stress-free eigenstrain ϵ^*

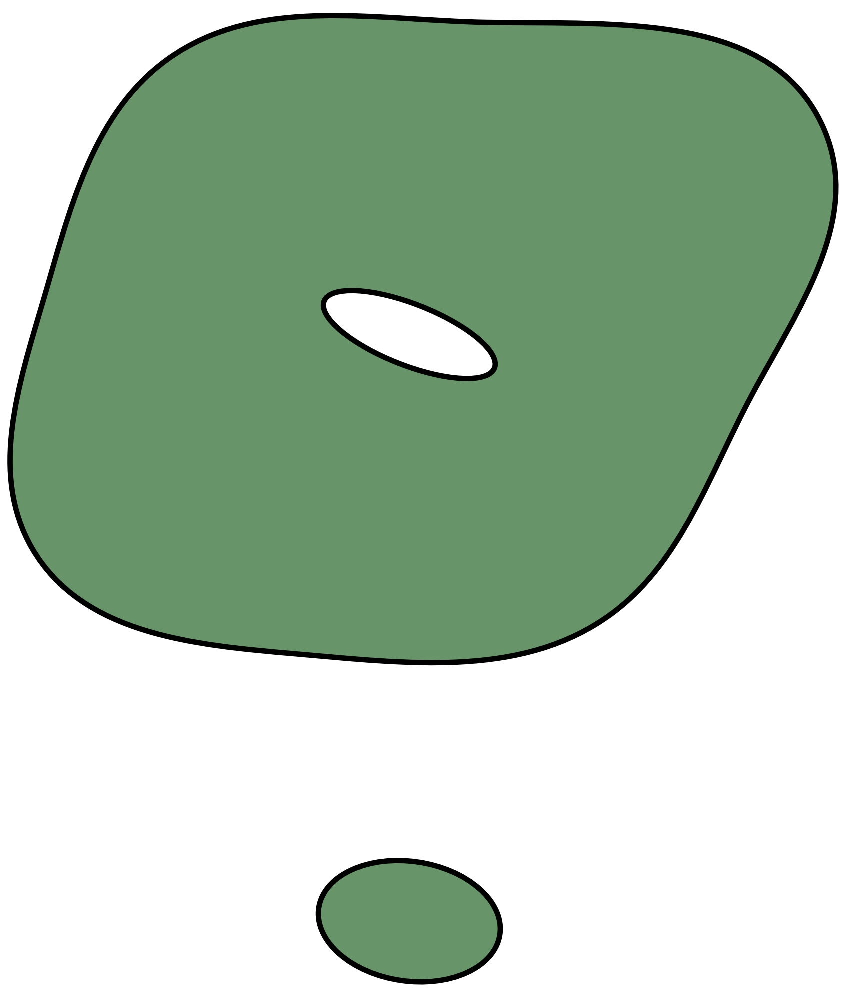

mean-field methods

Eshelby formalism

- cut out
- stress-free eigenstrain $\boldsymbol{\epsilon}^*$
- apply stress (or traction) $-\boldsymbol{\sigma}^*$

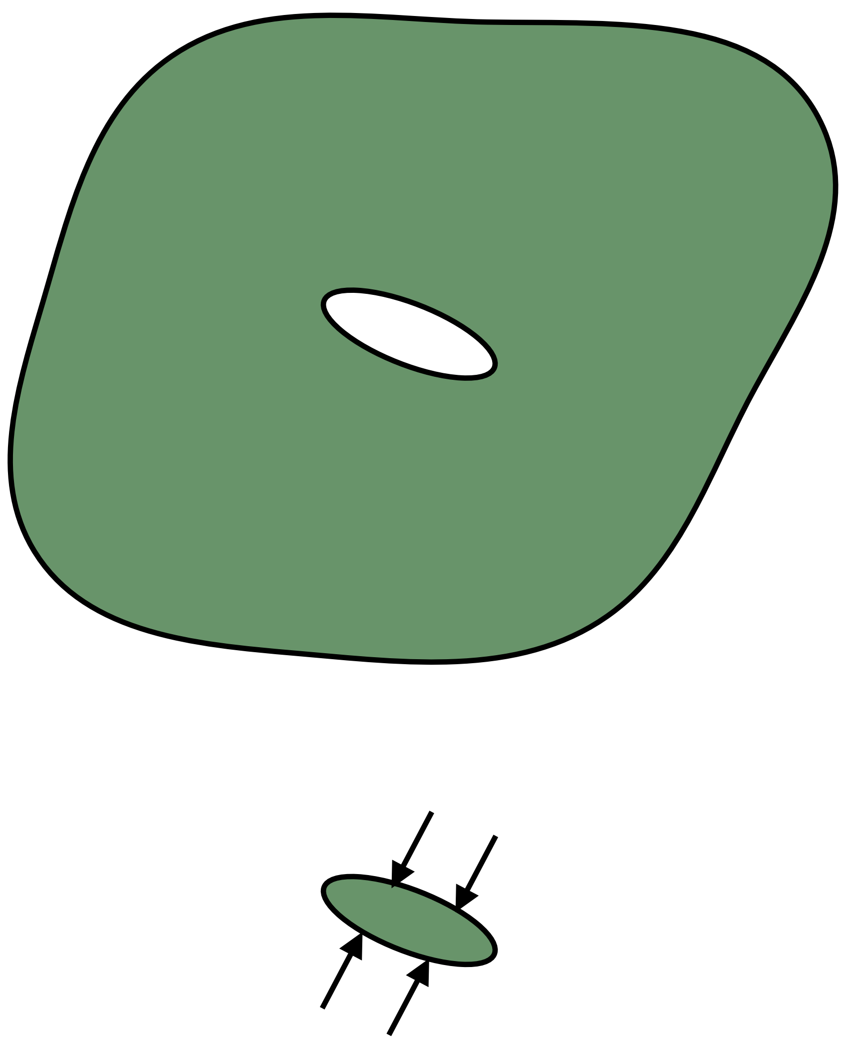

mean-field methods

Eshelby formalism

- cut out
- stress-free eigenstrain $\boldsymbol{\epsilon}^*$
- apply stress (or traction) $-\boldsymbol{\sigma}^*$
- put back

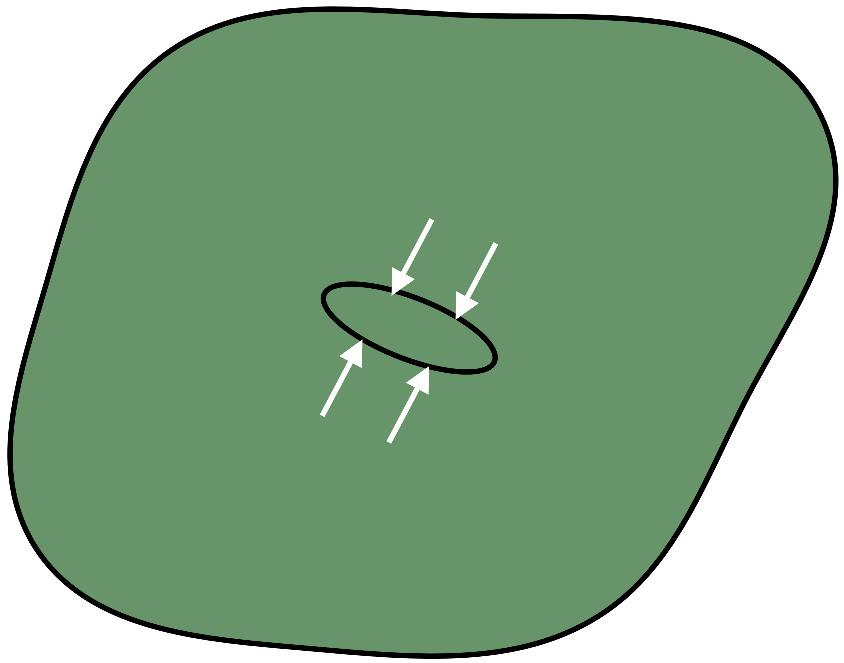

mean-field methods

Eshelby formalism

- cut out
- stress-free eigenstrain $\boldsymbol{\epsilon}^*$
- apply stress (or traction) $-\boldsymbol{\sigma}^*$
- put back

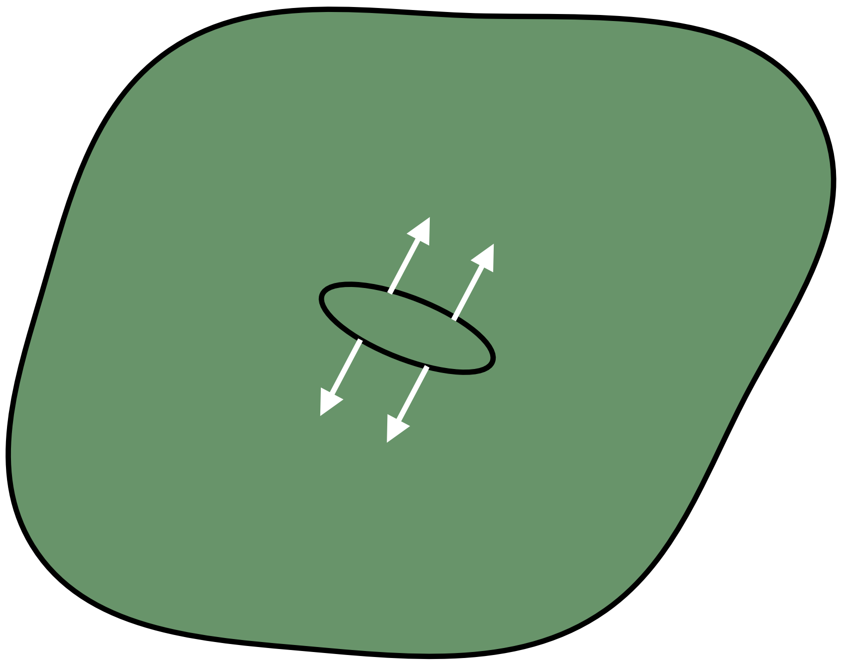

mean-field methods

Eshelby formalism

- cut out
- stress-free eigenstrain $\boldsymbol{\epsilon}^*$
- apply stress (or traction) $-\boldsymbol{\sigma}^*$
- put back
- release

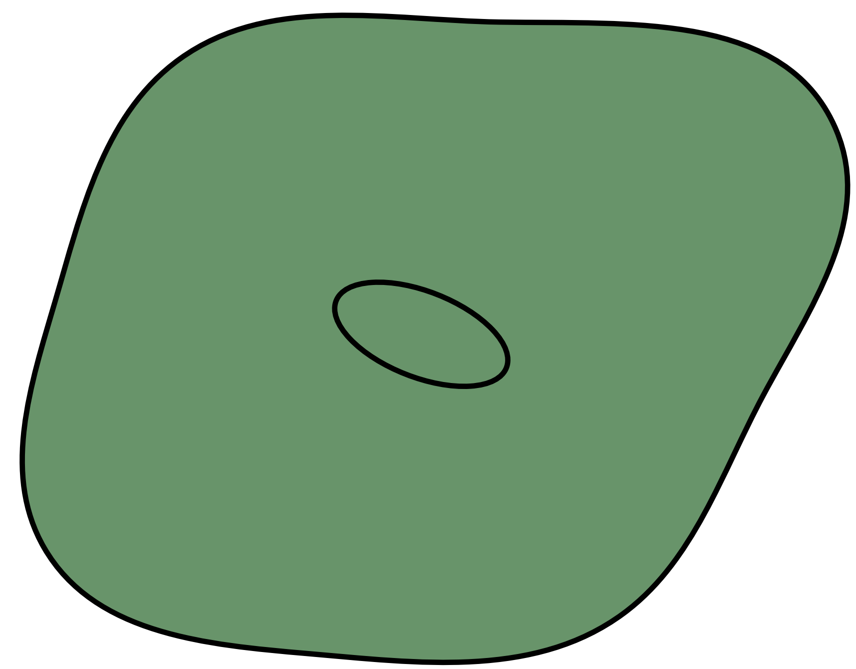

Eshelby tensor

Green’s function for displacement resulting from (point) body forces

$$\Rightarrow \boldsymbol{\epsilon}^{\mathrm{c}} = \mathbb{S}\,\boldsymbol{\epsilon}^* \equiv \mathrm{const}$$

within ellipsoidal inclusions

mean-field methods

isolated inclusion

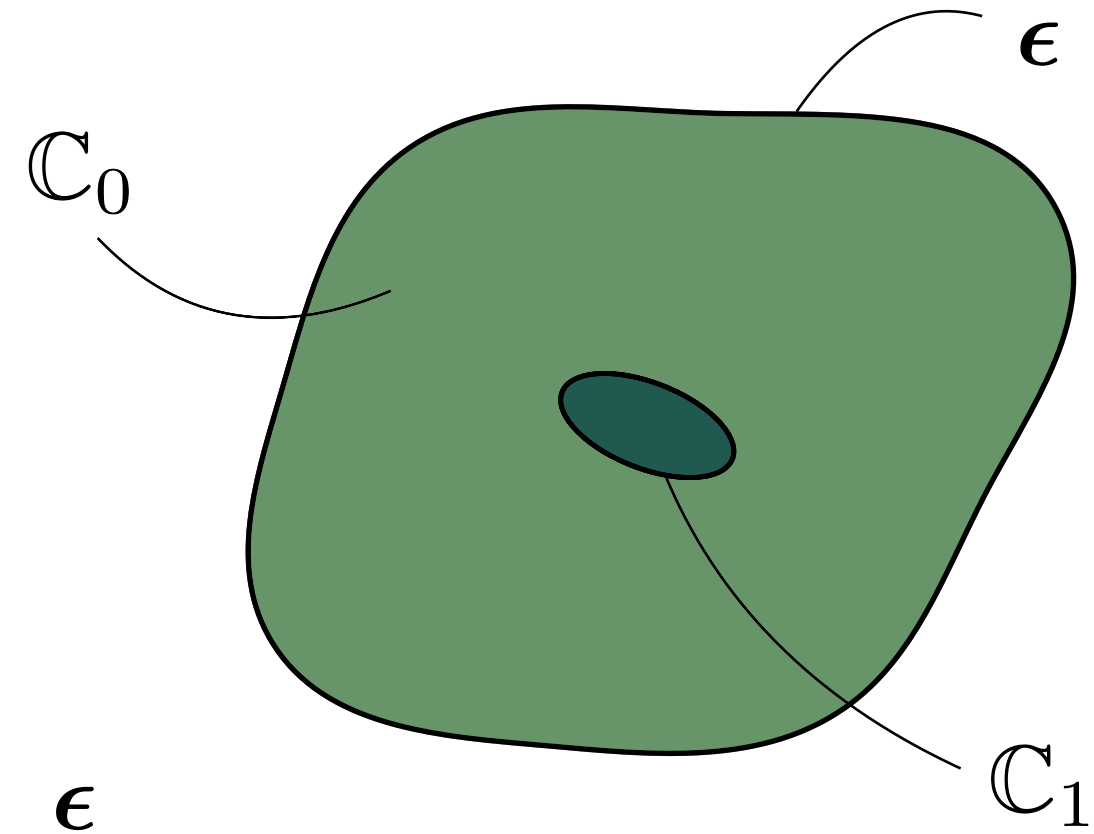

$$\boldsymbol{\epsilon}_1 = \underbrace{\mathbb{H}(I, \mathbb{C}_0, \mathbb{C}_1)}_{\left[\mathbb{I}+\mathbb{S}(I,\mathbb{C}_0):\mathbb{C}_0{}^{-1}:(\mathbb{C}_1-\mathbb{C}_0)\right]^{-1}} \boldsymbol{\epsilon}$$

shape (aspect ratios) and orientation of inclusion

mean-field methods

isolated inclusion

unknown composite modulus

- self-consistent

$$\boldsymbol{\epsilon}_1 = \mathbb{H}(I, \mathbb{C}, \mathbb{C}_1)\boldsymbol{\epsilon}$$

- Mori–Tanaka (1973)

$$\boldsymbol{\epsilon}_1 = \mathbb{H}(I, \mathbb{C}_0, \mathbb{C}_1)\boldsymbol{\epsilon}_0$$

inclusion experiences matrix strain as far-field strain

mean-field methods

summary

- inclined towards (relatively) isolated inclusions
  (no heterogeneous neighborhood)

- extension to non-linear materials not trivial

grain cluster methods

strategy

- partial relaxation of iso-strain assumption
- compatibility maintained on average
- stress equilibrium partly fulfilled

grain cluster methods

LAMEL

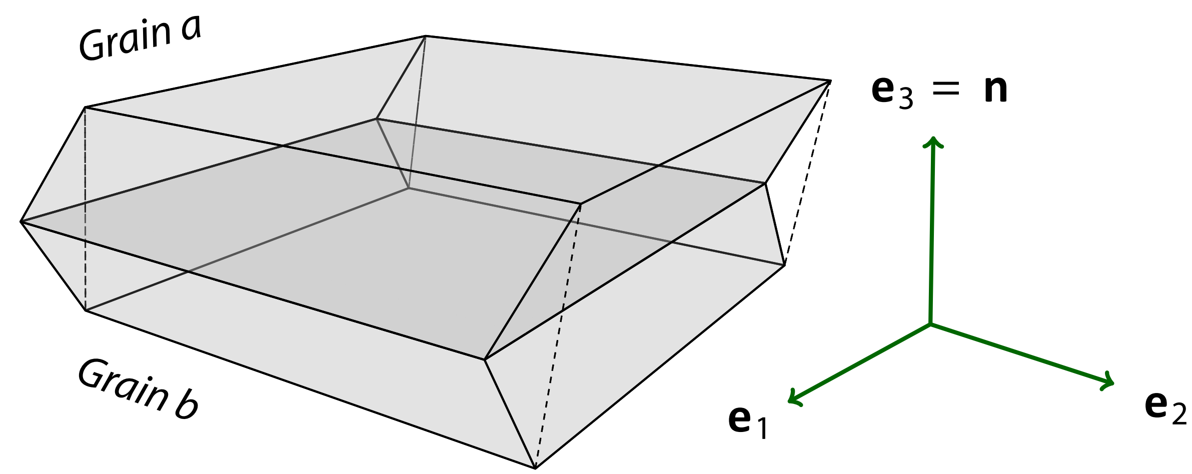

- stack of two “flat” grains
- stack experiences plastic velocity gradient
- each grain may deviate by two shear relaxation modes

$$\Delta\mathbf{L}_\mathrm{p} = \sum_{r=1}^{2} \dot{\gamma}^r_\mathrm{rlx}\mathbf{K}^r_\mathrm{rlx} = \dot{\gamma}^1_\mathrm{rlx}\begin{pmatrix}0 & 0 & 1\\ 0 & 0 & 0\\ 0 & 0 & 0\end{pmatrix} + \dot{\gamma}^2_\mathrm{rlx}\begin{pmatrix}0 & 0 & 0\\ 0 & 0 & 1\\ 0 & 0 & 0\end{pmatrix}$$

$$= \begin{pmatrix}0 & 0 & \dot{\gamma}^1_\mathrm{rlx}\\ 0 & 0 & \dot{\gamma}^2_\mathrm{rlx}\\ 0 & 0 & 0\end{pmatrix}$$

grain cluster methods

LAMEL

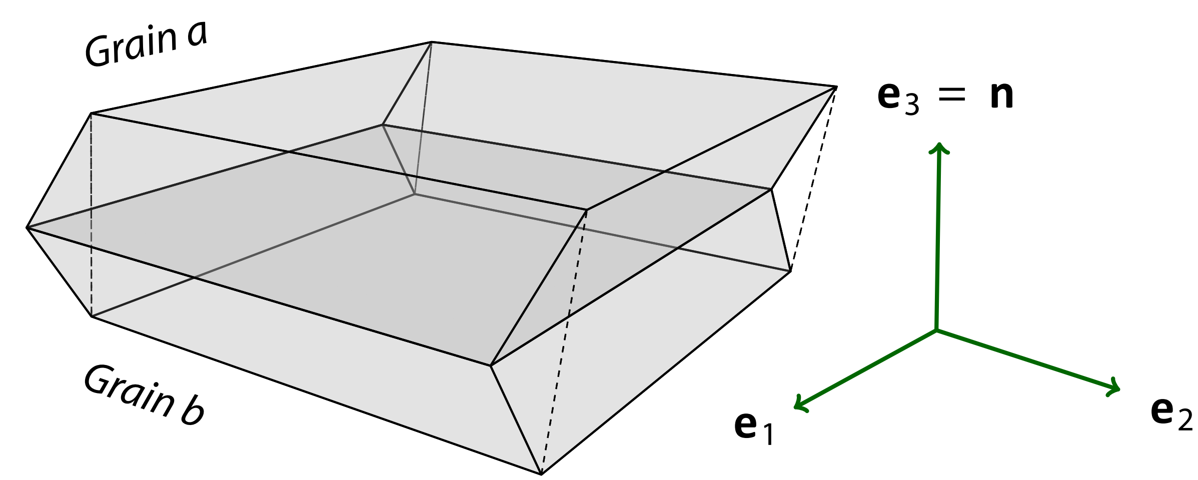

$$\mathbf{L}^a = \mathbf{L}_\mathrm{p} + \Delta\mathbf{L}_\mathrm{p} = \sum_{\alpha=1}^{N^a} \left(\mathbf{m}^\alpha \otimes \mathbf{n}^\alpha\right) \dot{\gamma}^\alpha$$

$$\mathbf{L}^b = \mathbf{L}_\mathrm{p} - \Delta\mathbf{L}_\mathrm{p} = \sum_{\beta=1}^{N^b} \left(\mathbf{m}^\beta \otimes \mathbf{n}^\beta\right) \dot{\gamma}^\beta \ ,$$

- symmetric distribution
  (valid for equal grain volume)

- usually slip system activity differs in both grains

grain cluster methods

LAMEL

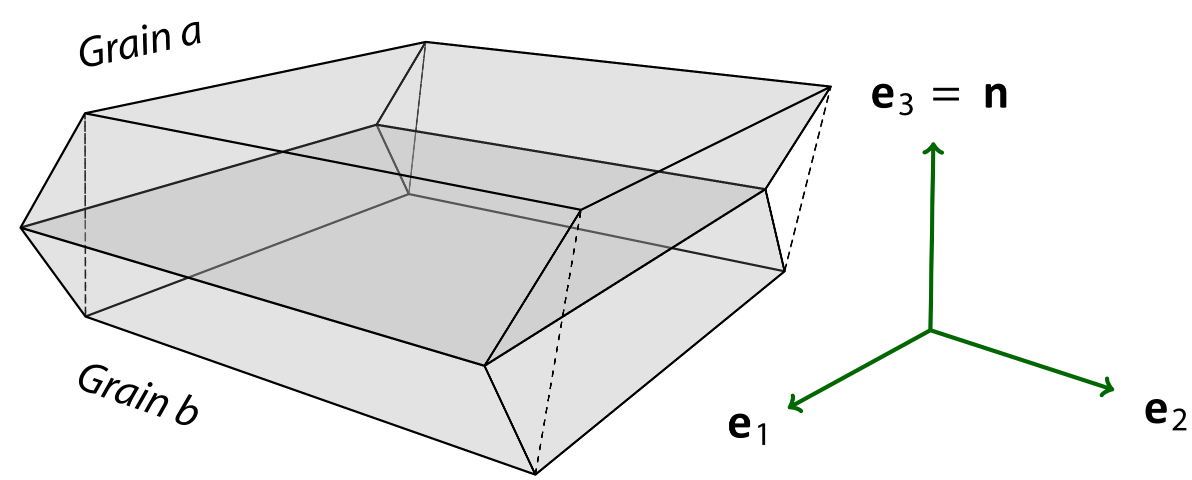

- solution minimizes plastic dissipation rate

$$\mathcal{P} = \sum_{\alpha=1}^{N^a} \tau^\alpha \, \dot{\gamma}^\alpha + \sum_{\beta=1}^{N^b} \tau^\beta \, \dot{\gamma}^\beta + \sum_{r=1} \tau^r_{\mathrm{rlx}} \, |\dot{\gamma}^r_{\mathrm{rlx}}| = \min$$

relaxation penalty stress

grain cluster methods

LAMEL advancements

- relax grain boundary neighborhoods

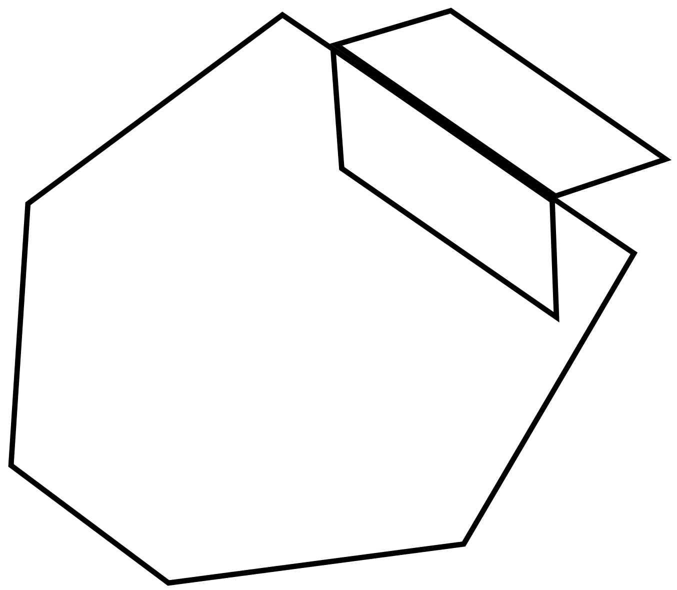

grain cluster methods

strategy

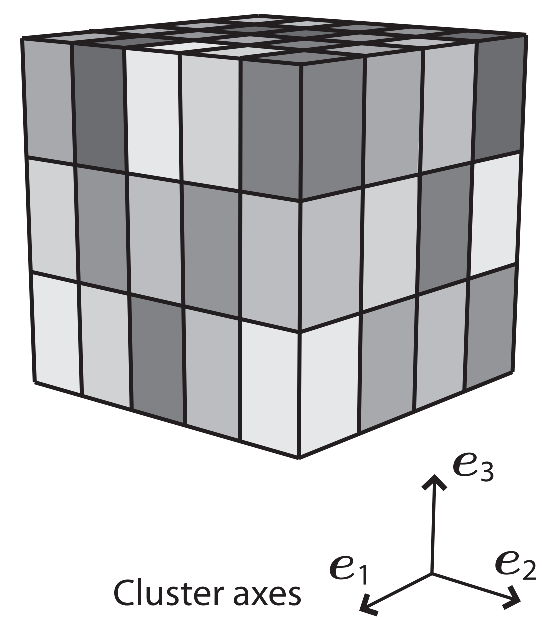

- extension of mono-directional to tri-directional “stack”

grain cluster methods

grain interaction (GIA) model (2 x 2 x 2 grains)

- relax all grain pairs stacked along the shortest and second shortest dimension as in LAMEL
- resulting incompatibility (excess/gaping) is translated into geometrically necessary dislocation density with associated (penalty) energy

- Wagner, P. (1994). Zusammenhange zwischen mikro- und makroskopischen Verformungsinhomogenitäten und der Textur. Ph.D. thesis, RWTH Aachen
- Crumbach, M., Pomana, G., Wagner, P., & Gottstein, G. (2001). A Taylor type deformation texture model considering grain interaction and material properties. Part I – Fundamentals. In G. Gottstein, & D. A. Molodov (Eds.), Recrystallisation and Grain Growth, Proceedings of the First Joint Conference (pp. 1053–1060). Berlin: Springer

grain cluster methods

relaxed grain cluster (RGC) model (p x q x r grains)

- generalization of GIA
  - finite strain
  - arbitrary relaxations
  - arbitrary cluster size

Tjahjanto, D. D., Eisenlohr, P., & Roters, F. (2010). A novel grain cluster-based homogenization scheme. Modelling and Simulation in Materials Science and Engineering, 18, 015006

grain cluster methods

relaxed grain cluster (RGC) model (p x q x r grains)

- relaxation vector displaces mutual interface

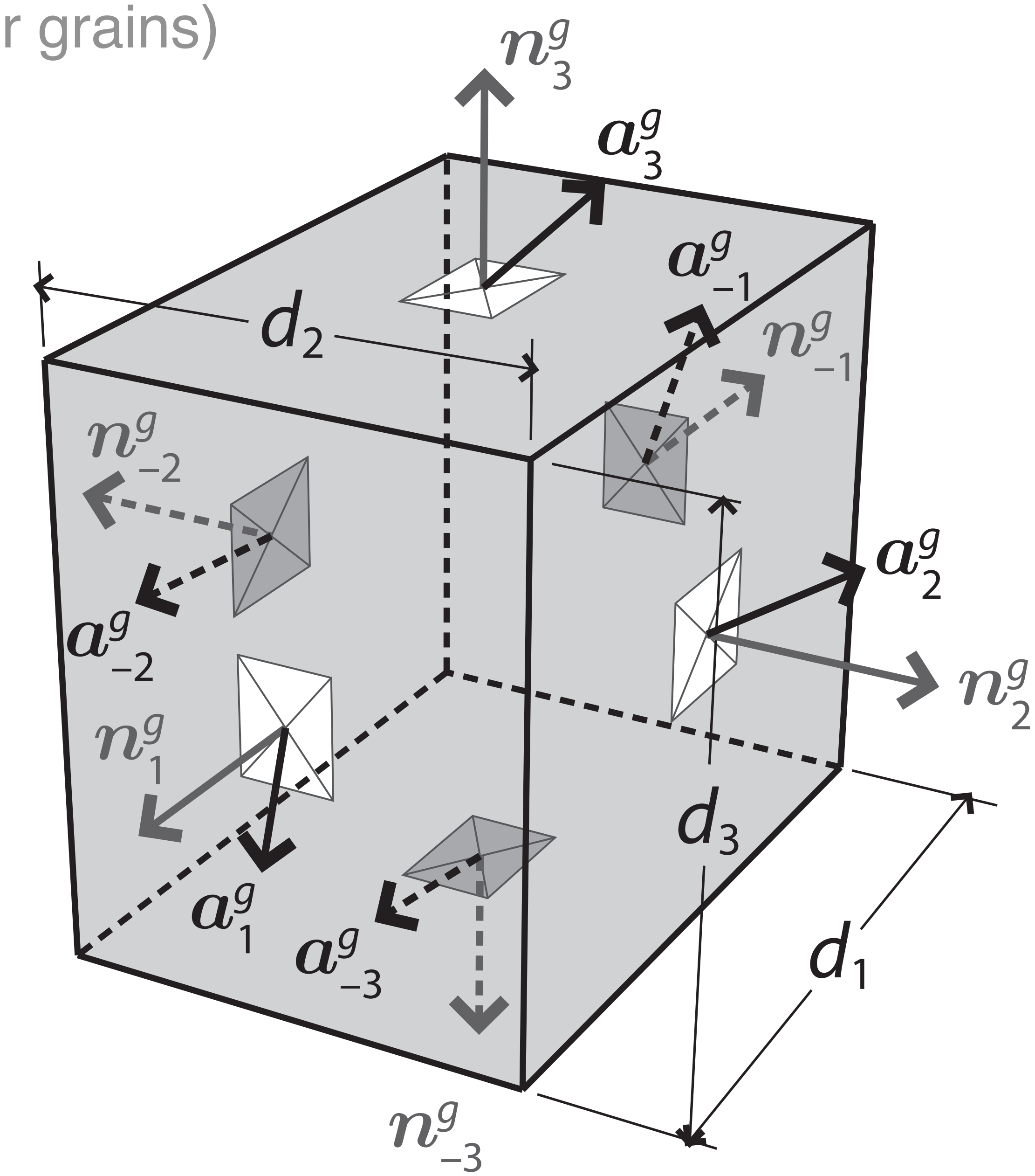

grain cluster methods

relaxed grain cluster (RGC) model (p x q x r grains)

- relaxation vector displaces mutual interface

- compatible relaxation

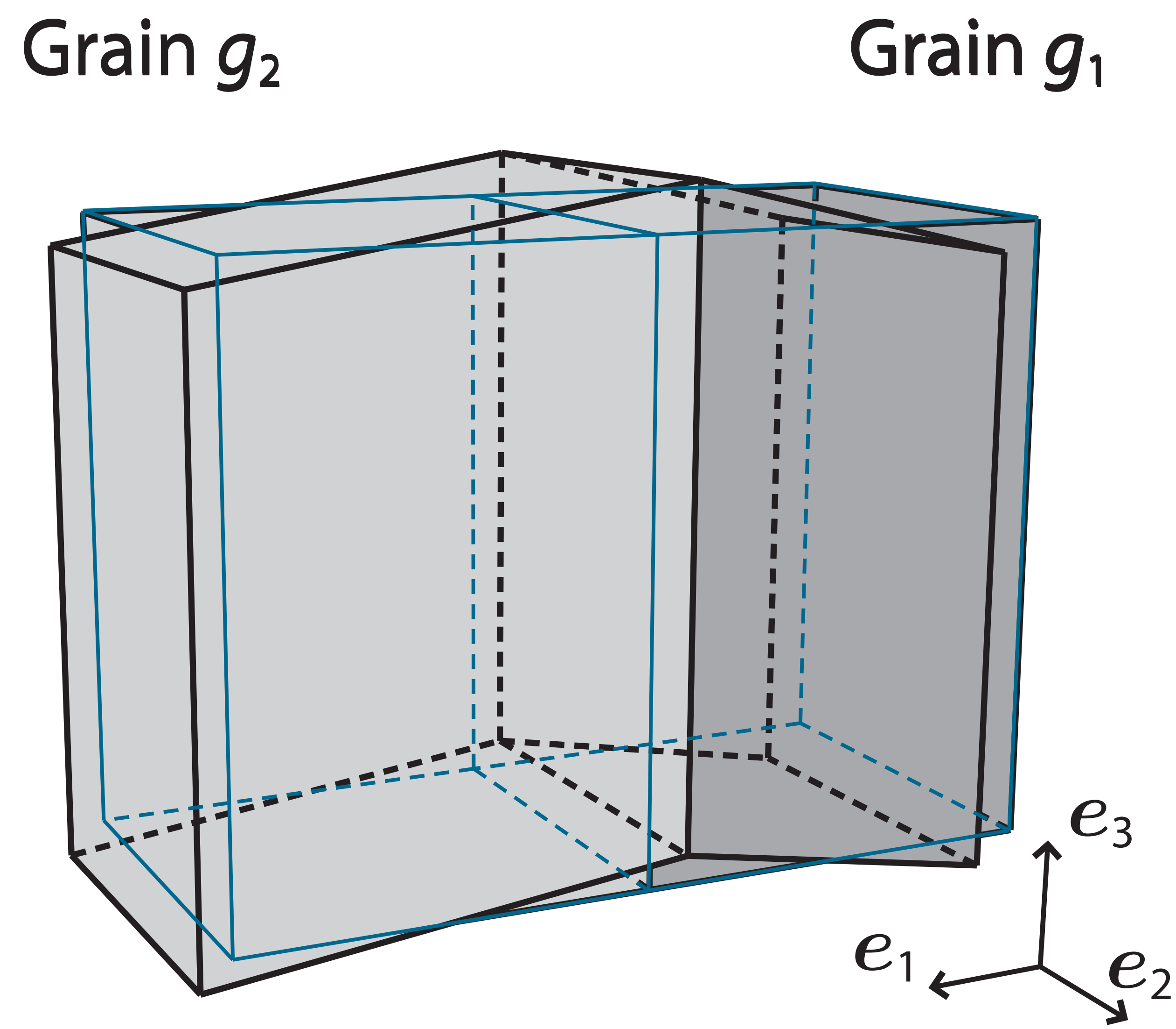

grain cluster methods

relaxed grain cluster (RGC) model (p x q x r grains)

- relaxation vector displaces mutual interface
- compatible relaxation
- incompatible relaxation

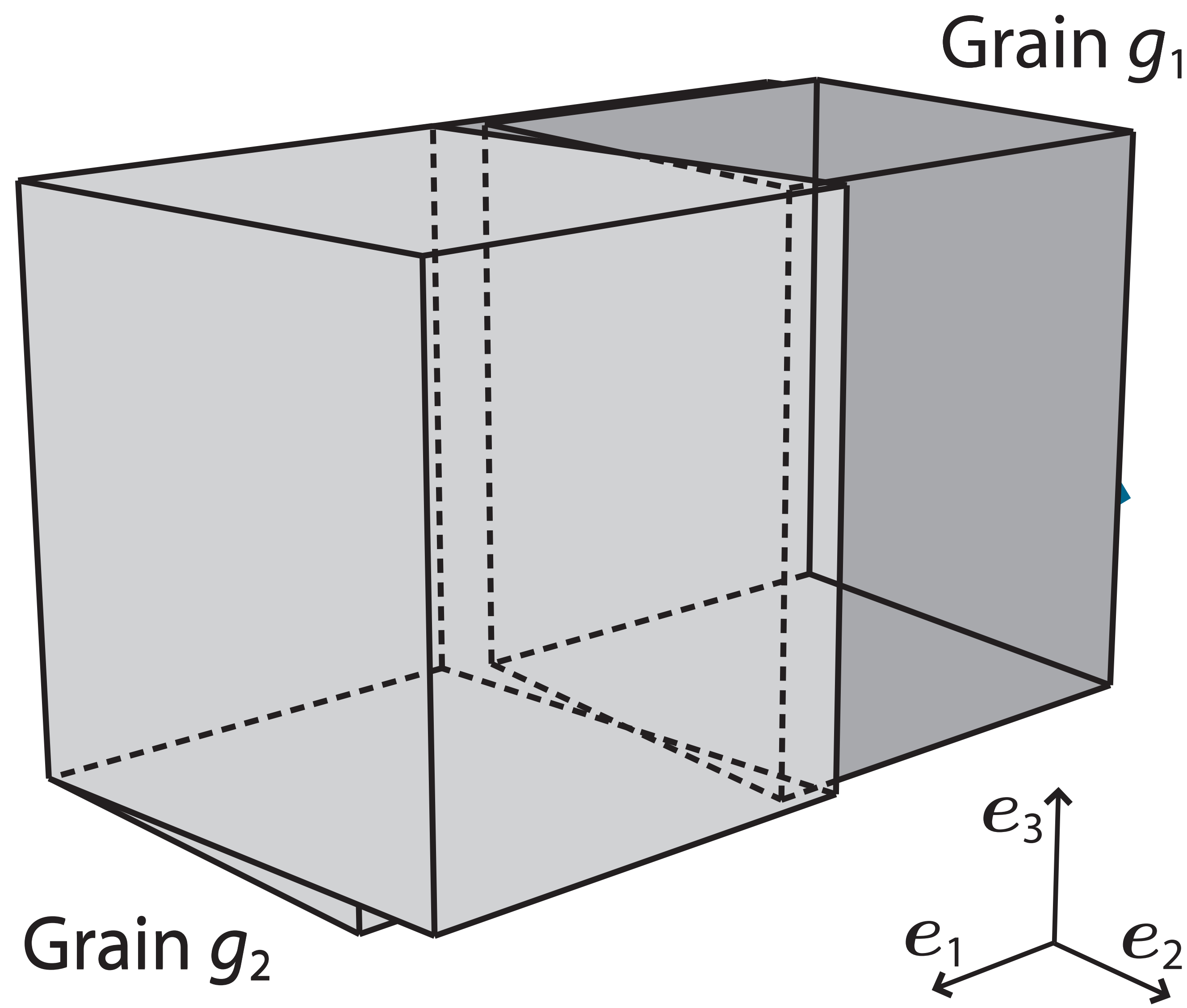

grain cluster methods

relaxed grain cluster (RGC) model (p x q x r grains)

- individual grain deformation gradient

$$\mathbf{F}^g = \bar{\mathbf{F}} + \sum_{\pm\alpha=1}^{3} \frac{1}{d_\alpha} \left(\mathbf{a}_\alpha^g \otimes \mathbf{n}_\alpha^g\right)$$

- mismatch (surface dislocation tensor) across interface

$$\mathbf{M}_\alpha^g = -\frac{1}{2}\left(\mathbf{n}_\alpha^g \times \Delta\mathbf{F}_\alpha^{g\,\mathrm{T}}\right)^\mathrm{T}$$

magnitude determines penalty energy density

computational homogenization

strategy

- spatially resolve the microstructure
- given boundary conditions from macroscopic material "point" $\overline{\mathbf{F}}$ $\overline{\mathbf{P}}$
- solve microscopic fields of displacement and stress

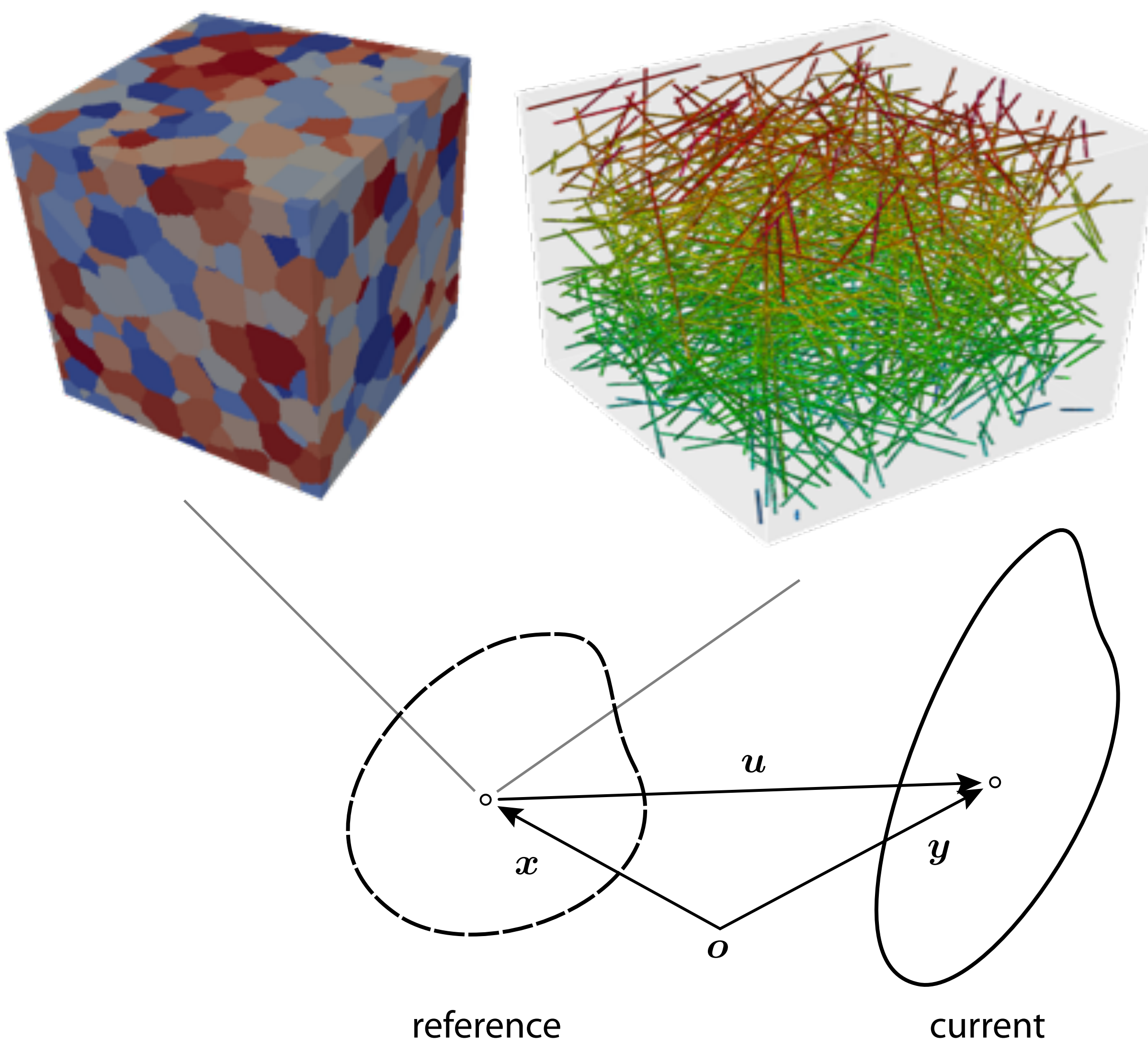

computational homogenization

microscopic displacement field

reference coordinates

$$\mathbf{y} = \overline{\mathbf{F}}\mathbf{x} + \widetilde{\mathbf{w}}$$

deformed coordinates

$$\frac{\partial \mathbf{y}}{\partial \mathbf{x}} = \overline{\mathbf{F}} + \frac{\partial \widetilde{\mathbf{w}}}{\partial \mathbf{x}}$$

$$\mathbf{F} = \overline{\mathbf{F}} + \widetilde{\mathbf{F}}$$

computational homogenization

average microscopic displacement gradient

$$
\begin{aligned}
\overline{\mathbf{F}} &= \int_{\mathcal{B}_0} \mathbf{F} \, \mathrm{d}V_0 \\
&= \int_{\mathcal{B}_0} \overline{\mathbf{F}} + \widetilde{\mathbf{F}} \, \mathrm{d}V_0 \\
&= \overline{\mathbf{F}} + \underbrace{\int_{\mathcal{B}_0} \widetilde{\mathbf{F}} \, \mathrm{d}V_0}_{\stackrel{!}{=} \mathbf{0}}
\end{aligned}
$$

computational homogenization

boundary conditions

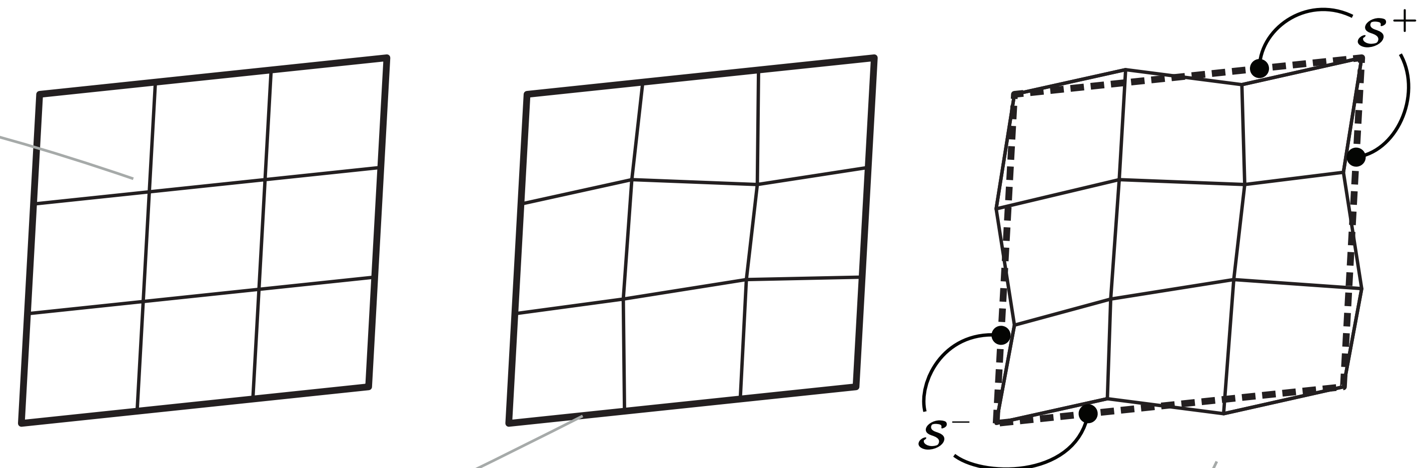

$$\mathbf{0} = \int_{\mathcal{B}_0} \widetilde{\mathbf{F}} \, \mathrm{d}V_0$$

$$= \int_{\mathcal{S}_0} \widetilde{\mathbf{w}} \otimes \mathrm{d}\mathbf{n}_0$$

$$= \int_{\mathcal{S}_0^-} \widetilde{\mathbf{w}}^- \otimes \mathrm{d}\mathbf{n}_0{}^- + \int_{\mathcal{S}_0^+} \widetilde{\mathbf{w}}^+ \otimes \mathrm{d}\mathbf{n}_0{}^+$$

computational homogenization

examples

ELSEVIER
Computational Materials Science 16 (1999) 344–354
COMPUTATIONAL MATERIALS SCIENCE

Multiscale FE^2 elastoviscoplastic analysis of composite structures

Frédéric Feyel
ONERA LCME/DMSE, BP 72, 29 Avenue de al Division Leclere, 92372 Chatillon Cedex, France

ELSEVIER
Comput. Methods Appl. Mech. Engrg. 183 (2000) 309–330
Computer methods in applied mechanics and engineering
www.elsevier.com/locate/cma

FE^2 multiscale approach for modelling the elastoviscoplastic behaviour of long fibre SiC/Ti composite materials

Frédéric Feyel, Jean-Louis Chaboche *
ONERA DMSE–LCME, 29 Avenue de la Division Leclerc, F-92320, Châtillon, France

Received 17 April 1998

computational homogenization

examples: turbine rotor

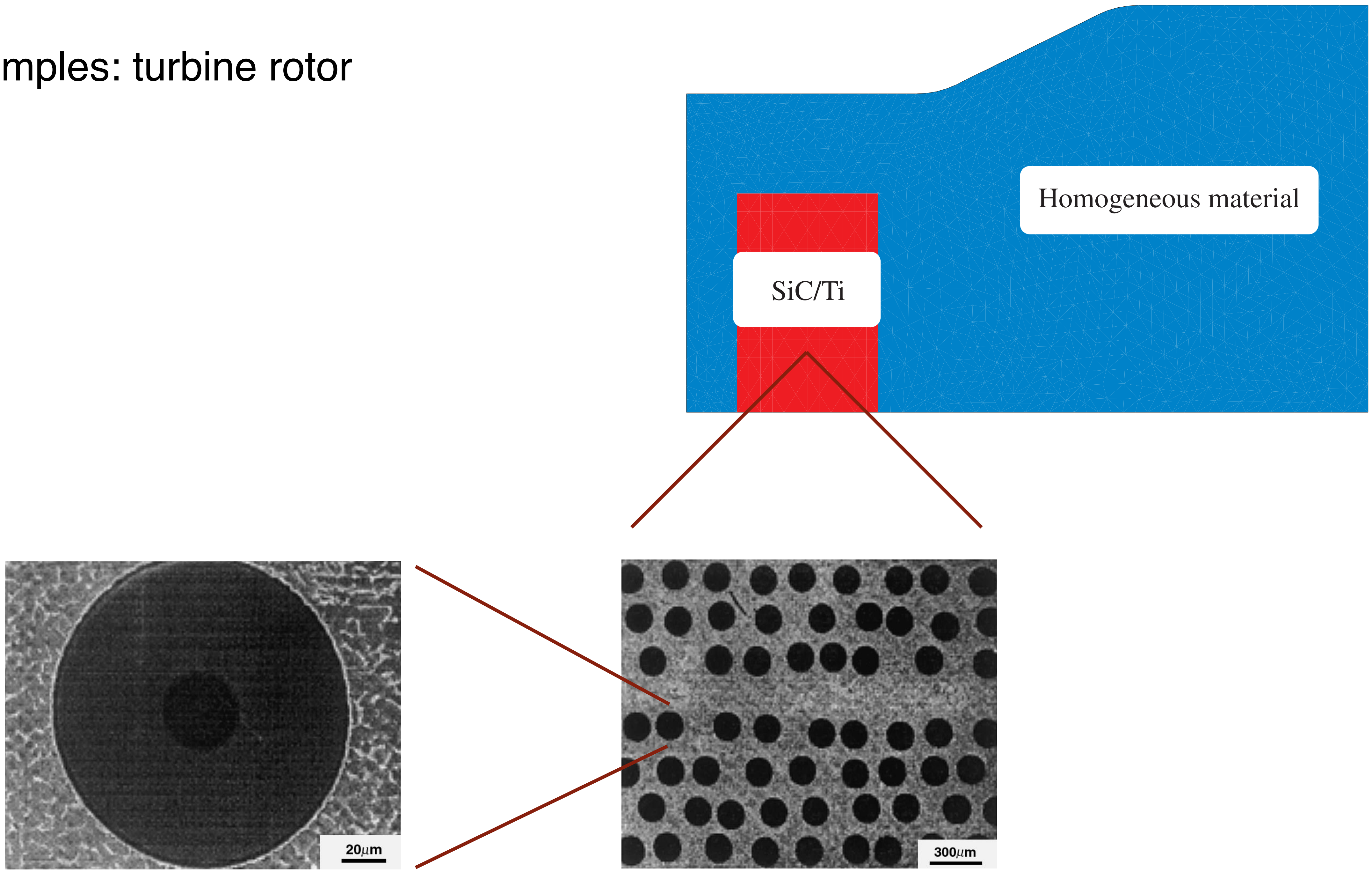

computational homogenization

examples: turbine rotor

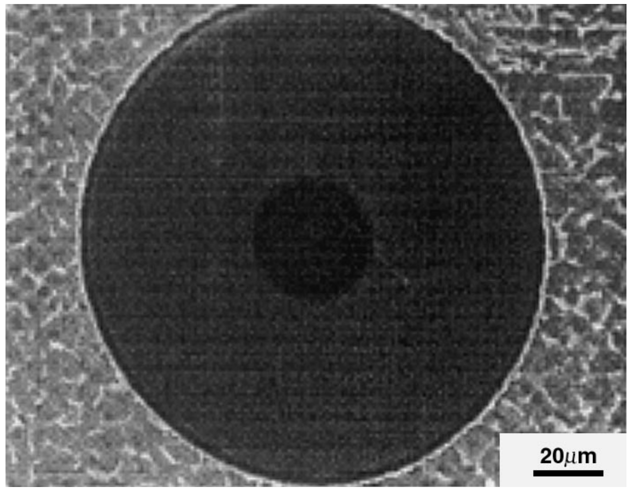

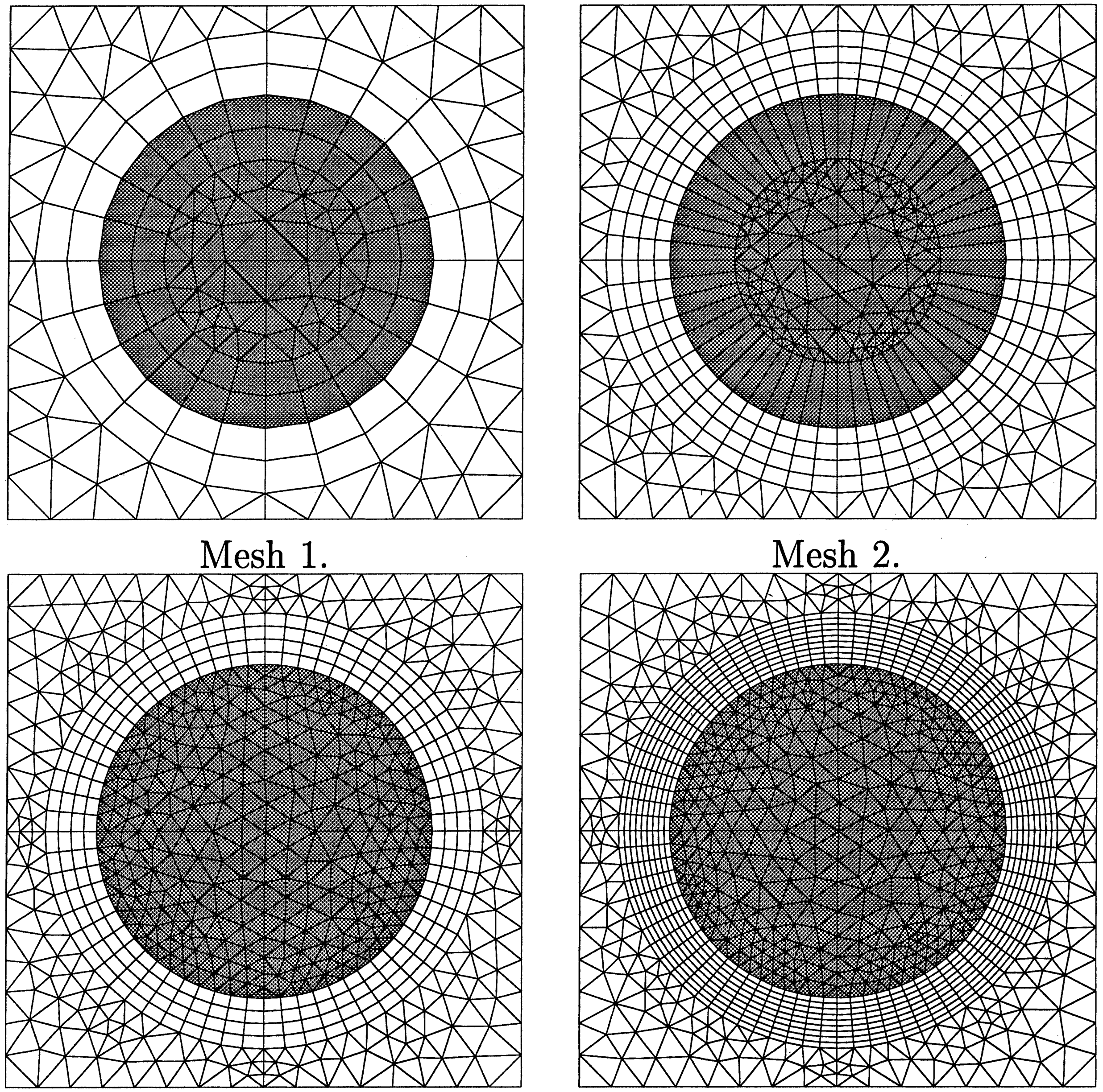

Mesh 1. Mesh 2.

Mesh 3. Mesh 4.

computational homogenization

examples: turbine rotor

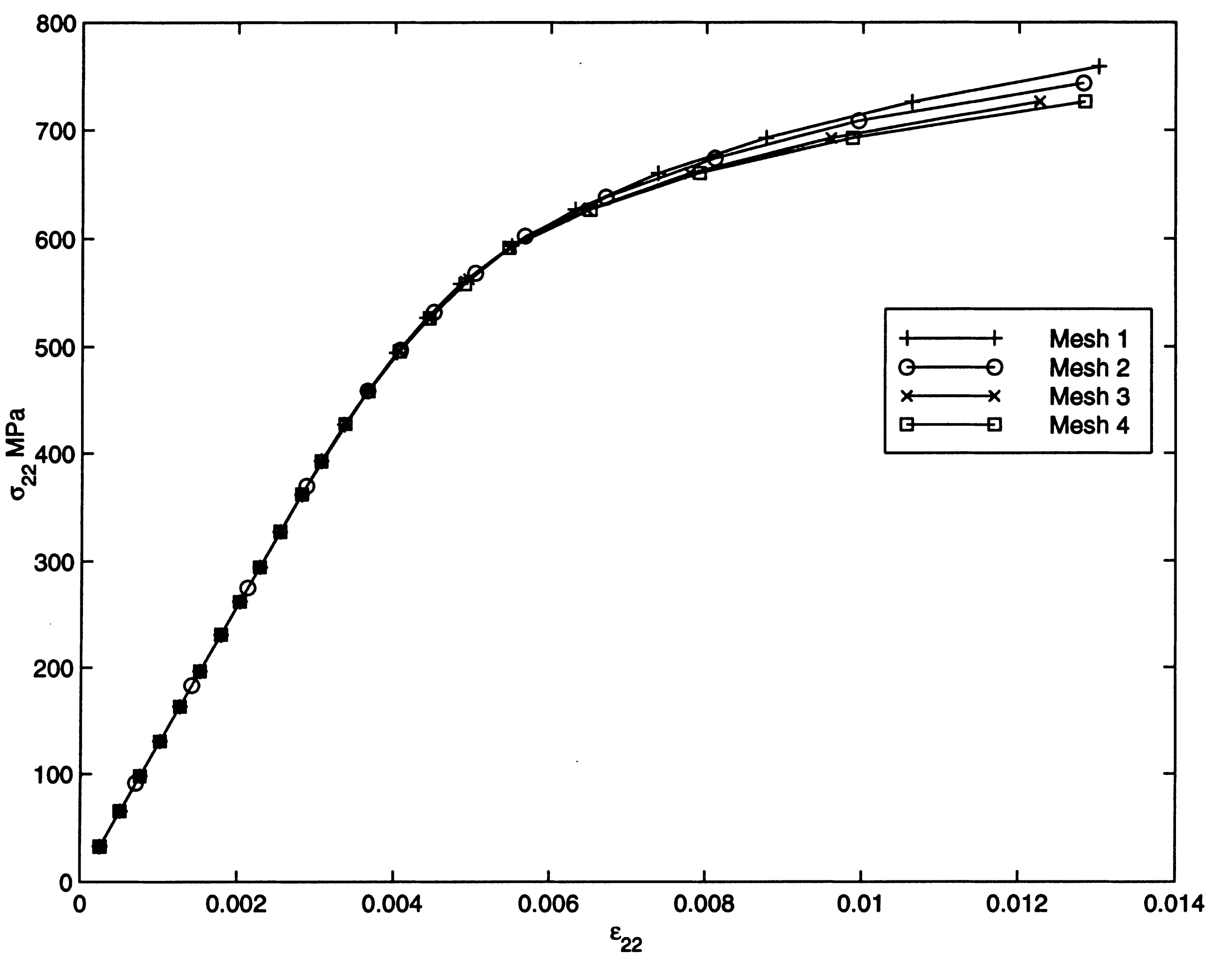

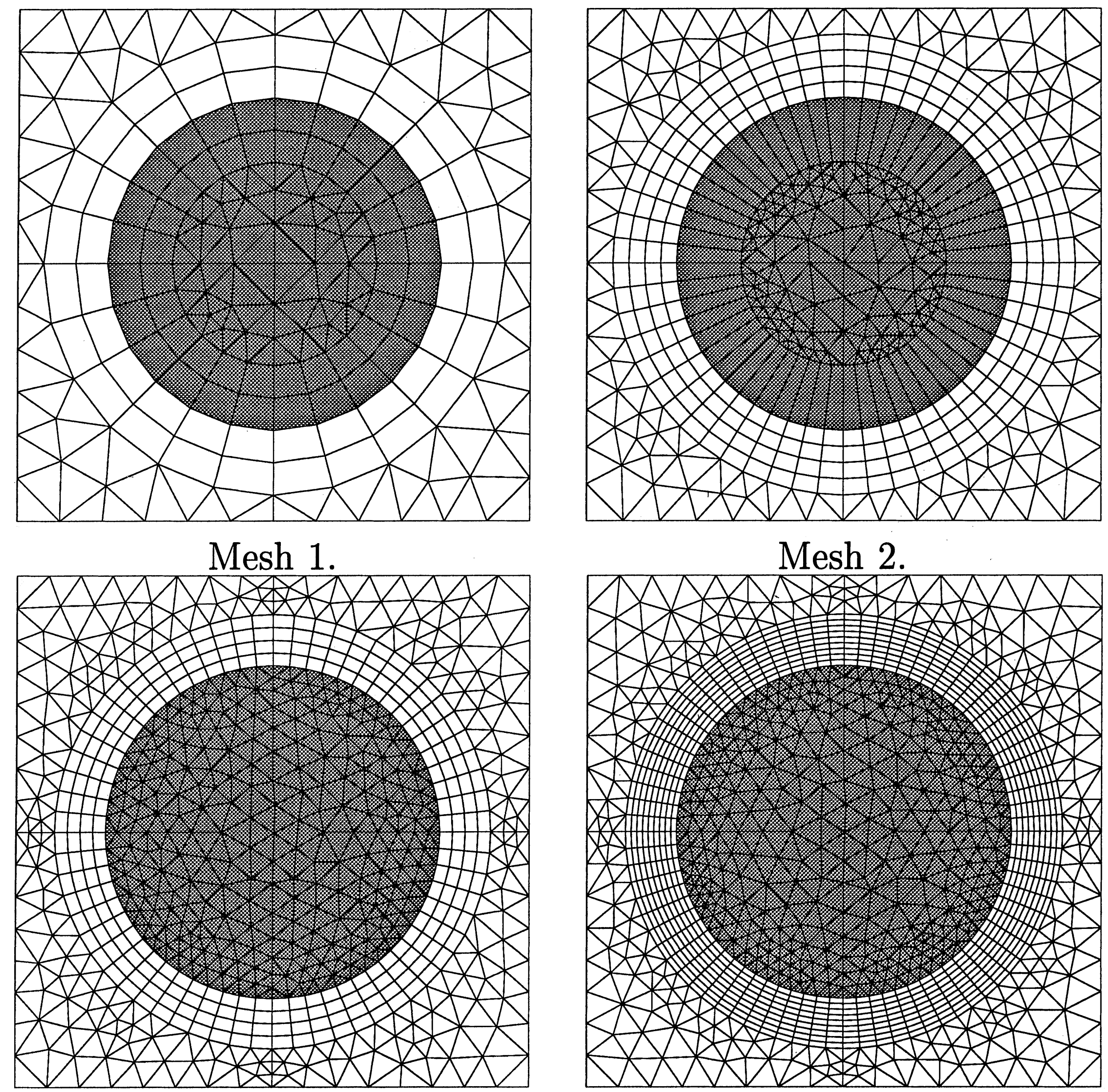

Mesh 1. Mesh 2.

Mesh 3. Mesh 4.

MICHIGAN STATE UNIVERSITY

computational homogenization

examples: turbine rotor

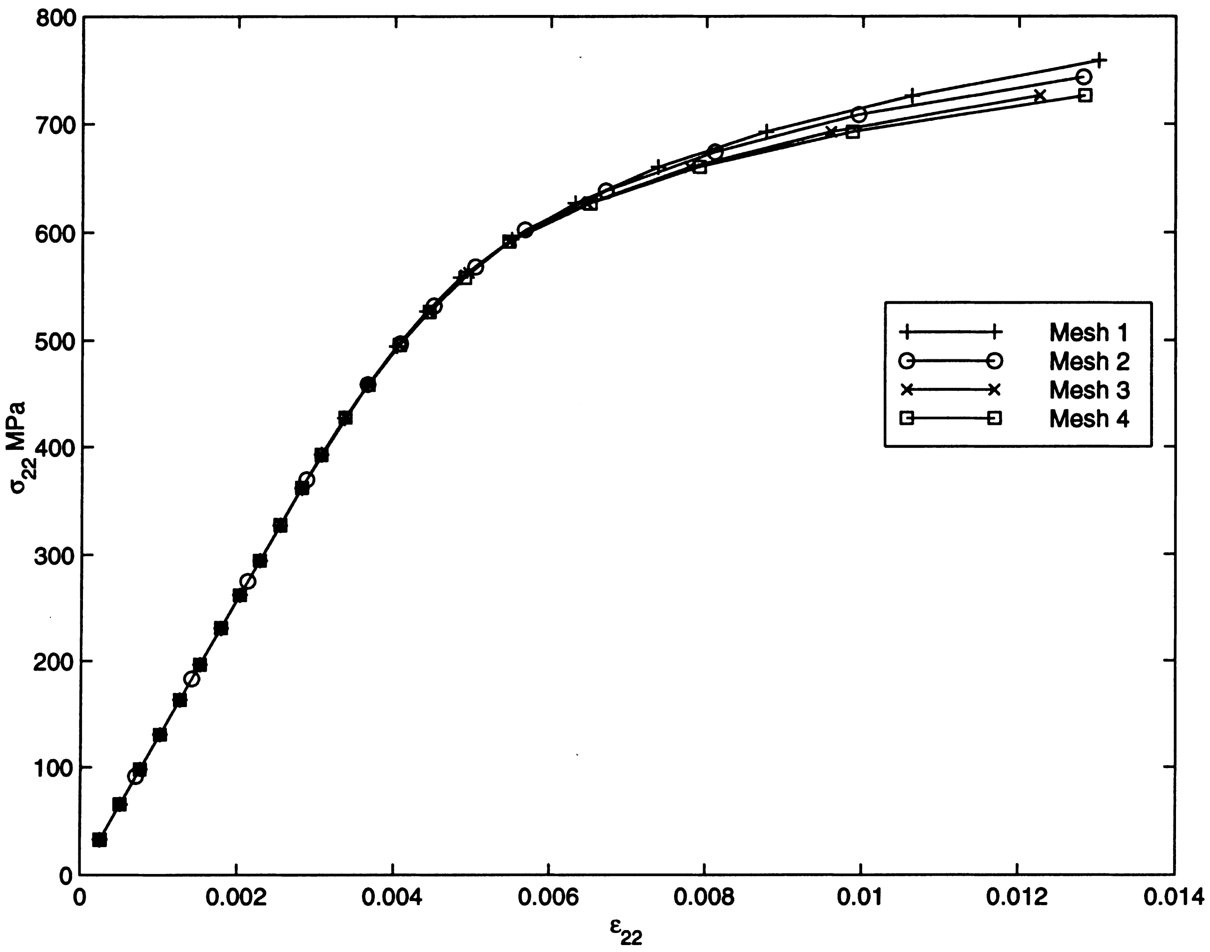

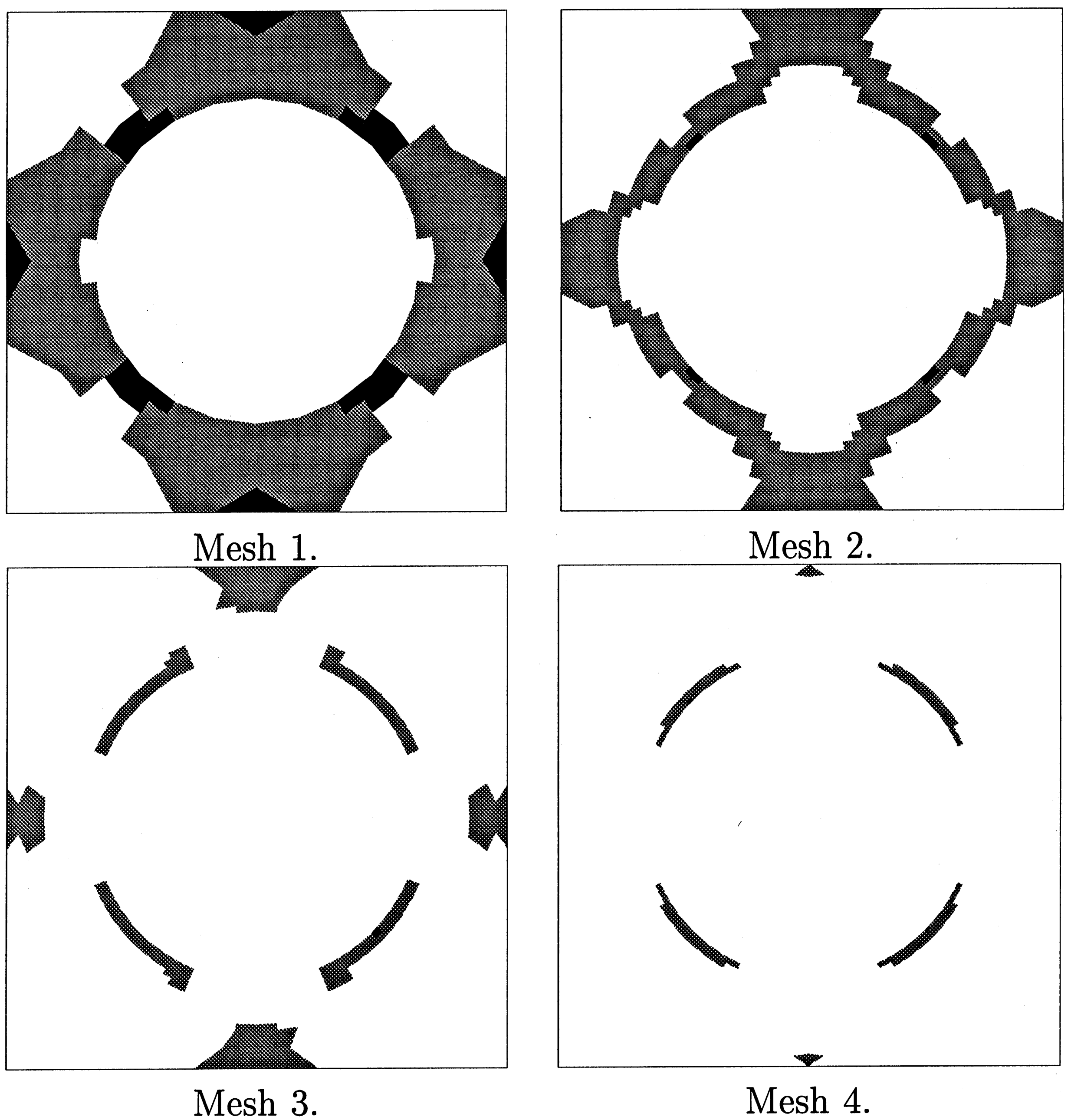

computational homogenization

examples: turbine rotor

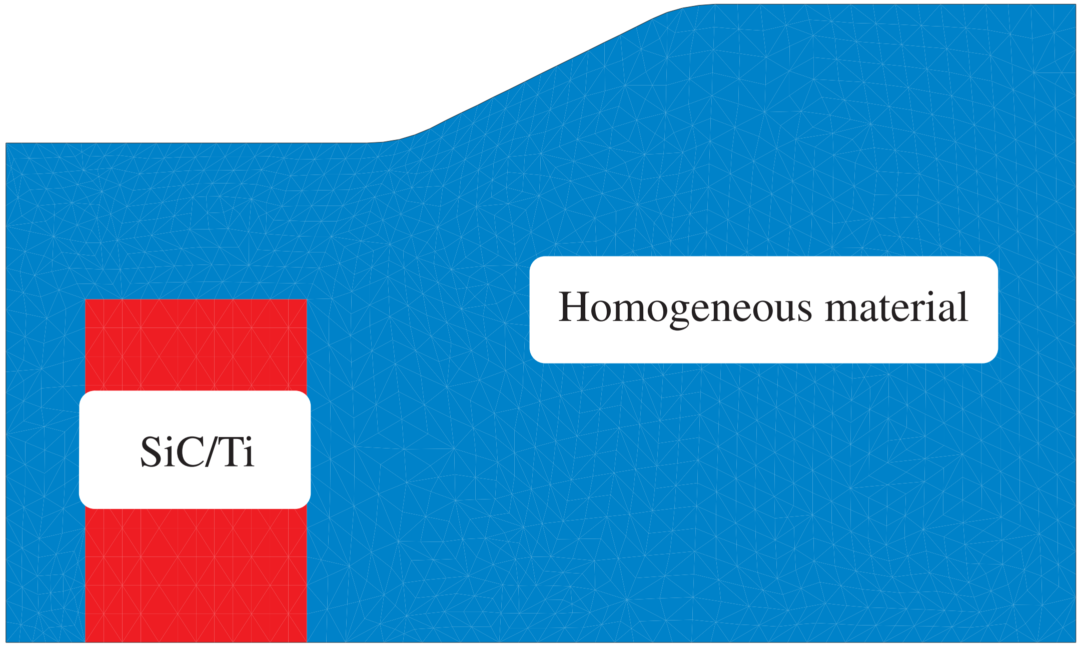

deformation 5x exaggerated

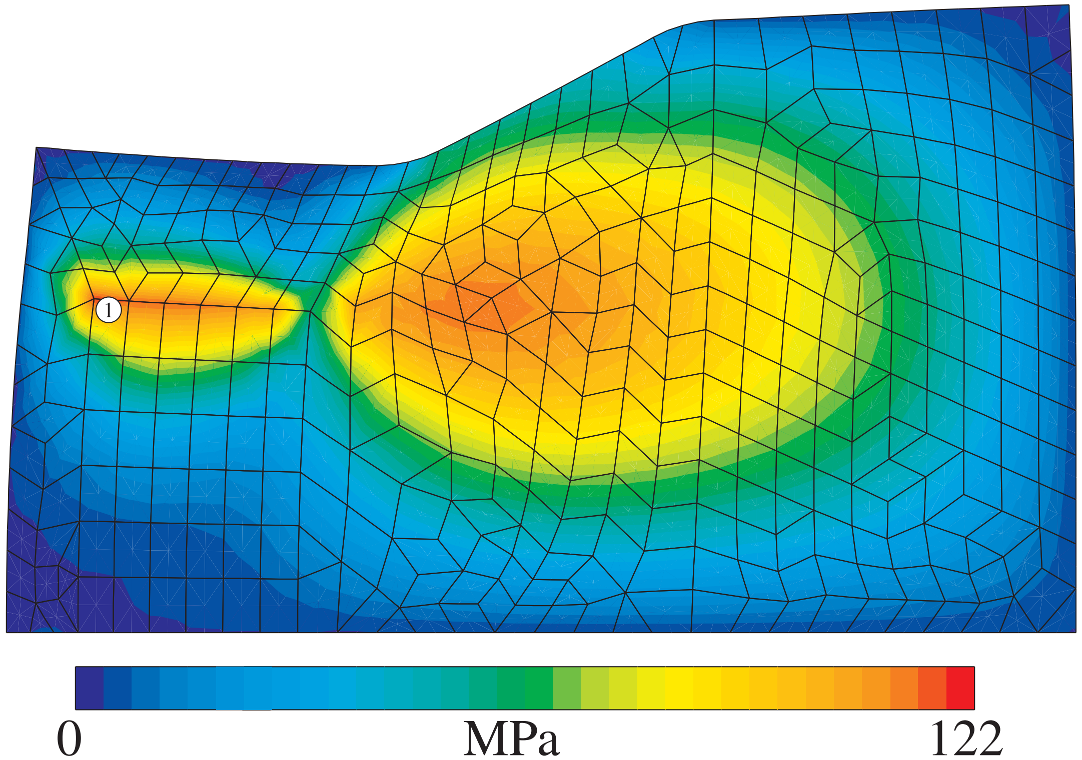

computational homogenization

examples

Computational Mechanics 27 (2001) 37–48 © Springer-Verlag 2001

An approach to micro-macro modeling of heterogeneous materials

V. Kouznetsova, W. A. M. Brekelmans, F. P. T. Baaijens

computational homogenization

examples: porous aluminum

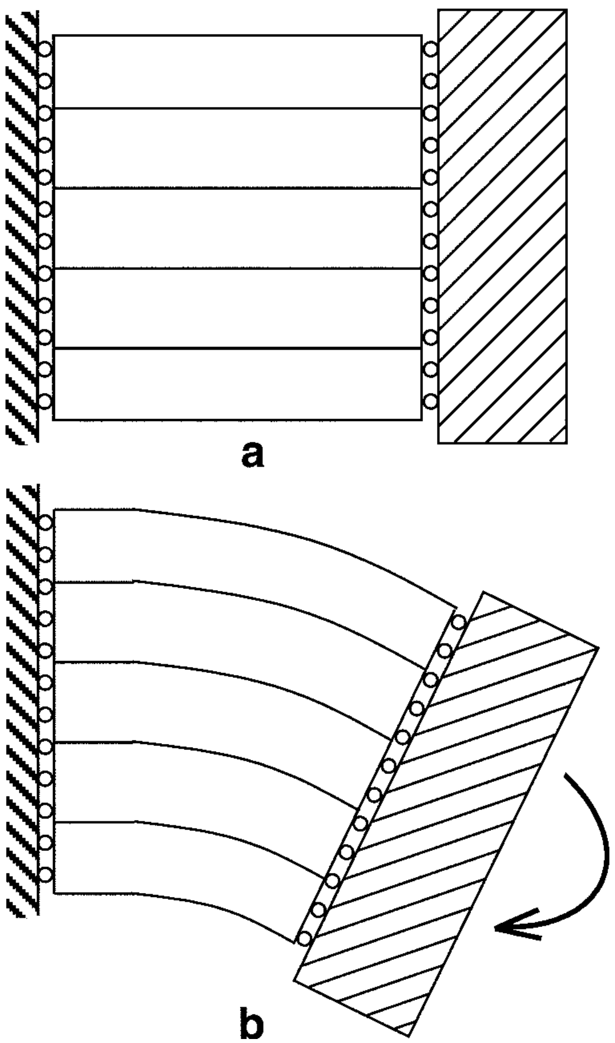

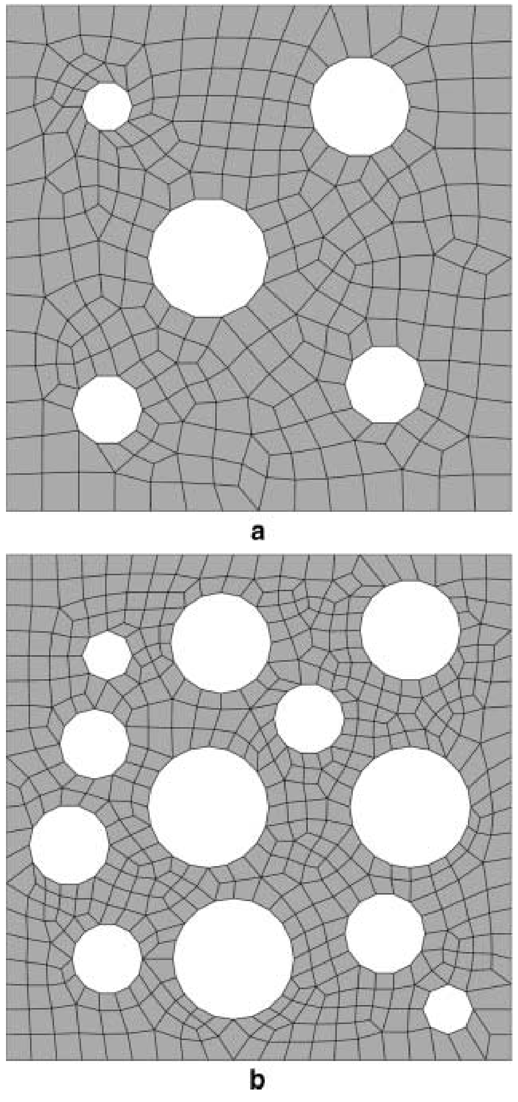

MICHIGAN STATE UNIVERSITY

computational homogenization

examples: porous aluminum

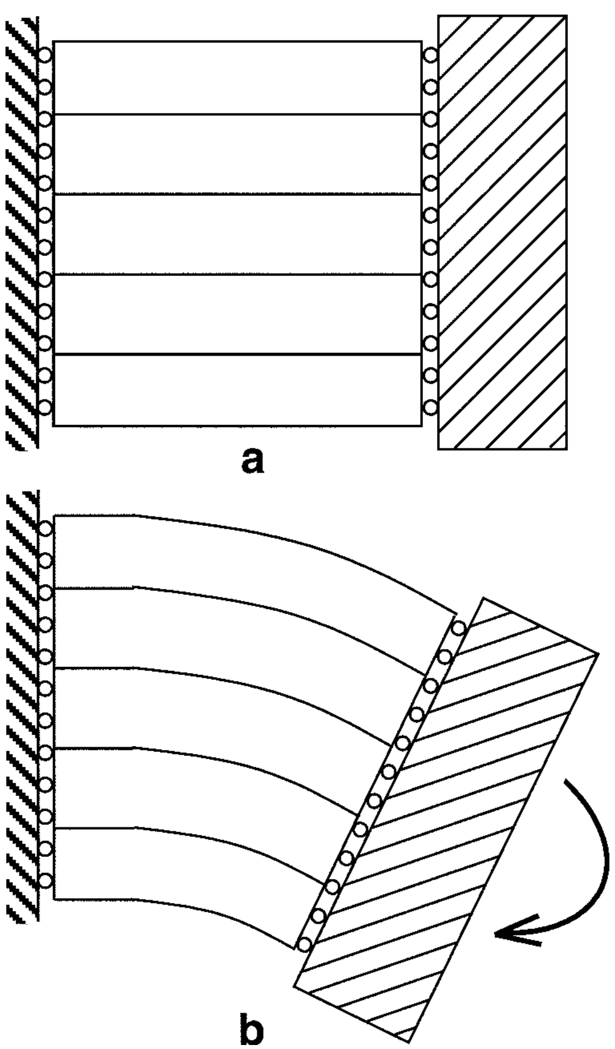

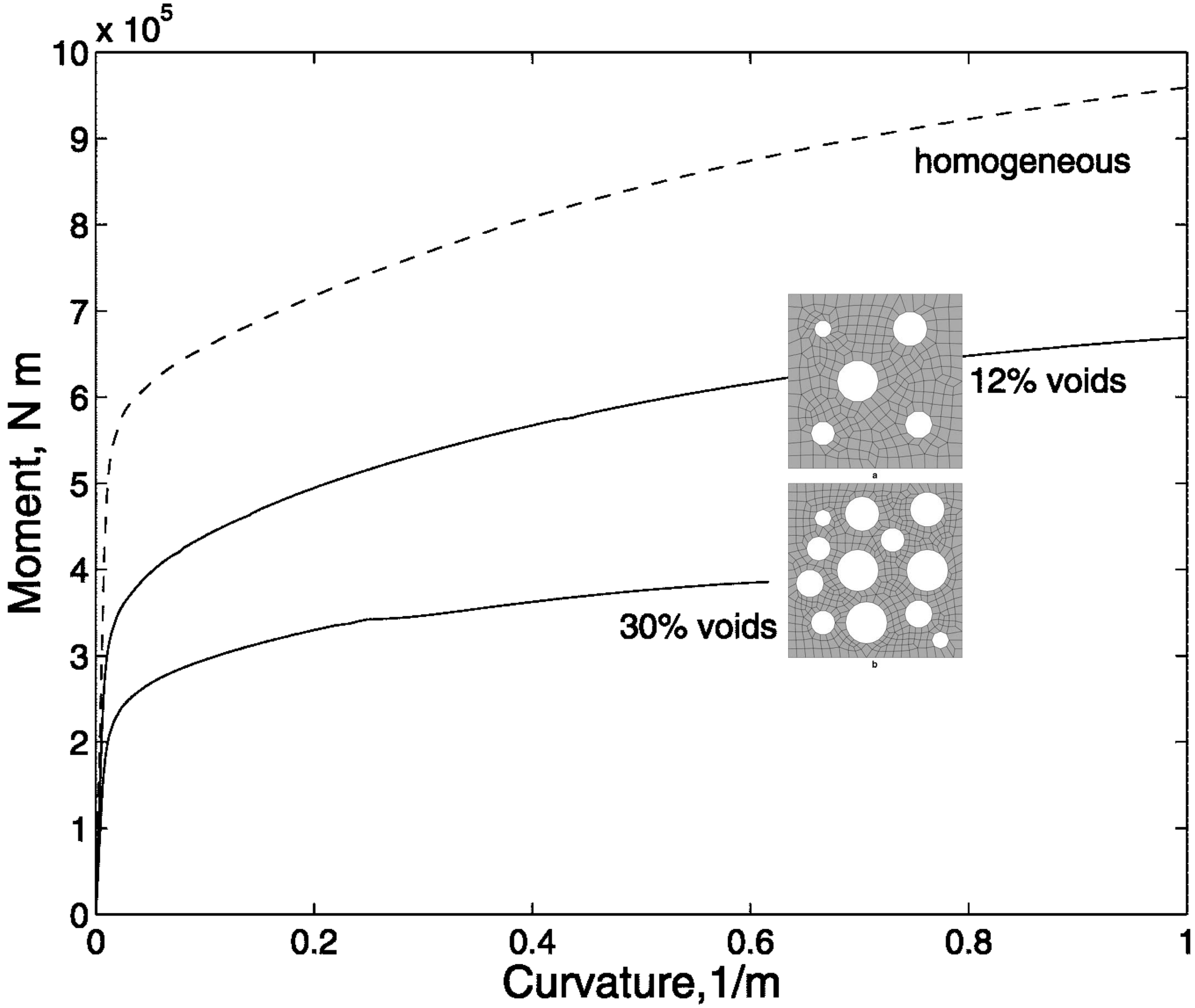

computational homogenization

examples: porous aluminum

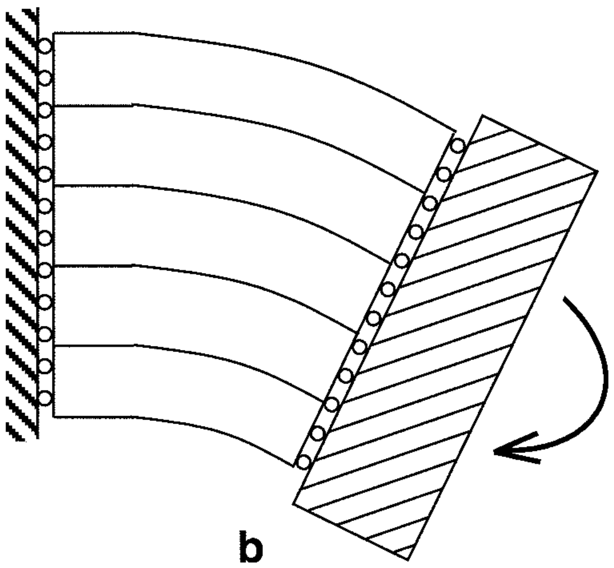

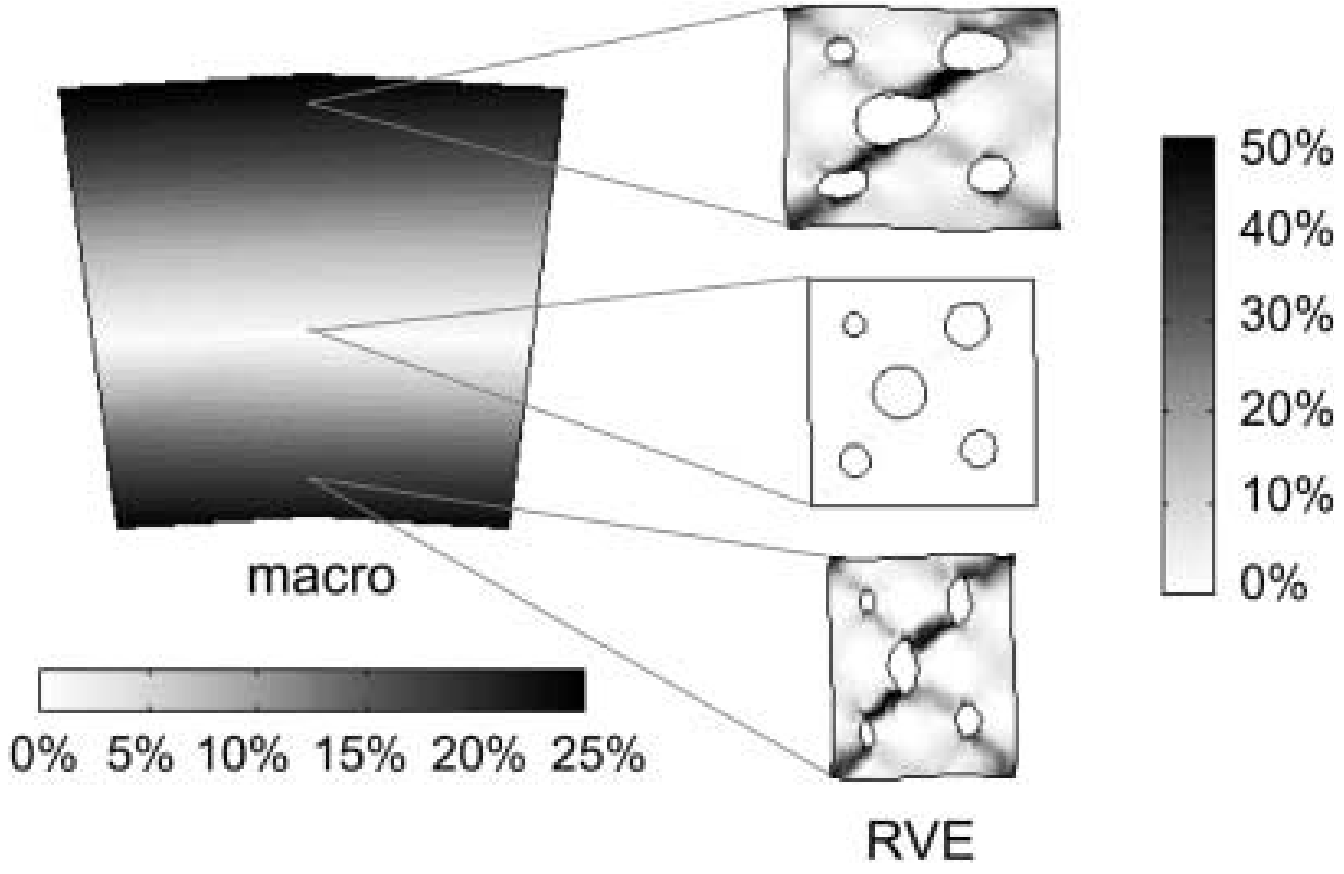

computational homogenization

examples: porous aluminum

- regular array (cubic unitcell)

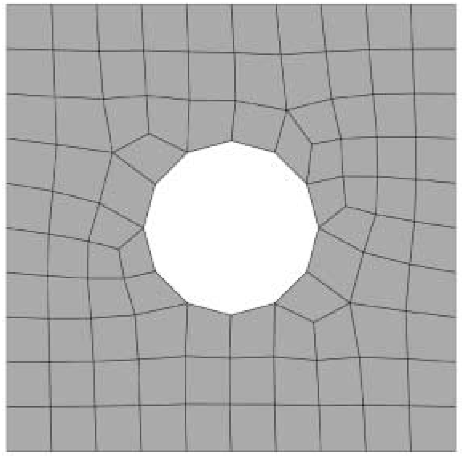

- random porosity

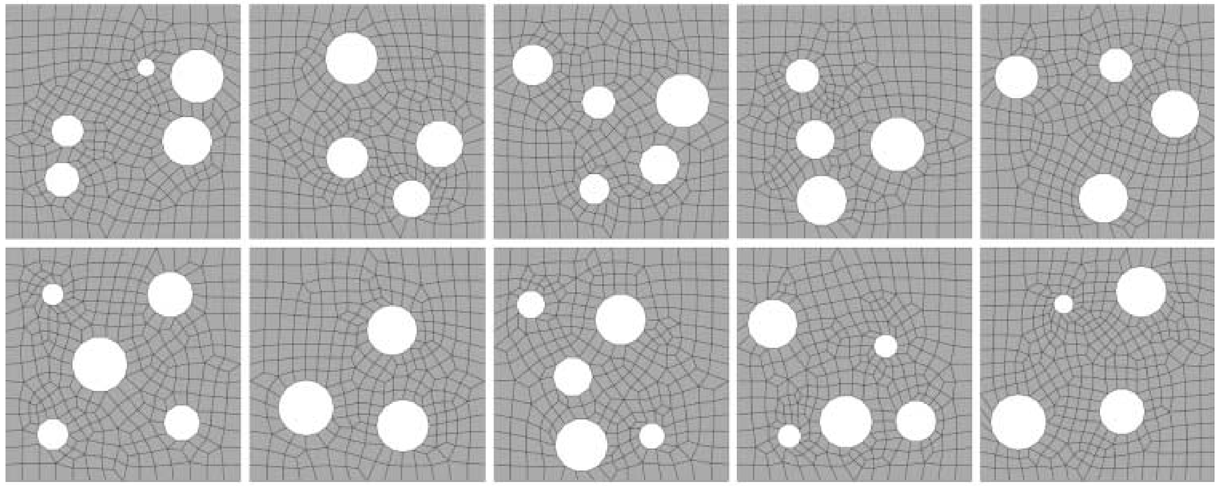

MICHIGAN STATE UNIVERSITY

computational homogenization

examples: porous aluminum

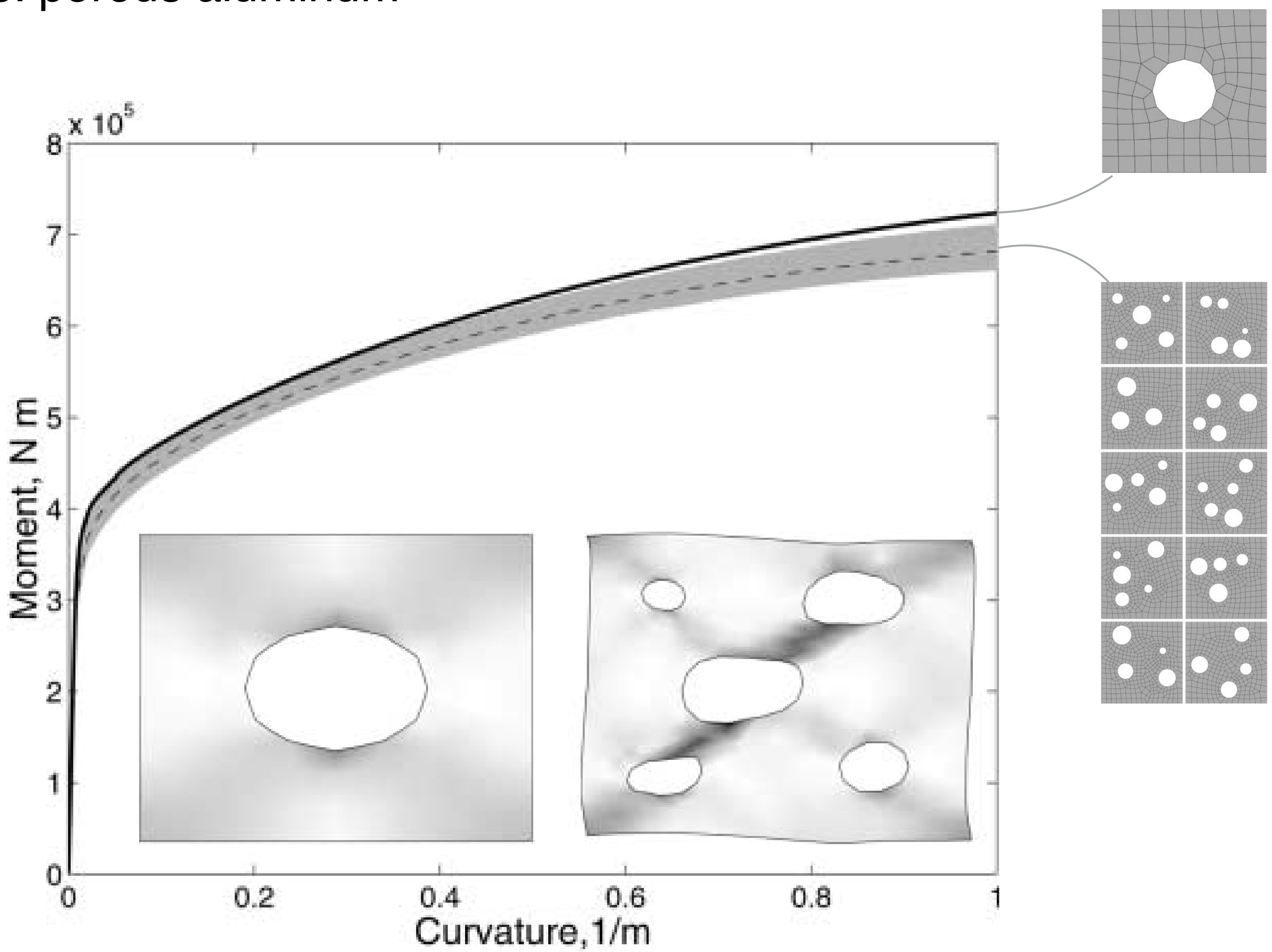

statistical representation of texture

crystallite orientation description

- rotation matrix relating reference to crystal frame

$$\begin{pmatrix} X \\ Y \\ Z \end{pmatrix} = \mathbf{Q} \begin{pmatrix} x \\ y \\ z \end{pmatrix}$$

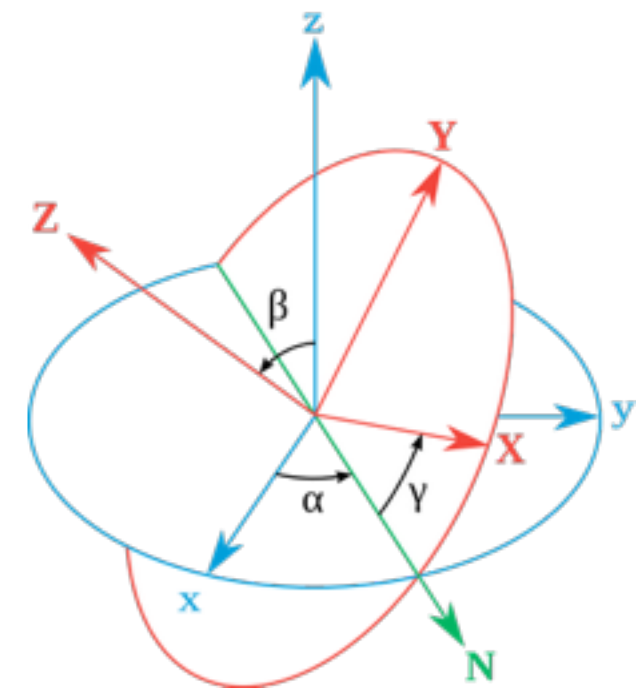

- probability density to find volume fraction of crystallites at a point in orientation space

infinitesimal volume of orientation space

$$\nu \equiv \frac{\mathrm{d}V}{V} = f(\mathbf{Q})\,\mathrm{d}Q$$

crystallite orientation distribution function (CODF)

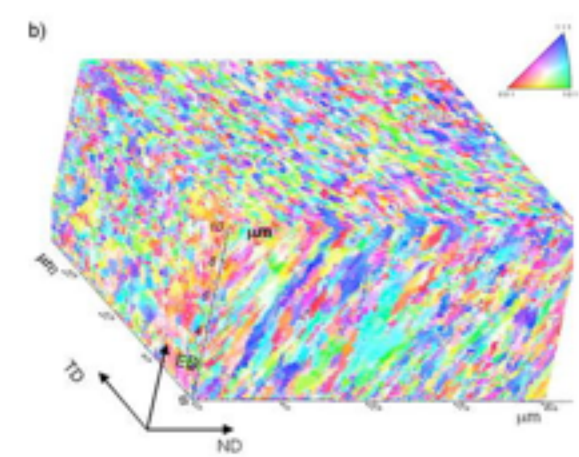

statistical representation of texture

orientation space

- Bunge (1982) z-x-z rotation

$$
\begin{aligned}
\mathrm{d}Q &= \frac{1}{8\pi^2}\,\mathrm{d}\varphi_1\,\mathrm{d}\cos\phi\,\mathrm{d}\varphi_2 \\
&= \frac{\sin\phi}{8\pi^2}\,\mathrm{d}\varphi_1\,\mathrm{d}\phi\,\mathrm{d}\varphi_2
\end{aligned}
$$

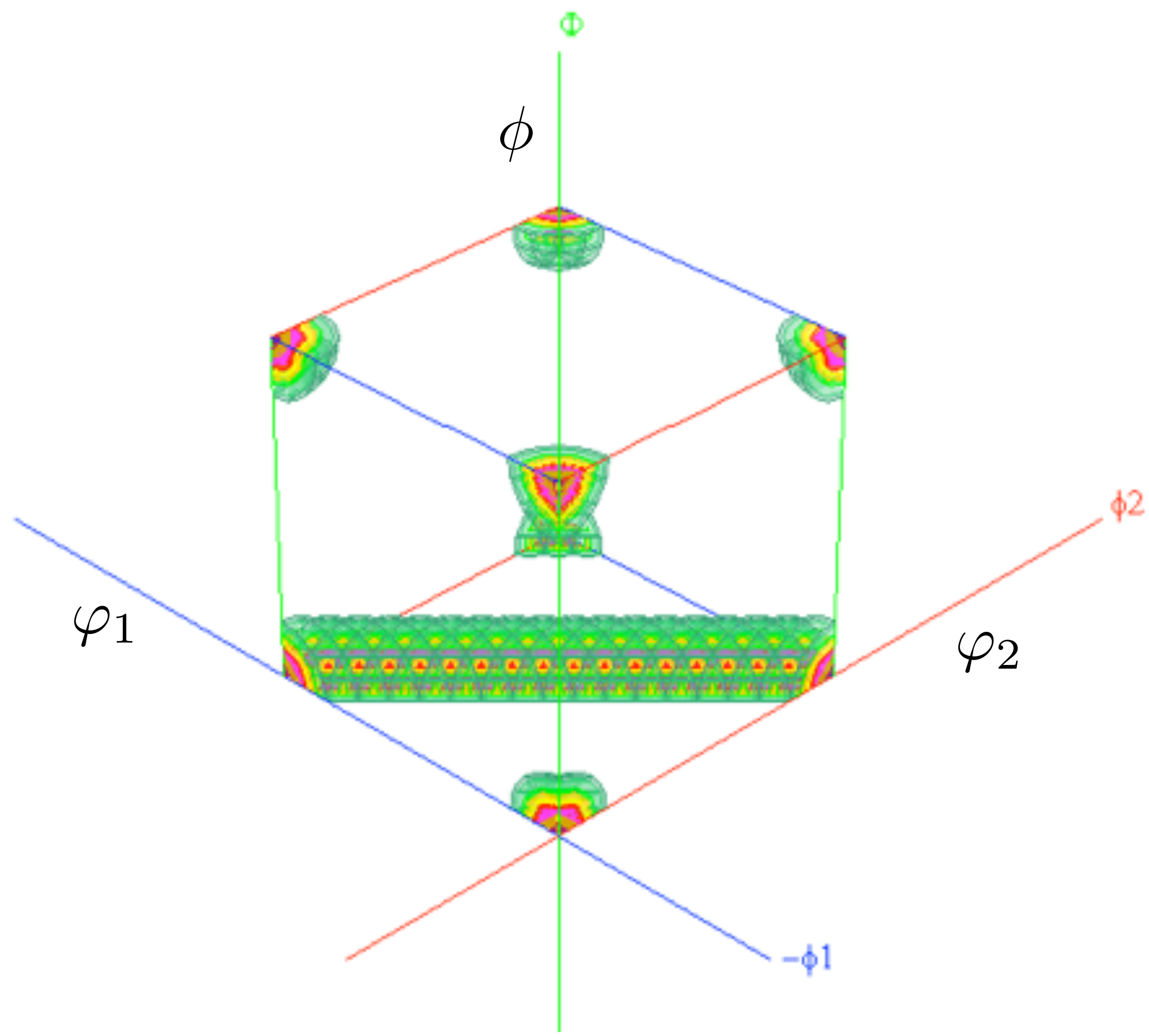

statistical representation of texture

orientation space discretization

- Bunge (1982) z-x-z rotation

$$\mathrm{d}Q = \frac{1}{8\pi^2}\,\mathrm{d}\varphi_1\,\mathrm{d}\cos\phi\,\mathrm{d}\varphi_2 = \frac{\sin\phi}{8\pi^2}\,\mathrm{d}\varphi_1\,\mathrm{d}\phi\,\mathrm{d}\varphi_2$$

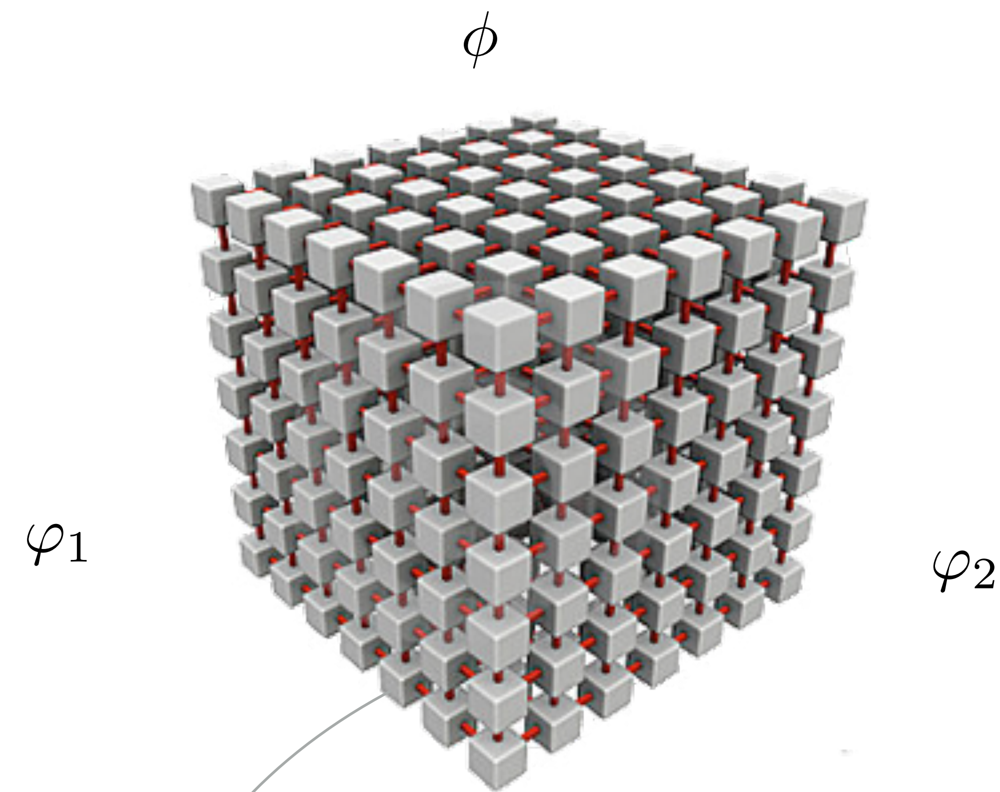

discrete volume of orientation space

$$f^i = \nu^i \Big/ \int_{\mathrm{box}^i} \mathrm{d}Q$$

statistical representation of texture

representation by discrete number of orientations

- how to select a given number of orientations to best represent an orientation distribution ?

$$p(\mathbf{Q}^i) = \frac{f^i \sin\phi^i}{\max(f \sin\phi)}$$

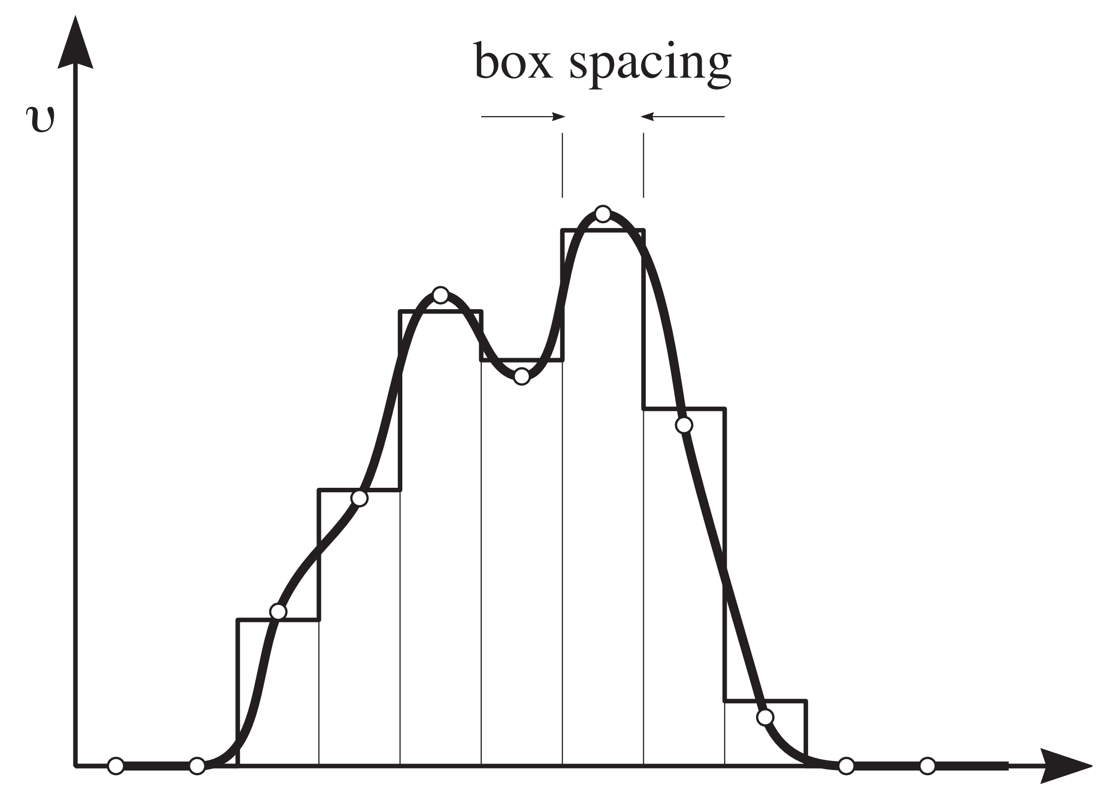

statistical representation of texture

representation by discrete number of orientations

- how to select a given number of orientations to best represent an orientation distribution ?

$$n^{*i} = \mathrm{round}(C\nu^i)$$

$$\sum_{i=1}^{N} n^{*i} \stackrel{!}{=} N^*$$

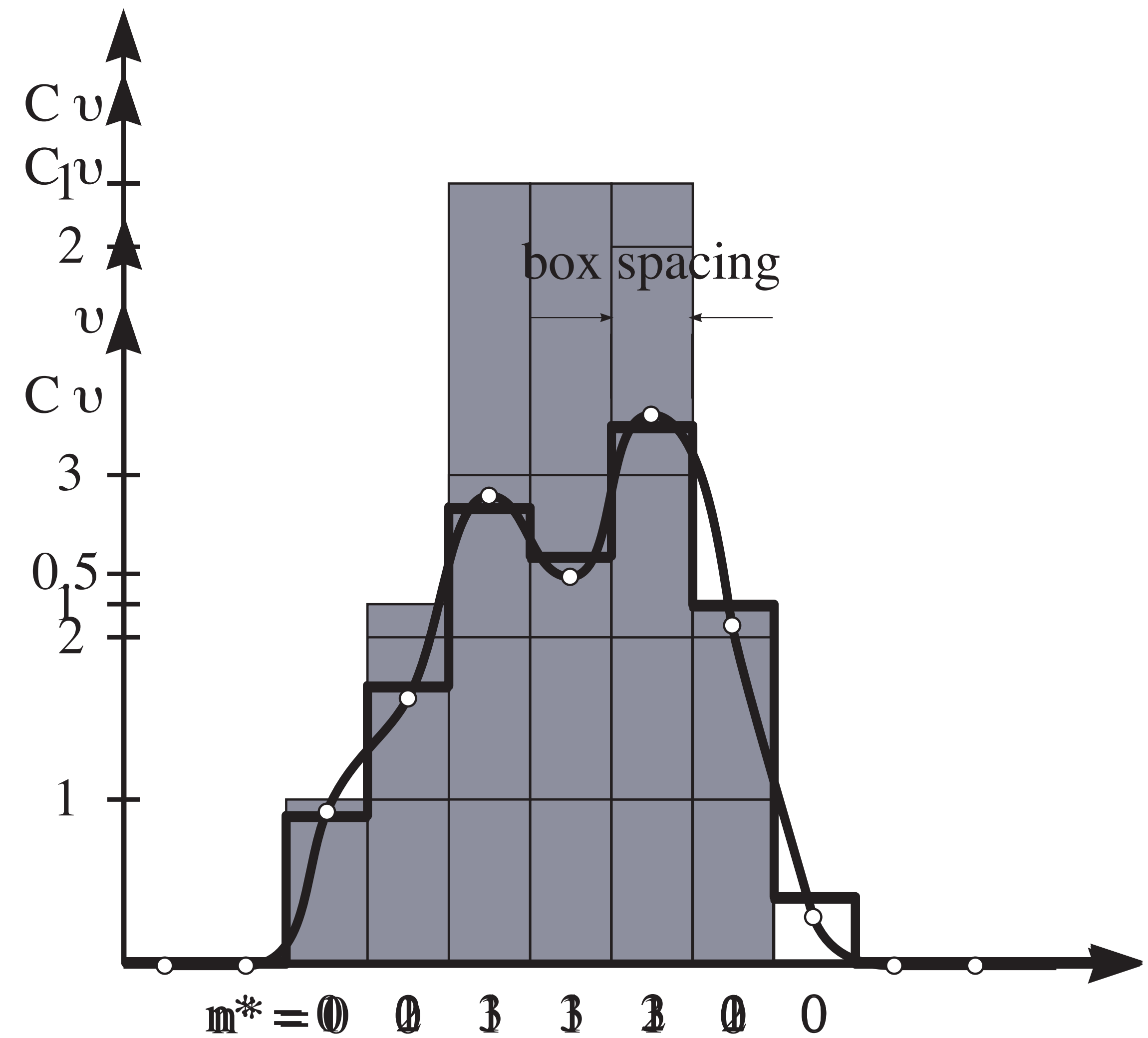

Eisenlohr, P., & Roters, F. (2008). Selecting sets of discrete orientations for accurate texture reconstruction. Computational Materials Science, 42(4), 670–678.

statistical representation of texture

representation by discrete number of orientations

- systematic over-prediction at (relatively) low numbers of discrete orientations

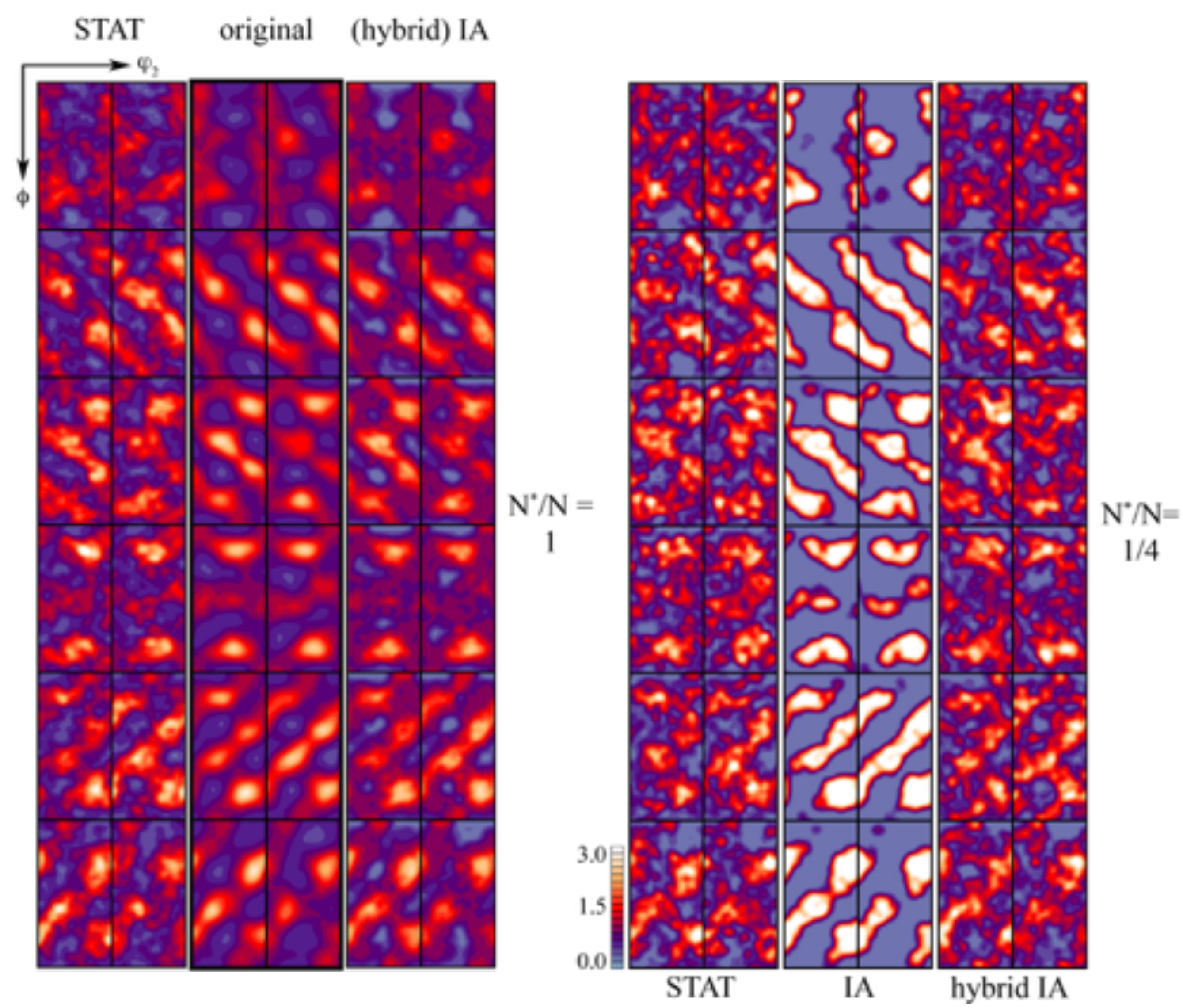

statistical representation of texture

representation by discrete number of orientations

- systematic over-prediction at (relatively) low numbers of discrete orientations
- blend of probabilistic and deterministic schemes ("hybrid")

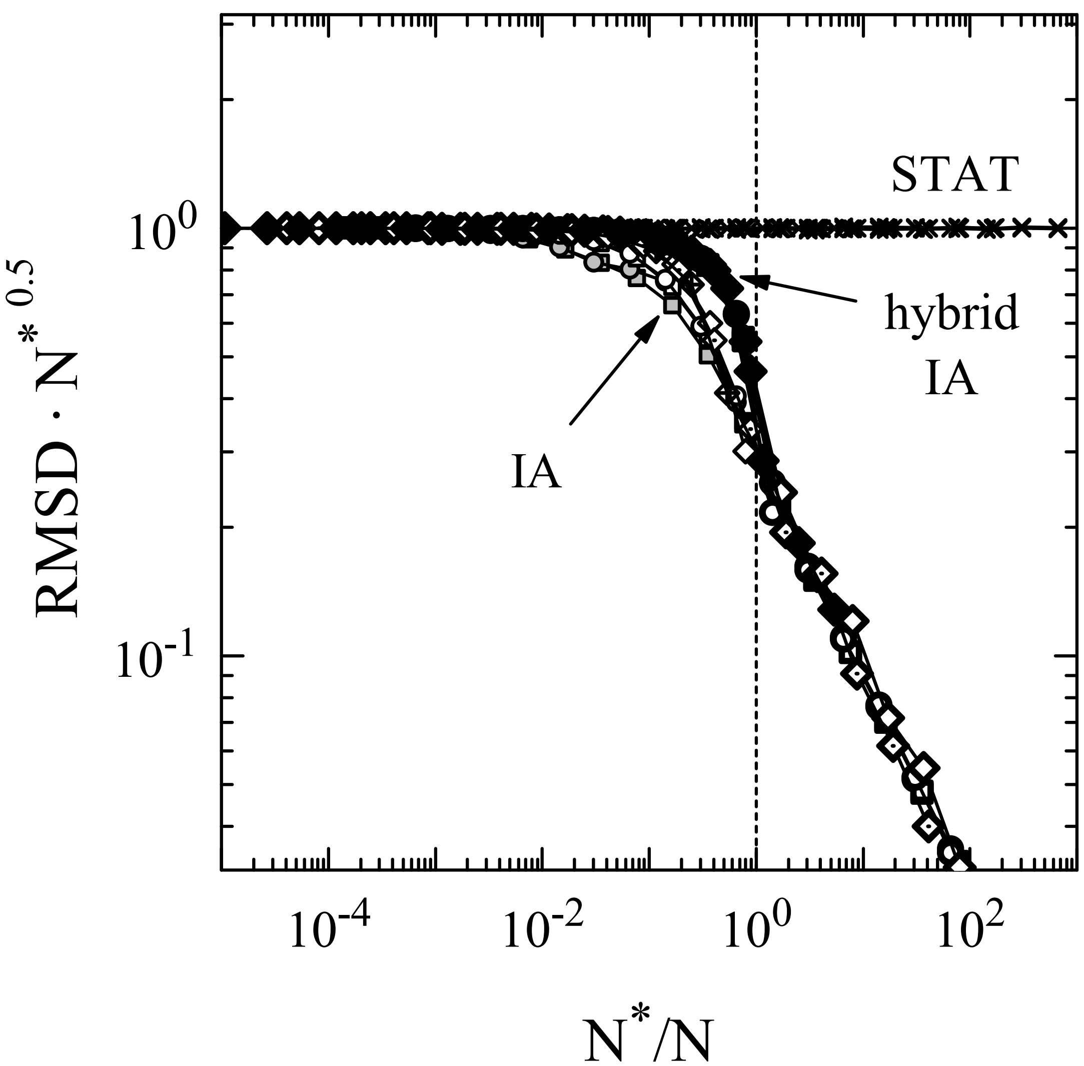

purpose

- generate an approximate solution to
- a boundary value problem (field problem) on
- an (irregular) domain
- governed by (a system of) partial differential equations (PDEs)

classification of PDEs

$$F(x, y, \ldots, u, u_{,x}, u_{,y}, \ldots, u_{,xx}, u_{,xy}, u_{,yy}, \ldots) = 0$$

independent variables

dependent variable

- order: highest derivative
- linear/non-linear: in dependent variable or its derivative

classification of second-order PDEs

$$A\, u_{,xx} + B\, u_{,xy} + C\, u_{,yy} = D$$

- elliptic (heat conduction, electrostatics) $\quad B^2 - 4\,A\,C < 0$

  $u_{,xx} + u_{,yy} = f(x,y)$

- parabolic (diffusion) $\quad B^2 - 4\,A\,C = 0$

  $u_{,xx} = u_{,t}$

- hyperbolic (wave equation) $\quad B^2 - 4\,A\,C > 0$

  $c^2\, u_{,xx} - u_{,tt} = 0$

governing PDE

u satisfies PDE everywhere

- strong form $$F = 0$$

u satisfies PDE on average in domain

- weak form $$\int_\Omega \eta \, F = 0$$

function space for u has infinite dimension…

discretization of function space and domain

- "triangulation" of domain
- low-order polynomial in each element

$$p = a_1 + a_2 x + a_3 y + a_4 xx + a_5 xy + a_6 yy + \ldots$$

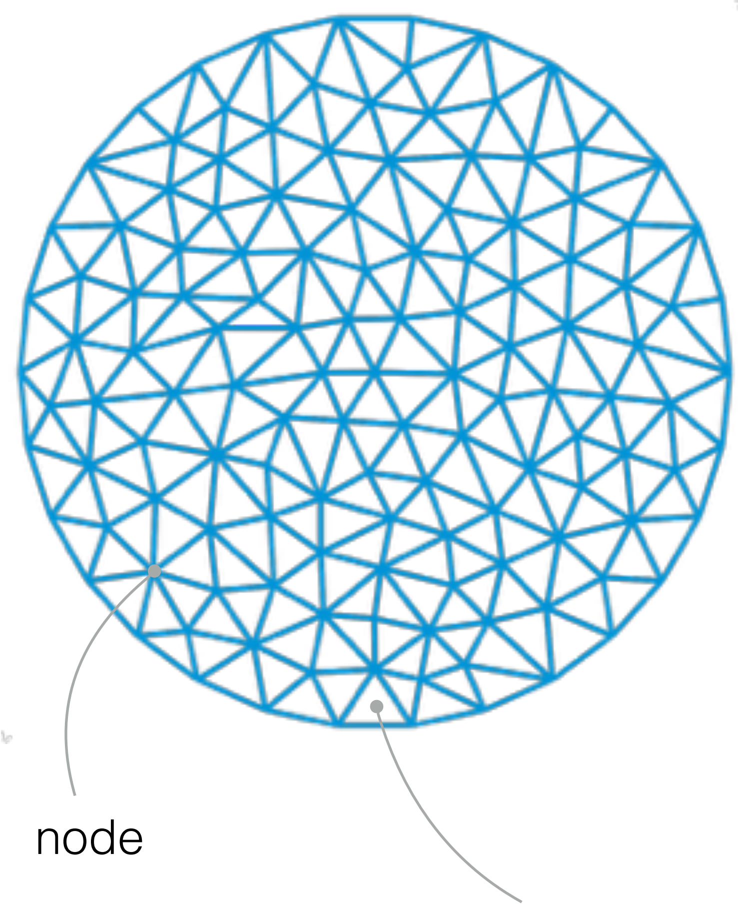

approximation within single element

- function determined by nodal values
- edge values only depend on values at shared nodes

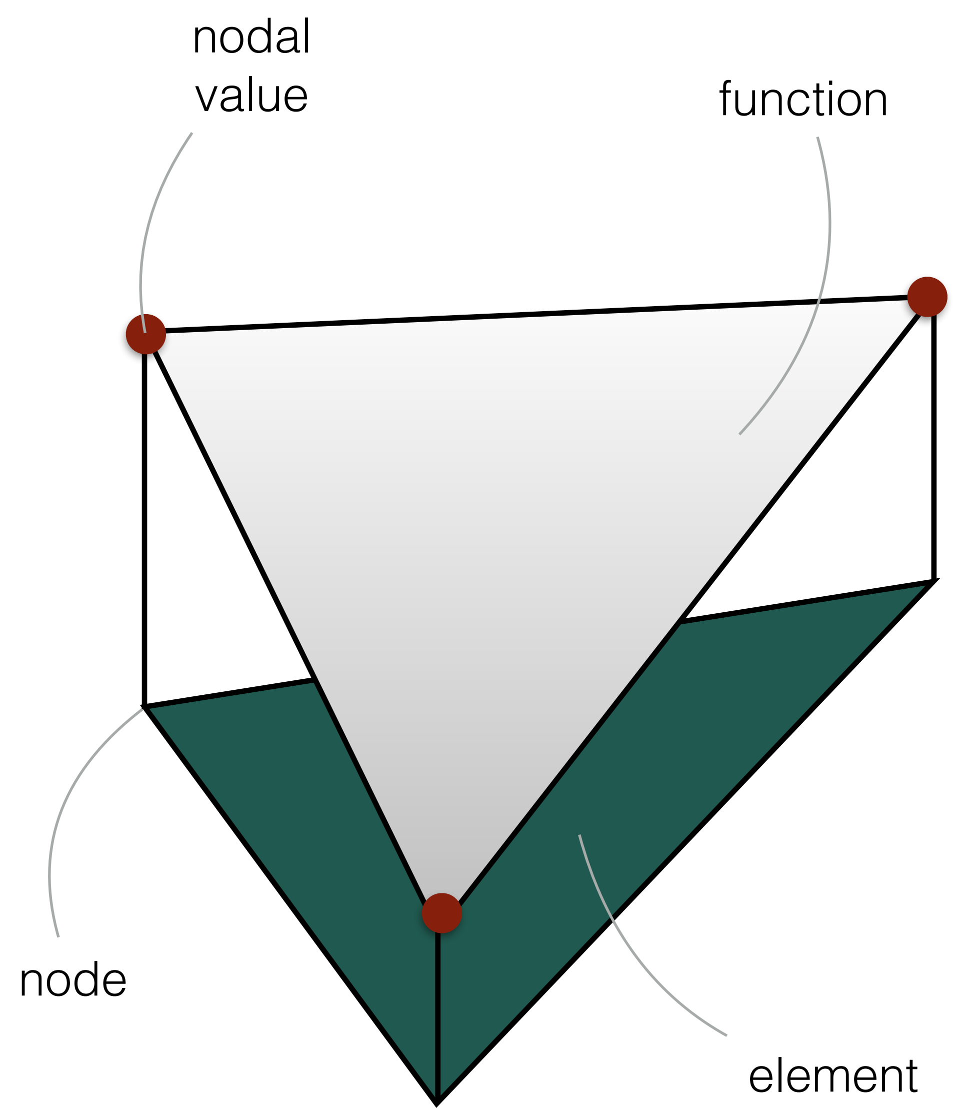

approximation within domain

- globally continuous

$$u(\mathbf{x}) = \sum_{i}^{N} u_i \, N_i(\mathbf{x})$$

- uniquely defined by set of nodal values

$$\{u_i\}$$

- interpolation by basis functions

$$N_i(\mathbf{x}_k) = \delta_{ik}$$

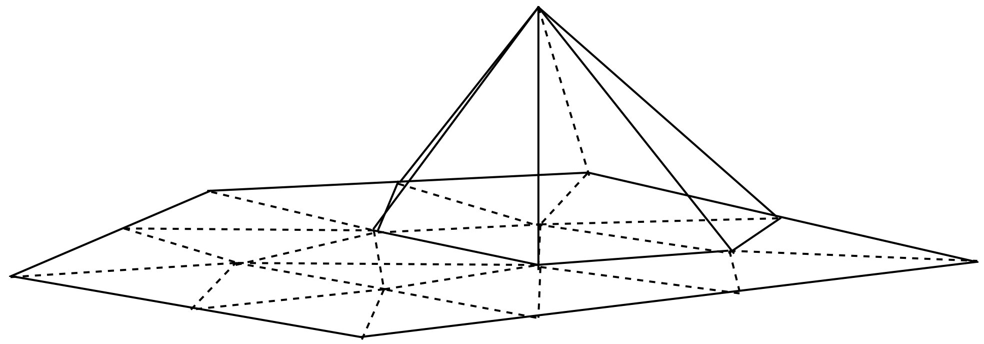

solution to weak form

- nodal basis functions as test function

$$\int N_i \, F = 0$$

system of N equations to solve for unknown nodal degrees of freedom

example problem: taut wire

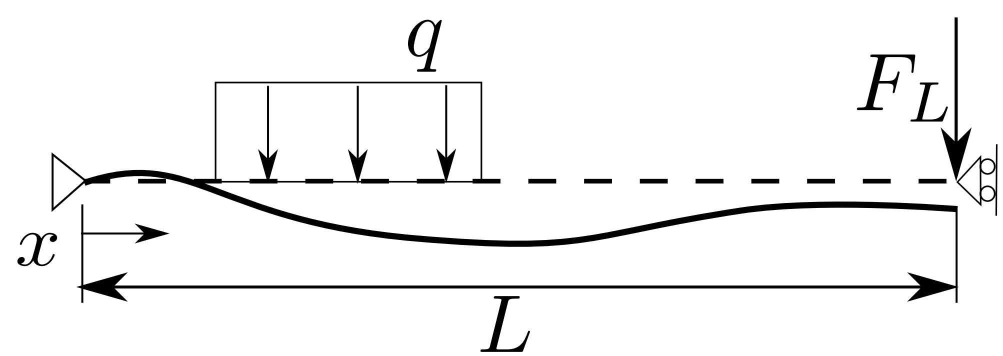

governing equation

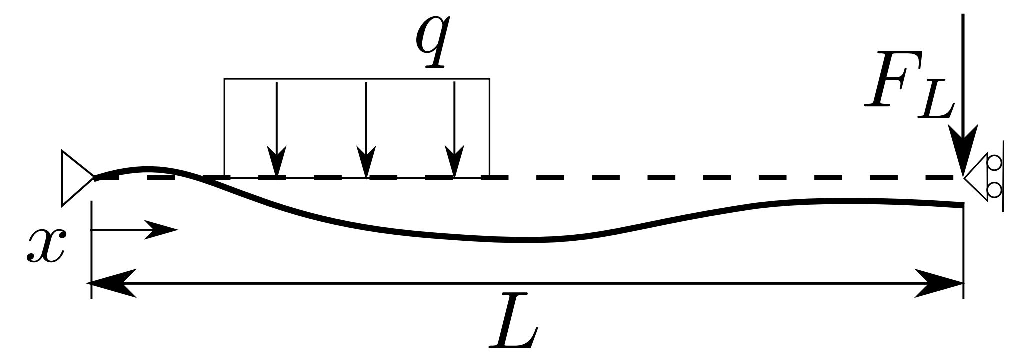

$$Pw'' + q = \mu\ddot{w}$$

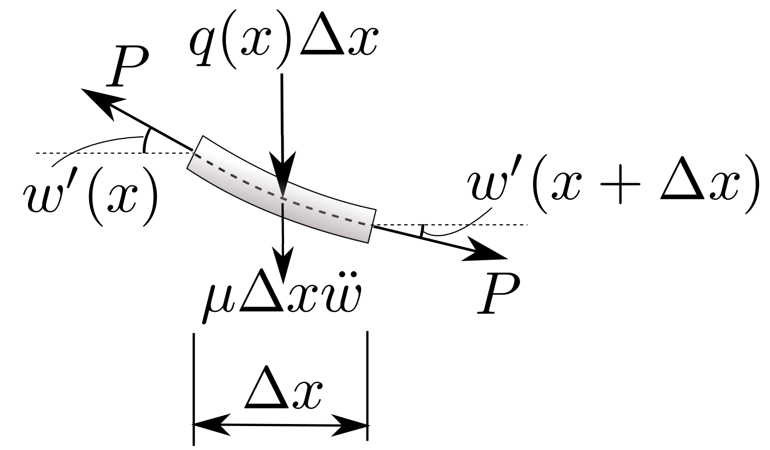

P. Krysl, Thermal and stress analysis with the finite element method, Pressure Cooker Press, 2010

boundary condition

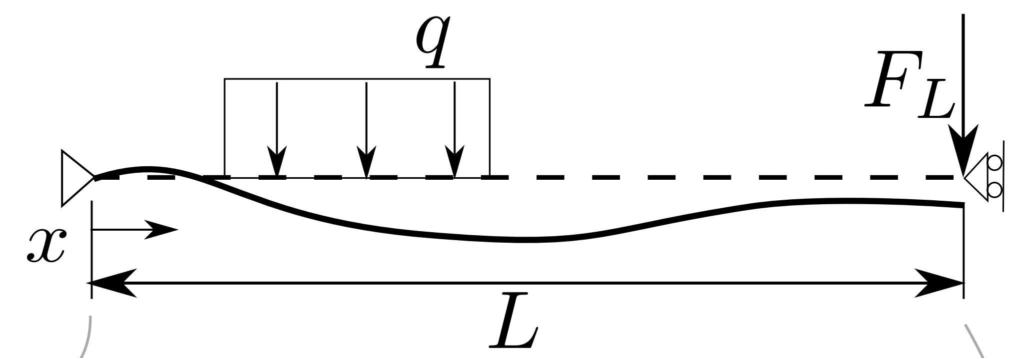

$$w(0,t) = \bar{w}_0(t)$$

“essential”
boundary condition

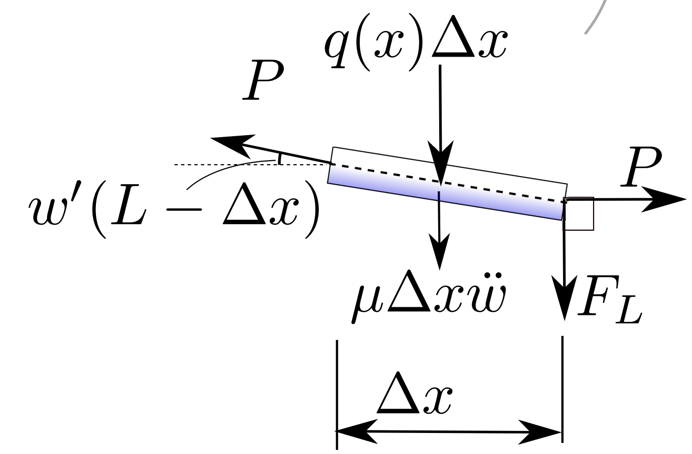

“natural” boundary
condition

$$P w'(L,t) = F_L(t)$$

P. Krysl, Thermal and stress analysis with the finite element method, Pressure Cooker Press, 2010

initial condition

- position $w(x,0) = \bar{w}(x)$
- velocity $\dot{w}(x,0) = \bar{v}(x)$

Galerkin method of weighted residual

static case for simplicity

- **approximate** fulfillment of the governing equation(s) by

$$Pw''(x) + q(x) = r_{\mathrm{B}}(x)$$

- **minimizing the residual**

$$\int_0^L r_{\mathrm{B}}(x)\,\mathrm{d}x \stackrel{!}{=} 0$$

- **weighting** the residual by **test function**

$$\int_0^L \eta(x)\,r_{\mathrm{B}}(x)\,\mathrm{d}x \stackrel{!}{=} 0$$

- use multiple test functions with limited support

$$\int_0^L \eta_j(x)\,r_{\mathrm{B}}(x)\,\mathrm{d}x \stackrel{!}{=} 0$$

shifting derivatives for piecewise linear approximation

$$\int_0^L \eta_j(x) r_B(x) \, \mathrm{d}x = \int_0^L \eta_j(x) P w''(x) \, \mathrm{d}x + \int_0^L \eta_j(x) q(x) \, \mathrm{d}x$$

$$(\eta_j P w')' = \eta_j{}' P w' + \eta_j P w''$$

only first derivatives

$$\int_0^L \eta_j P w'' \, \mathrm{d}x = \eta_j(L) P w'(L) - \eta_j(0) P w'(0) - \int_0^L \eta_j{}' P w' \, \mathrm{d}x$$

essential boundary condition

- fix the value(s) of the trial function

$$w(0) \equiv \bar{w}_0$$

natural boundary condition

- direct control of derivative not feasible

- introduce residual $$r_F = -Pw'(L) + F_L$$

$$\eta_j(L) r_F = \eta_j(L)(-Pw'(L) + F_L) = 0$$

MICHIGAN STATE UNIVERSITY

natural boundary condition

- combine both residuals

$$
\begin{aligned}
\int_0^L n_j\, r_\mathrm{B}\, \mathrm{d}x + n_j(L) r_\mathrm{F} &= n_j(L) P w'(L) - n_j(0) P w'(0) \\
&\quad - \int_0^L n_j' P w'\, \mathrm{d}x + \int_0^L n_j\, q\, \mathrm{d}x \\
&\quad + n_j(L)(-P w'(L) + F_L) \\
&= -\, n_j(0) P w'(0) \\
&\quad - \int_0^L n_j' P w'\, \mathrm{d}x + \int_0^L n_j\, q\, \mathrm{d}x \\
&\quad + n_j(L) F_L \\
&= 0
\end{aligned}
$$

force to zero

stiffness matrix and load vector

- residuals

$$\eta_j(L)F_L - \int_0^L \eta_j{}'P\sum_{i=1}^{N} N_i{}'w_i \,\mathrm{d}x + \int_0^L \eta_j q \,\mathrm{d}x = 0, \quad j = 1, ..., N$$

$$\eta_j(L)F_L - \sum_{i=1}^{N}\left(\int_0^L \eta_j{}'PN_i{}' \,\mathrm{d}x\right) w_i + \int_0^L \eta_j q \,\mathrm{d}x = 0$$

- stiffness matrix

$$K_{ji} = \int_0^L \eta_j{}'PN_i{}' \,\mathrm{d}x$$

- load vector

$$L_j = \eta_j(L)F_L + \int_0^L \eta_j q \,\mathrm{d}x$$

- algebraic system

$$\sum_{i=1}^{N} K_{ji}w_i = L_j, \quad j = 1, \ldots, N$$

outline

- background and opportunities
- methodology
- exemplary results
- limitations

background

macromechanics

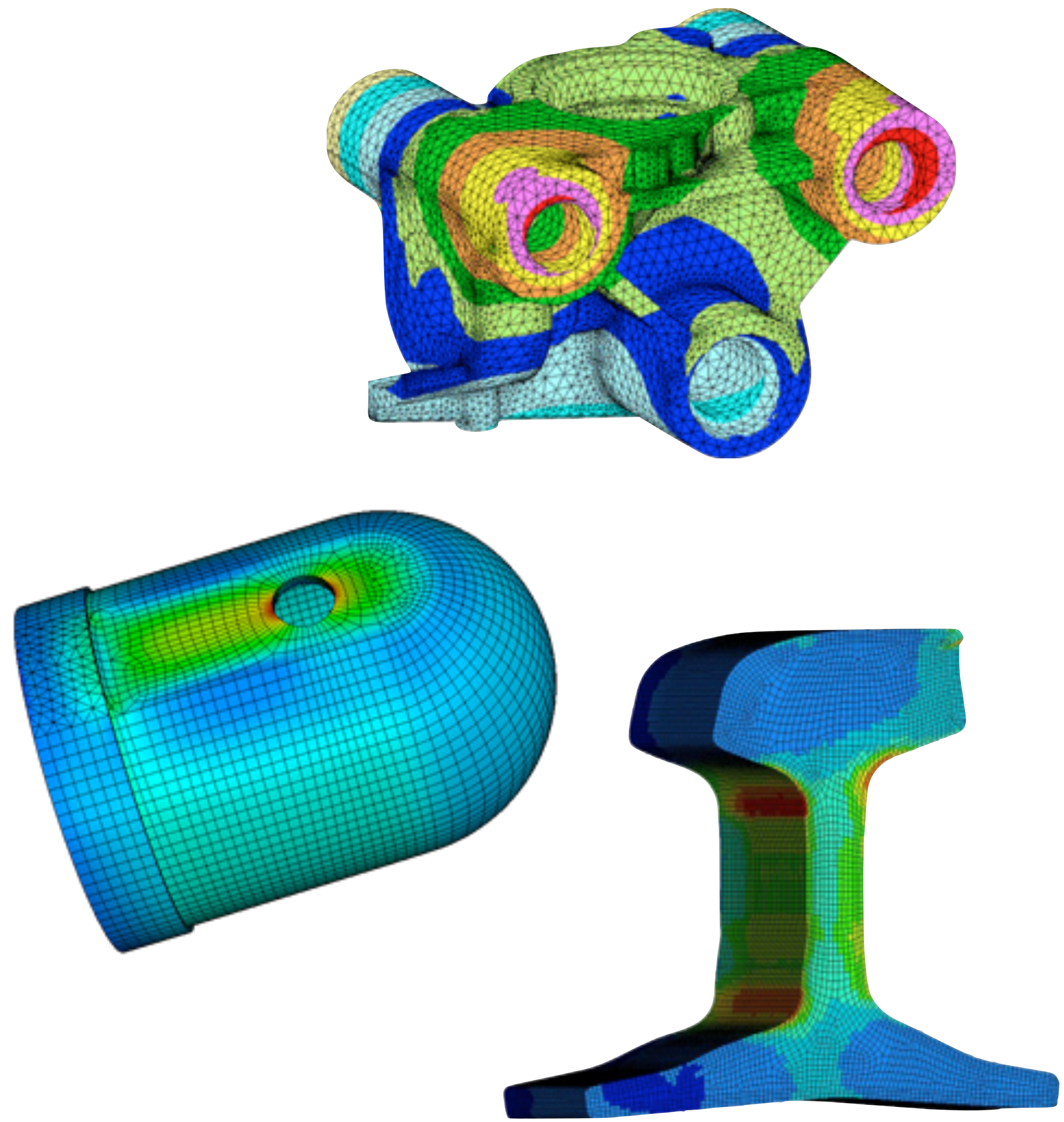

- complex geometry
- finite element method established

background

micromechanics

- periodic geometry
- shape-conforming mesh
- regular grid
- finite element method challenged by large number of degrees of freedom

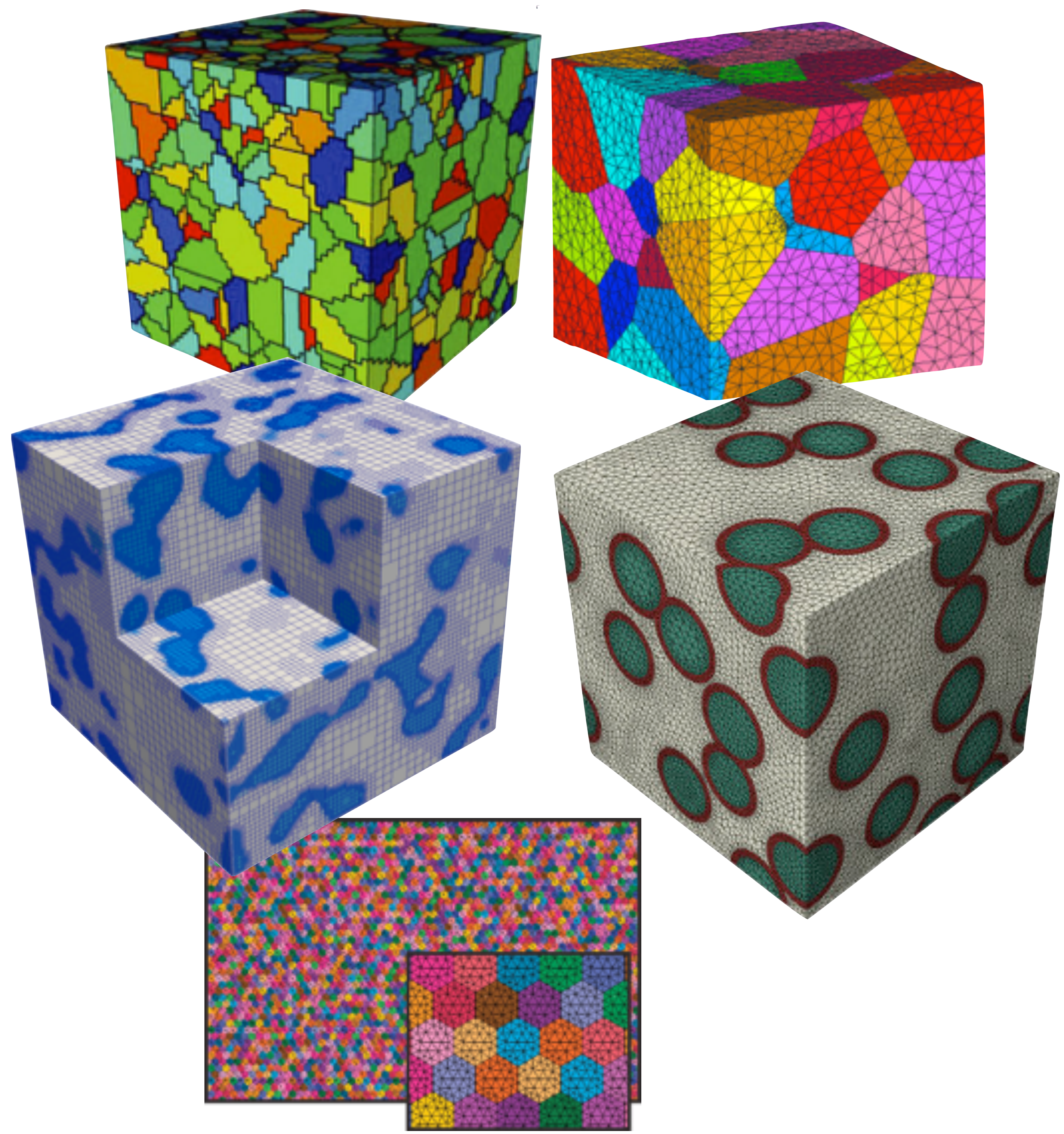

opportunities

- one-to-one comparison to experiment
    - verification of constitutive assumptions
- research and knowledge
    - influence of microstructural parameters
    - localization
    - hot spots
    - damage nucleation
- optimization
    - constituent properties
    - morphology
    - orientation distribution
    - misorientation distribution
- computational homogenization

methodology

historical development

- Moulinec, H., & Suquet, P. (1994).
  A fast numerical method for computing the linear and nonlinear properties of composites.
  C. R. Acad. Sci. Paris Ser. II, 318, 1417–1423.
- Moulinec, H., & Suquet, P. (1998).
  A numerical method for computing the overall response of nonlinear composites with complex microstructure.
  Computer Methods in Applied Mechanics and Engineering, 157(1-2), 69–94.
- Lebensohn, R. A. (2001).
  N-site modeling of a 3D viscoplastic polycrystal using Fast Fourier Transform.
  Acta Materialia, 49(14), 2723–2737.
- Lahellec, N., Michel, J. C., Moulinec, H., & Suquet, P. (2001).
  Analysis of inhomogeneous materials at large strains using fast Fourier transforms.
  In C. Miehe (Ed.), Proc. IUTAM Symposium (pp. 247–258). Solid Mechanics and its Applications, 108. Dordrecht, The Netherlands: Kluwer Academic Publishers.
- Lebensohn, R. A., Kanjarla, A. K., & Eisenlohr, P. (2012).
  An elasto-viscoplastic formulation based on fast Fourier transforms for the prediction of micromechanical fields in polycrystalline materials.
  Int. J. Plast., 32-33, 59–69.
- Eisenlohr, P., Diehl, M., Lebensohn, R. A., & Roters, F. (2013).
  A spectral method solution to crystal elasto-viscoplasticity at finite strains.
  Int. J. Plast., 46, 37–53.

methodology

finite strain kinematic framework

reference coordinates

$$\mathbf{y} = \overline{\mathbf{F}}\mathbf{x} + \widetilde{\mathbf{w}}$$

deformed coordinates

$$\frac{\partial \mathbf{y}}{\partial \mathbf{x}} = \overline{\mathbf{F}} + \frac{\partial \widetilde{\mathbf{w}}}{\partial \mathbf{x}}$$

$$\mathbf{F} = \overline{\mathbf{F}} + \widetilde{\mathbf{F}}$$

methodology

linear reference material

- arbitrary rate-dependent constitutive law

$$\mathbf{P}(\mathbf{x}) = \mathbf{f}(\mathbf{x}, \mathbf{F}, \dot{\mathbf{F}}, \mathbf{v})$$

- linear comparison material of stiffness

$$\begin{aligned}\mathbf{P}(\mathbf{x}) &= \mathbb{A}\mathbf{F}(\mathbf{x}) + \underbrace{\mathbf{P}(\mathbf{x}) - \mathbb{A}\mathbf{F}(\mathbf{x})} \\ &= \mathbb{A}\mathbf{F}(\mathbf{x}) + \qquad \boldsymbol{\tau}(\mathbf{x})\end{aligned}$$

polarization field

methodology

static equilibrium

- divergence-free stress field

$$\begin{aligned}\mathbf{0} &= \operatorname{Div}\mathbf{P}(\mathbf{x}) \\ &= \operatorname{Div}\left(\mathbb{A}\mathbf{F}(\mathbf{x}) + \boldsymbol{\tau}(\mathbf{x})\right) \\ &= \left\{\mathbb{A}\left[\boldsymbol{\chi}(\mathbf{x}) \otimes \nabla\right] + \boldsymbol{\tau}(\mathbf{x})\right\}\nabla\end{aligned}$$

- transformation into Fourier space

$$\begin{aligned}\mathbf{0} &= \frac{1}{(2\pi)^3}\int e^{i\,\mathbf{k}\cdot\mathbf{x}}\left\{\mathbb{A}\left[\boldsymbol{\chi}(\mathbf{k}) \otimes i\,\mathbf{k}\right] + \boldsymbol{\tau}(\mathbf{k})\right\} i\,\mathbf{k}\,\mathrm{d}\mathbf{k} \\ &= \mathcal{F}^{-1}\left(\left\{\mathbb{A}\left[\boldsymbol{\chi}(\mathbf{k}) \otimes i\,\mathbf{k}\right] + \boldsymbol{\tau}(\mathbf{k})\right\} i\,\mathbf{k}\right)\end{aligned}$$

- equilibrium fulfilled if

$$\mathbf{0} = \left\{\mathbb{A}\left[\boldsymbol{\chi}(\mathbf{k}) \otimes i\,\mathbf{k}\right] + \boldsymbol{\tau}(\mathbf{k})\right\} i\,\mathbf{k}$$

methodology

static equilibrium

- equilibrium condition $\mathbf{0} = \Big\{ \mathbb{A}\,[\boldsymbol{\chi}(\mathbf{k}) \otimes i\,\mathbf{k}] + \boldsymbol{\tau}(\mathbf{k}) \Big\}\, i\,\mathbf{k}$

- equivalent to $\mathbb{A}\,[\boldsymbol{\chi}(\mathbf{k}) \otimes \mathbf{k}]\,\mathbf{k} = \boldsymbol{\tau}(\mathbf{k})\, i\,\mathbf{k}$

$$\mathbf{A}(\mathbf{k})\,\boldsymbol{\chi}(\mathbf{k}) = \boldsymbol{\tau}(\mathbf{k})\, i\,\mathbf{k} \quad \text{for all} \quad \mathbf{k} \neq \mathbf{0}$$

- “acoustic tensor” $\mathbf{A}(\mathbf{k})\,\mathbf{a} = \mathbb{A}\,[\mathbf{a} \otimes \mathbf{k}]\,\mathbf{k}$

methodology

equilibrated deformation map

$$\mathbf{A}(\mathbf{k})\,\boldsymbol{\chi}(\mathbf{k}) = \boldsymbol{\tau}(\mathbf{k})\,i\,\mathbf{k} \quad \text{for all} \quad \mathbf{k} \neq \mathbf{0}$$

$$\boldsymbol{\chi}(\mathbf{k}) = \begin{cases} \mathbf{A}(\mathbf{k})^{-1}\boldsymbol{\tau}(\mathbf{k})\,i\,\mathbf{k} & \text{if } \mathbf{k} \neq \mathbf{0} \\ \boldsymbol{\chi}(\mathbf{0}) & \text{if } \mathbf{k} = \mathbf{0} \end{cases}$$

methodology

equilibrated deformation gradient

$$\boldsymbol{\chi}(\mathbf{k}) = \begin{cases} \mathbf{A}(\mathbf{k})^{-1} \boldsymbol{\tau}(\mathbf{k})\, i\, \mathbf{k} & \text{if } \mathbf{k} \neq \mathbf{0} \\ \boldsymbol{\chi}(\mathbf{0}) & \text{if } \mathbf{k} = \mathbf{0} \end{cases}$$

$$\begin{aligned} \mathbf{F}(\mathbf{k}) &= \begin{cases} -\mathbf{A}(\mathbf{k})^{-1} \boldsymbol{\tau}(\mathbf{k})\, (\mathbf{k} \otimes \mathbf{k}) \\ \mathbf{F}(\mathbf{0}) \end{cases} \\ &= \begin{cases} -\mathbb{\Gamma}(\mathbf{k})\, \boldsymbol{\tau}(\mathbf{k}) & \text{if } \mathbf{k} \neq \mathbf{0} \\ \overline{\mathbf{F}} & \text{if } \mathbf{k} = \mathbf{0} \end{cases} \end{aligned}$$

methodology

iterative algorithm

$$\boldsymbol{\tau} = \mathbf{P} - \mathbb{A}\mathbf{F}$$

$$\mathbf{F}(\mathbf{k}) = \begin{cases} -\mathbb{\Gamma}(\mathbf{k})\,\boldsymbol{\tau}(\mathbf{k}) & \text{if } \mathbf{k} \neq \mathbf{0} \\ \overline{\mathbf{F}} & \text{if } \mathbf{k} = \mathbf{0} \end{cases}$$

$$\begin{aligned} \widetilde{\mathbf{F}}(\mathbf{x}) &= -\mathbb{\Gamma}(\mathbf{x}) * \Big[\mathbf{P}(\mathbf{F}(\mathbf{x})) - \mathbb{A}\mathbf{F}(\mathbf{x})\Big] \\ &= -\mathbb{\Gamma}(\mathbf{x}) * \mathbf{P}(\mathbf{F}(\mathbf{x})) + \underbrace{\mathbb{\Gamma}(\mathbf{x}) * [\mathbb{A}\mathbf{F}(\mathbf{x})]} \\ &= -\mathbb{\Gamma}(\mathbf{x}) * \mathbf{P}(\mathbf{F}(\mathbf{x})) + \qquad \widetilde{\mathbf{F}}(\mathbf{x}) \end{aligned}$$

methodology

iterative algorithm

- fix-point iteration

$$\widetilde{\mathbf{F}}(\mathbf{x}) = -\mathbb{\Gamma}(\mathbf{x}) * \mathbf{P}(\mathbf{F}(\mathbf{x})) + \widetilde{\mathbf{F}}(\mathbf{x})$$

$$\{\mathbf{F}(\mathbf{x})\}_{n+1} = \{\mathbf{F}(\mathbf{x})\}_n - \mathcal{F}^{-1}\left(\begin{cases} \mathbb{\Gamma}(\mathbf{k})\ \{\mathbf{P}(\mathbf{k})\}_n & \text{if } \mathbf{k} \neq \mathbf{0} \\ \{\overline{\mathbf{F}}\}_n - \{\mathbf{F}_{\mathrm{BC}}\}_{n+1} & \text{if } \mathbf{k} = \mathbf{0} \end{cases}\right)$$

- boundary condition

$$\{\mathbf{F}_{\mathrm{BC}}\}_{n+1} = \{\overline{\mathbf{F}}\}_0 + \dot{\mathbf{F}}_{\mathrm{BC}}\,\Delta t - \left\{\frac{\overline{\partial \mathbf{F}}}{\partial \mathbf{P}}\right\}_n \left(\{\overline{\mathbf{P}}\}_n - \mathbf{P}_{\mathrm{BC}}\right)$$

exemplary results

comparison between FEM and spectral method

- load case

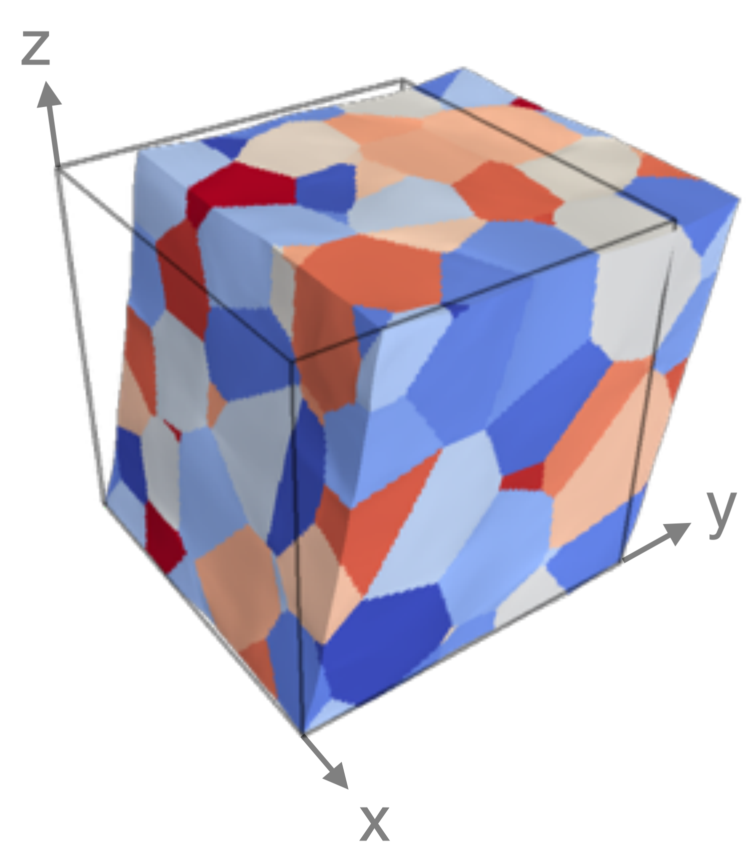

exemplary results

comparison between FEM and spectral method

- mesh convergence of volume-average response

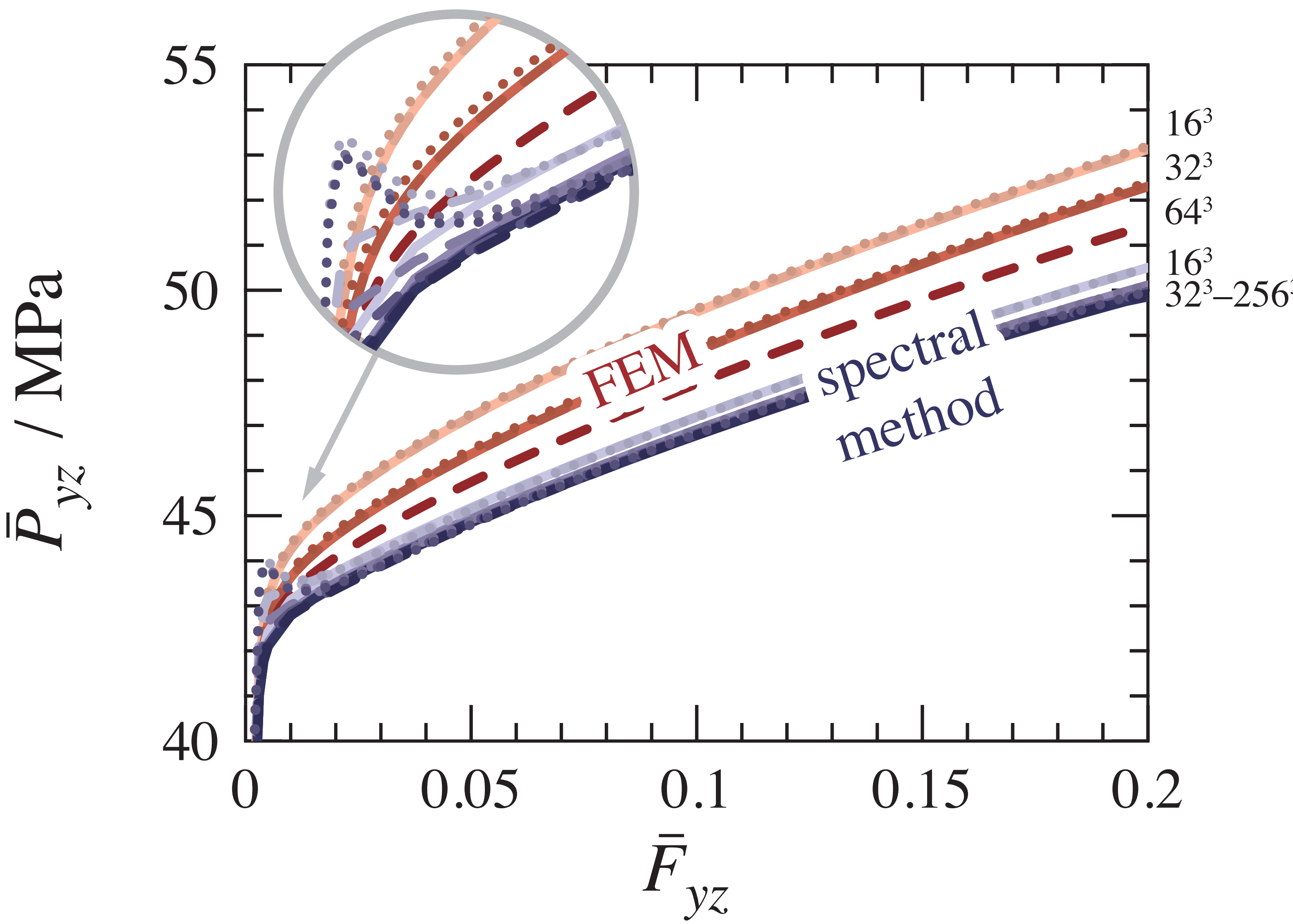

MICHIGAN STATE UNIVERSITY

exemplary results

comparison between
FEM and spectral method

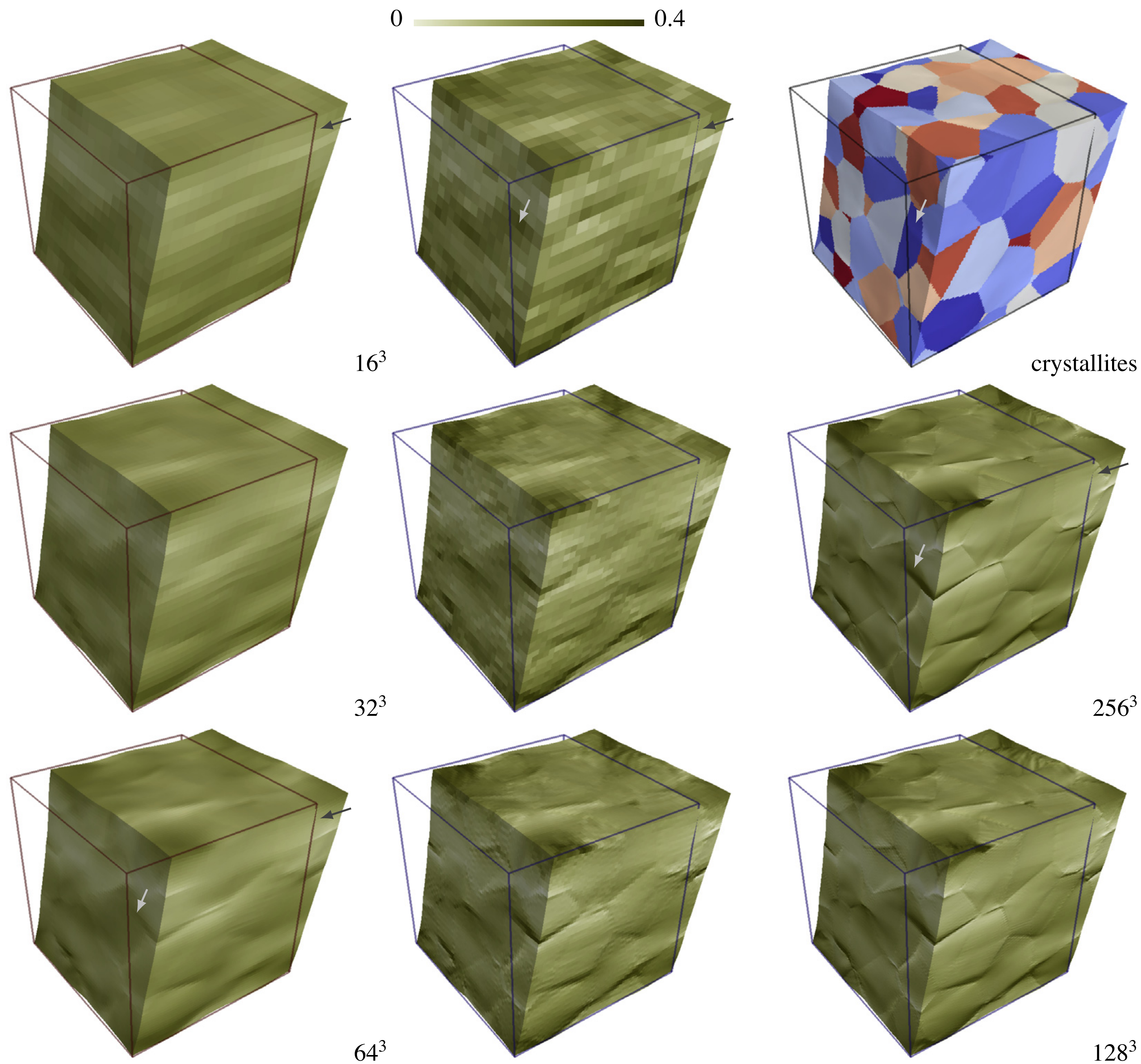

(a) Finite element method simulation (b) Spectral method simulation

MICHIGAN STATE UNIVERSITY

exemplary results

comparison between FEM and spectral method

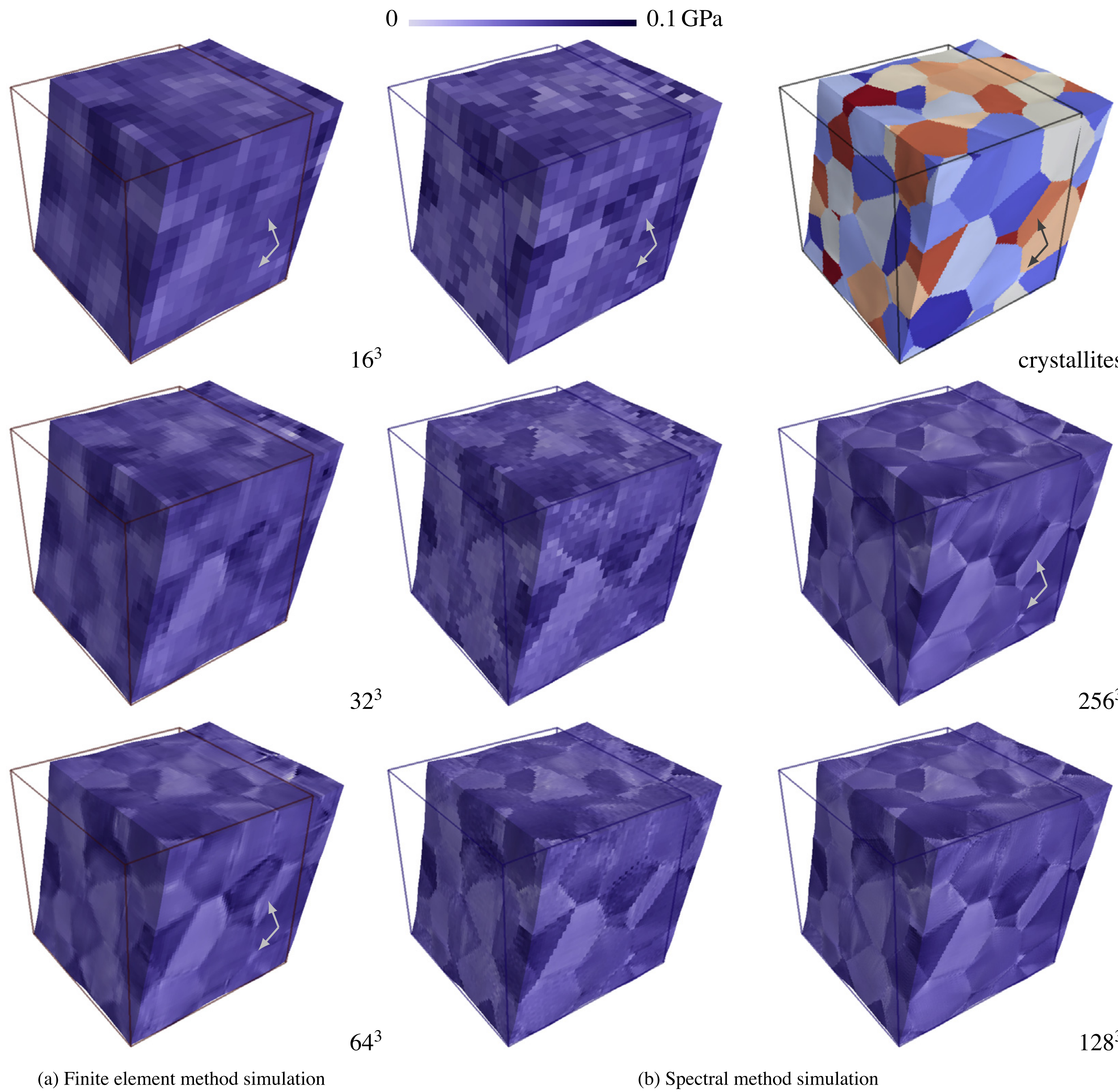

exemplary results

comparison between
FEM and spectral method

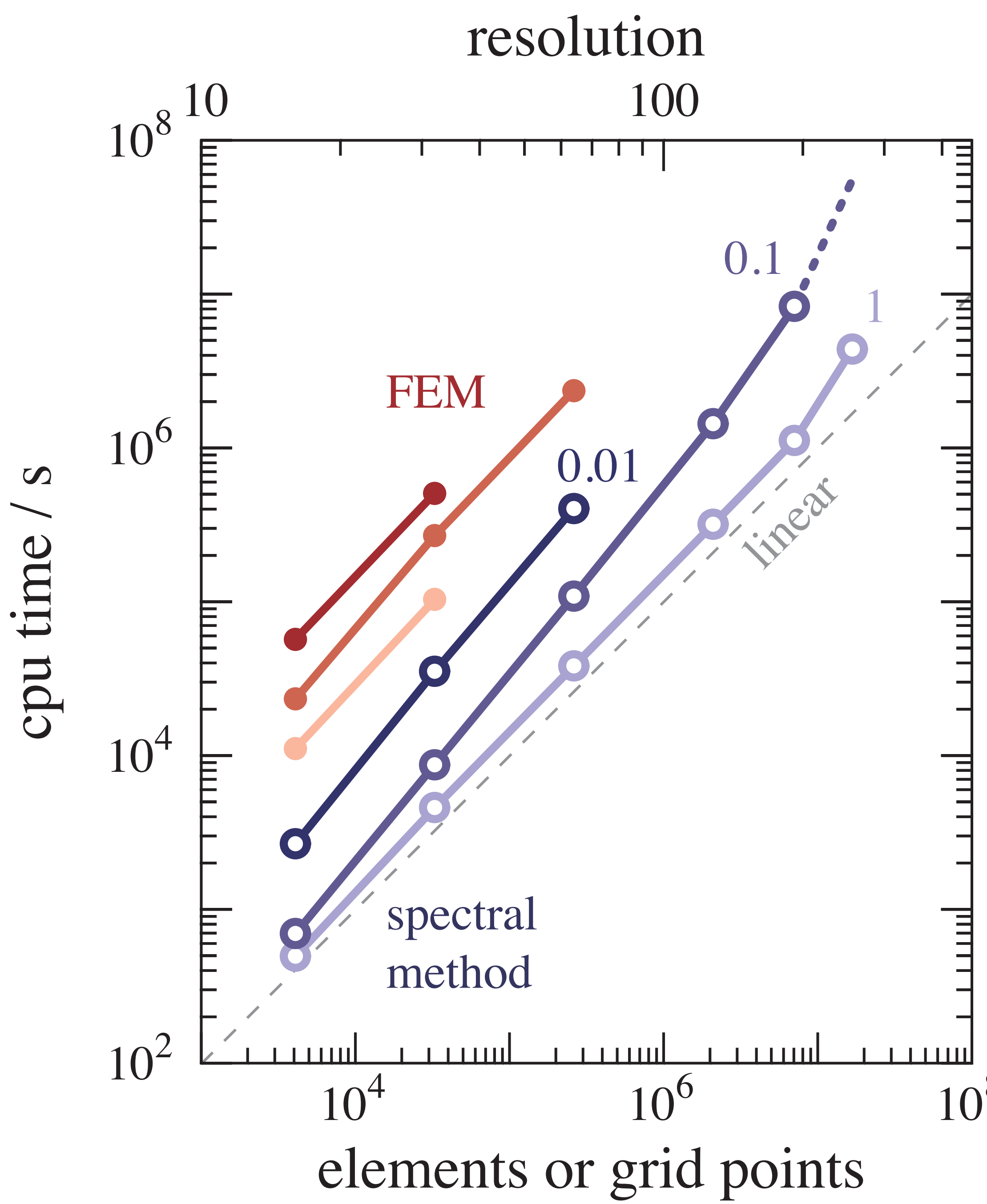

exemplary results

International Journal of Plasticity 27 (2011) 707–727

ELSEVIER

Contents lists available at ScienceDirect

International Journal of Plasticity

journal homepage: www.elsevier.com/locate/ijplas

Modeling the viscoplastic micromechanical response of two-phase materials using Fast Fourier Transforms

S.-B. Lee [a,*], R.A. Lebensohn [b], A.D. Rollett [a]

[a] Department of Materials Science and Engineering, Carnegie Mellon University, Pittsburgh, PA 15213, USA
[b] Materials Science and Technology Division, Los Alamos National Laboratory, Los Alamos, NM 87845, USA

exemplary results

- percolating vs granular matrix
- stress
- strain rate

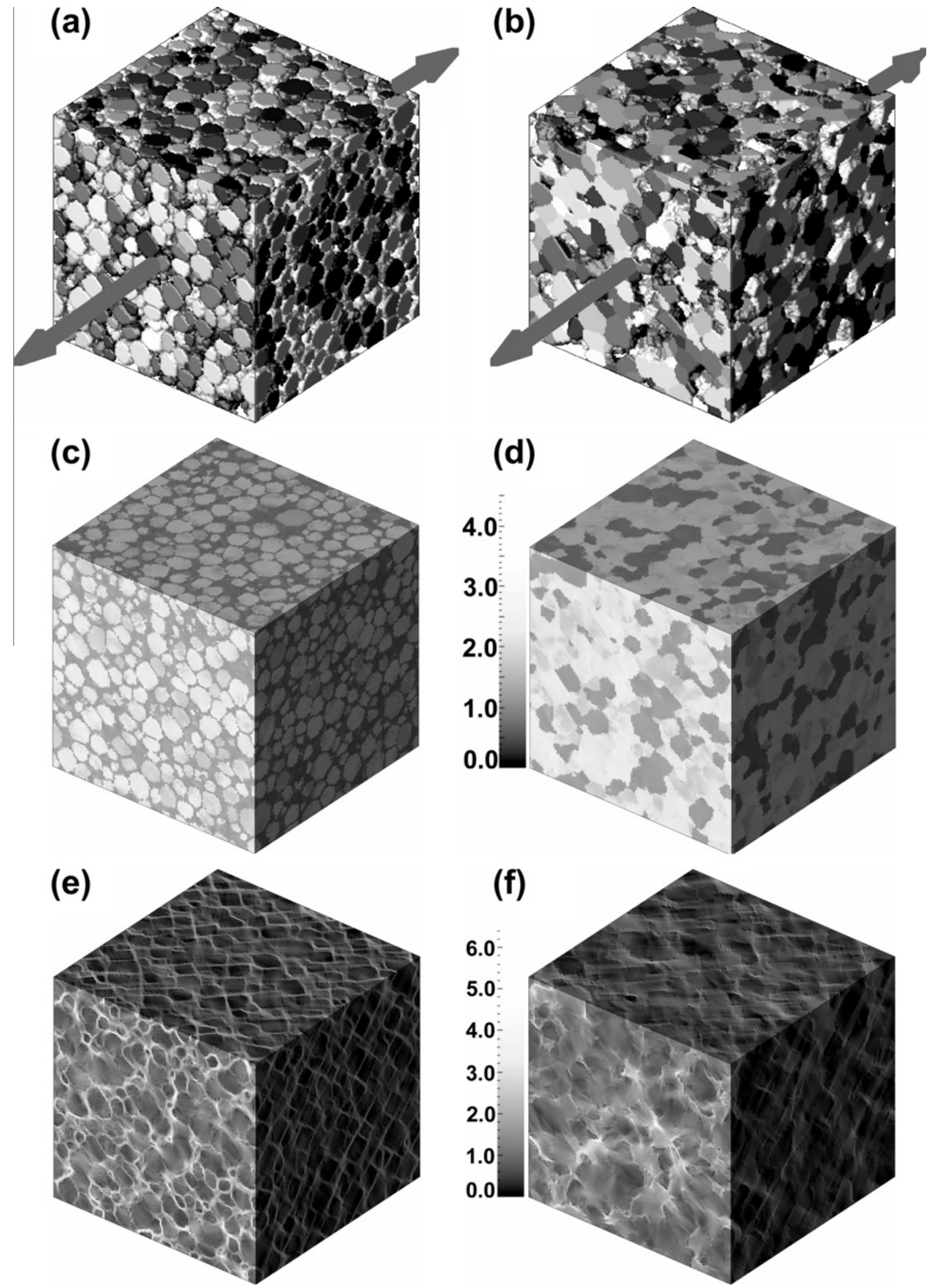

exemplary results

- different contiguity
- stress
- strain rate

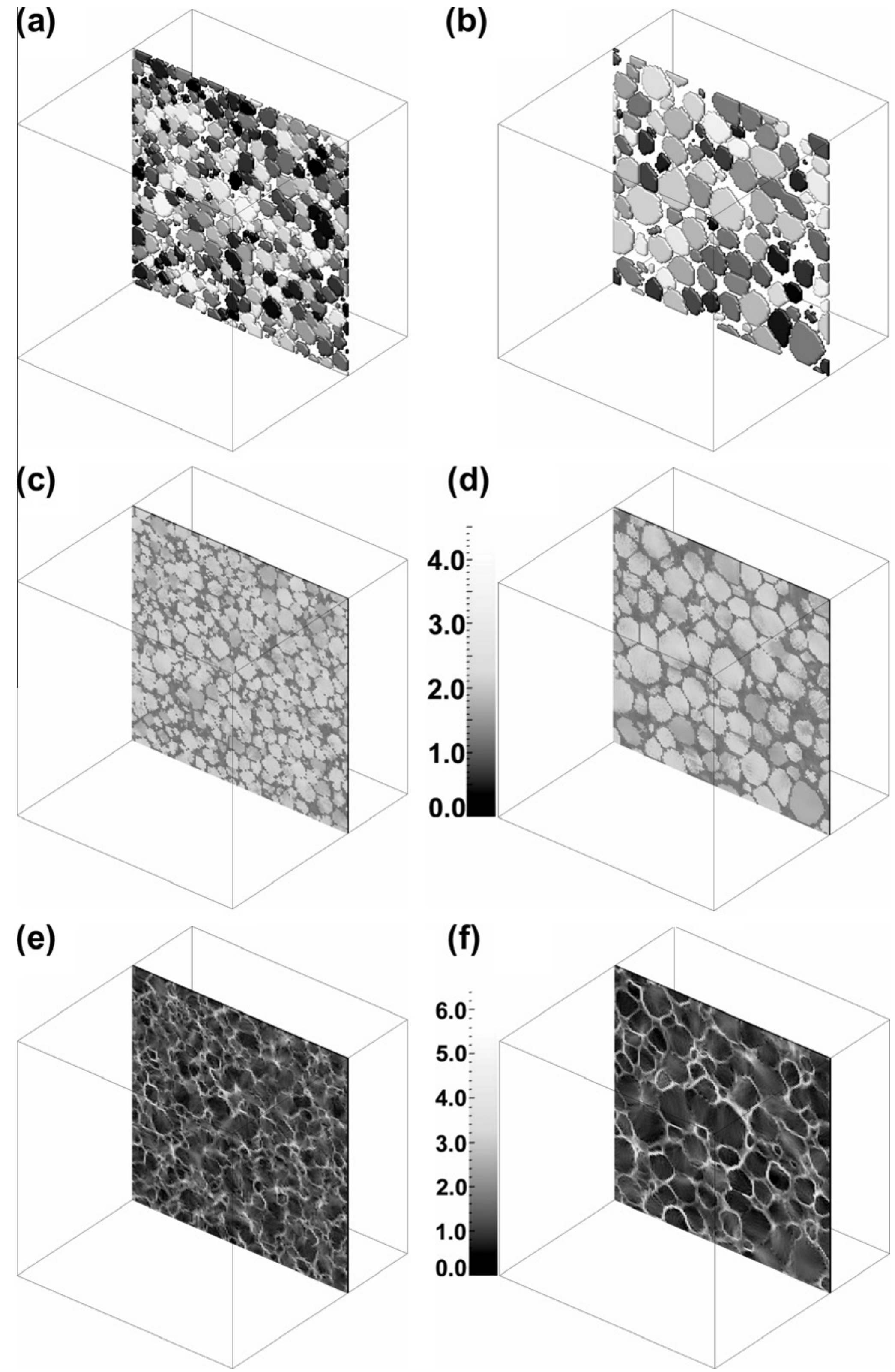

exemplary results

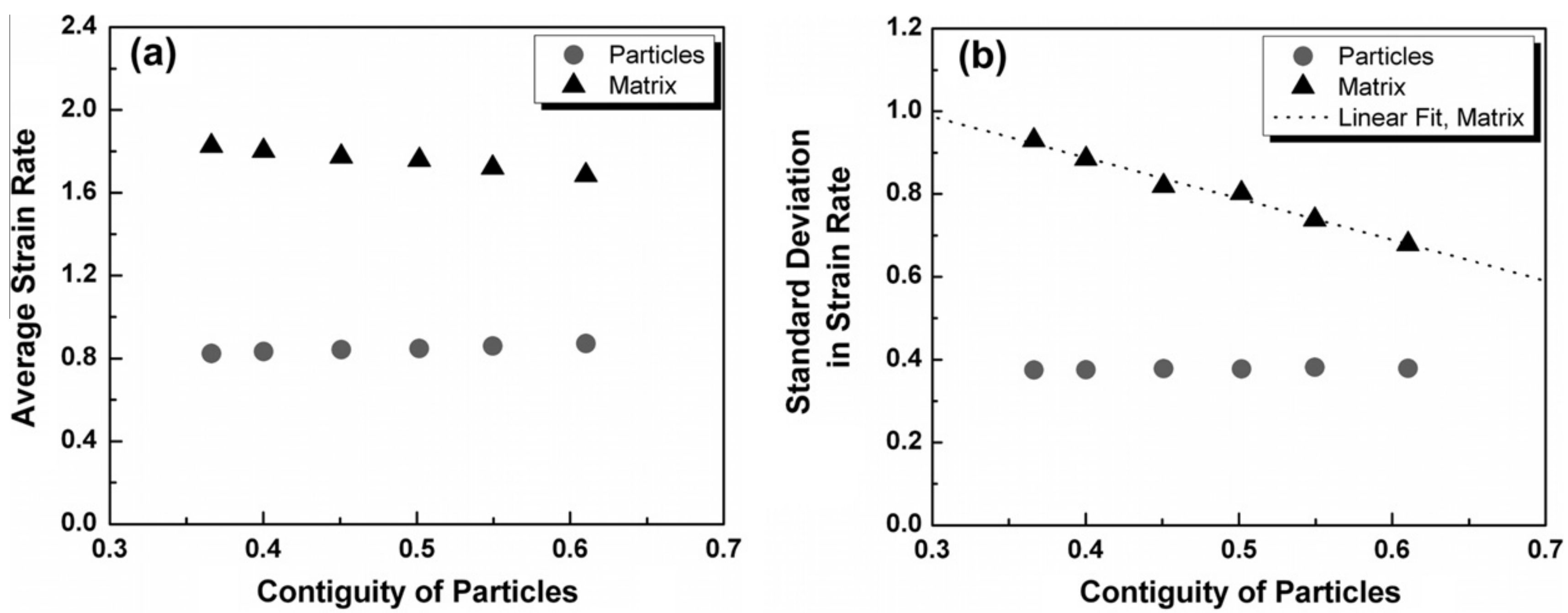

limitations

- periodic structure
- high property contrast
- strongly heterogeneous deformation

solution

- low-stiffness gaps
- alternative formulations
- regridding

homework

- finalize lab assignments of April 11 and 18
- due date April 27 (Sunday)

file transfer

mesh convergence (lab April 11)

- make a directory at /egr/research/CMM/MSE991/SpectralMeshConvergence/$USER
- copy
  - *.geom files of 20 and 40 grain structure
  - material.config
  - loadcase file
  - *.spectralOut binary result file

file transfer

kinematic variability in 3D and 2D (lab April 18)

- make a directory at /egr/research/CMM/MSE991/VariabilityColumnarEquiaxed/$USER
- copy
  - *.geom files of equiaxed and sliced structures
  - material.config
  - loadcase file
  - *.spectralOut files of all five simulations

convergence of basic scheme

linear elastic media

- spectral radius of "Gamma" operator

$$R = \frac{\max \mathbb{C}(\mathbf{x}) - \min \mathbb{C}(\mathbf{x})}{\max \mathbb{C}(\mathbf{x}) + \min \mathbb{C}(\mathbf{x})}$$

- distance to fix point

$$\epsilon \propto R^N$$

- rate of convergence proportional to contrast factor

Michel, J. C., Moulinec, H., & Suquet, P. (2001). A computational scheme for linear and non-linear composites with arbitrary phase contrast. Int. J. Numer. Meth. Engng., 52(12), 139–160.

dual-phase steel example

microstructure

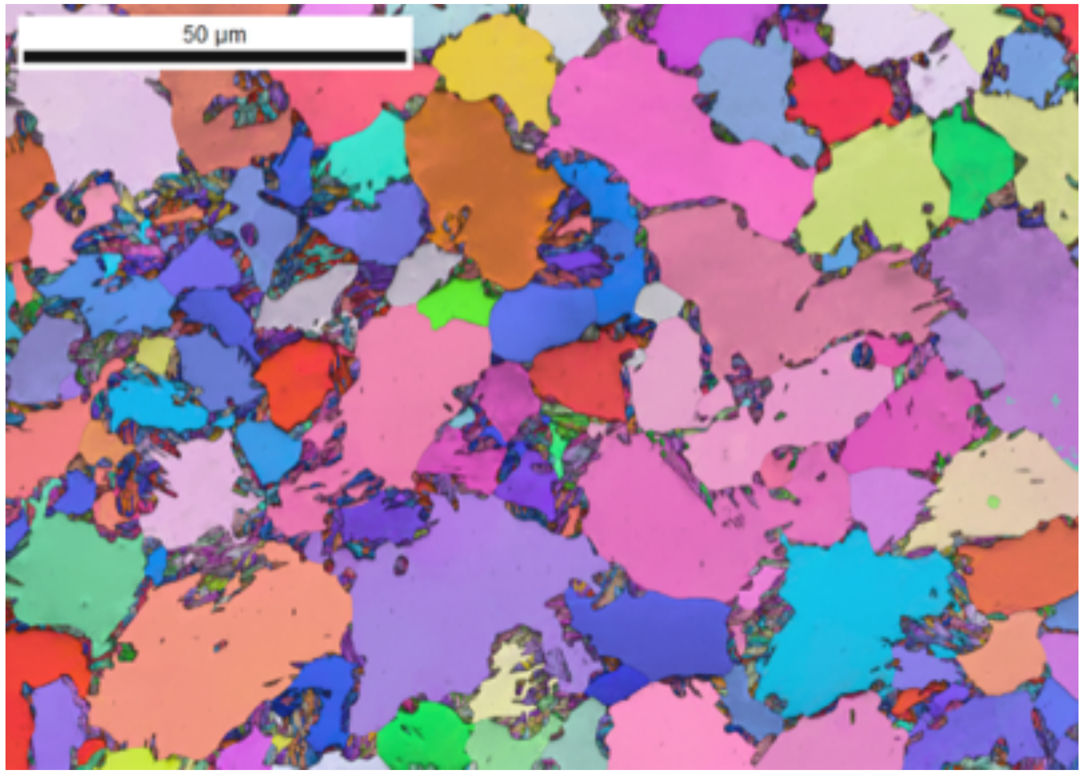

dual-phase steel example

basic spectral scheme

body force

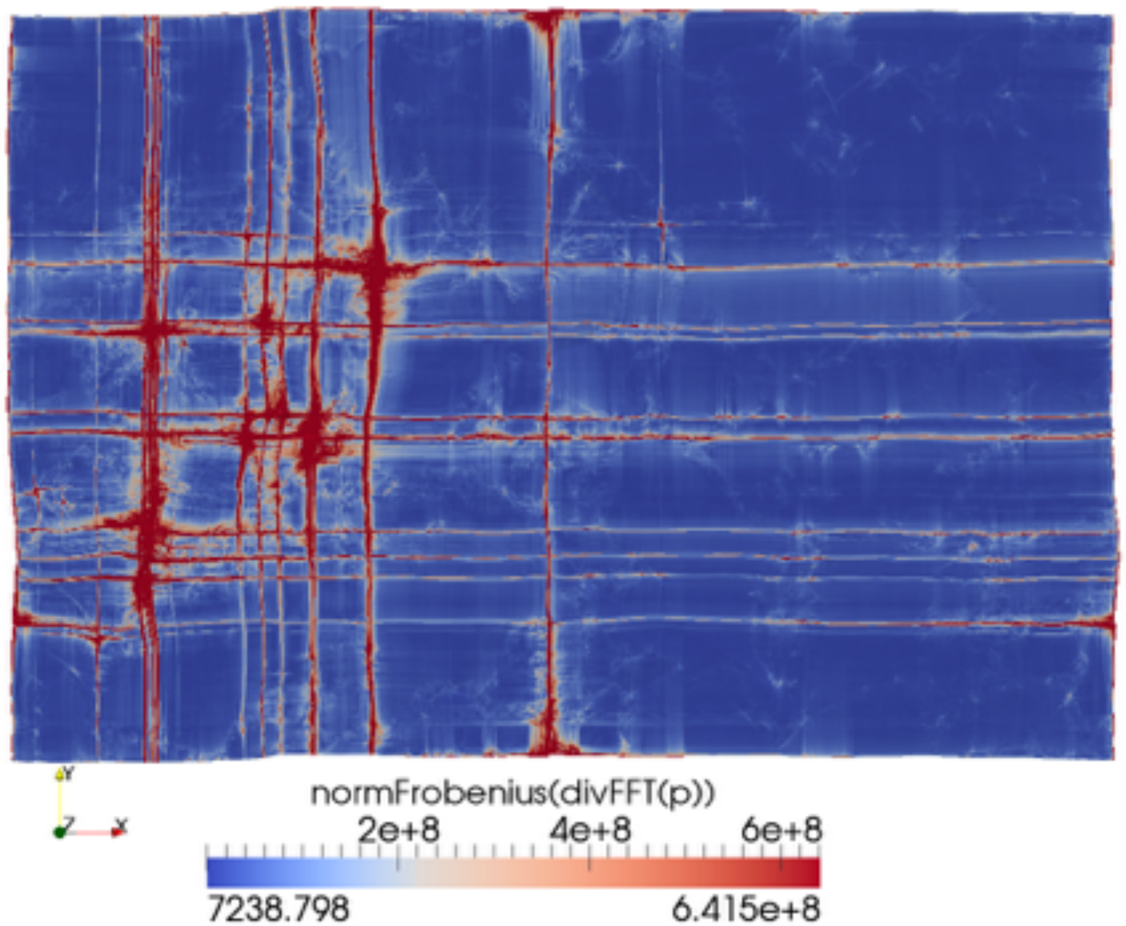

compatibility

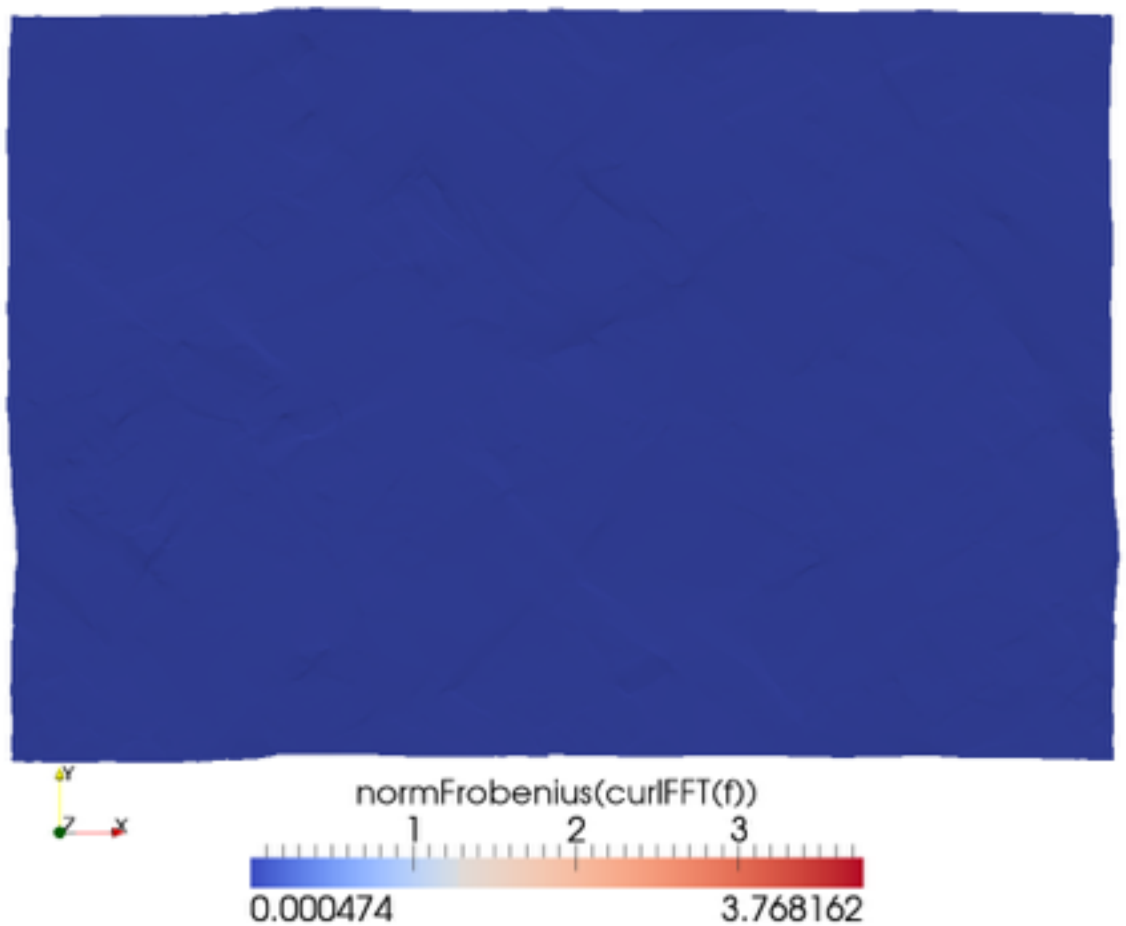

dual-phase steel example

Augmented Lagrangian spectral scheme

body force

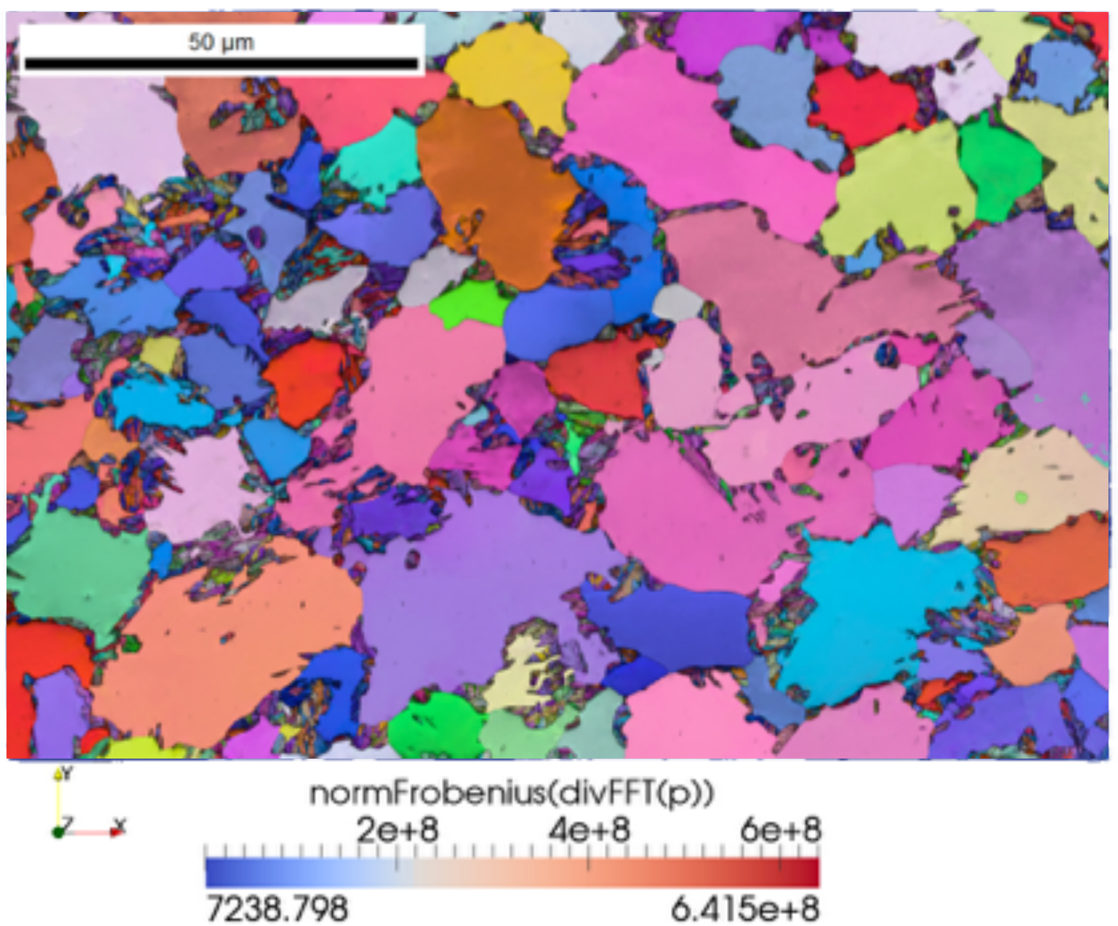

compatibility

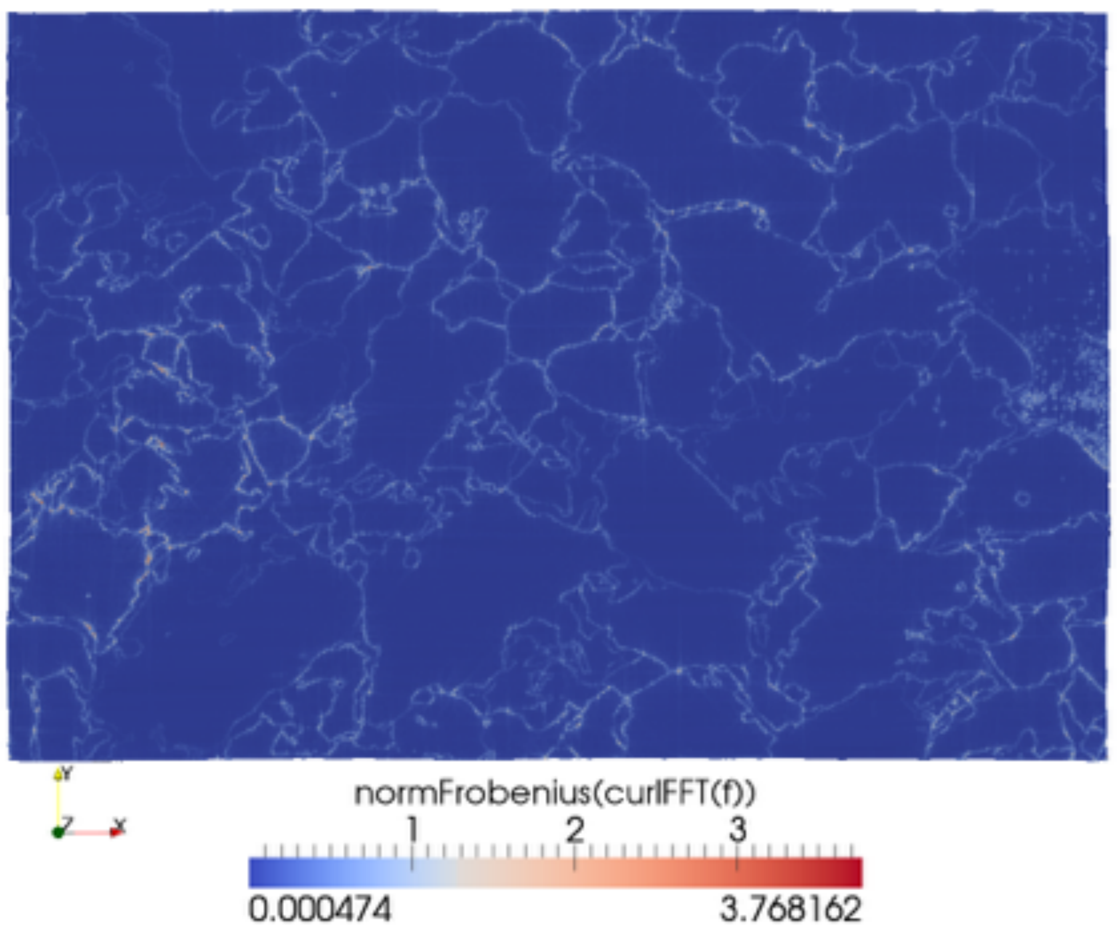

arbitrary rate-dependent constitutive law

strain energy density functional

$$\mathbf{P}(\mathbf{x}) = \frac{\delta \mathcal{W}}{\delta \mathbf{F}(\mathbf{x})} = \mathbf{f}(\mathbf{x}, \mathbf{F}, \dot{\mathbf{F}}, \boldsymbol{\xi})$$

first Piola–Kirchhoff stress

internal variables

direct variational formulation

inv. Fourier transform

$$\min_{\boldsymbol{\chi}} \mathcal{W} \implies \operatorname{Div} \mathbf{P}(\mathbf{x}) = \mathcal{F}^{-1}\left[\mathbf{P}(\mathbf{k})\, i\, \mathbf{k}\right] = \mathbf{0}$$

$$\widehat{\mathscr{F}}\left[\boldsymbol{\chi}(\mathbf{k})\right] := \mathbf{P}(\mathbf{k})\, i\, \mathbf{k} = \mathbf{0}$$

residual body force field

direct variational formulation

try to find that deformation map which causes the same body force field in a linear homogeneous reference medium

$$\widehat{\mathscr{F}}[\boldsymbol{\chi}(\mathbf{k})] := \mathbf{P}(\mathbf{k})\, i\, \mathbf{k} = \mathbf{0}$$

direct variational formulation

reference stiffness

$$\mathbf{P}(\mathbf{x}) = \mathbb{A}\mathbf{F}(\mathbf{x}) = \mathbb{A}\,\mathrm{Grad}\,\boldsymbol{\chi}$$

$$\widehat{\mathscr{P}}[\boldsymbol{\chi}(\mathbf{k})] := \mathbb{A}\,[\boldsymbol{\chi}(\mathbf{k}) \otimes i\,\mathbf{k}]\; i\,\mathbf{k} = \mathbf{A}(\mathbf{k})\,\boldsymbol{\chi}(\mathbf{k}) = \mathbf{0}$$

body force field in reference material

acoustic tensor

deformation map in reference material

MICHIGAN STATE UNIVERSITY

direct variational formulation

body force field in heterogeneous material

$$\widehat{\mathscr{P}}^{-1}\widehat{\mathscr{F}}\left[\chi(\mathbf{k})\right] = \left[\mathbf{A}(\mathbf{k})^{-1}\mathbf{P}(\mathbf{k})\, i\, \mathbf{k}\right] = \mathbf{0} \quad \forall\, \mathbf{k} \neq \mathbf{0}$$

deformation map in reference material

deformation gradient in reference material

$$\widehat{\mathscr{F}}_{\text{direct}}\left[\mathbf{F}(\mathbf{k})\right] := \Gamma(\mathbf{k})\, \mathbf{P}(\mathbf{k}) = \mathbf{0} \quad \forall\, \mathbf{k} \neq \mathbf{0}$$

mixed variational formulation

$$\min_{\mathbf{F}} \mathcal{W} \quad \text{subject to} \quad \mathbf{F} = \operatorname{Grad} \boldsymbol{\chi}$$

Lagrange multiplier

$$\begin{aligned}\mathcal{L}[\mathbf{F}, \boldsymbol{\chi}, \boldsymbol{\Lambda}] = \mathcal{W} & \\ & + \int_{\mathcal{B}_0} \mathbf{F}(\mathbf{x}) \boldsymbol{\Lambda}(\mathbf{x}) \cdot [\operatorname{Grad} \boldsymbol{\chi}(\mathbf{x}) - \mathbf{F}(\mathbf{x})] \, \mathrm{d}\mathbf{x} \\ & + \frac{1}{2} \int_{\mathcal{B}_0} [\operatorname{Grad} \boldsymbol{\chi}(\mathbf{x}) - \mathbf{F}(\mathbf{x})] \cdot \mathbb{A} \, [\operatorname{Grad} \boldsymbol{\chi}(\mathbf{x}) - \mathbf{F}(\mathbf{x})] \, \mathrm{d}\mathbf{x}\end{aligned}$$

penalty

mixed variational formulation

solution corresponds to saddle point

$$
\begin{aligned}
\frac{\delta \mathcal{L}}{\delta \mathbf{F}(\mathbf{x})} &= \mathbf{P}(\mathbf{x}) - \mathbf{F}(\mathbf{x})\boldsymbol{\Lambda}(\mathbf{x}) + \mathbb{A}\Big\{\mathbf{F}(\mathbf{x}) - \operatorname{Grad}\boldsymbol{\chi}(\mathbf{x})\Big\} = \mathbf{0},\\
\frac{\delta \mathcal{L}}{\delta \boldsymbol{\chi}(\mathbf{x})} &= \operatorname{Div}\,\Big[\mathbf{F}(\mathbf{x})\boldsymbol{\Lambda}(\mathbf{x}) - \mathbb{A}\Big\{\mathbf{F}(\mathbf{x}) - \operatorname{Grad}\boldsymbol{\chi}(\mathbf{x})\Big\}\Big] = \mathbf{0},\\
\frac{\delta \mathcal{L}}{\delta \boldsymbol{\Lambda}(\mathbf{x})} &= \operatorname{Grad}\boldsymbol{\chi}(\mathbf{x}) - \mathbf{F}(\mathbf{x}) = \mathbf{0}.
\end{aligned}
$$

mixed variational formulation

saddle point condition in Fourier space

$$\mathbf{P}(\mathbf{k}) - \mathbf{\Lambda}_{\mathrm{R}}(\mathbf{k}) + \mathbb{A}\Big\{\mathbf{F}(\mathbf{k}) - \boldsymbol{\chi}(\mathbf{k}) \otimes i\,\mathbf{k}\Big\} = \mathbf{0}$$

$$\boldsymbol{\chi}(\mathbf{k}) = \mathbf{A}(\mathbf{k})^{-1}\Big\{\mathbb{A}\mathbf{F}(\mathbf{k}) - \mathbf{\Lambda}_{\mathrm{R}}(\mathbf{k})\Big\}\, i\,\mathbf{k}$$

$$\boldsymbol{\chi}(\mathbf{k}) \otimes i\,\mathbf{k} - \mathbf{F}(\mathbf{k}) = \mathbf{0}$$

mixed variational formulation

saddle point

$$\widehat{\mathscr{F}}_{\text{mixed}}\left[\mathbf{F}(\mathbf{k}), \boldsymbol{\Lambda}(\mathbf{k})\right] := \left\{\begin{array}{r} \mathbf{P}(\mathbf{k}) - \boldsymbol{\Lambda}_{\mathrm{R}}(\mathbf{k}) + \mathbb{A}\Big\{\mathbf{F}(\mathbf{k}) - \mathbb{\Gamma}(\mathbf{k})\Big\{\mathbb{A}\mathbf{F}(\mathbf{k}) - \boldsymbol{\Lambda}_{\mathrm{R}}(\mathbf{k})\Big\}\Big\} \\ \mathbf{F}(\mathbf{k}) - \mathbb{\Gamma}(\mathbf{k})\Big\{\mathbb{A}\mathbf{F}(\mathbf{k}) - \boldsymbol{\Lambda}_{\mathrm{R}}(\mathbf{k})\Big\} \end{array}\right\}$$

$$= \mathbf{0}$$

numerical solution

discretization

- regular spatial grid
- associated Fourier grid

root finding algorithm

- non-linear Richardson
- non-linear GMRES
- inexact Newton-GMRES

elastic inclusion problem

- isotropic elasticity
- 2048 x 2048
- uniaxial tension

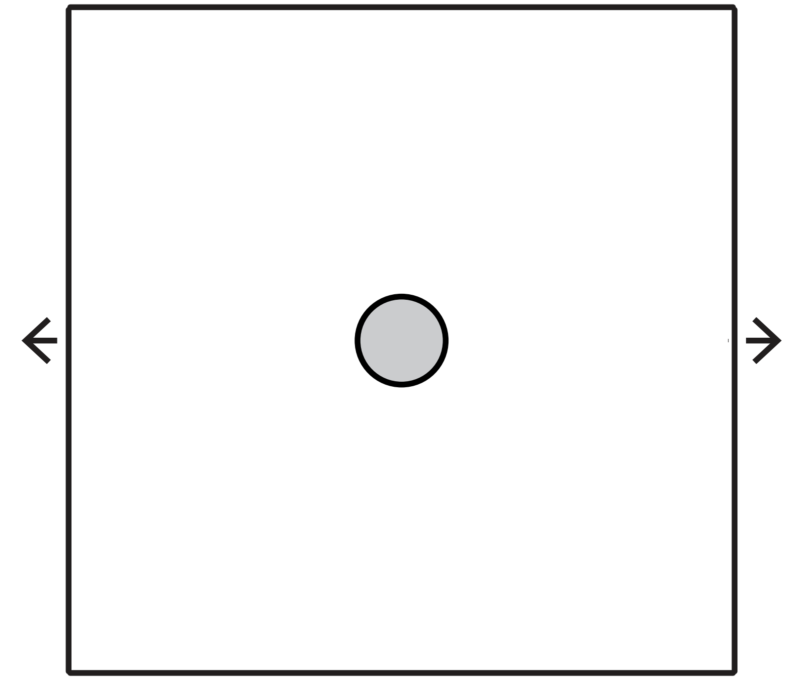

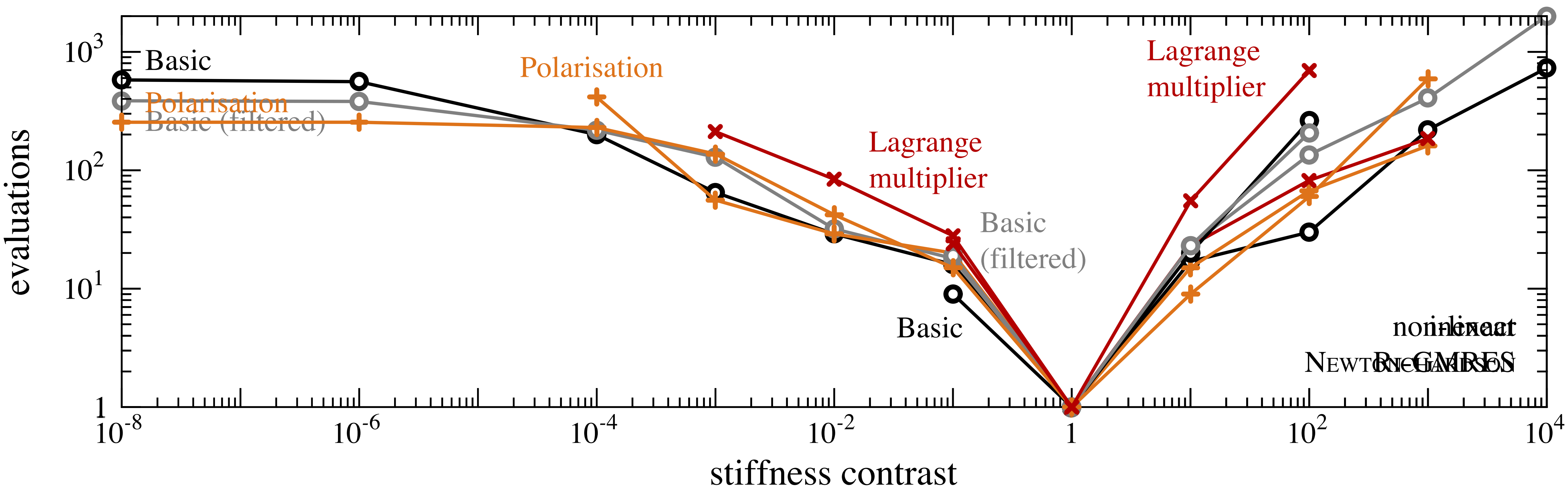

http://www.mathpages.com/home/kmath330/kmath330.htm